IL
NUOVO CIMENTO
ORGANO DELLA SOCIETÀ ITALIANA DI FISICA
SOTTO GLI AUSPICI DEL CONSIGLIO NAZIONALE DELLE RICERCHE

VOL. X, N. 5 *Serie decima* 1° Dicembre 1958

WOLFGANG PAULI

È MORTO

IL GIORNO 15 DICEMBRE 1958

W. Pauli

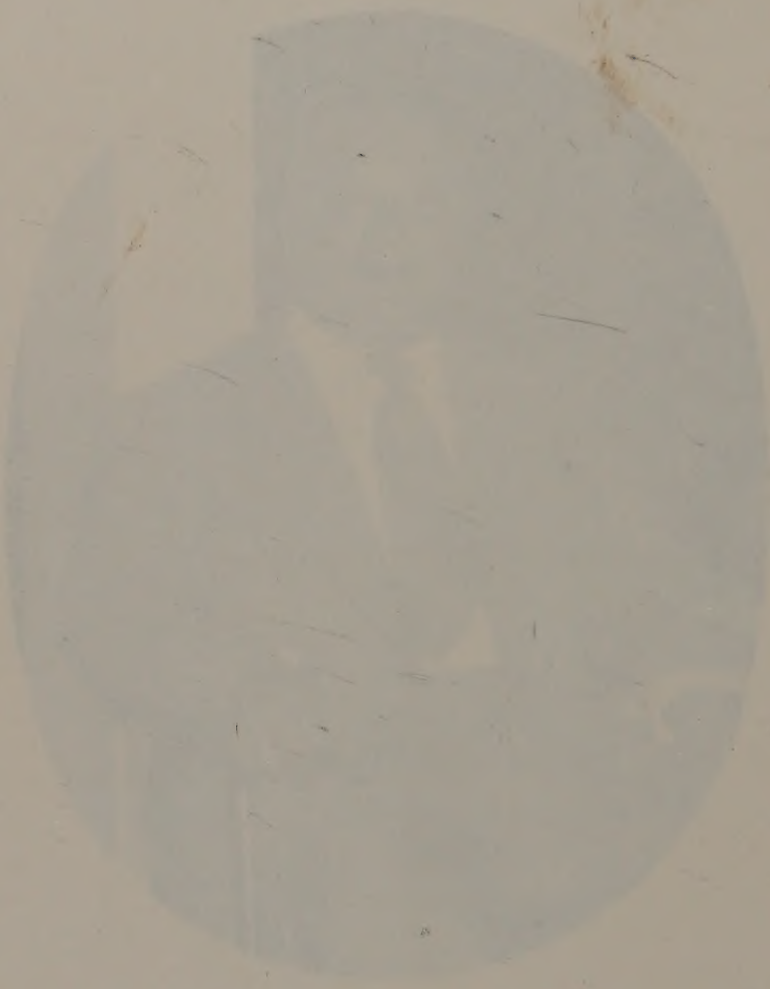

Questo quartino va preposto alla pag. 741.

IL NUOVO CIMENTO Vol. X, N. 5 1° Dicembre 1958

Nuclear Interactions in the Energy Region ($10^{10} \div 10^{14}$) eV.

P. Ciok, T. Coghen, J. Gierula, R. Hołyński, A. Jurak, M. Mięsowicz and T. Saniewska

Institute of Nuclear Research, Cosmic Ray Department - Kraków and Warszawa

J. Pernegr

Institute for Physics of Czechoslovac Academy of Sciences - Praha

(ricevuto il 16 Luglio 1958)

Summary. — Measurements of angular distributions of secondary particles in interactions of high energy primaries of cosmic radiation with the nuclei of photographic emulsion have been performed. A systematic increase in anisotropy of angular distribution in C.M. with increasing primary energy has been stated. It was found that in many high energy jets the number of secondaries in the vicinity of $\pi/2$ C.M. angle in smaller than that predicted by the theories of Heisenberg or Landau. For explaining these experimental results a model has been introduced in which the secondaries are emitted isotropically from two centres moving in opposite direction in the C.M. system. Some experimental arguments have been given for this isotropy. The relation between the velocity of two centres, the inelasticity coefficient, multiplicity and transversal momenta of secondaries has been discussed.

1. – Introduction.

Takagi [1] proposed a model of multiple meson production in nuclear collisions of very high energy based on the assumption that the generated particles are emitted independently from two centres moving in opposite directions in the C.M. system.

(1) S. Takagi: *Progr. Theor. Phys.*, **7**, 123 (1952).

TAKAGI assumed that the secondary particles are emitted isotropically in the frames associated with each centre and as a result the particles are concentrated in the forward and backward directions in the C.M. system.

KRAUSHAAR and MARKS [2] suggested a similar model in which the centres are assumed to be highly excited nucleons.

BHABHA [3] suggested a model based on the assumption of a spatial distribution of mass in the nucleons. This results in the emission of secondary particles from distinct regions which move in opposite directions in the C.M. system.

All authors mentioned above used the theories of FERMI [4] or HEISENBERG [5] for describing the phenomena of emission of secondaries from both centres.

KOBA [6] examined Takagi's model in comparison with Heisenberg's and Landau's [7] theories. This comparison concerned mainly the problem of multiplicity of secondary particles in high energy jets and their composition.

In a recently published paper [8] the authors used Takagi's model for describing the phenomena observed in high energy interactions. In that paper —which we shall further denote as « I »—the authors analysed the angular distributions of secondary particles using the method of DULLER and WALKER [9] and LINDERN [10]. As a result of this analysis we observed an increase of anisotropy in angular distributions in the C.M. system with increasing energy of the primary. It was found that the model under consideration—« two centres »—model as we called it in « I »—gave a consistent description of the observed experimental facts. For jets of the highest energies in which the narrow and the diffuse cone can be easily distinguished, the distribution observed in the cones taken separately was not in contradiction with an isotropic one in the centres own system. We found that the $\bar{\gamma}$ *i.e.* the γ-values of the emitting centres in C.M. system were much smaller than the corresponding values for nucleons.

We related the factor $\bar{\gamma}$ with the inelasticity coefficient K by means of the formula (1) given in « I » and formula (8) in the Sect. **6** of the present

---

(2) W. L. KRAUSHAAR and L. J. MARKS: *Phys. Rev.*, **93**, 326 (1954).
(3) H. J. BHABHA: *Proc. Roy. Soc. London*, **219**, 293 (1953).
(4) E. FERMI: *Phys. Rev.*, **81**, 683 (1951).
(5) W. HEISENBERG: *Zeits. Phys.*, **133**, 65 (1952).
(6) Z. KOBA: *Progr. Theor. Phys.*, **17**, 288 (1957).
(7) S. Z. BELEN'KIJ and L. LANDAU: *Suppl. Nuovo Cimento*, **3**, 15 (1956).
(8) P. CIOK, T. COGHEN, J. GIERULA, R. HOŁYŃSKI, A. JURAK, M. MIĘSOWICZ, T. SANIEWSKA, O. STANISZ and J. PERNEGR: *Nuovo Cimento*, **8**, 166 (1958).
(9) N. M. DULLER and W. D. WALKER: *Phys. Rev.*, **93**, 215 (1954).
(10) L. VON LINDERN: *Nuovo Cimento*, **5**, 491 (1957).

paper. The comparison of this formula with a very similar one given recently by EDWARDS *et al.* [11] will be given later.

A similar attempt to describe some events of high energy collisions known from the literature was then given by G. COCCONI [12].

The paper « I » was based on experimental material from our laboratories only. The present paper gives the results based on our extended material and on data from published papers [13] and private communications (*).

2. – Experimental procedure.

From the whole available material we selected for analysis only interactions with primary particles: p, n, α, and with low excitation of the target nucleus ($N_h \leqslant 5$).

In order to obtain sufficient statistical significance in the energy evaluation from the angular distribution we restricted the events by the condition $n_s \geqslant 6$.

We also used information about angular distributions of neutral pions in the few cases in which an analysis of electron-photon cascades was performed.

The events fullfilling these conditions were divided into 4 groups according to their primary energy (in eV)

$10^{10} < E_p < 10^{11}$	38 jets	374 tracks
$10^{11} < E_p < 10^{12}$	42 jets	611 tracks
$10^{12} < E_p < 10^{13}$	29 jets	475 tracks
$10^{13} < E_p$	10 jets	143 tracks

In separating the events into particular energy groups we used the formula [14]

$$\lg \gamma_c = \overline{\lg \operatorname{cotg} \theta_L} \tag{1}$$

---

[11] B. EDWARDS, J. LOSTY, D. H. PERKINS, K. PINKAU and J. REYNOLDS: *Phil. Mag.*, **3**, 237 (1958).

[12] G. COCCONI: private communication.

[13] M. SCHEIN, R. G. GLASSER and D. M. HASKIN: *Nuovo Cimento*, **2**, 647 (1955); A. DEBENEDETTI, C. M. GARELLI, L. TALLONE and M. VIGONE: *Nuovo Cimento*, **4**, 1142 (1956); M. KOSHIBA and M. F. KAPLON: *Phys. Rev.*, **97**, 193 (1955); V. D. HOPPER, S. BISWAS and J. F. DARBY: *Phys. Rev.*, **84**, 457 (1951); E. G. BOOS, A. H. WINNICKIJ, Z. S. TAKIBAEW and I. JA. CASNIKOW: *Žurn. Exp. Theor. Fyz.*, **34**, 622 (1958).

(*) We are very much indebted to Dr. D. H. PERKINS of the H. H. Wills Laboratory, Bristol and to Dr. K. LANIUS of the Kern-physikalisches Institut der Deutschen Akademie der Wissenschaften zu Berlin for kindly sending us the angular distributions of their material.

[14] C. CASTAGNOLI, G. CORTINI, D. MORENO, C. FRANZINETTI and A. MANFREDINI: *Nuovo Cimento*, **10**, 1539 (1953).

and

$$E_p = 2\gamma_c^2 - 1 , \tag{2}$$

γ_c is therefore the Lorentz factor of a system for which there is a symmetry in the forward and backward directions. In the case of nucleon-nucleon collision, γ_c is the energy of each nucleon in the C.M. system in rest mass units.

It may be remarked that the analyzed material consists at least in the high energy groups of jets with relatively small numbers of shower particles n_s. If we tentatively hold to the tunnel-model of nucleon-nucleus collision, and evaluate the average length of the tunnel expressed in the number of nucleons l in it, we get for the highest energy group in average $l < 1$ and in the group 10^{12} eV $\div 10^{13}$ eV $l \approx 2$ (see for instance ([15])).

The angular distribution was expressed in co-ordinates ([9])

$$x = \log (\gamma_c \operatorname{tg} \theta_L); \qquad y = \log \frac{F(\theta_L)}{1 - F(\theta_L)} , \tag{3}$$

where $F(\theta_L)$ is the fraction of tracks with an angle less than θ_L with the jet axis. It follows from the transformation formula

$$\gamma_c \operatorname{tg} \theta_L = \frac{\sin \bar{\theta}}{\beta_c/\beta_\pi + \cos \bar{\theta}} ,$$

where $\bar{\theta}$ and θ_L are the angles in the C.M. and laboratory system respectively, that in case $\beta_c \approx \beta_\pi \approx 1$ the angular distributions in such co-ordinates give angular distributions in the C.M. system. In these co-ordinates the isotropic distribution in the C.M. system is represented as a line of slope 2 and the anisotropic distribution of HEISENBERG ([16]) as a line of slope 1. The distribution given by the theory of LANDAU ([7]) is also an approximately straight line whose slope decreases slightly with increasing primary energy. The Landau distribution for the primary energy interval ($10^{12} \div 10^{13}$) eV is very similar to the Heisenberg distribution.

LINDERN ([10]) used $x = \lg (\gamma_c \operatorname{tg} \theta_L)$ for plotting differential distributions, and showed that the typical angular distributions in the C.M. system *e.g.* isotropic, Heisenberg's anisotropic, etc., could be well approximated by Gaussian curves, and the dispersion σ can be taken as a measure of anisotropy. For instance, for isotropy we get $\sigma = 0.36$ and for Heisenberg's anisotropic distribution $\sigma = 0.7$.

([15]) F. D. ROESLER and C. B. A. MCCUSKER: *Nuovo Cimento*, **10**, 127 (1953).

([16]) K. SYMANZIK: in *Kosmische Strahlung*, 2nd ed. (Berlin-Göttingen-Heidelberg, 1953).

3. – The dependence of anisotropy of angular distribution on the primary energy.

In Figs. 1. 2. 3 and 4 we see the experimental differential angular distribution $dN/d\lg(\gamma_c \operatorname{tg}\theta_L)$ *vs.* $\lg(\gamma_c \operatorname{tg}\theta_L)$, *i.e.* angular distributions in the C.M.

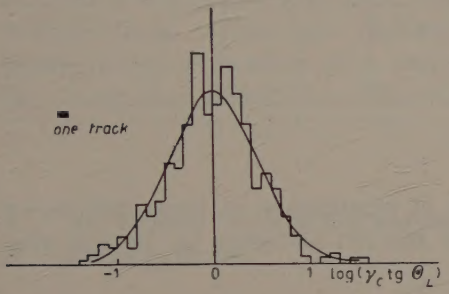

Fig. 1. – Differential angular distribution for jets in the energy interval 10^{10} eV to 10^{11} eV. The continous curve represents the best fit of a Gaussian curve to the experimental data with $\sigma = 0.46$.

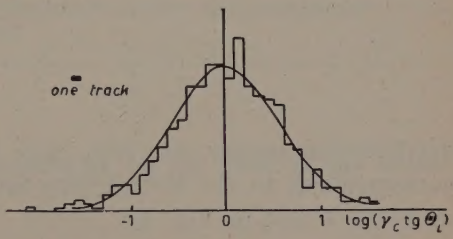

Fig. 2. – Differential angular distribution for jets in the energy interval 10^{11} eV to 10^{12} eV. The continous curve represents the best fit of a Gaussian curve to the experimental data with $\sigma = 0.55$.

system. These figures correspond to 4 energy intervals. As mentioned before the σ of these distributions may be considered as a measure of anisotropy. The values of σ for different energy intervals are given in Table I.

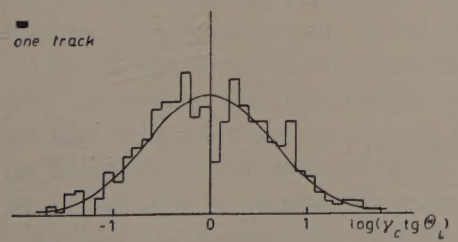

Fig. 3. – Differential angular distribution for jets in the energy interval 10^{12} eV to 10^{13} eV. The continous curve represents the best fit of a Gaussian curve to the experimental data with $\sigma = 0.66$.

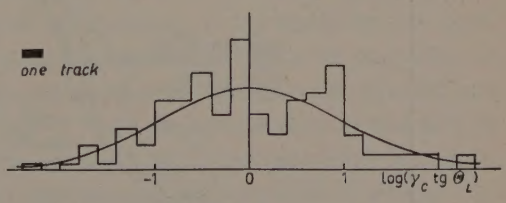

Fig. 4. – Differential angular distribution for jets with energy higher than 10^{13} eV. The continous curve represents the best fit of a Gaussian curve to the experimental data with $\sigma = 0.96$.

We see from Table I the general increase of the anisotropy—expressed by σ_{exp}—with increasing energy. The experimental material used in this investigation is sufficiently large to give significant differences in σ-values of

TABLE I.

$E_{primary}$ in eV	10^{10}	10^{11}	10^{12}	10^{13}	10^{14}
σ_{Landau}		0.49	0.63	0.77	0.96
σ_{exp}	0.46	0.55	0.66	0.96	
$\bar{\gamma}$	1.25	1.50	2.0	4.0	
$\alpha_{\Delta\sigma}$		33%	8%	12%	

neighbouring energy intervals. The levels of significance of these differences corresponding to the Kolmogorov-Smirnov test ([17]) are given in the last row of Table I and in Fig. 5.

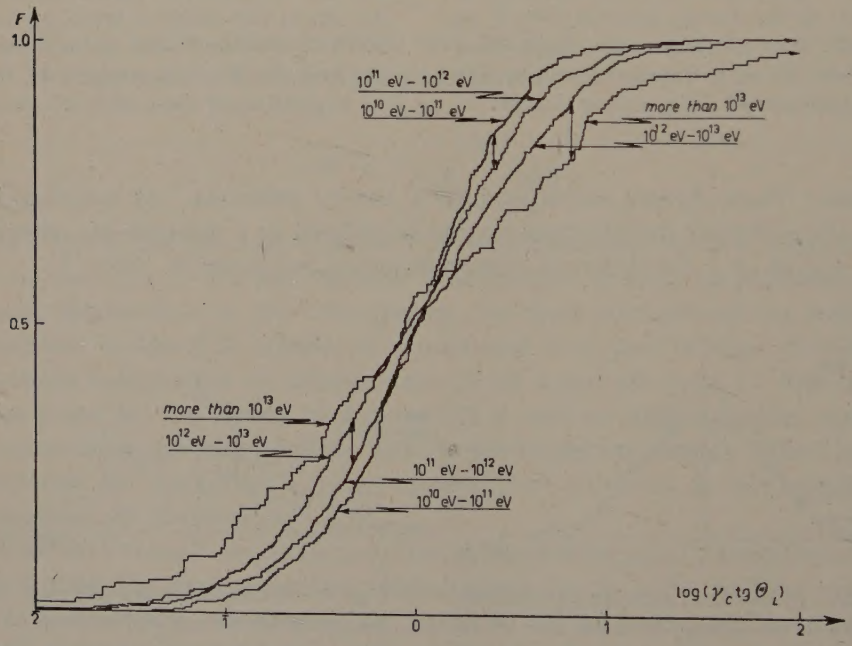

Fig. 5. – Integral angular distributions for four energy intervals of jets. The maximum differences corresponding to the Kolmogorow-Smirnow test between neighbouring distributions are marked.

([17]) A. KOLMOGOROW: *Giorn. dell'Ist. Ital. degli Attuari*, **4**, 1 (1933); H. SMIRNOW: *Recueil Math.*, N.S. **6**, 1 (1939); see also F. J. MASSEY: *Amer. Statist. Assoc. Journ.* (March 1951), p. 68.

The general dependence of anisotropy *i.e.* the σ-value of the distribution, on the primary energy is roughly consistent with the prediction of Landau's theory (7) as seen from the table. Besides we see that for lower energy intervals ($10^{10} \div 10^{11}$ and $10^{11} \div 10^{12}$) the experimental histograms are well approximated by Gaussian curves. However, for the energy interval ($10^{12} \div 10^{13}$) eV the agreement of the experimental histogram with the Gaussian curve of corresponding σ is rather a poor one. There is a characteristc lack of tracks in the neighbourhood of the C.M. angle $\pi/2$. For energies higher than 10^{13} eV the errors in the evaluation of γ_c and poor statistics make the comparison with any theoretical distribution difficult.

4. – An attempt to analyze angular distributions on the basis of the «two-centre» model.

In « I » the authors drew attention to the fact that in a number of high energy jets we observe a characteristic angular distribution which were shown for co-ordinates x, y (Fig. 7 in « I », Fig. 2 of Cocconi's paper (12) and Fig. 6 of the present paper). If these distributions significantly deviate from a straight line, as represented by the Heisenberg or Landau distributions, then we can say that the observed distribution is marked by a lack of tracks in the directions close to the angle $\pi/2$ in the C.M. system. In the differential distribution dN/dx *vs.* x this fact appears in the deviation from the Gaussian curve namely the dip in the vicinity $x = 0$, which seems to be present in Fig. 3 and 4. The authors attempted to discuss the characteristic angular distributions of the type shown in Fig. 6 on the basis of the two centre model.

Let us assume (as in « I ») that after the collision of the nucleons the emission takes place from two centres independently which move in opposite directions with the same velocity (in the simplest case) in the C.M. system and for which the corresponding value of γ is $\bar{\gamma}$. Let us assume that in the system associated with the centre the emission of particles is isotropic and let us assume that the particles are emitted in this system with a uniform energy E_π. These assumptions lead in a simple way to an angular distribution which, in the x, y co-ordinates have the characteristic shape seen in Fig. 6. In this figure are represented several events with distinctly differing narrow and diffuse cones. Besides the events given in « I » we have included in this paper the additional events Nos. 18 and 26 from our material and events P5 and P20 published in the paper of Edwards *et al.* (11).

For each event γ_c calculated from the formula $\lg \gamma_c = \lg \operatorname{cotg} \theta_L$ and γ_c' calculated from the individual cones by evaluations γ_1 and γ_2 for two emitting centres in the L system, in an analogous way to that introduced in the paper

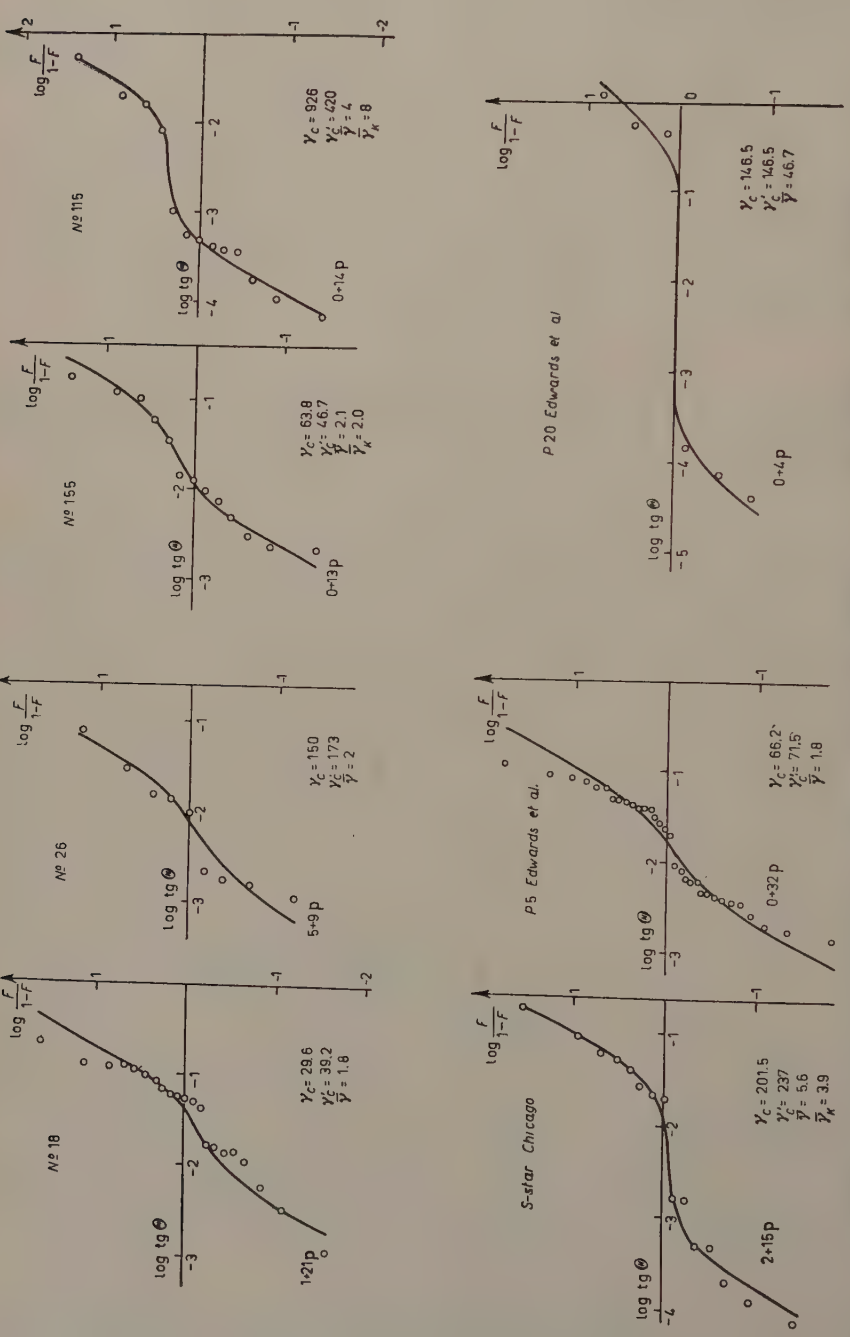

Fig. 6. – Integral angular distributions for some jets. The continuous curves represent the distributions based on the two-centre model. Notations: see text.

of CIOK *et al.* [18] are given in the figure. We have (see Appendix)

$$\gamma_c'^2 = \tfrac{1}{2}(\gamma_1\gamma_2 + \sqrt{\gamma_1^2-1}\,\sqrt{\gamma_2^2-1}+1) \approx \gamma_1\gamma_2 . \tag{4}$$

From the values γ_1 and γ_2 we also calculate the value of $\bar{\gamma}$ from the formula

$$\bar{\gamma} = \frac{\gamma_1+\gamma_2}{2\gamma_c'} . \tag{5}$$

In addition, the values of $\bar{\gamma}$ (denoted as $\bar{\gamma}_k$ in Fig. 6) calculated from the coefficients of inelasticity (formula (8)) are given for the events for which these coefficients were directly measured. The solid lines in Fig. 6 represent distributions calculated on the basis of the « two-centre model » for values of γ_c' and $\bar{\gamma}$ given in the figure.

5. – Angular distribution of secondary particles in the system of the emitting centre.

In the preceding Section we gave a comparison of the observed angular distribution for several events with the distribution calculated under the assumption of the « two-centre » model. Here we assume that emission in the system of the given centre is isotropic. There exists the possibility of checking this assumption experimentally. In the events where the cones are distinctly separated we can investigate the distributions in the individual cones treated as separate jets.

In « I » an analysis was made in this direction. Calculations of γ_1 and γ_2 from the formula

$$\log \gamma_{1,2} = \overline{\log \operatorname{cotg} \theta_L} , \tag{6}$$

were made for individual forward and backward cones of our jets Nos. 155, 115 and for the star « S ». Then the total integral angular distribution for this set of forward and backward « jets » was computed. Fig. 6 in « I » shows that there is no contradiction with the assumption of isotropy of the distribution if it is assumed that the particles in the individual cones are emitted by two centres moving with the Lorentz factors γ_1 and γ_2 in the L system. The results of such analysis are shown in Fig. 7 on the basis of more extensive material.

---

[18] P. CIOK, M. DANYSZ, J. GIERULA, A. JURAK, M. MIĘSOWICZ, J. PERNEGR, J. VRANA and W. WOLTER: *Nuovo Cimento*, **6**, 1409 (1957).

Represented here are the integral angular distributions for narrow and diffuse cones separately. We believe that the results presented here confirm the opinion expressed in « I » that both distributions can be regarded as isotropic.

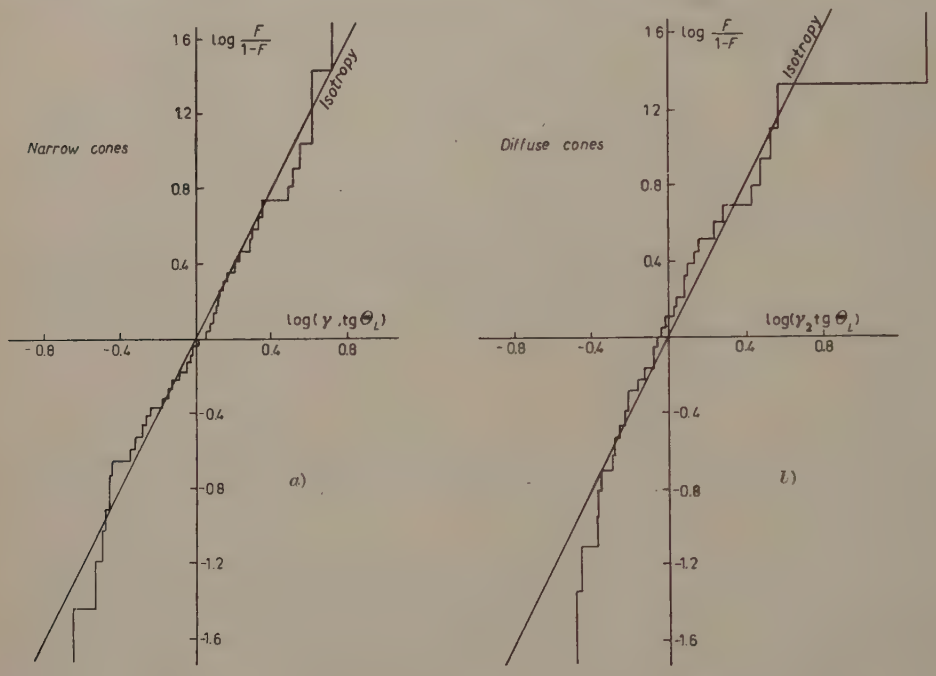

Fig. 7. – Integral angular distributions for narrow (*a*) and diffuse (*b*) cones treated separately as independent jets. Here are presented no. 115 [18], « S »-star [13], α5, P20. P20S4, P10 and P24S4 [11] and private communication from Dr. PERKINS.

6. – The problem of transversal momentum in the « two-centre » model.

Now we would like to consider the consequences, aside from the shape of the angular distribution, which result from the adoption of the « two-centre » model. In the work of the Bristol group [11] there was introduced a new definition of the coefficient of inelasticity K' from which the following relation results:

$$(7) \qquad (\operatorname{cosec}\bar{\theta})_{\mathrm{av}} = \frac{4}{3}\frac{K'}{p_T}\left(\frac{\gamma_c}{n_s}\right); \qquad \begin{array}{l}\bar{\theta} \text{ angle in C.M.;}\\ p_T \text{ transversal momentum.}\end{array}$$

As we have shown in « I » ((Eq. (1)) an analogous relation results from our model as an expression of the principle of the conservation of energy: the

total energy of the centres moving in the C.M. system with a γ-value equal to $\bar{\gamma}$ and emitting secondary particles with a mean energy E_π (total energy of a particle in the rest system of the centre) is equal to the energy available in the C.M. multiplied by the factor K (K, coefficient of inelasticity):

$$1.5 n_s E_\pi \bar{\gamma} = 2 K \gamma_c . \tag{8}$$

In our approach the measure of anisotropy introduced in the Bristol paper —$(\operatorname{cosec}\theta)_{av}$—finds physical expression in $\bar{\gamma}$. The mean $\bar{\gamma}$-values for each energy interval were determined and given in Table I (see also Appendix).

If we tentatively adhere to this model, we can, from the above relation determine:

a) the value E_π assuming that the upper limit of the quantity $n_s\bar{\gamma}/\gamma_c$ ($= 2K/1.5E_\pi$) for the set of all observed jets corresponds to the highest possible value of the inelasticity coefficient, *i.e.* $K = 1$ (say $E_\pi = (E_\pi)_{K=1}$);

b) assuming this value of $(E_\pi)_{K=1}$ as the energy of the emitted particles also for collisions with $K < 1$ we can establish the relation between the quantities $n_s\bar{\gamma}/\gamma_c$ and K, namely:

$$\frac{1.5}{2} (E_\pi)_{K=1} \left(\frac{n_s\bar{\gamma}}{\gamma_c}\right) = K . \tag{9}$$

We can check this relation for jets in which the inelasticity coefficient was determined by direct measurements (see the numerical data in Fig. 6).

Let us make this analysis, in effect, analogous to that of the Bristol group, for the entire experimental material at our disposal. The results are shown in Fig. 8. The quantity $n_s\bar{\gamma}/\gamma_c$ for jets in the energy range from 10^{10} eV to 10^{14} eV are shown as a function of γ_c. The quantity $\bar{\gamma}$ was determined from the angular distributions on the basis of the « two-centre » model (see Appendix). For energies below 10^{12} eV only the mean for the two groups of jets in the energy intervals 10^{10} eV $\div$ 10^{11} eV and 10^{11} eV $\div$ 10^{12} eV are given.

It should be stressed that value of $(E_\pi)_{K=1} \approx 0.4$ GeV estimated in this way is in good agreement with the measurements of the transversal momenta ([19,11]).

As may be seen from Fig. 8 the material investigated here characterized by a small excitation of the target nucleus ($N_h \leqslant 5$) confirms the conclusion given

([19]) O. Minakawa, Y. Nishimura, M. Tzuzuki, H. Yamanouchi, H. Aizu, H. Hasegawa, Y. Ishii, S. Tokunaga, Y. Fujimoto, S. Hasegawa, J. Nishimura, K. Niu, K. Nishikawa, K. Imaeda and M. Kazuno: *I. N. S. J.*-7, preprint (Tokyo, March 1958).

originally by the Bristol group [11] about the decrease of the mean value of K with increasing energy. From the smallness of K for very high energies and from the fact that $\bar{\gamma}$ is much smaller than γ_c it follows that it would be difficult to identify the centres of emission with two « excited nucleons ».

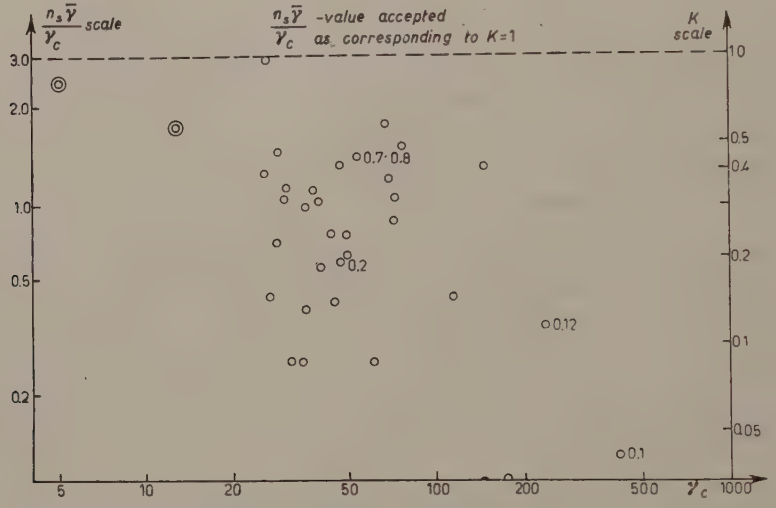

Fig. 8. – Analysis of the formula $1.5 n_s E_\pi \bar{\gamma} = 2K\gamma_c$, and the energy dependence of K based on the « two-centre » model. ○ correspond to jets with energy higher than 10^{12} eV. ◎ correspond to groups of jet energy smaller than 10^{12} eV. Numbers in the vicinity of some points denote experimental K-values. Other details: see text.

7. – Conclusions.

1) In interactions of nucleons of cosmic radiation with the nuclei of photographic emulsion (with $N_h \leqslant 5$) in the limits of energy 10^{10} eV $\div$ 10^{14} eV the angular distributions of secondary particles in the C.M. approximated by Gaussian curves show an increase in anisotropy with energy in agreement with the predictions of the Landau theory.

2) It was found, however, that in many high energy jets the angular distribution quite markedly departs from the angular distribution predicted by the theories of Landau and Heisenberg in their present form. This is also reflected in the total differential distribution by a dip in the vicinity of the angle $\pi/2$ in the C.M.

3) The « two-centre » model that has been introduced by TAKAGI seems to describe the shape of the angular distribution in the C.M. with better agree-

ment with experiment. In this model it is assumed that the secondary particles are emitted isotropically with the same energy from two centres moving in the C.M. with $\bar{\gamma}$ considerably less than the γ of the nucleons.

4) The « two-centre » model permits the factor $\bar{\gamma}$ of the centres in C.M. to be related to the coefficient of inelasticity, multiplicity, energy of secondary particles in the system of the centre and the energy of the primary nucleon, as $(\operatorname{cosec}\theta)_{av}$ was in the paper of Bristol group. From this relation and from the observed angular distributions the values of the transversal momentum obtained are in agreement with experiment.

* * *

The authors wish to thank Dr. A. Zawadzki and Dr. P. Zieliński for their comments on the statistical analysis of the experimental material.

Appendix

Formulae (4) and (5) can be derived in the following manner: Let γ_1, γ_2 be the Lorentz factors of the two emitting centres in L. If we assume the angles $\theta_{(1)}$ and $\theta_{(2)}$ formed with the shower axis by the two centres respectively $\theta_{(1)} = \theta_{(2)} = 0$ and the Lorentz factors $\bar{\gamma}$ of the two centres in the C.M. equal, than the usual transformation formulae from L. to C.M. read

$$\text{(10)} \qquad \begin{cases} \bar{\gamma} = \gamma_1\gamma_c' - \sqrt{\gamma_1^2 - 1}\,\sqrt{\gamma_c'^2 - 1}\,, \\ \bar{\gamma} = \gamma_2\gamma_c' - \sqrt{\gamma_2^2 - 1}\,\sqrt{\gamma_c'^2 - 1}\,, \end{cases}$$

or inversely

$$\text{(11)} \qquad \begin{cases} \gamma_1 = \bar{\gamma}\gamma_c' + \sqrt{\gamma_c'^2 - 1}\,\sqrt{\bar{\gamma}^2 - 1}\,, \\ \gamma_2 = \bar{\gamma}\gamma_c' - \sqrt{\gamma_c'^2 - 1}\,\sqrt{\bar{\gamma}^2 - 1}\,. \end{cases}$$

Comparing these equations and eliminating $\bar{\gamma}$ we immediately receive for the velocity of C.M. in L

$$\text{(12)} \qquad \beta_c = \frac{\gamma_1 - \gamma_2}{\sqrt{\gamma_1^2 - 1} - \sqrt{\gamma_2^2 - 1}} = \frac{\sqrt{\gamma_1^2 - 1} + \sqrt{\gamma_2^2 - 1}}{\gamma_1 + \gamma_2},$$

and for $\gamma_c' = 1/(\sqrt{1 - \beta^2})$ after some simple calculations,

$$\text{(13)} \qquad \gamma_c'^2 = \tfrac{1}{2}(\gamma_1\gamma_2 + \sqrt{\gamma_1^2 - 1}\,\sqrt{\gamma_2^2 - 1} + 1) \approx \gamma_1\gamma_2\,.$$

The right hand side of (12) can be directly obtained from energy and momentum conservation in L. $\bar{\gamma}$ can be obtained either directly from (10) or by adding equations (11)

$$\bar{\gamma} = \frac{\gamma_1 + \gamma_2}{2\gamma_c'} . \tag{14}$$

The value $\bar{\gamma}$ can be also evaluated if we know

$$\sigma = \sqrt{\frac{\sum [\log \gamma_c \operatorname{tg} \theta_L]^2}{n}} = \sqrt{\frac{\sum (x_i + \log \gamma_c)^2}{n}} . \tag{15}$$

If we assume isotropic emission from two centres, as in the model under consideration we get two groups of values, each having $\sigma = 0.36$ with respect to its mean value: $-\log \gamma_1$ or $-\log \gamma_2$ respectively. Let us denote the distance between these two values by 2δ. From equations (11) follows:

$$2\delta = \log \frac{\gamma_1}{\gamma_2} = \log \frac{\gamma_c \bar{\gamma} + \sqrt{\gamma_c^2 - 1}\sqrt{\bar{\gamma}^2 - 1}}{\gamma_c \bar{\gamma} - \sqrt{\gamma_c^2 - 1}\sqrt{\bar{\gamma}^2 - 1}} \approx 2 \log 2\bar{\gamma} , \tag{16}$$

(for large γ_c and not too small $\bar{\gamma}$).

For σ with respect to $-\log \gamma_c = -\frac{1}{2}(\log \gamma_1 + \log \gamma_2)$ we obtain immediately:

$$\sigma = \sqrt{0.36^2 + \delta^2} . \tag{17}$$

This relation enables us to evaluate $\bar{\gamma}$ in a very simple manner even if the narrow and diffuse cones can not be easily distinguished.

RIASSUNTO (*)

Si sono eseguite misure di distribuzioni angolari di particelle secondarie nelle interazioni di primari della radiazione cosmica coi nuclei dell'emulsione fotografica. Si è constatato un aumento sistematico dell'anisotropia della distribuzione nel sistema del centro di massa coll'aumento dell'energia primaria. Si è trovato che in molti jets di alta energia il numero dei secondari in prossimità dell'angolo $\pi/2$ nel sistema del centro di massa è minore di quello previsto dalle teorie di Heisenberg e di Landau. Per spiegare tali risultati sperimentali, è stato introdotto un modello nel quale i secondari sono emessi isotropicamente da due centri che si muovono in direzioni opposte nel sistema del centro di massa. Si espongono alcuni argomenti sperimentali a sostegno di tale isotropia. Si è discussa la relazione tra la velocità dei due centri, il coefficiente di inelasticità, la molteplicità e i momenti trasversali dei secondari.

(*) *Traduzione a cura della Redazione.*

IL NUOVO CIMENTO Vol. X, N. 5 1° Dicembre 1958

Possible Consequences of the Isobar and Fire Ball Models.

Z. Koba

Research Institute for Fundamental Physics, Kyoto University, Kyoto

S. Takagi

Department of Physics, Osaka University, Osaka

(ricevuto il 30 Luglio 1958)

Summary. — Two possible consequences, characteristic of the isobar model and the fire ball model of the multiple meson production, are discussed. One is the azimuthal asymmetry of secondary particles, and the other is the apparent anomaly of the inelasticity in meson-nucleon collision.

1. – Introduction.

Recently a model for multiple particle production at extremely high energy has been proposed by Niu [1], the Polish group [2], and Cocconi [3]. According to them, the collision of two energetic nucleons gives rise to two « fire

[1] K. Niu: *Utyusen-Kenkyu* (Mimeographed circular in Japanese for cosmic ray studies), **3**, 85 (1958); K. Niu: Lecture at the semi-annual meeting of the Physical Society of Japan (May 1958).

[2] P. Ciok, T. Coghen, J. Gierula, R. Hołyński, A. Jurak, M. Mięsowicz, T. Saniewska, O. Stanisz and J. Pernegr: preprint. We are grateful to these authors for sending us their work before publication.

[3] G. Cocconi: preprint. We are grateful to Prof. S. Hayakawa for showing us this work.

balls », each of which separates from the incident nucleon, flies out, and after a very short time disintegrates into a number of mesons.

This « fire ball model » (*) shares with the isobar model (+), which was presented by one of us (S. T.) (4) and later worked out by KRAUSHAAR and MARKS (5), the assumption of a hypothetical metastable state in the intermediate stage. In this note we should like to point out two possible consequences of such models, which might be detected experimentally.

2. – Azimuthal asymmetry of secondary particles.

In these models it is conceivable that the azimuthal distribution of secondary particles can sometimes show more asymmetry than is expected from simple statistical fluctuation.

Suppose that partial waves of very high angular momenta are effective in the collision process due to certain properties of interaction, and a larger part of this angular momentum is assigned to the intrinsic angular momentum (or spin, so to speak) of isobars or fire balls.

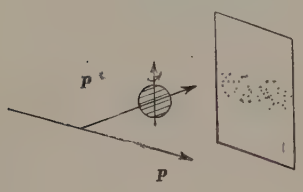

Fig. 1. – Emission with azimuthal asymmetry.

Let the isobar or the fire ball have linear momentum, $\boldsymbol{p}^*$, whose direction can be slightly different from that of the incident particle, $\boldsymbol{p}$. Thus the spin of the isobar or fire ball will be quantized in the direction of $\boldsymbol{p} \times \boldsymbol{p}^*$; this implies that a particular direction with respect to the azimuthal angle does exist. That is to say, the emission in the plane defined by $\boldsymbol{p}$ and $\boldsymbol{p}^*$ will be most favoured when the perpendicular component of the spin of the isobar or the fire ball happens to be large (×) (Fig. 1).

Detailed calculation of possible azimuthal asymmetry has already been carried out by KRAUSHAAR and MARKS (5). The point we should like to emphasize here is the essential role in the above argument played by the intermediate stage. One might be tempted to imagine the nucleon-nucleon collision as two classical balls, passing by each other at a certain distance ϱ (Fig. 2).

(*) Abbreviated hereafter as FB-model.

(+) Abbreviated hereafter as I-model.

(4) S. TAKAGI: *Prog. Theor. Phys.*, **7**, 123 (1952).

(5) W. L. KRAUSHAAR and L. J. MARKS: *Phys. Rev.*, **83**, 326 (1954).

(×) One can imagine emission from a spinning ball: most of the emitted particles will be found in the plane of equator.

Then the system would have an angular momentum ϱE in the direction perpendicular to the line defined by the two parallel tracks of incident balls, so that the system would again have a preferential direction with respect to the azimuthal angle, quite irrespective of the I model or FB-model. But such a reasoning is not correct, because here the quantum-mechanical system of two colliding nucleons is described by a plane wave (*) which has an axial symmetry around the direction of incidence; in other words, the system is represented by an equal-weight superposition of all the states which are obtained by rotating the Fig. 2 around the vector $\boldsymbol{p}$.

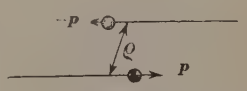

Fig. 2. – Classical picture of collision.

Thus it is obvious that the actual existence of a metastable state, which through the interaction with external fields defines the momentum $\boldsymbol{p}^*$ and consequently the plane $\boldsymbol{p} \times \boldsymbol{p}^*$, is a necessary condition for the detection of azimuthal asymmetry. The situation is analogous to the polarization experiment by a double scattering.

In this way we conclude that, if we find more azimuthal asymmetry than statistical fluctuations, then it would make the models with intermediate metastable states rather plausible, while the reverse argument does not hold, of course.

3. – Apparent inelasticity of the meson-nucleon collision.

Many of the secondary jet-showers are regarded as induced by mesons. In such cases there is no reason to believe that the collision will be symmetric. But experimentally most of the secondary showers exhibit symmetric angular distribution of emitted particles in suitably chosen reference systems. In the following we shall show that, according to the I- or FB-model, an asymmetric meson-nucleon collision can give rise to apparently symmetric distribution of secondary particles, and moreover, this circumstance can lead to an erroneous (sometimes unacceptable) estimation of the inelasticity.

It is plausible to imagine that a meson-nucleon collision will result in emission of not two, but one isobar or fire ball, which then disintegrates. In the I-model the isobar will stop in the center of mass system (+), if the incident meson loses its whole energy by the collision; but, in general, when the incident meson loses only a fraction of its original energy and goes on proceeding in

(*) In the actual condition the incident beam is located by the silver grain, which is infinitely large compared with the target, so that it can be described by a plane wave.

(+) Abbreviated hereafter as c.m.s.

the initial direction, the resulting isobar will move in the opposite direction to the incident meson in the c.m.s. In the FB-model we can imagine, as far as kinematical relations are concerned, that the above mentioned isobar separates further into a nucleon and a fire ball, the nucleon proceeding faster than the fire ball in the opposite direction to the incident meson. Thus the fire ball will be moving slower (*) in the c.m.s. than the isobar, when the inelasticity has a given value (cf. Fig. 3).

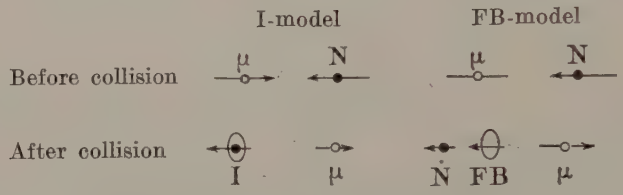

Fig. 3. – Partially inelastic collision.

Let us denote the Lorentz factor of the laboratory system (+) with respect to the c.m.s. by γ_c, and that of the isobar or the fire ball in the c.m.s. by γ_b. Then the Lorentz factor, γ_{ap}, of the isobar or the fire ball in the l.s. is given by

$$\gamma_{ap} = \gamma_b\gamma_c \mp \sqrt{\gamma_b^2 - 1}\sqrt{\gamma_c^2 - 1}\,, \tag{1}$$

where the minus and the plus signs correspond respectively to the directions of motion of the isobar or the fire ball in the c.m.s. being the opposite and the same as the incident meson.

Now it is obvious that, when we estimate the incident energy by the usual analysis of the angular distribution of secondary particles, the formula:

$$-\log\gamma = \frac{1}{n_s}\sum_{i=1}^{n_s}\log\operatorname{tg}\theta_i\,, \tag{2}$$

n_s: number of shower particles, θ_i: angle of emission of the i-th particle in c.m.s., will not give $\gamma = \gamma_c$, but $\gamma = \gamma_{ap}$, since the secondary particles are symmetrically emitted in the rest system of the isobar or the fire ball. (Here we neglect the effect of possible inclusion of the incident meson and the target nucleon in the summation of (2), since $n_s \gg 1$.)

Thus the estimation of the incident energy in the l.s. through the relation

$$E \simeq 2M\gamma_c^2\,, \tag{3}$$

(*) In algebraic sense. Sometimes the direction of motion in c.m.s. can be reversed (i.e. it can move in the direction of the incident meson).

(+) Abbreviated hereafter as l.s.

M being the mass of the target, will lead to an apparent value

$$E_{ap} \simeq 2M\gamma_{ap}^2 . \tag{4}$$

Consequently we shall obtain an apparent inelasticity:

$$\eta_{ap} = \eta\left(\frac{\gamma_c}{\gamma_{ap}}\right)^2 , \tag{5}$$

where η represents the « true » inelasticity and is defined by the ratio of energy loss to the total energy of the incident meson in the l.s. (*).

In the Appendix I and II it is proved that

$$\eta_{ap} = \eta' , \tag{6}$$

where η' stands for the rate of energy loss of the incident *nucleon* in the c.m.s. When the nucleon moves with the excited meson cloud (I-model), η' is put equal to 1.

Thus in the I-model the apparent inelasticity always turns out one, even if the incident meson loses only a small fraction of its energy. If by chance the energy of the incident meson, which has thus retained a large energy, is measured and taken into the sum of the energy of the secondary particles then it will lead to an unacceptable result: $\eta_{ap} > 1$. The situation in the FB-model model is more or less similar.

It is suggested, therefore, that we should be rather careful in the analysis of secondary jets and examine whether the above-mentioned effect really exists.

* * *

In conclusion, we should like to express our gratitude to the Kyoto, Osaka and Tokyo members of the research group of extremely high energy phenomena for their discussions.

Appendix I

Let the incident meson and nucleon lose fractions η and η' of their energies in the c.m.s. respectively. The energy, E^*, and momentum, p^*, of the fire ball are determined by the energy and momentum conservation:

$$2M\gamma_c = (1-\eta)M\gamma_c + (1-\eta')M\gamma_c + E^* , \tag{A.1}$$

$$0 = (1-\eta)M\gamma_c - (1-\eta')M\gamma_c - p^* . \tag{A.2}$$

(*) The inelasticity in the c.m.s. is $(\eta + \eta')/2$.

These relations are valid when $(1-\eta)\gamma_c \gg 1$, $(1-\eta')\gamma_c \gg 1$, but they hold also when $\eta = 1$ or $\eta' = 1$, provided that the nucleon moving with the cloud (isobar) is regarded as if it had disappeared and, instead, E^* and p^* are identified with energy and momentum of the isobar (*). We shall use, therefore, the above relations for all values of $0 \leqslant \eta \leqslant 1$, $0 \leqslant \eta' \leqslant 1$.

The Lorentz factor of the isobar or the fire ball in the c.m.s. is given by

$$\gamma_b = \frac{E^*}{(E^{*2} - p^{*2})^{\frac{1}{2}}}, \tag{A.3}$$

or, with the help of (A.1) and (A.2),

$$= \tfrac{1}{2}\left(\sqrt{\frac{\eta'}{\eta}} + \sqrt{\frac{\eta}{\eta'}}\right). \tag{A.4}$$

Now, by (1)

$$\gamma_{ap} = \gamma_b\gamma_c \mp \sqrt{\gamma_b^2 - 1}\sqrt{\gamma_c^2 - 1} \approx \gamma_c\{\gamma_b \mp \sqrt{\gamma_b^2 - 1}\}, \qquad \text{if } \gamma_c \gg 1, \tag{A.5}$$

($\mp$ corresponding to $\eta \lesseqgtr \eta'$).

We have from (A.4)

$$\sqrt{\gamma_b^2 - 1} = \begin{cases} \tfrac{1}{2}\left[\sqrt{\dfrac{\eta'}{\eta}} - \sqrt{\dfrac{\eta}{\eta'}}\right] & \text{if } \eta \leqslant \eta', \\ \tfrac{1}{2}\left[\sqrt{\dfrac{\eta}{\eta'}} - \sqrt{\dfrac{\eta'}{\eta}}\right] & \text{if } \eta \geqslant \eta', \end{cases} \tag{A.6}$$

so that, from (A.5) and (A.6)

$$\gamma_{ap} \approx \sqrt{\frac{\eta}{\eta'}}\,\gamma_c, \tag{A.7}$$

whence

$$\eta_{ap} = \eta\left(\frac{\gamma_c}{\gamma_{ap}}\right)^2 \approx \eta'. \tag{A.8}$$

Appendix II

The relation (6) can be easily understood by imagining a hypothetical collision of a hypothetical meson with the nucleon, which collision gives rise to a fire ball identical with that of the real collision, but in which both particles lose the same fraction η' of the incident energy (Fig. 4).

(*) In other words (A.1) and (A.2) hold, as far as we can neglect the effect of rest mass.

Let the hypothetical meson have an incident energy $(\eta/\eta')M\gamma_c$ (instead of $M\gamma_c$ of the real meson) in the original c.m.s. of the real collision. In this reference system the hypothetical meson and the nucleon lose the energy $\eta M\gamma_c$ and $\eta' M\gamma_c$ respectively, giving rise to a fire ball identical with the real one.

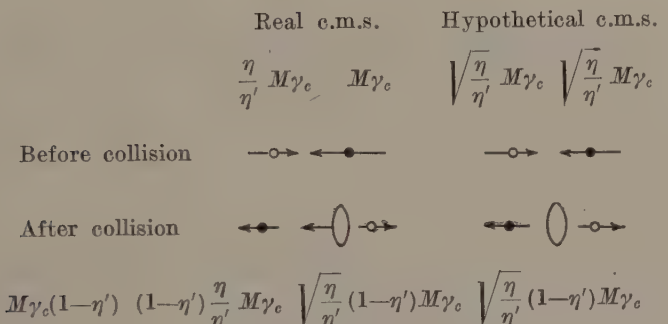

Fig. 4. – Hypothetical collision.

The rate of energy loss of the incident particles is η' for both of them, and as far as we can neglect the rest mass of nucleon and meson, this rate of energy loss is invariant with respect to the Lorentz transformation. Therefore in the c.m.s. of the hypothetical meson and the nucleon, the hypothetical collision will take place in a completely symmetric way, and the fire ball will be at rest and decay symmetrically.

We can further show, that the Lorentz factor of this hypothetical c.m.s. with respect to the l.s. is identical with the γ_{ap} given by (A.7). For this purpose let us first prove that the product of the energies of two incident particles is independent of the Lorentz frame as far as we can neglect the effect of rest mass. Due to a Lorentz transformation the energy of one particle is multiplied by a factor $\Gamma(1 + v)$, and that of the other by a factor $\Gamma(1 - v)$, where $\Gamma = (1 - v^2)^{-\frac{1}{2}}$ is the Lorentz factor of this transformation. Thus the product of both energies is multiplied by $\Gamma^2(1 - v)(1 + v) = 1$, that is, remains invariant. Consequently the incident energy ε of each particle (hypothetical meson and nucleon) in the hypothetical center of mass system is given by the geometrical mean of the incident energies in any system of reference:

$$\varepsilon^2 = \frac{\eta'}{\eta} M\gamma_c \cdot M\gamma_c ,$$

or

$$\varepsilon = \sqrt{\frac{\eta'}{\eta}}\, M\gamma_c . \tag{A.9}$$

Evidently this implies that the Lorentz factor of the hypothetical c.m.s. with respect to the l.s. is expressed as $\sqrt{\eta'/\eta}\cdot\gamma_c$, which is equal to γ_{ap} in (A.7).

Thus it is seen that, by analyzing the decay product of the fire ball with the assumption of a symmetric collision, we are led to the process of the hypothetical collision with the inelasticity η', and not to the real collision with the inelasticity η (or $((\eta + \eta')/2$ in the c.m.s.).

RIASSUNTO (*)

Si discutono due possibili conseguenze, caratteristiche del modello isobarico e del modello a « fire ball » della produzione multipla dei mesoni. Una è l'asimmetria azimutale delle particelle secondarie, l'altra è l'apparente anomalia dell'anelasticità della collisione mesone-nucleone.

(*) *Traduzione a cura della Redazione.*

IL NUOVO CIMENTO Vol. X, N. 5 1° Dicembre 1958

A Study of 540 τ-Meson Decays (*).

S. McKenna (+)

Physics Department, University College - Dublin

S. Natali

Istituto di Fisica dell'Università - Padova

M. O'Connell

Institute for Advanced Studies - Dublin

J. Tietge

Max-Planck Institut für Physik - Göttingen

N. C. Varshneya (×)

Max-Planck Institut für Physik - Göttingen
Institute for Advanced Studies - Dublin

(ricevuto l'8 Agosto 1958)

Summary. — A homogenous sample of 540 τ-meson decays found in emulsion stacks exposed to the Berkeley Bevatron has been studied. Most of the events have been located by track scanning, and the effects of geometrical and scanning biases have been minimized. The results are discussed in detail and then combined with those of a comparably large sample examined by Baldo-Ceolin *et al.* (2). The most probable spin-parity assignment is 0^- and the deviations of the positive and negative pion energy spectra from those predicted by the relativistic statistical factor, already noted by Baldo-Ceolin *et al.*, have been confirmed and estimated.

(*) A preliminary report on this study was presented at the *Padua-Venice Conference on Mesons and Recently Discovered Particles* (1957).

(+) Now at Dunsink Observatory, Institute for Advanced Studies, Dublin.

(×) Now at the College of Science, Pilani, India.

3725

1. – Introduction.

The energy and angular distributions of the three pions emitted in the decay of the τ-meson have been calculated by several authors [1] under various assumptions of spin and parity of the parent particle and of the angular momentum configuration in the decay. The approximations and assumptions in the derivation of these curves are discussed fully in these references. The experimental results agree best with the curves calculated for the spin-parity assignment (0^-).

BALDO-CEOLIN *et al.* [2] have given a useful bibliography of the earlier work, which we shall refer to as A.

The largest homogeneous sample of τ-meson decays studied hitherto has been that of 419 events reported in A. In this work, attention was drawn to certain apparent discrepancies between the experimental results and the calculated curves.

In the present work a second large homogeneous sample has been studied, with the aim, as far as possible, of avoiding selection bias.

The sample of τ-decay studied was comparable in size with that studied in A. It is a feature of the present experiment however, that almost all the events have been found by track-scanning, or modified track-scanning, in contrast to that of BALDO-CEOLIN *et al.*, in which most of the events were found by area scanning.

Of the events studied in the present work, 87 reported already by N. N. BISWAS *et al.* [3] have been re-examined in the light of the criteria laid down in Sect. **2**·1 and **2**·2.

The selection procedure, measurements and results are described in Sect. **2**·1, **2**·2, and **2**·3 respectively.

In Sect. **3** the results are discussed separately, and combined with the results of the 419 events of A.

---

(1) R. H. DALITZ: *Proc. Phys. Soc.*, **66**, 710 (1953); *Phil. Mag.*, **44**, 1068 (1953); *Phys. Rev.*, **94**, 1046 (1954); **99**, 915 (1955); *Proc. Phys. Soc.*, **69**, 527 (1956); E. FABRI: *Nuovo Cimento*, **11**, 479 (1954); *Suppl. Nuovo Cimento*, **12**, 205 (1954); G. COSTA and L. TAFFARA: *Nuovo Cimento*, **3**, 169, (1956). Y. EISENBERG, E. LOMON and S. ROSENDORFF: *Nuovo Cimento*, **4**, 610 (1956); I. S. SHAPIRO, E. I. DOLINSKY and A. P. MISHAKOVA: *Nucl. Phys.*, **3**, 60 (1957).

(2) M. BALDO-CEOLIN, A. BONETTI, W. D. B. GREENING, S. LIMENTANI, M. MERLIN and G. VANDERHAEGHE: *Nuovo Cimento*, **6**, 84 (1957).

(3) N. N. BISWAS, L. CECCARELLI-FABBRICHESI, M. CECCARELLI, K. GOTTSTEIN, N. C. VARSHNEYA and P. WALOSCHEK: *Nuovo Cimento*, **3**, 825 (1956).

2. – Experimental procedure and results.

2·1. *Method of scanning.* – All the events were found in 3 stacks of G5 nuclear emulsion strips 600 μm thick exposed to K^+-meson beams at the Bevatron, the K_1^- stack, the K_2^- stack of the European Collaboration, and a third smaller stack exposed on behalf of W. F. FRY.

289 events were found by track scanning in the course of experiments on the interactions of K^+ particles ([4]), 221 events by modified track scanning as described in ([5]), and 30 events by area scanning.

Due attention has been paid to minimizing the effects of bias discussed in detail in Sect. 2·1 of A, and the geometrical criteria proposed by BRENE *et al.* ([6]) have been strictly satisfied.

A decay configuration wicht might escape observation is that in which the negative π-meson is emitted in the direction of the primary τ-meson with low energy ~ 1 or 2 MeV, and results in a zero prong capture star.

In such a case, the change in grain density at the point of decay is liable to elude detection and the tracks of the 2 positive π-mesons, being fast and almost collinear, might be mistaken for a single crossing track.

An approximate calculation predicts an expectation of one such event in the present sample.

2·2. *Acceptance criteria and analysis of events.* – Only those τ-meson decay events were selected for study of which the origins lay at distances greater than 8 mm from the borders of the stacks. In this case, as shown by BRENE *et al.* ([6]), at least two secondary pions should be brought to rest within the stack, making it possible to deduce unambiguously the signs of the charge of the three decay products. 39 events failed to satisfy this criterion and were excluded. For 499 events, the angles included between the directions of the emitted secondary particles were measured, and such further observations were made that the sign of the charge could be deduced for each of the three π-mesons. A stereographic projection chart was used in the usual manner to reduce the projected angle and dip measurements to space angles. By use

---

([4]) N. N. BISWAS, L. CECCARELLI-FABBRICHESI, M. CECCARELLI, K. GOTTSTEIN, N. C. VARSHNEYA and P. WALOSCHEK: *Nuovo Cimento*, **5**, 123 (1957); M. BALDO-CEOLIN, M. CRESTI, N. DALLAPORTA, M. GRILLI, L. GUERRIERO, M. MERLIN, G. A. SALANDIN and G. ZAGO: *Nuovo Cimento*, **5**, 402 (1957); B. BHOWMIK, D. EVANS, S. NILSSON, D. J. PROWSE, F. ANDERSON, D. KEEFE, A. KERNAN and J. LOSTY: *Nuovo Cimento*, **6**, 440 (1957).

([5]) G. ALEXANDER, R. H. W. JOHNSTON and C. O'CEALLAIGH: *Nuovo Cimento*, **6**, 478 (1957).

([6]) N. BRENE, K. H. HANSEN, J. E. HOOPER and M. SCHARFF: *Nuovo Cimento*, **4**, 1059 (1956).

of the chart, the coplanarity of the three outgoing π-mesons was checked for each acceptable event. In no case, could a departure from coplanarity be established which was significant, taking into account the uncertainty (typically $\sim 1°$) in the individual measurements of the space angles. Range measurements were made on the secondary particles from 318 τ-decays. In 258 events, the energy of the π^--meson was found by direct range measurement, and in 60 of these, the range of one of the π^+-mesons was also measured. The energies of the two π^+-mesons were found by range measurement for 60 events.

For clarity this information is summarized in Table I.

TABLE I.

No. of events	π^-	π^+	π^+	Angles
1	Range	Range	Range	yes
60	No Range	Range	Range	yes
60	Range	Range	No Range	yes
197	Range	No Range	No Range	yes
181	No Range	No Range	No Range	yes
499	Fully analysed			
39	Excluded for reasons of geometry			
2	Could not be fully analysed, see text			
540	Total			

Apart from the 499 events fully analysed, 2 additional events were investigated which satisfied the selection criteria, but for which the energy of the π^- particle could not be determined. In each of these events, one particle escaped from the stack and one particle was positively charged. In one event the third particle interacted, and in the other came to rest between pellicles. See Appendix II for a partial analysis of these events. The ranges were carefully measured and the uncertainties in the measurement of length were estimated to lead to an uncertainty of $\sim 0.7\,\%$ in energy. This was neglected in comparison with the error in the energy estimate due to straggling ($\Delta E/E \sim 2\,\%$). When it was found impossible, or experimentally inconvenient, to measure directly the momentum of the π^--meson, owing to particles crossing cut edges or going into parts of the stacks not to hand, the ranges of the two positively charged secondaries were measured. Their energies having been deduced, the energy of the π^--meson was derived either by subtraction from the Q-value of the τ-meson decay 74.9 MeV, or by closing the momentum triangle. In 181 events the energies of the secondary particles were obtained from the

momentum triangle defined by the space angles at decay, normalizing the energies to the Q-value.

As a check, the energies of the 258 π^--mesons whose ranges were directly measured were also computed from the angles in this way. These energy estimates were in good agreement with those obtained from the range.

The range energy curves published by BARKAS *et al*, (7) were used in all cases to deduce the energies of the mesons from their ranges. No decay in flight of a τ-meson was observed.

2·3. *Experimental results.* – Fig. 1 shows the observed energy distributions of the negative and positive π-meson secondary to the 499 τ-meson decays,

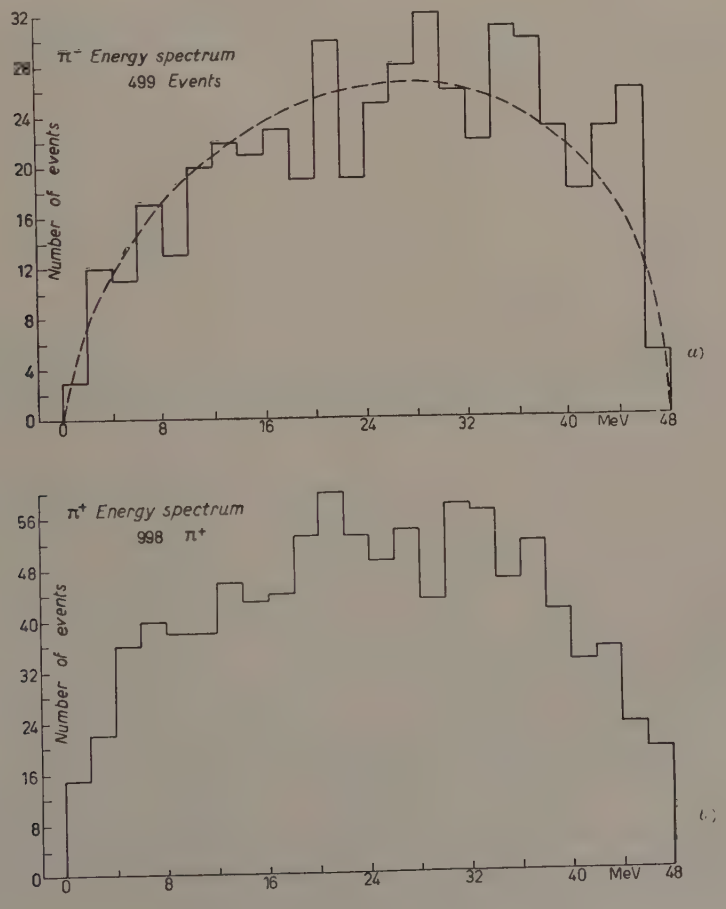

Fig. 1.

(7) W. H. BARKAS: U.C.R.L. Reports no. 3768, 3769.

plotted in class intervals of 2 MeV. Uncertainties in the energy estimates are greater for the higher than for the lower regions of the spectra since, in most cases, these energies were not estimated directly from the range of a single track, but depended rather on measurements of angles, or upon the measured ranges of two tracks of lower energy. Similarly, a large error is associated with the calculated energy of a secondary particle which is emitted opposite a small angle. The uncertainties introduced in this energy region exceed those due to straggling, namely $\pm$ 1.0 MeV at 48 MeV.

Table I shows the uncertainties set out as a function of energy for the energies of the negative pions of the present sample.

TABLE II.

Energy interval (MeV)	0÷4	4÷8	8÷12	12÷16	16÷20	20÷24	24÷28	28÷32	32÷36	36÷40	40÷44	44÷48
Error	10%	6%	4%	3%	3%	3%	3%	3%	2%	2%	3%	5%

3. – Discussion.

3·1. *Energy distribution.* – The energy and angular distributions have been calculated by DALITZ and FABRI. They are based on the assumption of an interaction radius roughly equal to the Compton wavelength of the τ-meson and an interaction independent of the orbital momentum quantum numbers l, l' (defined in reference (1)).

Coulomb effects and pion pion interactions in the final state are not considered.

Then, neglecting the possible influence of unknown partial or complete selection rules, the lowest order term in the expansion in terms of angular momentum eigenstates is by far the most important. The effects of this term on the energy distribution of the τ-meson decay are displayed by these authors for the spin and parity combinations 0^- 1^+ 1^- 2^+ 3^-. In Fig. 2 the experimental energy distribution for the negative pion is compared with the theoretical curves in the non-relativistic approximation. Also shown in Fig. 2 is the relativistic curve for the 0^- configuration. Energy distributions calculated in this way show a maximum sensitivity to the value of the spin in the extreme parts of the spectrum, since in these regions they are less dependent on the simplifying assumptions made.

Because of conservation of angular momentum the low energy negative pions must have a momentum dependence p^n where $n \geqslant 2$ for τ-mesons of odd spin and n can be zero for a τ-meson of even spin. Using the world data

available at the time, OREAR ([8]) showed that the results were consistent with $n = 0$ and strongly inconsistent with $n = 2$. This was done by calculating

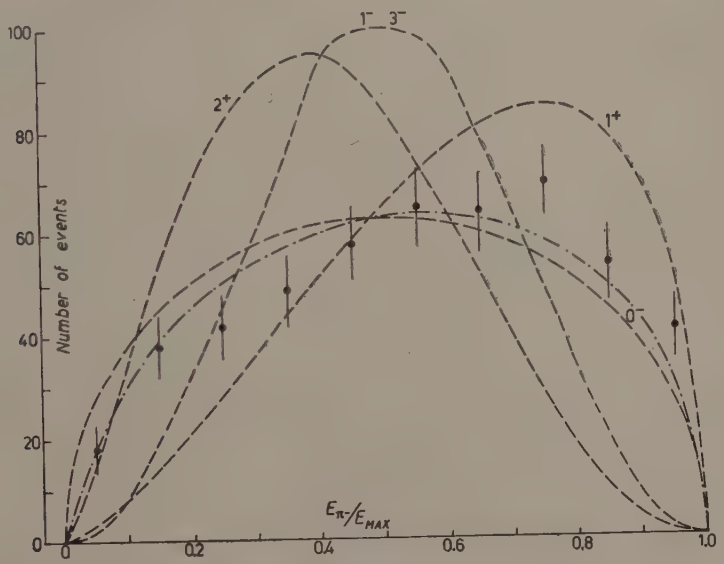

Fig. 2.

the probability that the low energy events occurred as they did, assuming 1^+ to be the true spin-parity, divided by the probability that they occurred as they did, assuming 0^- to be the true spin-parity assignment.

In the present work, the energy of the negative pion was found to be less than 10 MeV in 56 cases. The probability of spin zero to spin one was found to be 10^4. We can infer that it is extremely unlikely that the τ-meson has spin 1 or any odd value. It does not seem possible to exclude spin 2 for the τ-meson by means of a Dalitz type analysis alone.

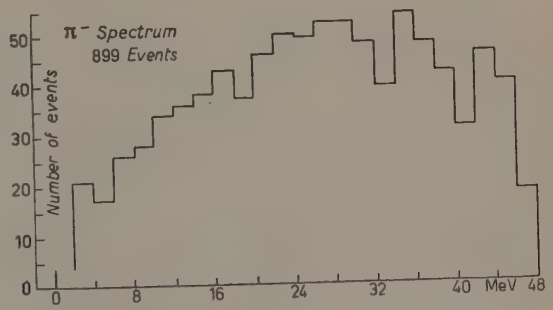

Fig. 3.

It has been found that the energy spectra of the negative and positive

([8]) J. OREAR: *Phys. Rev.*, **106**, 834 (1957).

π-mesons are not identical and show departures from that calculated from the variation with energy of the relativistically computed statistical factor. This effect has been observed also by BALDO-CEOLIN *et al.*, with their sample of 400 decays. Since the present work was performed with criteria similar to theirs, the results of the two large samples thus collected have been combined. The combined results of the 899 τ-meson decays are displayed in Fig. 3 (π^- spectrum) and fig. 4, (π^+ spectrum). In Table III, are given the coefficients of asymmetry and excess (γ_1 and γ_2 respectively) relative to the mean of the statistical factor for the spectra of Figs. 3 and 4, and for the statistical factor.

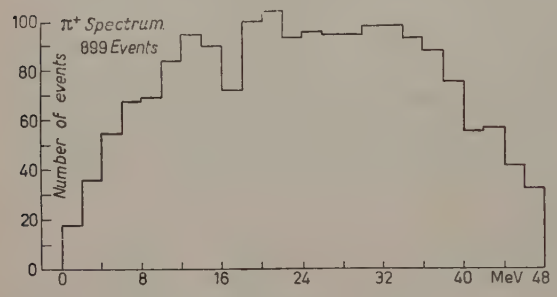

Fig. 4.

TABLE III.

Spectra of 499 Events			
	π^+	π^-	Theoretical
μ_2	145	148	144.34
μ_3	71.3	625	+ 118.94
μ_4	42588	42681	41850
γ_1	0.0407	— .3471	— 0.0686 ± 0.3137 (*)
γ_2	— 1.0044	— 1.0546	— 0.9913 ± 0.1058 (*)
Spectra of 899 Events			
	π^+	π^-	Theoretical
μ_2	139.36	144.50	144.34
μ_3	— 73.88	534.23	— 118.94
μ_4	39 210	41 755	41 850
γ_1	0.0449	— 0.3075	— 0.0686 ± 0.3137 (*)
γ_2	— 0.9815	— 1.0004	— 0.9913 ± 0.1058 (*)

μ_2 = moment of order 2 with respect to the theoretical mean, for the statistical distribution;
μ_3 = moment of order 3 etc.;
μ_4 = moment of order 4 etc.;
γ_1 = coefficient of skewness;
γ_2 = coefficient of excess.

(*) The errors given in column 4 have been calculated on the assumption that the individual pion energies have an error of 1 MeV.

The table shows that the experimental distributions depart somewhat from that predicted by the relativistic statistical factor (r.s.f.). For the spectrum of the negative pions, the departure is towards the higher energies, and for the positive pions, is towards the lower energies. These tendencies can be more easily appreciated in Figs. 5 and 6 where in each diagram the r.s.f. is

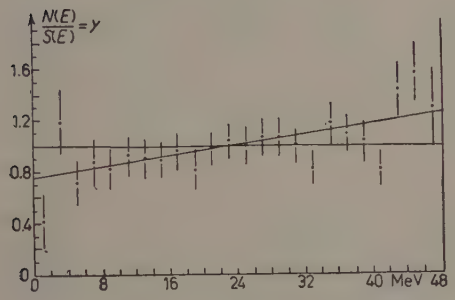

Fig. 5.

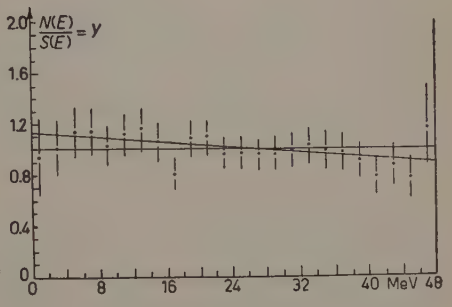

Fig. 6.

denoted by a horizontal straight line. Each ordinate is the ratio of the number of secondaries found experimentally with energies in a particular energy interval to the expected number of secondaries deduced from the same energy interval of the r.s.f.

To the sets of ordinates thus obtained, the following straight lines were fitted, using the method of least squares

$$Y(\pi^-) = (\quad 0.0105 \quad \pm 0.00164\ )X + (0.7578 \pm 0.0474)\,,$$

$$Y(\pi^+) = (-0.00507 \pm 0.000615)X + (1.1351 \pm 0.0165)\,.$$

The errors shown are the mean quadratic errors to be feared. It has been suggested by MITRA (9) that similar asymmetries in the energy spectra may be due to resonant pion-pion interactions, thus bringing about a certain momentum dependence in the various transition amplitudes. However, as pointed out by DALITZ (10) very little is known about the strength of π-π forces.

It is also possible that the discrepancy could be accounted for in terms of a difference between the non-relativistic and relativistic matrix elements, and that in extending the calculation to the relativistic case it is not a sufficiently good approximation to change only the statistical factor.

---

(9) A. N. MITRA: *Nucl. Phys.*, **6**, 404 (1958).
(10) R. H. DALITZ: *Rep. Progr. Phys.*, **20**, 163 (1957).

4. – Conclusions.

A homogeneous sample of 540 τ-decays has been studied under the strictest conditions of scanning and with every safeguard against appreciable bias. A comparison of the results with the curves calculated by several authors shows that the τ-meson decays in a state of zero spin and odd parity. The sample has been combined with the events of BALDO-CEOLIN *et al.* and the slight departure from symmetry in the distribution of the decay energy among the three pions already noted by these authors has been confirmed.

* * *

The authors wish to thank Professor M. MERLIN for his active interest in the work and Professor C. O'CEALLAIGH and Dr. D. KEEFE for useful discussions. Our best thanks are due to Dr. A. KERNAN (Dublin U.C.) for supplying 56 partially analysed events and Dr. M. CECCARELLI for valuable suggestions.

N.C.V. wishes to thank Professor C. O'CEALLAIGH and the staff of the Dublin Institute for Advanced Studies for their hospitality, also the D.I.A.S. and the Alexander von Humboldt Stiftung for maintenance grants at Dublin and Göttingen respectively. M.O'C. wishes to thank the Board of the School of Cosmic Physics, D.I.A.S. for a Scholarship. Miss R. RYAN drew the diagrams and Miss C. INIGHT prepared the typescript. Our best thanks are due to both.

APPENDIX I

The following is a list of the energies of the negative pions from the 499 τ-meson decays used in this analysis. Those which have been derived from angular measurements are marked with a cross (+); those from the energies of the two positive pions with an asterisk (*); the remaining pions were traced to rest, and their energies deduced from the measured range.

TABLE IV.

1.3	3.51+	5.19+	7.08	7.8*	9.3	10.45+	11.09+	12.62	13.21+
1.57+	3.61+	5.2	7.1	7.99	9.3	10.50	11.38	12.75+	13.4
1.7	3.72+	5.49	7.1	8.3	9.33+	10.60+	11.75	12.76+	13.6
2.0	3.8	5.65	7.11+	8.4	9.5	10.7	11.8	12.85	13.7
2.05+	3.82	5.8	7.16	8.6	9.8	10.8	11.8	12.90	13.7
2.4	4.00+	5.86+	7.19+	8.7	10.05	10.95	12.04+	12.9	13.89+
2.6	4.13	6.25	7.3	8.9	10.2	11.0	12.10+	12.9	13.99
2.85	4.14+	6.32	7.4	8.9	10.20+	11.0	12.13+	12.99+	14.28+
3.40	4.9	6.75	7.45	8.99+	10.3	11.00+	12.4	13.0	14.30
3.42	5.03+	6.84+	7.7	9.2	10.38+	11.03+	12.6	13.04+	14.41+

TABLE IV (*continued*).

14.53+	15.4	16.2	16.85+	17.93+	18.77	20.0	20.70+	21.5	22.01*
14.60	15.45+	16.2	16.9	18.0	18.90+	20.0	20.77+	21.5	22.1
14.86+	15.68+	16.24+	17.0	18.1	18.98+	20.22	20.8	21.55+	22.13+
14.87	15.78+	16.3	17.1	18.2	19.2	20.28+	21.06*	21.56+	22.32+
15.0	15.8	16.38+	17.13+	18.2	19.2	20.3	21.08+	21.6	22.5
15.02+	15.9	16.46+	17.2	18.2*	19.7*	20.3	21.2	21.6	22.60+
15.1	15.9*	16.6	17.6	18.27+	19.7	20.41+	21.3	21.6	22.63
15.13+	15.9	16.7	17.64+	18.3	19.8	20.5	21.34+	21.8	22.77+
15.2	16.13+	16.76+	17.8	18.52	19.91+	20.5	21.44+	21.94+	23.0
15.4	16.2	16.80	17.80+	18.56	19.92+	20.6	21.5	21.99	23.07+
23.1	24.09	24.68+	25.58+	26.58+	27.1	27.9	28.43+	29.00+	29.80+
23.35	24.10	24.75+	25.92+	26.74+	27.2	27.9	28.44+	29.08+	29.81+
23.44+	24.3	24.8	25.95+	26.75+	27.4	28.05	28.5	29.14+	29.85*
23.50	24.33+	24.9	25.99+	26.8	27.50+	28.07+	28.5	29.29+	29.92+
23.50	24.42+	25.0*	26.0	26.89+	27.5	28.10+	28.54+	29.3	30.02+
23.53+	24.46+	25.0	26.18+	26.9	27.5	28.11+	28.66+	29.5	30.05
23.6	24.46	25.2	26.30	26.9	27.59+	28.16+	28.70	29.5	30.24+
23.7	24.48+	25.41+	26.4	27.0	27.69	28.18+	28.75+	29.5*	30.37+
23.8	24.50	25.5	26.5	27.0	27.7	28.3	28.8	29.52+	30.5
24.0	24.5	25.5	26.5	27.05	27.8	28.4	29.0*	29.6	30.5
30.76+	31.5	32.03+	33.15+	33.99+	34.43*	35.26+	35.8	36.49+	37.0*
30.79+	31.5*	32.04+	33.2*	33.99	34.5	35.30	35.8	36.5	37.0
30.8	31.58*	32.2	33.3	34.04	34.5	35.3	35.84+	36.5	37.01
30.8*	31.64+	32.39+	33.35+	34.1	34.6	35.33+	36.0	36.5*	37.3
31.0	31.66+	32.4	33.5	34.17+	34.68*	35.4	36.01+	36.5*	37.4
31.0	31.67+	32.8	33.5	34.19	34.87+	35.4	36.1	36.6	37.5
31.04+	31.76+	33.0	33.5	34.19*	35.0	35.41*	36.10+	36.6	37.5*
31.36+	31.77+	33.00+	33.77*	34.21+	35.0	35.5	36.23+	36.74+	37.5
31.4	31.8	33.02+	33.8	34.32+	35.16+	35.75	36.4	36.98+	37.67+
31.5	31.88	33.13*	33.9	34.4	35.21+	35.76+	36.45*	37.0	37.74+
37.76+	38.90+	39.7	40.62*	41.6*	42.5*	43.56+	44.08*	44.70*	45.50+
37.9*	38.94*	39.70	40.69*	41.70+	42.5*	43.58+	44.09*	44.87+	45.73+
37.94	39.0*	39.79+	41.0	41.83+	42.5*	43.62+	44.13+	44.9*	45.8
38.29+	39.0	39.81*	41.0	41.9	42.5	43.75	44.2*	45.0*	46.1
38.4	39.0*	39.95+	41.0	42.2	42.54+	43.81*	44.2*	45.02*	46.2*
38.41+	39.02+	39.99	41.2	42.2*	42.7	43.84+	44.34+	45.05*	46.51+
38.5	39.09+	40.2	41.33+	42.3	43.04+	43.9*	44.5*	45.06+	47.0*
38.5	39.18+	40.46+	41.34+	42.4*	43.20	44.0*	44.57*	45.30+	47.0
38.59+	39.25	40.5*	41.5	42.5	43.4	44.01	44.59+	45.39+	—
38.6	39.5*	40.82+	41.58+	42.5*	43.5	44.06+	44.62+	45.5*	7.79

Appendix II

In the first event which cannot be fully analysed, one π^+ has an energy 15.4 MeV; another pion whose charge is unknown because its track ends between pellicles, has an energy 36.1 MeV; the third pion interacts. The energy of the negative pion is either 23.4 MeV or 36.1 MeV.

One π^+ from the second τ-decay has an energy 3.1 MeV and one pion interacts. 22.00 mm of the third track can be seen before it leaves the available pellicles and the residual range indicated by ionization measurements is 0.54 mm. Hence the energy of the negative pion is either 37.6 MeV or 34.2 MeV.

RIASSUNTO (*)

Si è studiato un campione omogeneo di 540 decadimenti τ trovati in pacchi di emulsioni esposti al bevatrone di Berkeley. La maggior parte degli eventi è stata individuata osservando lungo la traccia e si sono resi minimi gli effetti dovuti a fattori geometrici e d'osservazione. Si discutono i risultati in dettaglio e si combinano poi con quelli forniti da un campione di volume comparabilmente grande studiato da Baldo-Ceolin *et al.* (2). La più probabile assegnazione di spin-parità è 0^- e abbiamo potuto confermare e valutare le deviazioni degli spettri dell'energia positiva e negativa dei pioni dai valori predetti dal fattore statistico relativistico, già osservate da Baldo-Ceolin *et al.*

(*) *Traduzione a cura della Redazione.*

IL NUOVO CIMENTO Vol. X, N. 5 1° Dicembre 1958

Conversion Coefficient of the 87 keV Transition in ^{160}Dy.

M. C. Joshi, B. N. Subba Rao and B. V. Thosar

Tata Institute of Fundamental Research, Bombay

(ricevuto il 18 Agosto 1958)

Summary. — The K-conversion coefficient of the 87 keV, $E2$ transition in ^{160}Dy has been determined from the photoelectron spectrum and the internal conversion spectrum of ^{160}Tb investigated with the intermediate image β-ray spectrometer. α^K is found to be 2.0 ± 0.2 which is large compared with the theoretical value.

1. – Introduction.

The decay of ^{160}Tb ($T_{\frac{1}{2}} = 73$ d) has been studied by many workers ([1-6]) and there is good agreement regarding the low-lying excited states in ^{160}Dy. From these studies, it is well established that the first excited state is at 87 keV and that, in accordance with the systematics of even-even nuclei, this level has $2+$ assignment for its spin and parity. So, the 87 keV transition ($2+ \rightarrow 0+$) should be purely $E2$.

There is no accurate determination of α^K reported so far for this 87 keV transition and there seems to be disagreement among the values given by previous workers. Recently, McGowan *et al.* ([7]) found that experimental

([1]) S. B. Burson *et al.*; *Phys. Rev.*, **94**, 103, (1954).
([2]) V. Keshishian *et al.*: *Phys. Rev.*, **96**, 1050 (1954).
([3]) G. Bertolini, M. Bettoni and E. Lazzarini: *Nuovo Cimento*, **3**, 754, 1162 (1956).
([4]) M. A. Clark *et al.*: *BAPS*. II, **4**, 231 (1957).
([5]) O. Nathan: *Nucl. Phys.*, **4**, 125 (1957).
([6]) S. Offer: *Nucl. Phys.*, **5**, 331 (1957).
([7]) F. K. McGowan and P. H. Stelson: *Phys. Rev.*, **107**, 1674 (1957).

values of α^K for a few pure $E2$ transitions were consistently higher than the corresponding theoretical values. So, it was felt necessary to determine the conversion coefficient of this transition as accurately as possible.

2. – Experimental methods.

The ^{160}Tb source was obtained by neutron irradiation in the Harwell pile. A small amount of the powder was used as source. The diameter of the source was 0.4 cm. Sufficient amount of perspex was used to absorb primary electrons from the source. Tin, deposited by vacuum evaporation on a perspex disc was used as converter for obtaining the photoelectron spectrum. The diameter of the converter was about 2 cm and the source-converter distance was about 0.4 cm. Thickness of the converter was about 0.3 mg/cm².

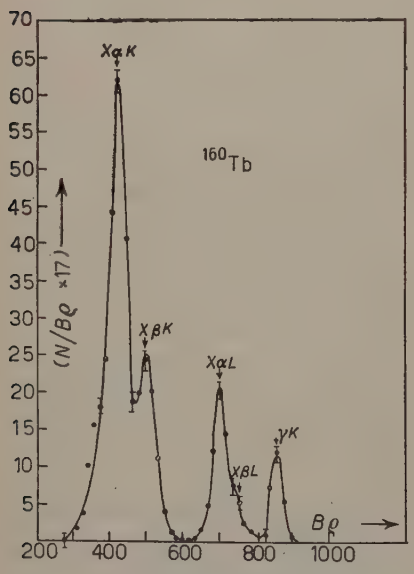

Fig. 1. - The photoelectron spectrum of γ-rays emitted in the decay of ^{160}Tb using tin as radiator (low energy part).

The photoelectron spectrum obtained with such an arrangement in the intermediate-image β-ray spectrometer is shown in Fig. 1. K- and L-photo-electron line (x_{α_K}, x_{β_K} and x_{α_L}, x_{β_L}) of K_x- and K_β-X-rays of Dysprosium and the K-photoline (γ_K) of the 87 keV γ-ray are seen in it. Background was determined in another run under identical conditions but without the converter.

The internal conversion spectrum of the low-energy portion, also observed in the intermediate image β-ray spectrometer using a thin source, is shown in Fig. 2. The most prominent lines were the K and $(L+M)$ conversion lines of the 87 keV transition, represented by K_1 and (L_1+M_1) in the figure. K_2 and (L_2+M_2) represent the conversion lines of the 197 keV transition. The latter are shown on a larger scale in the inset. Other conversion lines could not be clearly brought out indicating thereby that they are very weak compared even with K_2.

The area under the photoelectron peak may be represented ([8]) by

$$P = k \cdot I\tau tC\,, \tag{1}$$

([8]) A. C. G. Mitchell: *Beta- and Gamma-ray Spectroscopy* (1955), p. 229.

where I is the intensity of the incident electromagnetic radiation, τ is its photoelectric absorption coefficient, t is the thickness of the converter, C is a factor

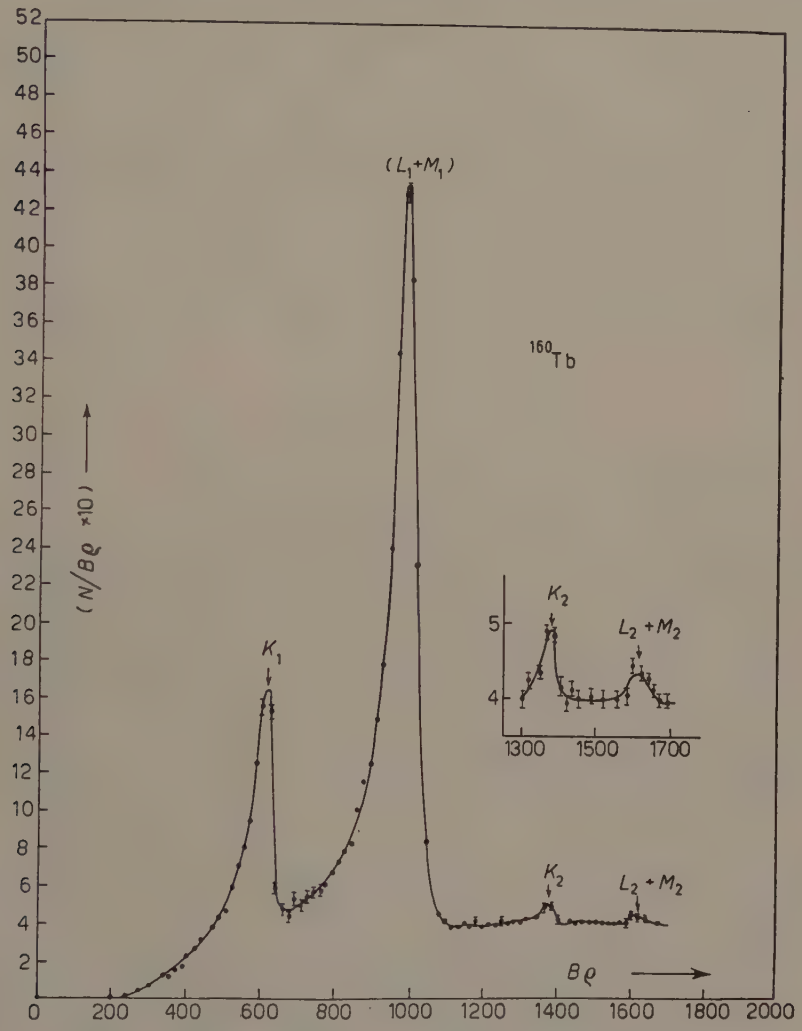

Fig. 2. - Internal conversion electron spectrum (^{160}Tb).

representing the effect of angular distribution of photoelectrons with respect to the incident photon momentum and k is a constant which depends on the transmission of the spectrometer and geometry of the source-converter assembly. Then the ratio of the areas under the photoelectron peaks due to X-ray and γ-ray may be written,

$$\frac{P_X}{P_\gamma} = \frac{I_X}{I_\gamma}\frac{\tau_X}{\tau_\gamma}\frac{C_X}{C_\gamma}. \tag{2}$$

From this one can determine I_X/I_γ, using theoretical values for τ_X and τ_γ. provided C_X/C_γ is known. The energy of X-rays of Dysprosium is about 50 keV and the energy of the γ-ray is 87 keV. The corresponding separation of the maxima of intensity distributions of photoelectrons with angle is expected theoretically to be about 10°. Further, such an angular distribution for low photoenergy is a fairly slowly varying function ([9]) of ϑ around ϑ_{max}, for a given energy of photoelectrons. The measurement of the K conversion-coefficient ([10]) of the 144 keV transition in $^{141}Pr_{59}$, by two independent methods, one based on β-spectrum and conversion line intensities and the other one being the same as the one adopted here, led to the same value within experimental errors though the separation between the maxima was about 20°. These considerations indicate that, for the experimental arrangement used here, $C_X/C_\gamma \approx 1$.

3. – Results and discussion.

By adopting the procedure described above, $I_X/I_\gamma\omega_K$ was found to be (2.2 ± 0.2), where ω_K is the K-fluorescence yield ([12]) of Dysprosium ($\omega_K = 0.93$) But the X-ray intensity determined above is not due to the internal conversion of 87 keV transition alone. In order to account for this, the K-conversion line intensity of this transition relative to the total of all K-conversion line intensities occuring in the β^--decay of ^{160}Tb was used. From our observations of internal conversion spectrum, it was found that $K_1/(K_1+K_2) = 0.94$. Using the conversion data of O. NATHAN ([5]), M. A. CLARK *et al.* ([4]) and M. P. AVOTINA *et al.* ([13]) also K_1/K was found to be 0.91 ± 0.03. Thus, the right value of $I_\gamma/I_X\omega_K = \alpha^K = 2.0 \pm 0.2$.

The theoretical value due to ROSE ([14]), based on the « no penetration » model which takes into account all static effects, for the K-conversion coefficient of the 87 keV $E2$ transition in Dysprosium is $\alpha_2^K = 1.53$. The experimental value is clearly larger than this. This gives for the ratio $\alpha^K_{exp}/\alpha^K_{theor} = 1.29 \pm 0.13$. MCGOWAN *et al.* ([7]) in their study of the K-conversion coefficient of $E2$ transitions —the 80 keV transition in ^{166}Er, the 84 keV transition in ^{170}Yb and the 89 keV transition in ^{176}Hf—find this ratio to range from 1.13 to 1.23. We also find

---

([9]) C. M. DAVISSON and R. D. EVANS: *Rev. Mod. Phys.*, **24**, 79 (1952).
([10]) M. C. JOSHI, B. N. SUBBA RAO and B. V. THOSAR: *Nuovo Cimento*, **9**, 600 (1958).
([11]) C. M. DAVISSON: *Beta- and Gamma-ray Spectroscopy* (1955) p. 836.
([12]) I. BERGSTROM: *Beta- and Gamma-ray Spectroscopy* (1955) p. 630.
([13]) M. P. AVOTINA *et al.*: *Doklady. Akad. Nauk. SSRR*, **119**, 1127 (1958).
([14]) M. E. ROSE: Privately circulated tables.

the K-conversion coefficient of the 84 keV $E2$ transition in ^{170}Yb, determined by the method described in this work, to be nearly the same as that reported by McGowan *et al.* (7). These determinations indicate that experimental α_2^K are larger than the corresponding theoretical values by about 20%.

* * *

Our thanks are due to Mr. C. V. Panat and Mr. S. D. Bhagwat for their assistance during this work.

RIASSUNTO (*)

Il coefficiente di conversione K della transizione $E2$ di 87 keV del ^{160}Dy è stato determinato dallo spettro dei fotoelettroni e lo spettro di conversione interna del ^{160}Tb è stato studiato con lo spettrometro β a immagine intermedia. Si trova che α^K è 2.0 ± 0.2, valore alto rispetto al valore teorico.

(*) *Traduzione a cura della Redazione.*

IL NUOVO CIMENTO Vol. X, N. 5 1° Dicembre 1958

The Effect of the Final State Interaction on the Decay of Hyper-^{5}He (*).

Y. C. Tang (+)

University of Illinois - Urbana, Ill.

(ricevuto il 18 Agosto 1958)

Summary. — The effect of the final state interaction on the decay of hyper-^{5}He has been studied. It is found that the strong interaction between the α-particle and the proton produced in this decay plays a significant role in determining the energy spectra and the angular distributions of the final particles. With the α-p force taken into account as determined by the experimental phase shifts, a simplified calculation indicates that the pion is emitted in the energy range from about 21 to 30 MeV for approximately 90% of the events, and that the proton is scattered predominantly in the backward direction in the α-p center of mass system. These findings are in fair agreement with Hill's analysis of recent experimental observations on the decay of hyper-^{5}He.

1. – Introduction.

A recent study by Hill (1) has shown that the decay patterns are quite similar for all of the known cases of « uniquely defined » decays of hyper-^{5}He. The energy of the pion produced in this decay shows a strong tendency to lie within the range approximately from 21 to 29 MeV, and for eight of the nine cases studied, the proton is projected in a backward direction in the center of mass of the α-p system. In view of these observed regularities, Hill therefore suggested that the strong interaction between the α-particle and the proton must play a significant role in the decay of this hyper-nucleus.

If the interactions among the final particles ^{4}He, p and π^- produced in this decay are completely neglected, then the energy spectra and the angular distributions of those particles can be readily calculated. However, the results so obtained are quite inconsistent with the experimental observations. Instead

(*) Assisted by a joint program of the U. S. Atomic Energy Commission and the U. S. Office of Naval Research.

(+) Now at the Florida State University, Tallahassee, Florida.

(1) R. D. Hill: *Nuovo Cimento*, **8**, 459 (1958).

of a prominent backward scattering asymmetry, the theoretical calculation indicates that the proton should rather be scattered in a forward direction in the center of mass of the α-p system. In addition, the energy spectrum of the pion obtained in this manner does not show any distinct preference for the region above 21 MeV. These discrepancies, therefore, necessitate the consideration of the final state interactions in the decay process.

According to the theoretical study of WATSON ([2]), three conditions would have to be met if the final state interaction is to seriously modify the characteristics of a reaction. These conditions are *a*) that the primary reaction must be confined to a certain volume V of order a^3, where a is the range of the primary interaction, *b*) that the relative energies of the particles whose interaction is under consideration must be comparatively low, and *c*) that the final state interaction must be strong and attractive. For the decay of the hyper-^{5}He, the primary reaction, which is the free decay of a Λ^0, takes place in a sphere with a radius of the order of $0.5 \cdot 10^{-13}$ cm. In the α-p system, for which the interaction is most important, the relative energy of interest is around 10 MeV, corresponding to a wave number k of about $6 \cdot 10^{12}$ cm^{-1}. The magnitude of ka is therefore only about 0.3, which is small compared to unity. As for the third condition, it is well known that, although the s-state interaction in the α-p system may be repulsive, the p-state interaction is strongly attractive. Thus, all three conditions are satisfied; consequently, we expect the final state interaction to be significant.

It is fortunate that the influence of the final state interaction is calculable in our case. The α-p force may be inferred from the experimentally determined phase shifts, which have been listed quite extensively for relative energies up to about 20 MeV ([3-6]). The interaction between π^- and α can be neglected, since in the decay of hyper-^{5}He, the energy of the pion never exceeds 33.4 MeV.

2. – Formulation of the problem.

The matrix element U which determines the probability of the decay mode

$$(1) \qquad {}^5\mathrm{He}_\Lambda \to {}^4\mathrm{He} + \mathrm{p} + \pi^- \qquad \text{(1)}$$

may be written as

$$(2) \qquad U = \int \psi_\alpha^* \psi^*(\boldsymbol{r}) \exp\left[-i\boldsymbol{K}\cdot\left[\boldsymbol{r}_1 - \frac{1}{5}(\boldsymbol{r}_1 + 4\boldsymbol{r}_\alpha)\right]\right]\left(s + p\,\frac{\boldsymbol{\sigma}\cdot\boldsymbol{K}}{K_\Lambda}\right)\psi_i \,\mathrm{d}\tau\,, \qquad \text{(2)}$$

([2]) K. M. WATSON: *Phys. Rev.*, **88**, 1163 (1952).
([3]) C. L. CRITCHFIELD and D. C. DODDER: *Phys. Rev.*, **76**, 602 (1949).
([4]) D. C. DODDER and J. L. GAMMEL: *Phys. Rev.*, **88**, 520 (1952).
([5]) K. W. BROCKMAN: *Phys. Rev.*, **108**, 1000 (1957).
([6]) P. E. HODGSON: *Adv. in Phys.*, **7**, 1 (1958).

where $\boldsymbol{\sigma}$ denotes the baryon spin vector, while s and p denote the amplitudes for the $l_\pi = 0$ and $l_\pi = 1$ channels in free Λ-decay, respectively. The vector $\boldsymbol{r}$ is defined as $(\boldsymbol{r}_1 - \boldsymbol{r}_\alpha)$, where $\boldsymbol{r}_1$ and $\boldsymbol{r}_\alpha$ are the position vectors of the Λ-particle and the α-core. $\hbar\boldsymbol{K}$ is the momentum of the pion in the three-body decay mode of ${}^5\mathrm{He}_\Lambda$, and $\hbar K_\Lambda$ is its value in the free decay of a Λ-particle. Finally, ψ_α, ψ and ψ_i represent the wave functions of the α-core, the α-p system and the hyper-nucleus ${}^5\mathrm{He}_\Lambda$, respectively.

Since the binding energy of the Λ-particle in the hyper-^{5}He is rather low, it is appropriate to assume the wave function to be in the form of a product; that is,

$$\psi_i = \psi_\alpha u_\Lambda(\boldsymbol{r})\chi_i\,, \tag{3}$$

where $u_\Lambda(\boldsymbol{r})$ represents the orbital motion of the Λ-particle relative to the α-core, and χ_i is the spin function.

If we make a further assumption that the α-core is not distorted by the presence of the Λ-particle ([7]), then Eq. (2) may be simplified, yielding

$$U = \int \psi^*(\boldsymbol{r}) \exp[-ib\boldsymbol{K}\cdot\boldsymbol{r}]\left(s + p\,\frac{\boldsymbol{\sigma}\cdot\boldsymbol{K}}{K_\Lambda}\right) u_\Lambda(\boldsymbol{r})\chi_i\,\mathrm{d}\tau\,, \tag{4}$$

with b equal to $\frac{4}{5}$.

For the α-p system, the wave function must be so chosen that it represents a plane wave modified by an ingoing spherical wave ([8]). Taking into account the spin-orbit force, we may therefore write $\psi(\boldsymbol{r})$ as

$$\begin{aligned}\psi(\boldsymbol{r}) = \sum_{l=0}^{\infty} i^l[\pi(2l+1)]^{\frac{1}{2}}\cdot \\ \cdot\{C_{l,\frac{1}{2}}(l+\tfrac{1}{2}, M; 0, M)[h_l^{(1)}(kr) + \exp[-2i\delta_l^+]h_l^{(2)}(kr)]\,\mathcal{Y}^M_{l+\frac{1}{2},l,\frac{1}{2}} + \\ + C_{l,\frac{1}{2}}(l-\tfrac{1}{2}, M; 0, M)[h_l^{(1)}(kr) + \exp[-2i\delta_l^-]h_l^{(2)}(kr)]\,\mathcal{Y}^M_{l-\frac{1}{2},l,\frac{1}{2}}\}\,,\end{aligned} \tag{5}$$

in which C is the Clebsch-Gordan coefficient and h_l is the spherical Hankel function. $\hbar\boldsymbol{k}$ is the relative momentum in the α-p system, $\mathcal{Y}$ is the eigenfunction of the total angular momentum ([9]), and δ_l is the anomalous phase shift which has been determined extensively for various energies ranging up to around 20 MeV ([3-6]). In this work, we shall use only the terms involving

([7]) According to R. H. Dalitz (to be published), the optimum compression of the α-particle core is only about 5% for the hyper-nucleus ^{5}He.

([8]) G. Breit and H. A. Bethe: *Phys. Rev.*, **93**, 888 (1954).

([9]) J. M. Blatt and V. F. Weisskopf: *Theoretical Nuclear Physics* (New York), p. 790.

$l=0$ and $l=1$ in Eq. (5), since in the α-p system, the relative energy of interest does not exceed 20 MeV, at which the values of δ_l for $l \geqslant 2$ are quite small.

For the wave function $\psi(\boldsymbol{r})$ shown in Eq. (5), we have not considered the repulsive Coulomb interaction, since a proper account of it by the modified Coulomb wave function would involve analytical difficulties in the integration procedure that follows. We, therefore, choose to use at this point the plane-wave approximation, keeping in mind that a modification has yet to be made after the integration process is completed.

To find the transition probability of the decay mode (1), it is necessary to take the square of the matrix element U, and then average over the spin states and the outgoing directions of the pion. Using Eqs. (4) and (5), and with due consideration of the volume in phase space, we get for the transition probability per unit pion energy per unit solid angle

$$\frac{\mathrm{d}^2T}{\mathrm{d}E_\pi\,\mathrm{d}\Omega_\tau} = D\left(s^2+p^2\frac{K^2}{K_\Lambda^2}\right)kK\left[2\,|I_1|^2+|I_2|^2+|I_3|^2\right], \tag{6}$$

where D is a constant, and

$$I_j=\int \psi_j^*(\boldsymbol{r})\exp\left[-ib\boldsymbol{K}\cdot\boldsymbol{r}\right]u_\Lambda(\boldsymbol{r})\,\mathrm{d}^3\boldsymbol{r}\,, \tag{7}$$

$$\psi_1(\boldsymbol{r})=\exp\left[i\boldsymbol{k}\boldsymbol{r}\right]-\sum_{l=0}^{\infty} i^{l+1}\left[4\pi/(2l+1)\right]^{\frac{1}{2}}Y_l^0\,h_l^{(2)}\cdot \tag{8}$$

$$\cdot\left[(l+1)\sin\delta_l^+\exp\left[-i\delta_l^+\right]+l\sin\delta_l^-\exp\left[-i\delta_l^-\right]\right],$$

$$\psi_2(\boldsymbol{r})=\sum_{l=0}^{\infty} i^l\left[\pi/(2l+1)\right]^{\frac{1}{2}}\left[l(l+1)\right]^{\frac{1}{2}}Y_l^1\,h_l^{(2)}\left\{\exp\left[-2i\delta_l^+\right]-\exp\left[-2i\delta_l^-\right]\right\}, \tag{9}$$

$$\psi_3(\boldsymbol{r})=\sum_{l=0}^{\infty} i^l\left[\pi/(2l+1)\right]^{\frac{1}{2}}\left[l(l+1)\right]^{\frac{1}{2}}Y_l^{-1}\,h_l^{(2)}\left\{\exp\left[-2i\delta_l^+\right]-\exp\left[-2i\delta_l^-\right]\right\}. \tag{10}$$

The wave function $u_\Lambda(\boldsymbol{r})$ will be obtained by using a variational procedure. Since the Λ-particle is known to be in the s-state, a trial function of the Hulthen form

$$u_\Lambda(\boldsymbol{r})=N\left(\exp\left[-\alpha r\right]-\exp\left[-\beta r\right]\right)/r \tag{11}$$

will be employed, in which α is related to the binding energy of the hyper-^{5}He, and β is the variational parameter. Assuming a K-exchange interaction for the Λ-n force, and using the results of the Stanford experiments ([10]) on the

([10]) R. HOFSTADTER: *Rev. Mod. Phys.*, **28**, 214 (1956).

shape and radius of the α-particle core, the potential seen by the Λ-particle is then

$$V(r) = -V_0 \exp[-(r/R)^2], \tag{12}$$

where R is equal to $1.31 \cdot 10^{-13}$ cm.

Since the binding energy of the Λ-particle in ${}^5\mathrm{He}_\Lambda$ is known, we can obtain by the variational method ([11]) the value $\beta = 3.4\alpha$, which corresponds to V_0 of about 57 MeV. The total volume integral for this particular well depth is then found to be 720 MeV f^3, a value in good agreement with the results of other authors, in particular, that of DALITZ ([12]).

3. – Energy spectra and angular distributions.

The energy spectrum of the pion may be obtained by integrating Eq. (6) over the element of solid angle $\mathrm{d}\Omega_\tau$ in the center of mass of the α-p system. With the use of Eq. (11) for u_Λ, the evaluation of $\mathrm{d}T/\mathrm{d}E_\pi$ is straightforward. As the wave function ψ used in the integrals does not take into account the repulsive Coulomb force between the α-particle and the proton, the spectrum so obtained still needs to be corrected for this interaction. In view of the fact that the Coulomb field accelerates the proton away from the α-particle, we must, therefore, represent its effect in modifying the spectrum of the pion by including the Coulomb correction factor F ([13]), and by observing that in Eq. (5), k is to be replaced by $[k^2 - (2\mu/\hbar^2)V(r_0)]^{\frac{1}{2}}$, in the presence of the Coulomb interaction, where $V(r)$ is the Coulomb potential between the α-particle and the proton, and μ is the reduced mass. As a reasonable estimate, we shall take for r_0 the radius at which the wave function u_Λ has its maximum value; consequently, $V(r_0)$ is found to be approximately equal to 1.7 MeV. However, it is to be emphasized that treating the Coulomb interaction in this way is not very accurate, especially when the relative energy in the α-p system is low. Thus, for energies of the pion exceeding about 31 MeV, the values of $\mathrm{d}T/\mathrm{d}E_\pi$ so obtained may be quite inaccurate, and should be taken only as an indication of the order of magnitude.

The energy spectrum of the pion is shown in Fig. 1. The curve *a*) is for

---

([11]) See, for example, R. G. SACHS: *Nuclear Theory* (Cambridge, Mass.), p. 33.

([12]) R. H. DALITZ: *Proc. of the Sixth Annual Rochester Conference on High-Energy Nuclear Physics* (New York, 1956), Sect. **5**, p. 40.

([13]) For the meaning of the Coulomb correction factor F, see ref. ([9]), p. 680.

the case in which the final state interaction has been taken into consideration, and the curve (*b*) is for the case of no interactions ([14]) among the final particles. Both curves have been plotted with p set equal to zero.

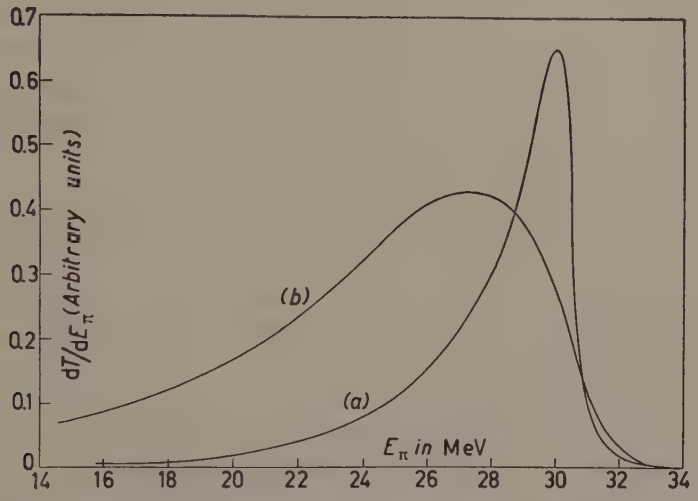

Fig. 1. – The energy spectrum of the pion: (*a*) with final state interaction and (*b*) without final state interaction.

To arrive at the energy spectrum of the pion, the expression (5) for ψ, while valid only in the region outside of the range of the α-p potential, has been used throughout the entire domain of integration. The accuracy of our result is, however, not greatly impaired by this approximation since the contribution to the integrals comes mostly from regions of space larger than that for which the α-p potential is important.

When the Λ-particle lies within the core nucleus, it is likely to decay by the non-mesonic mode, with the consequence that no pion appears among the final particles. To show the effect of this mode on the shape of the pion energy spectrum, we have evaluated I_l of Eq. (7) by integrating from a radius R_0 (taken to be approximately equal to the intrinsic range of the Λ-α potential, *i.e.*, $2 \cdot 10^{-13}$ cm) to infinity; the use of R_0 as a limit of integration comes from the consideration that when the Λ-particle is within the sphere of radius R_0, non-mesonic decay mode will probably dominate. The energy spectrum of the pion calculated in this manner exhibits the same general features as those for the case in which the non-mesonic decay mode is neglected, and hence will not be given any further attention here.

([14]) By no interaction among the final particles, it is meant that we set the anomalous phase shifts δ_l equal to zero.

We shall now determine the angular distribution of the final particles. Let θ be the angle between the direction of emission of the proton in the center of mass of the α-p system and the direction opposite to that of emission of the pion, and let us define

$$(13) \qquad \begin{cases} I_f = \int_0^{\pi/2} \frac{\mathrm{d}^2 T}{\mathrm{d}E_\pi \mathrm{d}\Omega_\tau} \sin\theta \, \mathrm{d}\theta \,, \\ I_b = \int_{\pi/2}^{\pi} \frac{\mathrm{d}^2 T}{\mathrm{d}E_\pi \mathrm{d}\Omega_\tau} \sin\theta \, \mathrm{d}\theta \,, \end{cases}$$

then with the use of Eq. (6), the ratio I_b/I_f can be found quite readily. As is clear from the definitions of I_f and I_b expressed by Eq. (13), the ratio I_b/I_f has the following meaning: for I_b/I_f greater than unity, the angle θ, for a given pion energy, will probably be between 90 and 180 degrees; for I_b/I_f less than unity, θ will likewise lie between 0 and 90 degrees.

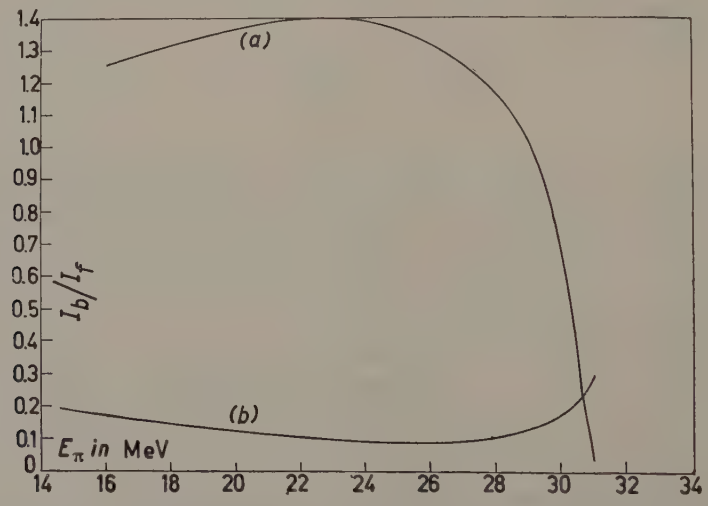

Fig. 2. – The ratio of probabilities for backward to forward scattering of the proton in the center of mass of the α-p system: (*a*) with final state interaction and (*b*) without final state interaction.

The ratio I_b/I_f is plotted against the energy of the pion in Fig. 2, again with the curve (*a*) for the case in which the final state interaction is considered, and the curve (*b*) for the case of no interactions among the final particles.

4. – Discussions and conclusions.

The energy spectrum of the pion as shown by the curve (*a*) of Fig. 1 shows that for approximately 90% of the events, the pion is emitted with an energy in the range from about 21 to 30 MeV. This is in good agreement with Hill's analysis of recent experimental observations, which indicates that in only one of the nine events studied, the pion has an energy less than 21 MeV. On the other hand, the curve (*b*) which is calculated by setting the anomalous phase shifts equal to zero, demands that the pion should be emitted with an energy not exceeding 21 MeV for about 30% of the events, a conclusion not in good accord with the results of the experimental findings.

The distinct peak near 30 MeV in the calculated energy spectrum of the pion indicates that there should be a number of decay events of $^5\mathrm{He}_\Lambda$ recorded with the pion energy in the neighborhood of this value. However, only one event was reported. This discrepancy may therefore be used as a strong argument against the validity of our theoretical calculations. It is to be noted, however, that this disagreement might conceivably come from the fact that it is difficult to observe low energy α-particles in photographic emulsions. For instance, with E_{π^-} equal to 30 MeV, the energy of the α-particle is $[1.48 + 1.47 \cos(180° - \theta)]$ MeV. Since at this pion energy, I_b/I_f is equal to about 0.6, θ is likely to be less than 90 degrees. Therefore, the energy of the α-particle may be quite low; for example, with $\theta = 30°$, the energy is 0.2 MeV, which will leave a track length less than a micron in the emulsion. In fact, some of the helium hyperfragment decays which are now classified as non-uniquely defined cases of $^5\mathrm{He}_\Lambda$, because the recoil He tracks are too short for accurate identification, could be cases of relatively high energy pion emission. It is quite probable that the inclusion of these cases would bring the experimental distribution into better agreement with the calculated curve.

According to the curve (*a*) of Fig. 2, the ratio I_b/I_f has an average value of about 1.35 in the range of pion energy from 21 to 28 MeV. On this basis, the expected number of decay events with θ larger than 90° is then 5.2, which is only slightly more than one standard deviation from the observed number of 8. On the other hand, within the same energy range, the average value on I_b/I_f for the curve (*b*) is only about 0.1, which is in total disagreement with the experimental evidence.

In view of the above discussions, we conclude that the final state interaction must play an important role in determining the energy spectra and the angular distributions of the final particles in the decay of the hyper-^{5}He. When this interaction is considered, the decay characteristics of this hypernucleus can be reasonably well understood. In addition, it is worth noting that the shape of the calculated energy spectrum of the pion may permit the

determination of the ratio p/s of the s- and p-channel amplitudes in free Λ-decay. However, this determination does not appear feasible at present, since the number of $^5He_\Lambda$ decay events reported is still too few to justify such a calculation.

* * *

The author wishes to thank Professor R. D. Hill for suggesting the problem and for helpful discussions. He is indebted to Professor H. W. Wyld for his continued encouragement and guidance. Valuable advice by Professor J. D. Jackson is also gratefully acknowledged.

RIASSUNTO (*)

Si è studiato l'effetto dell'interazione dello stato finale sul decadimento dell'iper-^{5}He. Si trova che l'interazione forte tra la particella α e il protone prodotto in questo decadimento ha una parte importante nella determinazione degli spettri d'energia e delle distribuzioni angolari delle particelle finali. Tenendo conto della forza α-p che si determina in base agli spostamenti di fase sperimentali, un calcolo semplificato indica che il pione è emesso nell'intervallo d'energia da circa 21 a 30 MeV per circa il 90% degli eventi, e che lo scattering del protone avviene prevalentemente in direzione retrograda nel sistema del centro di massa dell'α-p. Questi risultati sono in buon accordo con l'analisi di recenti osservazioni sperimentali sul decadimento dell'hiper-^{5}He fatta da Hill.

(*) *Traduzione a cura della Redazione.*

IL NUOVO CIMENTO Vol. X, N. 5 1° Dicembre 1958

A Note on the Inelastic Contributions to the Elastic Scattering of High-Energy Electrons from Helium (*).

P. O. Davey (+) and H. S. Valk

Department of Physics, University of Oregon - Eugene, Oreg.

(ricevuto il 19 Agosto 1958)

Summary. — An estimate is made of the contribution of non-radiative inelastic processes to the elastic scattering of high-energy electrons from ^{4}He. It is shown that at the presently available energies and scattering angles the dominant process is electrodisintegration, and that this and other effects may be expected to give a correction to the differential elastic scattering cross-section of several percent, the maximum values occurring at high-energies and backward scattering angles.

1. – Introduction.

In view of the continuing experiments (1) on the scattering of high-energy electrons from ^{4}He, it is of interest to extend earlier estimates (2) of the inelastic contributions to elastic scattering from light nuclei to include helium. For this purpose, it is convenient to employ the phenomenological treatment used in I.

(*) A preliminary report of this work was given at the Ithaca, N.Y. meeting of the American Physical Society, H. S. Valk and P. O. Davey: *Bull. Am. Phys. Soc.*, II, **3**, 268 (1958).

(+) Present address: Physics Department, University of Nevada, Las Vegas, Nevada.

(1) G. R. Burelson and R. Hofstadter. We wish to thank Dr. Hofstadter for informing us of the progress of this work.

(2) H. S. Valk: *Nuovo Cimento*, **6**, 173 (1957), referred to as I.

It has been shown in I that the differential elastic scattering cross-section, including inelastic corrections, can be written in first Born approximation as

$$\mathrm{d}\sigma_{\mathrm{el}}/\mathrm{d}\Omega = (\mathrm{d}\sigma_{\mathrm{el}}/\mathrm{d}\Omega)_0(1 + C)\,, \tag{1}$$

where $\mathrm{d}\sigma_{\mathrm{el}}/\mathrm{d}\Omega$ represents the observed cross-section, $(\mathrm{d}\sigma_{\mathrm{el}}/\mathrm{d}\Omega)_0$ is the uncorrected cross-section, and C is the inelastic correction term given by

$$C = \frac{\sigma_{\mathrm{in}}^2(k/4\pi)^2\,|\,g(\boldsymbol{q})\,|^2\cos^2(\vartheta/2)}{\mathrm{d}\sigma_{\mathrm{el}}/\mathrm{d}\Omega - \sigma_{\mathrm{in}}^2(k/4\pi)^2\,|\,g(\boldsymbol{q})\,|^2\cos^2(\vartheta/2)}\,. \tag{2}$$

Here, σ_{in} is the total non-radiative inelastic cross-section (which for incoherent processes is the sum of the individual cross-sections for these processes), k is the electron reduced wave number, ϑ is the angle of scattering, and $g(\boldsymbol{q})$ is an « inelastic form factor » (a function of the momentum transfer $\boldsymbol{q}\hbar$) taken to be of the form corresponding to an exponential type interaction,

$$g(\boldsymbol{q}) = (1 + a^2q^2)^{-2}\,, \tag{3}$$

where a is a parameter characteristic of the range of the particular inelastic process being considered.

Since the helium nucleus possesses only one bound state, the principal contributions to σ_{in} will come from excitation to the continuum (electrodisintegration) and pion production. As will be shown later, however, the former will make the dominant contribution for incident electron energies below 600 MeV.

2. – Inelastic contributions.

In order to calculate the correction C in Eq. (1) it is necessary to determine the total inelastic cross-section, σ_{in}, arising from both electrodisintegration and pion production.

The main contribution to the former will come from reactions of the type:

$$\text{(A)} \qquad \begin{cases} \mathrm{e}^- + {}^4\mathrm{He} \to \mathrm{e}^- + {}^3\mathrm{He} + \mathrm{n}\,, \\ \mathrm{e}^- + {}^4\mathrm{He} \to \mathrm{e}^- + {}^3\mathrm{H} + \mathrm{p}\,. \end{cases}$$

As pointed out in a recent paper by MUTO and SEBE [3], any other modes of disintegration may be expected to be of much lesser importance ($\sim 10\,\%$) and may be safely neglected in our calculations.

The differential inelastic scattering cross-section for the reactions (A) has

(3) T. MUTO and T. SEBE: *Progr. Theor. Phys.* (*Japan*), **18**, 621 (1957).

recently been derived ([3]) using gaussian wave functions containing empirical spread parameters determined by comparison with the earlier Stanford experimental data ([4]). It should be pointed out that the values selected for these spread parameters are such as to give an rms radius for the α-particle of 1.69 fermi rather than the 1.41 fermi appropriate to point nucleons ([4,5]). In this manner the finite nucleon size effects are roughly included without introducing any explicit form factor for the proton ([6]).

Thus the contribution to σ_{in} from (A) can be obtained by a direct numerical integration of Muto and Sebe's expression over final electron energies and angles. Since, however, we are concerned with the ultrarelativistic case, we can employ their simplified Eq. (39) rather than the more exact Eq. (32). Unfortunately, all of these cross-sections diverge as the scattering angle approaches zero, so that a logarithmic extrapolation has to be used in the angular integrations for $\vartheta < 40°$. Since a sizeable fraction of the electrodisintegration contribution, σ_{in}^{e}, to σ_{in} comes from this small angle region, the results obtained in such a manner can only be expected to provide, at best, rough estimates.

By using the above procedure for computing σ_{in}^{e} at 400 and 600 MeV, we find the values 51 μb, and 34 μb, respectively. It is encouraging to note that these numbers are approximately twice those previously reported for ^{2}H in I, corresponding to the fact that we are considering a system having essentially two modes of disintegration instead of one. At such energies where the binding effects are quite small, one may well expect the cross-section for one of the processes (A) to be about the same as for electrodisintegration of the deuteron.

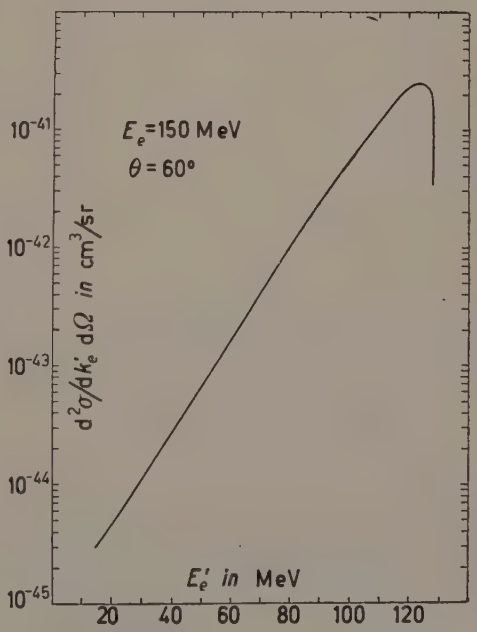

Fig. 1. – Differential inelastic cross-section at 150 MeV and 60°.

([4]) R. McAllister and R. Hofstadter: *Phys. Rev.*, **102**, 851 (1956) and R. Hofstadter: *Rev. Mod. Phys.*, **28**, 214 (1956); *Ann. Rev. Nucl. Sci.*, **7**, 231 (1957).

([5]) Actually a better choice of these parameters would be $\mu_t^{-\frac{1}{2}} = \mu_\alpha^{-\frac{1}{2}} = 4.3$ fermi, leading to an rms radius of 1.61 fermi in agreement with the experimental data; however, this difference will not affect our results significantly.

([6]) We would like to express our thanks to Dr. T. Muto for an interesting letter on this phase of his work with Dr. Sebe.

In addition to the preceding calculation, and as a supplement to Muto and Sebe's paper, we have computed representative values of the inelastic differential cross-section over a selected range of laboratory energies and angles so that their Eq. (39) can be more easily compared with experimental data when they become available. These results are shown in Figs. 1-5. All of

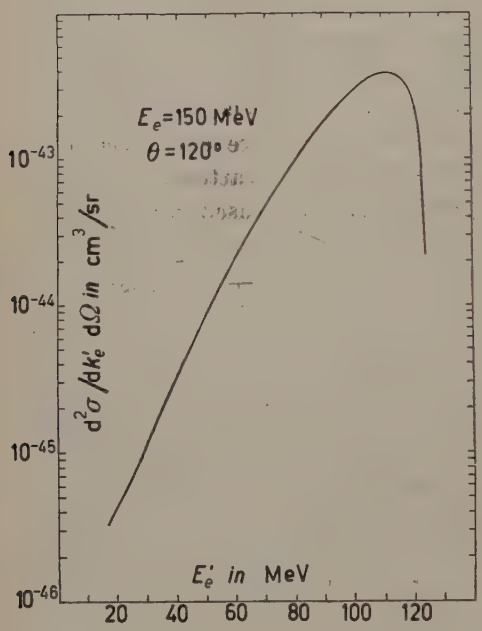

Fig. 2. – Differential inelastic cross-section at 150 MeV and 120°.

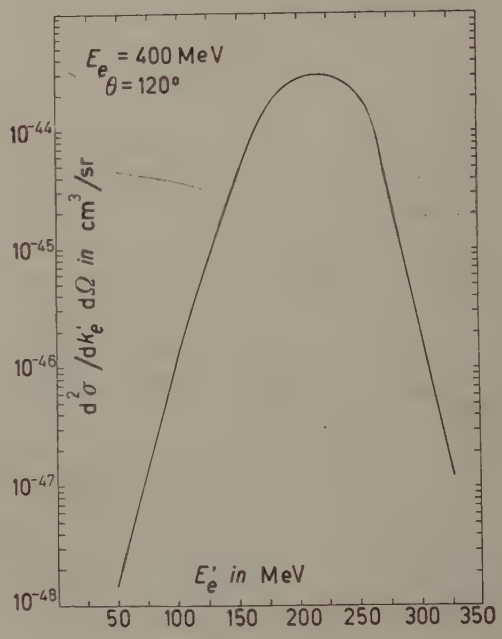

Fig. 3. – Differential inelastic cross-section at 400 MeV and 120°.

them demonstrate the expected kinematical behavior with regard to energy and scattering angle: 1) The more the energy of the incident electron, the more probable it is that the electron will have to lose a greater amount of energy in order to be scattered into the same angle. 2) For a given incident energy, the greater the scattering angle, the more probable it is that the electron will lose a greater amount of energy.

As in I, some estimate of the pion production contribution to σ_{in} can be obtained by considering the reactions (here we again neglect multiple production as a much smaller effect):

(B)
$$\begin{cases} e^- + p \to e^- + n + \pi^+ & e^- + n \to e^- + p + \pi^- \\ e^- + p \to e^- + p + \pi^0 & e^- + n \to e^- + n + \pi^0 \end{cases}$$

to arise virtually from the corresponding photo-production processes. The latter have studied extensively over the entire range of nuclei ([7,8]) and the results would indicate that for light nuclei:

$$(5) \qquad \sigma_{\gamma}^{\pi^+}(Z, N) \approx Z\sigma_{\gamma}^{\pi^+}(p) \; ; \qquad \sigma_{\gamma}^{\pi^0}(Z, N) \approx \sigma_{\gamma}^{\pi^0}(p)(Z + N) \, .$$

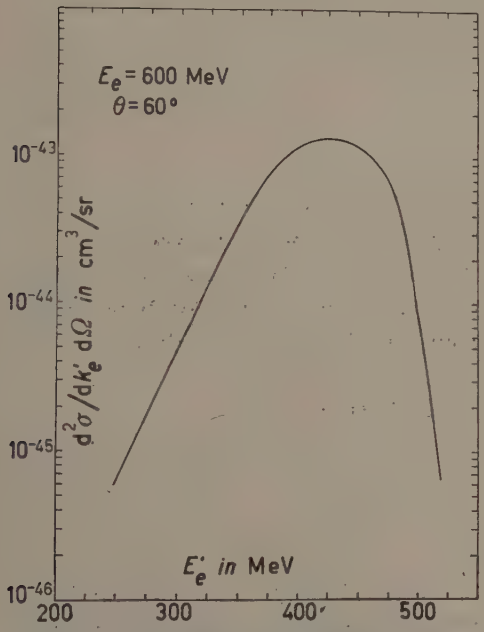

Fig. 4. – Differential inelastic cross-section at 600 MeV and 60°.

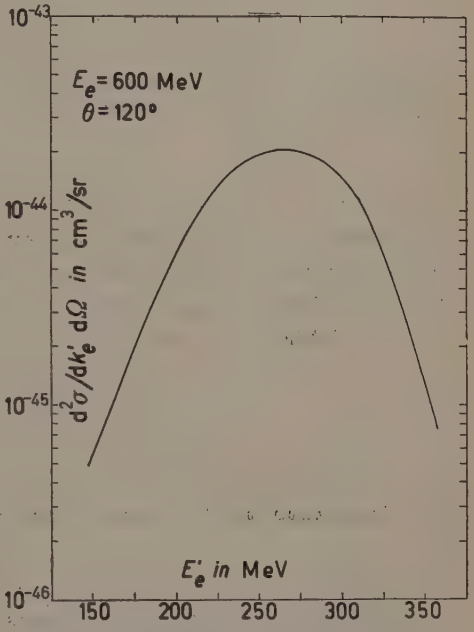

Fig. 5. – Differential inelastic cross-section at 600 MeV and 120°.

Since ^{4}He falls into this category we will assume that its photo-pion cross-sections are given by Eq. (5) with the additional supposition that $\sigma_{\gamma}^{\pi^-}$ (n) $\approx$ $\approx \sigma_{\gamma}^{\pi^+}(p)$. We can then write in the Weizsäcker-Williams approximation ([9]) the same relations between the electro-pion cross-sections and make use of the values found in I. This procedure gives the results shown in Cols. 2-4 of Table I. It may be expected that these values represent overestimates in so far as pion production is concerned because of the Pauli inhibition against

([7]) W. Williams, K. Crowe and R. Friedman: *Phys. Rev.*, **105**, 1840 (1957) and W. Imhof, E. Knapp, H. Easterday and V. Perez-Mendez: *Phys. Rev.*, **108**, 1040 (1957).

([8]) B. Govorkov, V. Goldanskij, O. Karpuhin, A. Kutsenko and V. Pavlovskaia: *Sov. Phys. Dokl.*, **2**, 4 (1957).

([9]) This method is discussed in R. Dalitz and D. Yennie: *Phys. Rev.*, **105**, 1598 (1957).

producing charged pions; however, this is more than offset by our neglect of the other electrodisintegration processes. The increasing relative importance of pionic effects can be seen from Table I: At 400 MeV, the pion contribution is only 20% of the total, while at 600 MeV it has risen to 38%.

TABLE I. – *Values of the total cross-sections.*

E_{lab}	σ_{in}^{e}	$\sigma_{in}^{\pi^0}$	$\sigma_{in}^{\pi^+}$	σ_{in}^{π}	σ_{in}
400 MeV	51 μb	6 μb	4 μb	14 μb	65 μb
600 MeV	34 μb	9 μb	6 μb	21 μb	55 μb

As a very rough check on the order of magnitude of the preceding results and the use of the logarithmic extrapolation procedure, we employed the latter to find the elastic differential scattering cross-section at zero angle along with the total elastic cross-section, σ_{el}. These results were then combined with those in Table I and found to satisfy the optical theorem inequality ([10]):

$$(6) \qquad (\mathrm{d}\sigma_{el}/\mathrm{d}\Omega)_{\vartheta=0^0} \geqslant k^2(\sigma_{el}+\sigma_{in})^2/16\pi^2 .$$

3. – Calculation of the inelastic correction and discussion.

The calculation of C according to Eq. (2) requires, in addition to σ_{in}, some knowledge of the appropriate inelastic form factor $g(\boldsymbol{q})$. This function has a shape and range dependent upon the nature of the inelastic processes being considered. Since the only conditions placed on it mathematically are that $g(0)=1$ and $g(\boldsymbol{q})\ll 1$ for $|\boldsymbol{q}|<\pi a^{-1}$, there are many admissible functions that can be chosen, each corresponding to a different form of the additional term in the Hamiltonian. Of these possibilities, perhaps the simplest is the Yukawa type chosen in I; this function, however, corresponds to an interaction possessing a non-physical singularity at the origin, thus placing undue emphasis on the region of high momentum transfer, and leading to unreasonably large values of the inelastic correction. The invalidity of such a model is verified by comparing the results of Eq. (1) (using $a=1.61$ fermi) with the experimental data at 400 MeV: Eq. (1) predicts too rapid a change in the total form factor for increased angles of scattering. Physically, one would expect the strength of the inelastic term to increase with decreasing radius r, until $r=a$, after which it would level off or increase to a finite maximum in the

([10]) See, for example, L. I. LAPIDUS: *Journ. Exp. Theor. Phys.* (*Sov. Phys.*), **4**, 937 (1957).

manner of a gaussian or exponential function. Here a would represent some characteristic distance of the order of nuclear dimensions.

For the present estimate we have chosen $g(\boldsymbol{q})$ to be of the form of an exponential, Eq. (3), and taken $a = 1.61$ fermi, the rms radius of the α-particle. The only remaining factor is that for the elastic cross-section $(\mathrm{d}\sigma_{\mathrm{el}}/\mathrm{d}\Omega)$. According to the Stanford data, this may be taken as

$$(\mathrm{d}\sigma_{\mathrm{el}}/\mathrm{d}\Omega) = [e^2/(k\hbar c)]^2[\cos^2(\vartheta/2)/\sin^4(\vartheta/2)]\,|F(\boldsymbol{q})|^2\,, \tag{7}$$

where

$$F(\boldsymbol{q}) = \exp[-q^2a^2/6] \tag{8}$$

is the form factor and a has its previous meaning.

Using Eqs. (2), (3), (7), and (8) and the values from Table I, we have computed C as a function of scattering angle in the electron-^{4}He barycentric system. The results are shown in Table II.

TABLE II. – *Values of the inelastic correction C.*

E_{lab} \ ϑ	40°	60°	80°	100°
400 MeV	$4.6\cdot10^{-6}$	$7.3\cdot10^{-6}$	$2.1\cdot10^{-5}$	$8.7\cdot10^{-5}$
600 MeV	$5.0\cdot10^{-6}$	$3.5\cdot10^{-5}$	$7.1\cdot10^{-4}$	$2.4\cdot10^{-2}$

As in the earlier cases of the proton and deuteron we see that the correction term increases with increasing momentum transfer. Especially noteworthy is the sharp rise with increasing angle, characteristic of the corresponding decrease in the elastic cross-section. This, of course, is due to the rapid decrease of the form factor, Eq. (8), over the same range. In all cases it can be seen that the correction is not greater than 10%. It should be noted, however, that although the correction term is small at the present experimentally available energies and angles, as represented in Table II, it tends to become much larger at increased backward angles. We have not considered this region in the present paper since the uncertainties in the inelastic form factor at high momentum transfer and the limitations on the present theory imposed by the use of first Born approximation do not warrant it. Such large values of the correction must be taken only as indicative of the increasing importance of inelastic effects at high momentum transfer and no more. Indeed, more knowledge of the inelastic form factor $g(\boldsymbol{q})$ for large $\boldsymbol{q}$ is required before further quantitative results can be given. It is clear, however, that if the strength of the electron-nuclear inelastic term levels off appreciably for $r \leqslant a$

$g(\boldsymbol{q})$ will decrease more rapidly for increasing $\boldsymbol{q}$ than $(1+q^2a^2)^{-2}$. In such a case the correction can be expected to remain of the order of magnitude of the values listed in Table II over the entire range of momentum transfer.

* * *

The authors would like to thank Professors H. PRIMAKOFF and H. EASTERDAY for enlightening discussions on various aspects of this work. In addition we would like to express our appreciation to Mr. A. JOHNSON for supplying us with his helium wave function calculations before publication.

RIASSUNTO (*)

Si valuta il contributo dei processi elastici non radiativi allo scattering elastico degli elettroni di alta energia derivanti da ^{4}He. Si dimostra che alle energie e sotto gli angoli di scattering attualmente disponibili il processo dominante è l'elettrodisintegrazione e che presumibilmente questo o altri effetti debbono apportare una correzione di alcuni percento alla sezione d'urto elastica differenziale, presentandosi i valori massimi alle alte energie e sotto angoli di scattering retrogradi.

(*) *Traduzione a cura della Redazione.*

IL NUOVO CIMENTO Vol. X, N. 5 1° Dicembre 1958

On the Relation between Velocity and Mass of the Electron (*).

S. Raboy and C. C. Trail

Argonne National Laboratory, Lemont - Ill.

(ricevuto il 30 agosto 1958)

Summary. — It is suggested that the elastic scattering of electrons from electrons be used to verify the Lorentz law of mass variation with velocity. The kinematics of such a process yield angular dependences which are sensitive to the model used. An independent measurement of the velocity of the incident particle is necessary to complete the measurement in a logical fashion. It is shown that two other experiments reported in the literature are deficient in this respect.

1. – Introduction.

In a recent article, Faragó and Jánossy (1) reviewed the experimental evidence supporting the Lorentz formula relating the mass of a particle to its velocity. They conclude that the Lorentz formula has less experimental support than is desired for such a fundamental relation. While the experiments indicate that mass does vary with velocity, a distinction cannot be made between the Lorentz formula and the results from other theories such as that of Abraham (2). Furthermore, the experiments actually determine the variation of e/m with velocity. In view of the universal use of a special functional form relating the mass to the velocity, it is desirable to design an experiment which will achieve that specific measurement.

(*) Work performed under the auspices of the U. S. Atomic Energy Commission.

(1) P. S. Faragó and Jánossy: *Nuovo Cimento*, **5**, 1411 (1957).

(2) M. Abraham: *Ann. der Phys.*, **10**, 105 (1902). We have translated this article into English and reprints are available upon request.

In 1932, CHAMPION [3] reported a cloud chamber measurement which purported to confirm the Lorentz law of mass variation quantitatively. His error assignments were criticized by FARAGÓ and JÁNOSSY, but were defended by CHAMPION [4]. We would like to add some additional comments about the measurement and to comment on another paper which describes a similar measurement. We will attempt to demonstrate that it is impossible in principle for these measurements to provide unambiguous verification of the Lorentz formula.

2. – Discussion.

We suggest an experiment which will indeed measure the variation of the mass with velocity. Such an experiment involves scattering electrons from electrons, measuring the angle between the scattered electron and the recoil electron, and measuring the velocity of the incident electrons, perhaps with a time-of-flight technique. Fig. 1 is a schematic diagram of the proposed experiment.

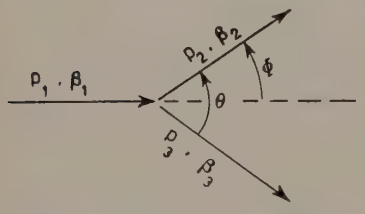

Fig. 1. – Schematic diagram of the electron-electron scattering experiment.

Application of the principles of conservation of momentum and energy yields the following collision equations.

$$(1) \qquad p_1 = p_2 \cos\varphi + p_3 \cos(\theta - \varphi) ,$$

$$(2) \qquad p_2 \sin\varphi = p_3 \sin(\theta - \varphi) ,$$

$$(3) \qquad E_1 + E_0 = E_2 + E_3 ,$$

where p is the magnitude of the momentum and E is the energy, E_0 is the rest energy φ is the angle one of the recoil particles makes with the incident direction and θ is the angle between the paths of the recoil particles. The subscript 1 designates the incident particle, 2 denotes the scattered particle, and 3 the recoiling particle. All quantities are measured in the laboratory coordinate system. Classically, θ is always 90° since the particles have the same mass.

To obtain a solution of these equations one specifies that momentum and energy are related by an equation which depends upon the model. Classically this relation is

$$(4) \qquad p^2 = 2mE .$$

---

[3] F. C. CHAMPION: *Proc. Roy. Soc.*, A **136**, 630 (1932).
[4] F. C. CHAMPION: *Nuovo Cimento*, **7**, 122 (1958).

The Lorentz model gives

$$E^2 = p^2c^2 + m^2c^4 , \tag{5}$$

and in this theory

$$p = \frac{m}{(1-\beta^2)^{\frac{1}{2}}}\beta c , \tag{6}$$

$$E = \frac{m}{(1-\beta^2)^{\frac{1}{2}}}c^2 , \tag{7}$$

where β is the ratio of the speed of the particle to the speed of light. The expressions for the energy and momentum based upon the Abraham model [5] may be written

$$p = \frac{3}{8}mc\left[\frac{1+\beta^2}{\beta^2}\log\frac{1+\beta}{1-\beta} - \frac{2}{\beta}\right]. \tag{8}$$

$$E = \frac{3}{4}mc^2\left[\frac{1}{\beta}\log\frac{1+\beta}{1-\beta} - 1\right]. \tag{9}$$

Fig. 2 shows the relation between p and β for the latter two models. A similar curve is obtained for the energy relations. Fig. 3 shows how the energy varies with momentum. These curves illustrate the similarity between the models and, more importantly, show that those experiments which depend exclusively upon the relationship between energy and momentum are not very sensitive to the model used. Indeed in the extreme relativistic case ($\beta \sim 1$), $E = pc$ for both models and the solution to the collision equations (1), (2) and (3) are identical for both models.

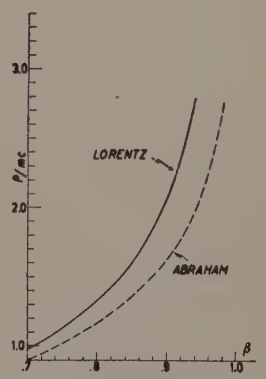

Fig. 2. – Relation between momentum and velocity for the Abraham and Lorentz models.

For purposes of designing an experiment [6], we present in Figs. 4, 5 and 6 relationships between θ, φ, and β_1. In Figs. 4 and 5 the difference between θ and 90° is plotted against φ for different values of β_1 for the two models. Fig. 6 gives the relationship between $(90° - \theta)$ and β_1 for $\varphi = 40°$. These

---

[5] In Abraham's expression for the rigid sphere with uniform surface charge, we have identified the coefficient $e/6\pi ac^2$ with the rest mass where e is the charge and a is the radius of the electron. This identification gives proper classical limits for the kinetic energy and momentum but the rest energy becomes (3/4) mc^2. However, in the collision equations these coefficients drop out.

[6] M. B. Scott, A. O. Hanson and E. M. Lyman: *Phys. Rev.*, **84**, 638 (1951).

quantities have been calculated with the digital computer GEORGE at Argonne National Laboratory. From Figs. 4 and 5 it is seen that the two theories give quite different results for the same β_1, but the shapes of the curves are similar and, for example, the curve for $\beta_1 = 0.99$ in the Abraham theory nearly coincides with that for $\beta_1 = 0.95$ in the Lorentz theory. This illustrates the need for an independent measurement of the velocity.

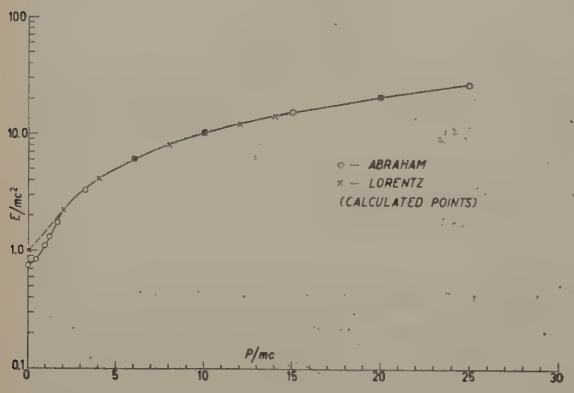

Fig. 3. – Relation between momentum and energy for the Abraham and Lorentz models.

This type of experiment has three virtues: 1) No assumption need be made concerning the relationship between charge and velocity. All other experiments of which we are aware involve the measurement of the ratio of charge to mass and the assumption is made that the charge is independent of velocity. 2) No law of force between the particles is assumed. Only conservation of momentum and energy is required. 3) The coefficients involving the rest energy cancel, removing an ambiguity in the Abraham model.

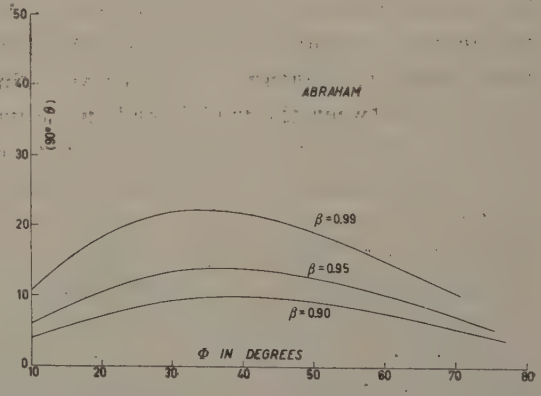

Fig. 4. – Variation of $(90° - \theta)$ with φ for the Abraham model.

An uncertainty in the experiment is introduced by the motion of the electrons in the atoms of the target. FORD and MULLIN (7) have shown that in the case of a beryllium target the spread in θ is about 3°, but this spread decreases as Z^2. Our calculations (8) show that it is necessary to obtain the velocity to 0.1% and the angles to 0.1° if one is to verify a particular model to 0.1%.

(7) G. W. FORD and C. J. MULLIN: *Phys. Rev.*, **110**, 520 (1958), and private communication.

(8) Calculations on the Abraham model have been made for $0.7 < \beta_1 < 0.99$ and all permissible laboratory angles. These results are available upon request.

Such measurements seem just possible if a Van de Graaf generator is used as a source of electrons, and movable scintillation counters in a scattering chamber are used to measure θ and φ. As mentioned above, the incident β_1 must be determined with a time-of-flight measurement. It appears that an optimum β_1 is about 0.9.

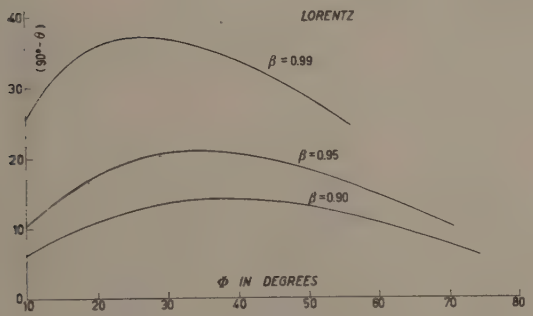

Fig. 5. – Variation of $(90° - \theta)$ with φ for the Lorentz model.

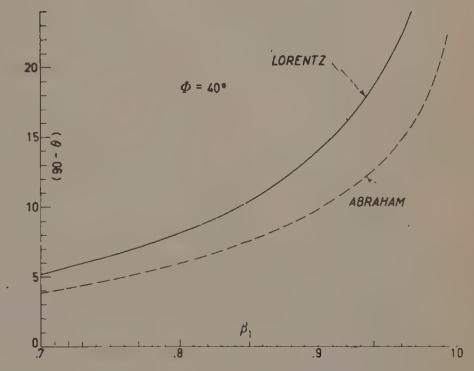

Fig. 6. – Variation of $(90° - \theta)$ with β for $\varphi = 40°$.

We discuss now the results of two experiments which we will call the Champion experiment ([3]) and the Illinois experiment ([6]).

Equations (1), (2) and (3) reduce, upon assumption of the Lorentz model, to the equation

$$\cos\theta = \frac{(\gamma_1 - 1)\sin\varphi\cos\varphi}{\left\{(\gamma_1 + 1)^2\sin^2\varphi + 4\cos^2\varphi\right\}^{\frac{1}{2}}},$$

where $\gamma = (1 - \beta^2)^{-\frac{1}{2}}$.

In 1932 CHAMPION, who used radium E as the source of electrons, reported some results from electron-electron scattering in a cloud chamber. His measurements of φ and θ for various incident velocities are given in Table I. The subscript (obs) is used to indicate the observed angle θ. The incident velocity β_L in Table I was determined by measuring the curvature of the path of the particle in a magnetic field. This measurement gives momentum (actually $He\varrho$) and one must assume a model to obtain the velocity. Apparently CHAMPION assumes the Lorentz model and obtains a consistency check as indicated in Table I. We have calculated the corresponding quantities on the Abraham model and find that the angle θ calculated from this model agrees with Champion's experimental results. We do not agree with the footnote on p. 634 in CHAMPION'S article. He reports $\theta_A = 58°$ for $\beta_L = 0.91$. We find $\theta_A = 76.3°$ for this collision.

TABLE I. – *Champion's* [3] *measured angle between the recoil and the scattered particles compared with the angle calculated with the Lorentz model and with the Abraham model.* Here β_L and β_A are the velocities of the incident electron (in units of the velocity of light) as calculated from the measured momentum from the Lorentz and Abraham model, respectively. The uncertainties in β_L and β_A result from the uncertainties in the measurement of the momentum. Angles φ and θ_{obs} are as defined in the text and their accompanying uncertainties result from the errors of measurement. Angles θ_L and θ_A are calculated from the respective models with resulting uncertainties caused by errors in the corresponding β and φ.

β_L	β_A	$\varphi \pm 0.5$ (°)	θ_{obs} (°)	θ_L (°)	θ_A (°)
0.85±0.01	0.90±0.01	20.0	83.6±1.0	82.7±1.0	82.9±1.0
0.83±0.01	0.88±0.01	26.6	81.2±1.0	81.7±1.0	82.3±1.0
0.83±0.01	0.88±0.01	31.4	81.0±0.1	81.0±1.0	81.8±1.0
0.82±0.01	0.86±0.01	22.0	84.1±1.0	83.2±1.0	83.9±1.0
0.85±0.01	0.90±0.01	22.2	82.2±1.0	81.7±1.0	82.2±1.0
0.83±0.01	0.88±0.01	22.4	82.1±1.0	82.3±1.0	83.1±1.0
0.84±0.01	0.89±0.01	23.4	82.7±1.0	81.7±1.0	82.4±1.0
0.90±0.02	0.95±0.02	24.5	79.6±1.0	77.4±1.5	78.2±1.5
0.88±0.01	0.93±0.01	35.4	76.8±0.5	77.3±1.0	78.3±1.0
0.85±0.01	0.90±0.01	21.1	82.7±1.0	81.8±1.0	82.6±1.0
0.91±0.02	0.95±0.02	36.9	75.2±0.5	75.2±1.5	76.3±1.5
0.93±0.02	0.97±0.02	29.6	72.5±0.5	72.6±1.5	74.1±1.5
0.85±0.01	0.90±0.01	21.8	82.4±1.0	81.4±1.0	82.4±1.0
0.82±0.01	0.86±0.01	36.9	80.6±0.5	81.0±1.0	82.2±1.0
0.87±0.02	0.92±0.02	24.7	83.6±1.0	79.6±2.0	80.6±2.0

These results lead us to conclude that the Champion experiment gives no evidence to support the Lorentz model. If, however, a direct measurement of the incident velocity (or of the velocity of one of the recoil particles) is made, then a check of the validity of the models can be made. This measurement of velocity must be made independent of momentum-energy relations.

We close with a brief discussion of the Illinois experiment. That experiment was similar to Champion's except that a magnetic analyzer was used to measure p_2 as a function of φ for a fixed p_1. (The Lorentz energy of the incident particle was 15.7 MeV). However, to compare the data with theory it was necessary to obtain a relation between momentum and energy. We have seen above that the models are not sensitive to these relations and in fact become identical for β_1 close to 1. We conclude that this paper offers no evidence for believing that the Lorentz model describes the electron more accurately than the Abraham model. It should be noted that the Illinois group does not claim a decisive experiment in this respect.

* * *

We wish to express our thanks to Dr. DAVID PHILLIPS of the Argonne Applied Mathematics Division for making the calculations.

RIASSUNTO (*)

Si suggerisce di usare per la verifica della legge di Lorentz sulla variazione della massa con la velocità lo scattering elastico degli elettroni su elettroni. La cinematica di tale processo fornisce dipendenze angolari soggette all'influenza del modello usato. È necessario eseguire indipendentemente la misura della velocità della particella incidente per completare la misura in modo logico. Si dimostra che a tale riguardo altri due esperimenti riportati in letteratura sono deficienti.

(*) *Traduzione a cura della Redazione.*

IL NUOVO CIMENTO Vol. X, N. 5 1° Dicembre 1958

Space-Charge Effects in Electron-Synchrotrons.

C. Bernardini

Istituto Nazionale di Fisica Nucleare
Laboratori Nazionali del Sincrotrone di Frascati

(ricevuto il 16 Settembre 1958)

Summary. — Space charge effects are considered (taking into account positive ions) with the aim of deciding whether they can set up serious intensity limitations for the beams of weak focusing electron synchrotrons, or not. The possibility of linear resonances and non linear beam splitting is shown. An estimate of the rate of production of positive ions in the doughnut is given.

1. – Introduction.

Space charge effects in electron-synchrotron are usually settled on by the statement that, if the injection energy is high enough, magnetic forces compensate nearly at all electrostatic forces (the well known $1-\beta^2$ factor [1]). This statement is, of course, valid in view of the till now obtained intensities for such machines, *i.e.* having in mind a figure of 10^{10} for the order of magnitude of the number of circulating electrons per pulse.

It is still assumed, even if not explicitly said, that the electron beam moves in vacuum but for the problem of scattering losses. Consideration of scattering losses gives an intensity independent rule for a troubleless pressure of the residual gas; now, we want to show that this rule does not eliminate the possibility of ion production, in the beam-occupied region, in such a quantity as to give rise to troubles with the focusing properties of the external magnetic field plus space charge forces.

---

[1] See for instance: W. Harman, *Fundamentals of Electronic Motion* (New York, 1953), pag. 291.

A complete formulation of the problem of positive ions production and of their interaction with the electron beam is complicated by the number of concomitant circumstances; nevertheless, orders of magnitude and semiqualitative results can be obtained by the use of simple models.

Two main results will be shown in the following paragraphs:

a) The possibility of reaching dangerous resonant values of the betatron frequencies.

b) The possibility of beam-splitting into two or more parallel beams.

It is hard to maintain that the strange facts observed in some electron-synchrotron laboratories (2) find an explanation in the results of this paper. However, we think that such results can give a guide for an easy experimental program with the aim of deciding if positive ion effects are to be accounted for (or rejected) in planning high intensity machines.

Eventually, we anticipate that typical appearance values of the effects in weak focusing machines (which we are interested in) are $5 \cdot 10^{-6}$ mm Hg for the pressure, $5 \cdot 10^{10}$ for the number of electrons per pulse. The main perturbation parameters depend on the product pressure $\times$ intensity.

2. – Resonance effects.

In this paragraph we want to study the effect of an uniformly distributed sea of positive ions, charge $+\zeta e$, on the betatron oscillation of the electrons in the beam. We think of the ion density as constant.

Let us call N_e the total number of circulating electrons, N_+ the number of ions in the beam occupied region and put

$$\varepsilon = \frac{\zeta N_+}{N_e} .$$

Suppose for semplicity the beam is made up of four bunches, uniformly filled, with electrons and cylindrical in shape, the length, along the axis (parallel to the direction of the bunch), being $R\Delta\Phi$, the circular section having a radius r_0. The total radial force on an electron of the beam, at a distance r from the beam axis will be

$$F_r = \frac{1}{2} N_e \frac{e^2}{R\Delta\Phi r_0^2} (1 - \beta^2 - \varepsilon) r .$$

(2) *CERN symposium*: **1**, 67, 301 (1956).

The $1-\beta^2$ dependent part is due to electron-electron forces, the ε part is due to electron-ion forces.

We neglect the $1-\beta^2$ part, thus assuming

$$1-\beta^2 \ll \varepsilon \ ;$$

the equations of betatron oscillations take the form

$$x''+(1-n+\delta n)x=0 \qquad \text{(radial motion)}$$

$$z''+(n+\delta n)z \quad =0 \qquad \text{(vertical motion)},$$

where

$$\delta n = \frac{1}{2}\,\varepsilon N_e \frac{e^2 R}{mc^2 \Delta\Phi r_0^2},$$

and the other symbols need no explanation.

The dependence on electron energy of this space charge parameter δn is not easy to guarantee: one could say that the quantity $m\Delta\Phi r_0^2$ behaves roughly as $B^{-\frac{1}{2}}$ (B being the main magnetic field in the machine) due to adiabatic dampings. But this energy dependence could be wrong because of a number of influencing circumstances (like scattering, radiation fluctuations or space charge effects themselves). We take a constant δn value, corresponding to injection values of the parameters; « injection values » means, of course, values reached soon after RF capture, when the electron beam density is nearly steady.

For typical values as

$$R = 360 \text{ cm}, \qquad (mc^2)_{\text{injec.}} = 2.5 \text{ MeV},$$

$$r_0 = 1 \text{ cm}, \qquad \Delta\Phi = 1 \text{ rad},$$

one obtains

$$\delta n = 0.1\,\varepsilon \left(\frac{N_e}{10^{10}}\right).$$

We can write down a resonance relation for the betatron frequencies, for a racetrack synchrotron with four straight sections of length L, in the form:

$$p+\left(1+\frac{L}{\pi R}\right)(q\sqrt{1-n+\delta n}+r\sqrt{n+\delta n})=0\,,$$

where p, q, r are integers ($\gtrless 0$) ([3]).

([3]) E. Persico: report T1 della Sez. Acc. dell'INFN (1953).

In the case of $L/\pi R = 0.106$, $n = 0.61$ (as for the Frascati machine), there are three *linear* resonances near the unperturbed working point, namely

$$p = 1 \qquad q = 0 \qquad r = -1 \qquad \delta n \simeq 0.2$$

$$p = -2 \qquad q = 1 \qquad r = 1 \qquad \delta n \simeq 0.3$$

$$p = 1 \qquad q = -1 \qquad r = 0 \qquad \delta n \simeq 0.4$$

The first resonance ($\delta n = 0.2$) reveals itself by the build up of vertical oscillations due to first harmonic median plane irregularities. The second one ($\delta n = 0.3$) is a coupling resonance excited by field or median plane second harmonic irregularities. The last resonance ($\delta n = 0.4$) is a field first harmonic excited radial motion (*).

Non-linear resonances are not considered here because of the surely longer amplitude build-up time, which could allow for ion density rearrangements destroying the resonant value of δn.

3. – The ion density.

We want to estimate the quantity δn as a function of pressure, beam intensity, atomic number Z of the residual gas, etc. We neglect the secondary electron production since, as can be easily shown, secondary electron velocities are $\gg$ than ion velocities, so that they rapidly leave the beam region.

Let us call N the number of the atoms per cm^3. At 300 °K of temperature:

$$N = 3.2 \cdot 10^{16} P \ (\mathrm{cm}^3)^{-1},$$

where P is the pressure in mm Hg.

σ_i is the ionization cross-section: it is energy independent for relativistic electrons ([4]). We shall take as in reference ([4])

$$\sigma_i \simeq 0.2 Z \cdot 10^{-18} \ \mathrm{cm}^2 .$$

Put t_w for the time an ion needs to escape from the beam-occupied region.

(*) Resonant blow up of the beam, of the just considered kind, seems likely to be observable only in the vertical direction because of the need of having ions over the whole path of the electrons during the oscillation amplitude build up time. This has been kindly pointed out to me by doctor A. TOLLESTRUP.

([4]) M. J. MORAVCSIK: *Phys. Rev.*, **100**, 1009 (1955).

It follows that

$$N_+ \simeq c\sigma_i N \int_0^t N_e(t') \exp\left[-t'/t_w\right] \mathrm{d}t' \ .$$

We suppose N_e is made up of two parts:

$$N_e = N_a + N_p \exp\left[-t/\tau\right] ,$$

where N_a and N_p are constant; τ is a characteristic time of slow losses.

When $t \gg t_w$, τ, ε reaches a steady value

$$\varepsilon = \zeta c t_w \sigma_i N \left(1 + \frac{\tau}{\tau + t_w} \frac{N_p}{N_a}\right);$$

the factor $1+(\tau/(\tau+t_w))(N_p/N_a)$ is likely to be about two, so that

$$\varepsilon \simeq 2\zeta c t_w \sigma_i N \ .$$

The main problem is to calculate t_w: The ions, since the time of their production, move along the lines of force of the external magnetic field, that is along the z axis. Thus, for an ion moving with velocity v, and produced at a random point of the beam section,

$$t_w = \frac{8 r_0}{3\pi |v|} \ .$$

What we need is the average $\langle 1/t_w \rangle$ over the possible $|v|$ values, $|v|$ being the modulus of the z component of the ion velocity (see Appendix A). One could take the average on thermal velocities (*), thus obtaining

$$\frac{1}{t_w} = \frac{3}{2 r_0} \left(\frac{2\pi k T}{M}\right)^{\frac{1}{2}} ,$$

(*) Recoil energies of the ions do not change appreciably the termal energy distribution. The transferred momenta q are certainly less than 10 keV/c in a collision, so that the ion mean recoil energy is certainly less than

$$\frac{q^2}{2M} \sim \frac{10^8}{4Z10^9} = \frac{0{,}025}{Z} \text{ eV} ,$$

which is less than thermal energies by a factor $1/Z$.

where M is the mass of the ions; but ion-ion and electron-ion electrostatic effects are certainly not negligible from the point of view of the ion distribution. There is the possibility of ion trapping by the main beam, which we shall examine in Appendix B. For the moment being, assume that the thermal distribution of velocities is valid; it follows that

$$t_w \simeq 3 r_0 \sqrt{z} \ \mu\text{s} \qquad (r_0 \text{ in cm})$$

assuming $M \simeq 2Z$ (mass of the H atom).

The formula giving ε is

$$\varepsilon \simeq 1200\, \zeta r_0 Z^{3/2} P ,$$

where P is in mm Hg. The formula for δn is thus

$$\delta n \simeq 120 \frac{\zeta Z^{\frac{3}{2}} P}{r_0} \left(\frac{N_e}{10^{10}} \right) \qquad \begin{cases} r_0 \text{ in cm} \\ P \text{ in mm Hg} . \end{cases}$$

We see that for

$$\zeta = 1 , \quad Z = 10 , \quad P = 5 \cdot 10^{-6} , \quad r_0 = 1 \text{ cm} , \quad N_e = 5 \cdot 10^{10}$$

one obtains

$$\delta n \simeq 0.1 .$$

4. – Beam splitting.

So far we were concerned with a simplified model having cylindrical symmetry. Beam splitting effects can be put in evidence by simply removing this assumption.

We will treat in Appendix C the general case of ion distribution; for the sake of clearness we now consider a simple model in wich the ion distribution has elliptic asymmetry:

$$n_+(r, \varphi) r \, \mathrm{d}r \, \mathrm{d}\varphi = \frac{N_+}{4\pi r_0^2 R \, \Delta\Phi} \frac{1 + 2e_0 \sin^2 \varphi}{1 + e_0} r \, \mathrm{d}r \, \mathrm{d}\varphi \qquad r < r_0$$

$$= 0 \qquad r > r_0$$

where n_+ stays for the ion density as a function of polar co-ordinates around

the electron beam axis, r and φ. e_0 is a constant measuring the ellipticity, satisfying $e_0 > -\frac{1}{2}$ because of $n_+ > 0$.

The electric field components due to such a charge distribution are, at points far from the head or tail of a bunch

$$E_x = C\left(1 - \frac{2e_0}{1+e_0}\left(\frac{3}{4} + \ln\frac{r}{r_0}\right)\frac{x^2 - z^2}{r^2}\right)x - 4C\,\frac{e_0}{1+e_0}\left(\frac{1}{4} + \ln\frac{r}{r_0}\right)\frac{xz}{r^2}\,z\,,$$

$$E_z = C\left(1 - \frac{2e_0}{1+e_0}\left(\frac{3}{4} + \ln\frac{r}{r_0}\right)\frac{x^2 - z^2}{r^2}\right)z + 4C\,\frac{e_0}{1+e_0}\left(\frac{1}{4} + \ln\frac{r}{r_0}\right)\frac{xz}{r^2}\,x\,,$$

where

$$x^2 + z^2 = r^2\,, \qquad z = x\,\mathrm{tg}\,\varphi\,,$$

$$C = \frac{1}{2}\,\frac{\zeta e N_+}{r_0^2 R\,\Delta\Phi}\,.$$

Limiting the analysis of possible motions to a simple case, *i.e.* to the motion on the median plane $z = 0$, we see that the equations of betatron oscillations for the electrons of the main beam are of the following kind:

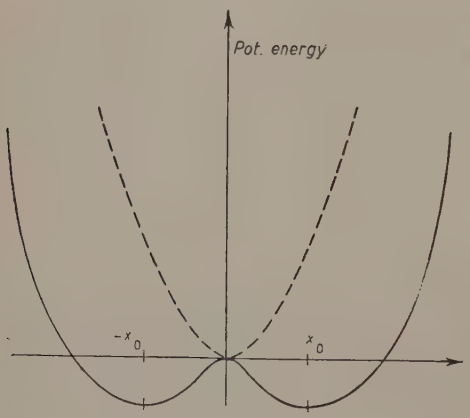

Fig. 2.

$$(1) \qquad \ddot{x} + \left(\omega_0^2 + e_0\omega_1^2 \ln\frac{|x|}{r_0}\right)x = 0\,.$$

The log term is a new feature for betatron oscillations; ω_0, ω_1, are two constants readily obtainable in terms of the parameters defining the fields E_x, E_z and the external magnetic field.

The motion described by eq. (1) can be visualized by means of the graph (Fig. 1) of the potential energy of the force

$$\left(\omega_0^2 + e_0\omega_1^2 \ln\frac{|x|}{r_0}\right)x\,,$$

for the case $e_0 > 0$. (Were actually $e_0 < 0$, the same conclusions hold true for the motions out of the median plane, round $x = 0$).

Two equilibrium positions are found for the beam; the axis ($x = 0$) is no more a stable equilibrium position.

The parameters defining the well-depth and well centers are quite sensitive to the ellipticity e_0; in the case shown here, for instance,

$$|x_0| = r_0 \exp\left[-\frac{\omega_0^2}{e_0\omega_1^2}\right],$$

where $\pm x_0$ are the well-center co-ordinates (*).

5. – Conclusion.

This report summarizes a list of possibilities for space charge effects due to residual gas in the doughnut.

We do not maintain these effects will be so strongly evident in a well working machine as can be conjectured from some of the reported formulas: these are, in fact, rough calculations containing too many unknowns.

Nevertheless we are afraid that intensity limitations for weak focusing machines follow on this reasoning line; the point is whether they are so near the actual working points as here shown or not and this, we think, can be only decided by a suitable experimental program.

* * *

We would like to thank Professor G. SALVINI for stimulating help.

APPENDIX A

Simple Boltzmann equation for the ion density.

Let us call $n_+(x, z, v, t)$ the density of ions in a space of coordinates x, z, v (v being the z component of the velocity). Put $n_e(x, z, t)$ for the electron density in the beam and $f(v)$ for the maxwellian distribution function of the velocity v. Then

$$\frac{\partial n_+}{\partial t} = -v\frac{\partial n_+}{\partial t} + \sigma_i N c n_e(x, z, t) f(v) .$$

Let us consider the case in which

$$n_e(x, z, t) = \psi(x, z)\, N_e(t) ,$$

(*) Once two beams are produced further splitting could be envisaged for each one of the two beams on the same basic mechanism. Prof. R. WILSON pointed out to me this possibility.

where

$$\iint_{\text{whole space}} \psi(x, z)\, \mathrm{d}x\, \mathrm{d}z = 1 .$$

A solution is readily found with the only condition that there are no ions at the time $t = 0$.

$$n_+(x, z, v, t) = c\sigma_i N f(v) \int_0^t \psi[x, z - v(t' - t)]\, N_e(t')\, \mathrm{d}t' .$$

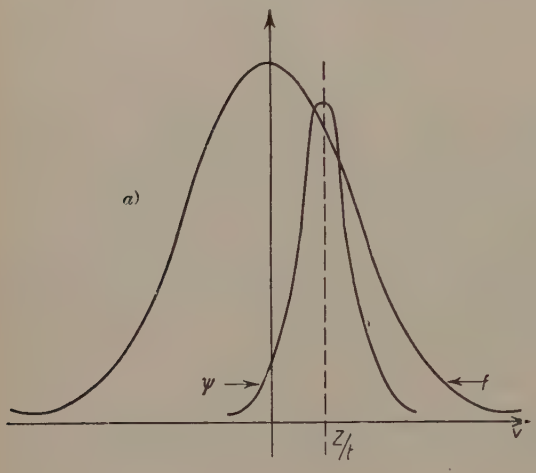

This formula allows us to perform the correct average over the velocities. Namely, what we need is

$$I(z, x, t) = \int_{-\infty}^{+\infty} f(v)\, \psi(x, z - vt)\, \mathrm{d}v .$$

Now, $f(v)$ is a gaussian function of width $\langle v^2 \rangle$; ψ, as a function of $z - vt$, is a strongly peaked function around the value $z - vt = 0$ of the argument. The width of this peak is of the order r_0. When (Fig. 2*a*)

$$\langle v^2 \rangle t^2 \gg r_0^2 ,$$

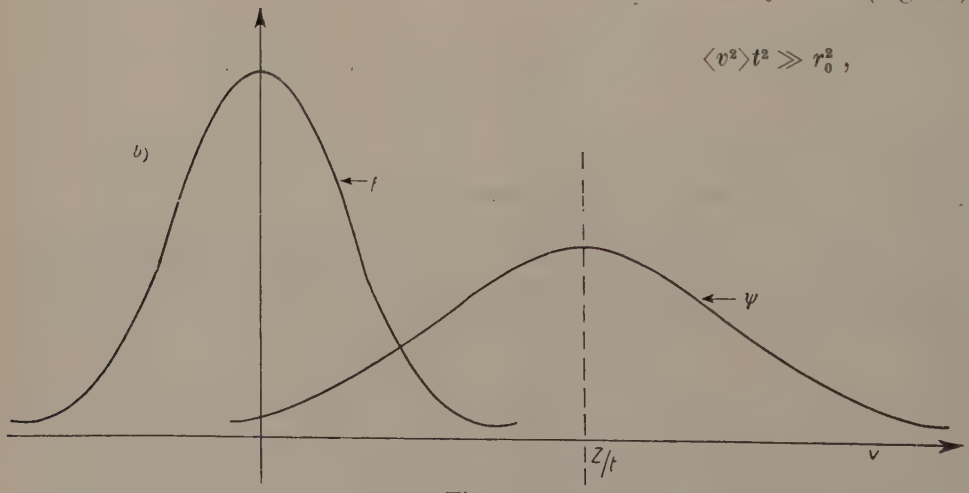

Fig. 2.

we can substitute for ψ a δ function:

$$\psi(x, z) \simeq u(x)\delta(z - vt) .$$

Here u takes into account the x dependence. Thus, for this case

$$I(x, z, t) \simeq \frac{1}{|t|} u(x)\left(\frac{M}{2\pi kT}\right)^{\frac{1}{2}} \exp\left[-\frac{Mz^2}{2kT}\cdot\frac{1}{t^2}\right] \simeq \frac{1}{|t|} u(x)\left(\frac{M}{2\pi kT}\right)^{\frac{1}{2}}.$$

The last approximation comes out from the fact that we are mainly interested in z values less than r_0.

On the other hand, if

$$\langle r^2\rangle t^2 \ll r_0^2 ,$$

and if $z \neq 0$, the $\psi(z - vt)$ function, as a function of v, displaces its peak toward infinity as $t \to 0$, so that it does not overlap appreciably with the velocity distribution, (Fig. 2*b*).

There is an intermediate region in which

$$z^2 < t^2\langle v^2\rangle < r_0^2 ,$$

where things are somewhat more complicated. This region is, however, of no interest for the final result. One can check all the qualitative considerations just made by calculating what happens for a gaussian shaped ψ. Eventually one obtains that:

$$\left.\begin{aligned} I(x, z, t) &\simeq 0 \qquad\qquad , \qquad \langle v^2\rangle\, t^2 < r_0^2 \\ &\simeq \frac{1}{|t|} u(x)\left(\frac{M}{2\pi kT}\right)^{\frac{1}{2}}, \qquad \langle v^2\rangle\, t^2 > r_0^2 \end{aligned}\right\} |z| < r_0 .$$

Using this result to calculate

$$\langle n_+\rangle = \int_{-\infty}^{+\infty} n_+ \,\mathrm{d}v ,$$

one obtains

$$\langle n_+\rangle = c\sigma_i N \int_0^t N_e(t')\, I(x, z, t - t')\,\mathrm{d}t' \simeq c\sigma_i N u(x)\left(\frac{M}{2\pi kT}\right)^{\frac{1}{2}} \int_{r_0/\sqrt{\langle v^2\rangle}}^t N_e(t - t')\,\frac{\mathrm{d}t'}{t'} ;$$

neglecting the time dependence of N_e:

$$\langle n_+\rangle \simeq \frac{1}{2} c\sigma_i N u(x)\left(\frac{M}{2\pi kT}\right)^{\frac{1}{2}} N_e \ln\left(\frac{\langle v^2\rangle\, t^2}{r_0^2}\right) = \frac{1}{2} c\sigma_i N u(x)\left(\frac{M}{2\pi kT}\right)^{\frac{1}{2}} N_e \ln\left(\frac{2kTt^2}{Mr_0^2}\right).$$

The log term is of no importance.

$$N_+ \simeq r_0 \int \langle n_+ \rangle \, \mathrm{d}x = \frac{1}{2} c\sigma_i N r_0 \left(\frac{M}{2\pi k T}\right)^{\frac{1}{2}} N_e \ln\left(\frac{2kTt^2}{Mr_0^2}\right).$$

This calculation shows that the qualitative arguments of Sect. **3** can be followed with some confidence.

Appendix B

Ion trapping.

The ion trapping mechanism can be described by means of matrix technique as follows: the ions in a given azimuthal position are periodically inside a bunch of electrons for a time $R\Delta\Phi/c$, outside of the bunches for a time $(R/c)((\pi/2) - \Delta\Phi)$.

When inside, the ions equations of motion are of the form

$$\ddot{z} + \omega_e^2 z = 0;$$

when outside, however,

$$\ddot{z} - \omega_+^2 z = 0,$$

where

$$\omega_e^2 = \frac{1}{2} \frac{\zeta N_e e^2 (1 - \varepsilon)}{R\Delta\Phi M r_0^2}$$

$$\omega_+^2 = \frac{1}{2} \frac{\zeta N_e e^2 \varepsilon}{R\Delta\Phi M r_0^2}.$$

This is a time alternating focusing defocusing structure, whose matrix trace is given by

$$\frac{1}{2} \operatorname{Tr} (\text{transf. matrix}) =$$

$$= \cosh \gamma_1 \sqrt{\varepsilon} \cos \gamma_2 \sqrt{1 - \varepsilon} - \frac{1}{2} \frac{1 - 2\varepsilon}{\sqrt{\varepsilon}\sqrt{1 - \varepsilon}} \cdot \sinh \gamma_1 \sqrt{\varepsilon} \sin \gamma_2 \sqrt{1 - \varepsilon}.$$

where we put for brevity

$$\begin{pmatrix} \gamma_1 \\ \gamma_2 \end{pmatrix} = \left(\frac{\zeta N_e R e^2}{2 M c^2 r_0^2 \Delta\Phi}\right)^{\frac{1}{2}} \begin{pmatrix} (\pi/2) - \Delta\Phi \\ \Delta\Phi \end{pmatrix} = \gamma \begin{pmatrix} (\pi/2) - \Delta\Phi \\ \Delta\Phi \end{pmatrix}.$$

When $\gamma \ll 1$ the analysis of the trace is quite easy:

$$\tfrac{1}{2} \operatorname{Tr} (\text{transf. matrix}) \simeq 1 - \tfrac{1}{2} \gamma_2(\gamma_1 + \gamma_2) + \tfrac{1}{2} \varepsilon(\gamma_1 + \gamma_2)^2,$$

and there follows that trapping is possible until ε reaches the value

$$\varepsilon = \frac{2\Delta\Phi}{\pi};$$

the assumption of this ε value as equilibrium value would lead to a pressure independent shift of betatron frequencies. But the just described trapping mechanism must be interpreted with some care: in fact we claim that the situation we shew in Sect. **3**, based on thermal motion considerations for free ions, is more likely to be true for the following reasons. Let us suppose an ion oscillates along the z axis (i.e. it is trapped). If it leaves the beam axis with a velocity $\langle v\rangle$ (thermal average), the amplitude of its oscillations will be $\langle v\rangle/\Omega$ where Ω is the characteristic frequency of the composite structure we deal with in this appendix. Trapping is effective only if

$$\frac{\langle v\rangle}{\Omega} < r_0,$$

because if the ion goes outside the electron beam boundary repulsive space charge forces prevail and make it reach the doughnut's walls. Now Ω is given, in the $\gamma \ll 1$ approximation, by $\Omega \simeq \sqrt{8\pi}\gamma(\Delta\Phi - (\pi/2)\varepsilon)^{\frac{1}{2}}(c/R)$ and

$$\frac{\langle v\rangle}{\Omega} \simeq \frac{R}{\sqrt{8\pi}\gamma} \frac{1}{(\Delta\Phi - (\pi/2)\varepsilon)^{\frac{1}{2}}} \frac{\langle v\rangle}{c} \simeq 4\cdot 10^{-3} r_0 \left[\frac{R\Delta\Phi}{\zeta(N_e/10^{10})(\Delta\Phi - (\pi/2)\varepsilon)}\right]^{\frac{1}{2}},$$

and this shows that trapping will be effective in fastening the ion cumulation but, as soon as $\Omega \to 0$, the trapping mechanism becomes less efficient and the pure thermal motion considerations give a good approximation.

We remark that because of this phenomenon the pressure dependence of ε could be far from linear.

Appendix C

The ion distribution. General case.

To show the possibility of appearance of log terms in the electric field formula, we develop here the potential due to an ion distribution of density $n_+(r, \varphi)$. The potential $V(r, \varphi)$ is given by

$$V(r,\varphi) = \text{const} - 2\zeta e \int_0^{2\pi} \mathrm{d}\bar{\varphi} \int_0^{\infty} \bar{r}\,\mathrm{d}\bar{r}\, n_+(\bar{r}, \bar{\varphi}) \ln \sqrt{r^2 + \bar{r}^2 - 2r\bar{r}\cos(\varphi - \bar{\varphi})} =$$

$$= \text{const} - 2\zeta e K(r, \varphi),$$

Expanding in Fourier series

$$n_+(r, \varphi) = \sum_{-\infty}^{+\infty} q_k(r) \exp[ik\varphi] \qquad (q_k = q^*_{-k})$$

and

$$K(r, \varphi) = \pi \ln r \int_0^r \bar{r} q_0(\bar{r})\, \mathrm{d}\bar{r} + \pi \int_r^\infty \bar{r} \ln \bar{r} q_0(\bar{r})\, \mathrm{d}\bar{r} -$$

$$- \frac{\pi}{2} \sum_{-\infty}^{+\infty}{}_{k \neq 0} \frac{\exp[ik\varphi]}{|k|} \left\{ \frac{1}{r^{|k|}} \int_0^r \bar{r}^{|k|+1} q_k(\bar{r})\, \mathrm{d}\bar{r} + \int_r^\infty \frac{1}{\bar{r}^{|k|-1}} q_k(\bar{r})\, \mathrm{d}\bar{r} \right\}.$$

Logarithmic terms can appear in the last term of the expansion, whenever

$$q_k(r) \sim r^{|k|-2} \qquad \text{(for not too large } r;\ k \neq 0)$$

The case we studied in Sect. **4** is that of $q_{\pm 2} = \text{const}$ for $r < r_0$. Attention must be given to the condition $n_+(r, \varphi) > 0$; in the model of Sect. **4** this condition requires, for instance, $e_0 > -\frac{1}{2}$.

RIASSUNTO

Si studiano gli effetti di carica spaziale (tenendo conto della presenza di ioni positivi) per stabilire se possono dar luogo a serie limitazioni per l'intensità del fascio di un elettrosincrotrone a focalizzazione debole. Si mostra che sono possibili effetti lineari di risonanza ed effetti non lineari di sdoppiamento del fascio. Si valuta inoltre il numero di ioni positivi prodotti nella camera a vuoto.

IL NUOVO CIMENTO Vol. X, N. 5 1° Dicembre 1958

Lagrangian Formalism in Relativistic Hydrodynamics of Rotating Fluid Masses.

F. Halbwachs, P. Hillion and J.-P. Vigier

Institut Henri Poincaré - Paris

(ricevuto il 17 Settembre 1958)

Summary. — The general theory of relativistic moving fluid masses is studied in terms of a new set of variables originally proposed by Einstein and Kramers. The general equations of motion established directly by Bohm and one of us (J.-P. V.) then appear as conservation equations deduced from a scalar Lagrange function of these new variables. This procedure paves the way for a quantization of the internal motion of a model of extended particles in real space: model strongly suggested by the experimental results of Hofstadter.

Introduction.

In a recent paper the general theory of the relativistic mechanical behaviour of rotating fluid masses has been treated by Bohm and one of us (1) and it was possible to show that the motion of various significant global physical quantities (such as the total linear momentum G_μ, the total angular momentum $M_{\mu\nu}$, the center of mass, and the center of matter density) satisfy equations of motion which generalize simple relations postulated by Weyssenhoff (2). The problem we want to treat here consists in the deduction of these equations as conservation equations resulting from a scalar Lagrangian depending on a new set of variables connected with global properties of the droplet.

Such a theory is interesting from two main points of view.

(1) D. Bohm and J.-P. Vigier: *Phys. Rev.*, **109**, 1882 (1958). In this paper we have used, as far as possible, the same notations. Greek indices such as μ vary from one to four; latin indices such as k, from one to three. Indices repeated twice are summed over all possible values. We work in Minkovski's space-time.

(2) J. Weyssenhoff: *Acta. Phys. Pol.*, **9**, 8 (1947).

First it might pave the way to treat in a covariant way the problem of the classical and quantal behaviour of particles extended in space. This seems absolutely necessary in the present stage of physics for various experimental and theoretical reasons.

As one knows, all recent experiments of high energy scattering between various types of elementary particles seem to indicate that such particles are not point-particles but have indeed a real extension in space (with a radius of the order of $0.6 \cdot 10^{-13}$ cm).

This results from many indirect evidences (which we shall not analyze here) and also from the remarkable proton-electron scattering experiments of HOFSTADTER and his collaborators ([3]).

On the other hand many of the divergences of quantum theory result precisely from the point-like character assumed arbitrarily for all particles in the present field theory.

As a consequence it is not unreasonable to hope to eliminate them by starting *a priori* from a classical extended model.

Secondly it provides a convenient basis to study internal stable excited quantum states of such droplets; thus generalizing the classical non relativistic treatment of POINCARÉ ([4]) and other authors. Indeed as we shall show in a subsequent paper resulting of common research in Bristol with Prof. BOHM, such states are characterized by a set of quantum numbers which reproduce exactly a classification analogous to the classification proposed by TIOMNO ([5]) for elementary particles. This classification differs from the Nishijima Gell-Mann scheme by the essential fact that fermions and bosons are respectively isofermions and isobosons.

However before following these lines of research it is necessary to give a Lagrange formulation of the equations of motion of such extended models in terms of convenient parameters.

At first sight such a step raises many difficulties.

If one drops the point-like character of particles and assumes them to be comparable to some field densities enclosed within a limited time-like tube (with radii of the order of 10^{-13} cm) we are immediatly faced by the well known trouble that in relativity such a model depends evidently on an infinite number of variables. This results from the fact that it is not possible to extend to the relativistic domain the non relativistic theory of rigid bodies, thus reducing that infinite number to a few characteristic variables (such as the Euler angles and the position of the center of mass).

([3]) R. HOFSTADTER: *Rev. Mod. Phys.*, **28**, 214 (1956).
([4]) H. POINCARÉ: *Acta. Math.*, **7**, 259 (1885).
([5]) J. TIOMNO: *Nuovo Cimento*, **6**, 69 (1957).

However, as we shall see, there exists a way of surmounting this trouble. If we consider the extended particle as a droplet enclosed within a time-like tube in space-time and define it in the most general way by an energy-momentum density $t_{\mu\nu}$ and a current density j_μ inside the tube, we can introduce integral tensor quantities defined by integration over the total volume of the droplet. These quantities have been shown to satisfy relations which determine their behaviour in time. In this way we describe a global sort of average motion of the body as a whole which leaves aside finer and irrelevant detailed motions within the droplet. Such an average hydrodynamical treatment evidently reduces the number of mechanical variables needed.

In fact as we shall see, the general equations of motion need only a limited number of variables which correspond to average physical properties of the droplet considered as a whole (such as the total angular momentum $M_{\mu\nu}$, the total linear-momentum G_μ, etc.).

In principle it is then possible to determine a Lagrange function depending on such global parameters which gives these global equations of motion as necessary consequences of its Euler equations.

This brief analysis determines the plan of this paper. In Sect. **1** we shall briefly recall the fundamental equations of motion of rotating fluid masses. In Sect. **2** we shall introduce the Einstein-Kramers « beingrössen » variables and introduce a general Lagrangian for the general case of rotating particles. In Sect. **3** finally we shall treat the particular case of liquid droplets satisfying Weyssenhoff's conditions and discuss further possible extensions of the general theory.

1. – According to our programm let us first give a brief summary of the relativistic liquid droplet theory. If one assumes that such a droplet is defined by a current density j_μ (equal to zero outside the time-like tube which encloses the droplet motion) and a symmetrical energy-momentum density tensor $t_{\mu\nu}$, both satisfying the conservation relations

$$\text{(1)} \qquad \begin{cases} \partial_\mu j_\mu = 0 \\ \partial_\nu t_{\mu\nu} = 0 \end{cases}$$

we can define the four-vector energy-momentum

$$G_\mu = \frac{1}{ic} \int_\Sigma t_{\mu 4} \, \mathrm{d}v_0 \,,$$

constant in time, where $\mathrm{d}v_0$ represents the three-dimensional volume element associated with a space-like plane cross-section.

This four-vector allows us to determine a special Lorentz frame Π_0 in which $G_i^{(0)} = 0$. In this frame we can define two physically important points:

— the center of matter density Y_k determined by the relation

$$Y_k^0 \left\{ \int_{\Sigma_0} j_4^0 \, \mathrm{d}v_0 \right\} = \int_{\Sigma_0} \varkappa_k^0 j_4^0 \, \mathrm{d}v_0 \,,$$

where the index 0 denotes the fact that the quantities are evaluated in the frame Π_0. This center, which corresponds to the classical geometrical center of the particle, moves along a world-line within the tube characterized by a proper time τ and a unitary tangent four-velocity v_μ

$$(v_\mu v_\mu = -c^2) \,;$$

— the center of gravity X_k determined by the relation

$$X_k^0 \left\{ \int_{\Sigma_0} t_4^0 \, \mathrm{d}v_0 \right\} = \int_{\Sigma_0} \varkappa_k^0 t_4^0 \, \mathrm{d}v_0 \,,$$

which moves in a straight line with a four-velocity parallel to G_μ.

We can also define a total angular momentum of the droplet with respect to the center of matter density by the relation

$$M_{\mu\nu} = \frac{1}{ic} \int_{\Sigma} [(\varkappa_\mu - Y_\mu) t_{\nu 4} - (\varkappa_\nu - Y_\nu) t_{\mu 4}] \, \mathrm{d}v \,.$$

Now the essential point on which is based this paper is that the global quantities G_μ, v_μ and $M_{\mu\nu}$ are (as a consequence of equations (1)) bound together by two sets of equations of motion, that is the four relations:

$$\dot{G}_\mu \equiv \frac{\mathrm{d}}{\mathrm{d}\tau} G_\mu \equiv v_\nu \, \partial_\nu G_\mu = 0 \,, \tag{2}$$

and the six relations:

$$\dot{M}_{\mu\nu} \equiv \frac{\mathrm{d}}{\mathrm{d}\tau} M_{\mu\nu} \equiv v_\lambda \, \partial_\lambda \, M_{\mu\nu} = G_\mu v_\nu - G_\nu v_\mu \,, \tag{3}$$

where $\dot{A}$ denotes $\mathrm{d}A/\mathrm{d}\tau$, the derivative along the world line followed by the center of matter density.

Evidently these set of 10 equations do not determine completely the motion of the 6 $M_{\mu\nu}$, 4 G_μ and 3 v_μ, so that 3 more equations are needed which represent various physical restrictions on the states of the droplet. One can

utilize for example the well known Weyssenhoff conditions

$$M_{\mu\nu}v_\nu = 0 \tag{4}$$

or various other sets such as those introduced by one of us (F.H.) [6].

To simplify the Lagrange formulation, we can adopt the usual method of passing from the isolated particle point of view to an hydrodynamical one, that is we substitute to the isolated particle a fluid of such particles without interaction [6]. More precisely, if we neglect the dimensions of the particles, we can consider such a fluid as a continuous distribution of variables multiplied by a scalar density ϱ which is assumed to be conservative. The center of matter density of each particle will follow a four-dimensional line of flow of that fluid, so we can multiply $M_{\mu\nu}$ and G_μ by ϱ and we have the 11 equations for the 11 quantities ϱ, $g_\mu = \varrho G_\mu$, $m_{\mu\nu} = \varrho M_{\mu\nu}$:

$$\left\{\begin{aligned} \dot{\varrho} &= 0\,, && (5)\\ \dot{g}_\mu &= 0\,, && (2)\\ \dot{m}_{\mu\nu} &= g_\mu v_\nu - g_\nu v_\mu\,, && (7) \end{aligned}\right.$$

where the dot denotes derivatives of tensor densities along the line of flow [2] (for instance $\dot{g}_\mu = \partial_\lambda(g_\mu v_\lambda)$).

The condition of Weyssenhoff is then:

$$m_{\mu\nu}v_\nu = 0\,. \tag{8}$$

The next step is now to look for a Lagrange function.

If we first concentrate on the 10 equations of motion (6) and (7) we can make the following remark:

Suppose we dispose of a Lagrange function depending on parameters q^λ. If the Lagrangian contains only the first derivatives of the variables:

$$\mathcal{L}(q^\lambda,\ \partial_\mu q^\lambda)\,.$$

BELINFANTE [7] and ROSENFELD [8] have established the following theorem: the expression $t_{\mu\nu} = (\partial\mathcal{L}/\partial(\partial_\nu q^\lambda))\,\partial_\mu q^\lambda - \delta_{\mu\nu}\mathcal{L}$ satisfies the 4 conservation relations

$$\partial_\nu t_{\mu\nu} = 0 \tag{9}$$

---

[6] F. HALBWACHS: *Théorie relativiste des fluides à spin* (Thèse de Paris, 1958) to be published further.

[7] F. J. BELINFANTE: *Physica*, **7**, 887 (1939).

[8] A. H. ROSENFELD: *Acad. Roy. Belgique*, **18**, 6 (1940).

as a consequence of the Euler equations on the q^λ's. Moreover if one denotes by $Z^{rs}_{[\mu\nu]}$ the operator corresponding to an infinitesimal Lorentz transform on the variables q^r, then the expression

$$f_{[\mu\nu]\alpha} = Z^{rs}_{[\mu\nu]} \frac{\partial \mathcal{L}}{\partial(\partial_\alpha q^r)} q^s ,$$

(where the indices r and s take all possible values of λ) satisfies the 6 conservation relations,

$$\partial_\alpha f_{\mu\nu\alpha} = t_{\mu\nu} - t_{\nu\mu} , \tag{9'}$$

also because of the Euler equation on the q^λ's.

We see then immediately that the 10 conservation equations (9) and (9') furnish exactly equations (6) and (7) provided that the $t_{\mu\nu}$ and the $f_{\mu\nu\alpha}$ deduced from the Lagrange function take the general forms:

$$t_{\mu\nu} = g_\mu(q^\lambda) \cdot v_\nu(q^\lambda) , \tag{10}$$

$$f_{\mu\nu\alpha} = \tfrac{1}{2} m_{\mu\nu}(q^\lambda) \cdot v_\alpha(q^\lambda) . \tag{11}$$

As a consequence, the general problem of deducing the equations of motion (6) and (7) of a liquid droplet from a Lagrange function depends now on our ability to discover a physically reasonable Lagrange function with corresponding $t_{\mu\nu}$ and $f_{\mu\nu\alpha}$ of the form (10) and (11).

Naturally, such a Lagrangian gives also Euler equations determining directly the behaviour of the variables q^λ. From these relations we can deduce in principle 3 relations which complete the set (6) and (7) and play the same role as Weyssenhoff's relation $m_{\mu\nu} v_\nu = 0$. The number of Euler equations is of course not restricted since a complete description of the motion of the droplet needs in principle an infinite number of variables q^λ. The more variables introduced, the more complete the description will be. However we must evidently try to introduce reasonable global variables in limited number which will define some sort of global average simplified behaviour of our droplet leaving aside details which evidently escape complete description. This treatment is somewhat analogous to the kinetic theory of gases or of plasmas, and the variables introduced play the role of collective variables corresponding to average regular motions inside the droplet.

The deduction of such Lagrangians will be attempted in the next two sections.

2. – Our first problem now is to introduce a convenient set of parameters q^λ which will correspond to global properties of the droplet.

A first variable is evident, namely the velocity v_μ of the center of matter density which we shall write henceforward $icb_\mu^{(4)}$ for reasons which will appear later (the index 4 is not a tensor index, but caracterises the vector).

The Lagrange function must evidently contain a term generalizing the classical total energy of rotation of the droplet. Such a term should be the product of the angular momentum by a term corresponding to the angular velocity, so it can be tentatively written in the form $T = \frac{1}{2} M_{\alpha\beta}\omega_{\alpha\beta}$, where $\omega_{[\alpha\beta]}$ is the realtivistic generalization of a global angular velocity.

Now it is very difficult *a priori* in hydrodynamics to define what is an angular velocity for the droplet considered as a whole with respect to a given point (such as the center of matter density) inside the droplet.

The simplest procedure is to go to the rest frame Σ_I of the center of matter density. In this frame we postulate that there exists a three-dimensional set of axes $b_\mu^{(i)}$, whose instantaneous rotation describes the instantaneous global rotation of the droplet, so that it is bound to its global distribution of matter. (We can take for example the principal axes of inertia with the aid of the bare matter density j_4^I). The projections of these axes on fixed axes constitute a rotation matrix C_k^j which naturally satisfies the relation:

$$C_k^j C_j^i = \delta_k^i .$$

The total instantaneous relativistic motion is then evidently obtained by adding to this space-rotation a Lorentz transform with the velocity $\boldsymbol{v}$ along the four velocity $b_\mu^{(4)}$, $\boldsymbol{v}$ and $b_\mu^{(4)}$ being related through:

$$b_j^{(4)} = \frac{1}{ic}\alpha v_j \qquad b_k^{(4)} = \alpha \qquad \alpha = (1 - v^2/c^2)^{-\frac{1}{2}} .$$

In other words, the three space-like vectors $b_\mu^{(k)}$ and the four-velocity $b_\mu^{(4)}$ form an orthogonal set of unitary vectors moving with the body, which satisfies the relations expressing the Lorentz transform (9):

$$b_\mu^{(4)} = -iv_\mu ,$$

$$b_4^{(k)} = iC_j^k v_j ,$$

$$b_i^{(k)} = C_i^k + \frac{C_j^k v_j v_i}{1 - iv_4} ,$$

and furthermore the following set of equivalent equations expressing their

(9) T. TAKABAYASI: *Nuovo Cimento*, **7**, 118 (1958).

orthogonality and unitary character:

$$b_{\mu}^{(\xi)} = \varepsilon^{\xi\eta\zeta\iota}\, \varepsilon_{\mu\nu\alpha\beta}\, b_{\nu}^{(\eta)} b_{\alpha}^{(\zeta)} b_{\beta}^{(\iota)} \tag{12}$$

$$b_{\mu}^{(\xi)} b_{\nu}^{(\xi)} = \delta_{\mu\nu}\,, \tag{13}$$

$$b_{\mu}^{(\xi)} b_{\mu}^{(\eta)} = \delta^{\xi\eta}\,, \tag{14}$$

(where $\varepsilon_{\mu\nu\alpha\beta}$ or $\varepsilon^{\xi\eta\zeta\iota}$ is the completely antisymmetrical symbol of Levi-Civita)

The instaneous angular velocity associated with this moving frame Σ_b is just ([6])

$$\omega_{\mu\nu} = \tfrac{1}{2}(\dot{b}_{\mu}^{(\xi)} b_{\nu}^{(\xi)} - \dot{b}_{\nu}^{(\xi)} b_{\mu}^{(\xi)}) \tag{15}$$

and we assume that this is the term which we must introduce in the kinetic energy T and which defines quantities $\varepsilon_{\alpha\beta}$ canonically conjugate to the $m_{\alpha\beta}$ Physically these assumptions could be justified by saying that during a very short interval of proper time the droplet rotates in the rest frame like a rigid body.

We can define directly such quantities in special cases. Suppose for instance that the current density j_{μ} inside the droplet varies very slowly. Then if we denote by u_{μ} the unitary four-vector parallel to j_{μ} it is well known that one can write:

$$\omega_{\mu\nu} = \tfrac{1}{2}(\partial_{\mu} u_{\nu} - \partial_{\nu} u_{\mu})\ ([10])\,.$$

But this is not true in general since the droplet can contain subvortices and many complex motions so that one cannot suppose that u_{μ} varies slowly over the droplet as a whole.

However we can still define such a quantity even in more complex cases. Suppose for instance that the current motion inside the droplet can be split into a regular slowly changing part, and an irregular part. If this latter part is sufficiently complex, we can neglect it in average and define $\omega_{\mu\nu}$ with the help of the regular part.

Independently of these physical considerations, we can say that the components $b_{\mu}^{(\xi)}$ constitute a set of variables attached to the global kinematical properties of the droplet. These variables where first introduced in physical theories by Einstein and Kramers and so we shall call them henceforward EK variables.

A next step is to express $m_{\mu\nu}$ in terms of suitable tensor variables. This can be easily made in relation with the preceeding EK variable $b_{\mu}^{(4)}$. As was

---

([10]) L. Brillouin: *Les tenseurs en mécanique et en élasticité* (Paris, 1938).

shown by BOHM and one of us (J.-P. V.) [1] one can use $b_\mu^{(4)}$ to split $m_{\mu\nu}$ in a sum of two bivectors, namely:

$$m_{\mu\nu} = \varrho \varepsilon_{\mu\nu\alpha\beta} s_\alpha b_\beta^{(4)} + i\varrho(b_\mu^{(4)} t_\nu - b_\nu^{(4)} t_\mu) , \tag{16}$$

where the vectors s_μ and t_μ are respectively:

$$s_\mu = \frac{1}{2\varrho} \varepsilon_{\mu\nu\alpha\beta} b_\nu^{(4)} m_{\alpha\beta} , \tag{17}$$

$$t_\mu = \frac{i}{\varrho} m_{\mu\nu} b_\nu^{(4)} . \tag{18}$$

It is then clear that s_μ and t_μ, which lie both in the space of Σ_1, define a set of six independent variables which determine $m_{\mu\nu}$.

Before we go any further in the Lagrangian, let us make a physical remark. It is not astonishing that $m_{\mu\nu}$ and $\omega_{\mu\nu}$ are in general different skew tensors. As we have seen, it is a characteristic property of liquids that conjugate variables are not parallel in general. Thus g_μ and v_μ are not colinear, except in very particular cases, such as the spinless fluid. Physically, it can be understood in the following way: the angular velocity moves over the droplet and changes its shape as it rotates, so that the internal tensions change in general, modifying the angular momentum in a complex way. The special case where the two tensors are parallel, which is the general case for rigid classical bodies, cannot be used in relativistic theories (*).

To complete the Lagrangian, we must evidently add to T the term corresponding to the rest mass energy of the matter: $\varrho \mathcal{M}_0 c^2$.

The sum of these two terms corresponds evidently to the total energy. Furthermore we must add a certain number of terms with Lagrange multiplyiers imposing restrictions on our variables. The first term imposing the conservation of the current (5) can be written:

$$ic\varrho b_\mu^{(4)} \partial_\mu S .$$

And then we must have a term imposing unitarity and orthogonality to the $b_\mu^{(\xi)}$ EK variables, that is $\lambda_{\mu\nu}(b_\mu^\xi b_\nu^\xi - \delta_{\mu\nu})$ ($\lambda_{\mu\nu}$ is evidently symmetrical). Finally, we get the following Lagrangian

$$\mathcal{L} = \varrho \mathcal{M}_0 c^2 + \frac{ic}{2} \varrho [\varepsilon_{\mu\nu\alpha\beta} s_\alpha b_\beta^{(4)} + i(b_\mu^{(4)} t_\nu - b_\nu^{(4)} t_\mu)] b_\lambda^{(4)} \partial_\lambda b_\mu^{(\xi)} b_\nu^{(\xi)} + \\ + ic\varrho b_\mu^{(4)} \partial_\mu S + \lambda_{\mu\nu}(b_\mu^{(\xi)} b_\nu^{(\xi)} - \delta_{\mu\nu}) , \tag{19}$$

(*) In a sense this is analoguous to the well known fact that in the neutron case the charge repartition is such that there is no total charge but there remains an anomalous magnetic moment.

in which we frequently replace for the sake of simplicity the bracket by m_μ. and $ic b_\mu^{(4)}$ by v_μ.

Before we derive the equations of motion, it is necessary to remember that the droplet is describable by a set of 10 dynamical variables (G_μ, $M_{\mu\nu}$) and 6 kinematical ones describing the angular velocity. These 10 variables, plus $b_\mu^{(4)}$, satisfy the 10 conservation equations, so that these equations leave 3 degrees of freedom open. In fact there exist 3 more degrees, because of the $b_\mu^{(r)}$, which do not appear explicitly in these equations. Now any given Lagrangian determines all variables through the corresponding Euler equations, that is, in our general case, 16 variables. As we have shown, Weyssenhoff's case is very special in the sense, that 3 relations more between $b_\mu^{(\xi)}$ and $m_{\mu\nu}$ were introduced, and must be derived as Euler equations from the Lagrangian.

As a consequence the 13 equations (6), (7), (8) can be integrated separately, but the other 3 variables $b_\mu^{(r)}$ are also determined according to the 3 remaining Euler equations which evidently depend on the explicit form of the Lagrangian chosen. Of course, many Lagrangians give the correct set of the 13 relations; so that Weyssenhoff's motion for the center of matter density can be associated with many modes of internal motions of the liquid droplet, which correspond to various possible distributions of the internal Poincaré stresses which hold its elements together.

Let us now write the equations of motion. First the Euler equations relative to the variables S and $\lambda_{\mu\nu}$ provide immediately the condition of conservation for ϱ, and the condition (13) for the set of EK variables. Then we can use some of the Euler equations to eliminate the redundant variables, namely the Lagrange coefficients $\partial_\mu S$ and $\lambda_{\mu\nu}$. The equation relative to the variable ϱ gives:

$$\mathcal{M}_0 c^2 + \frac{1}{2}\frac{m_{\mu\nu}}{\varrho}\dot{b}_\mu^{(\xi)} b_\nu^{(\xi)} + \dot{S} = 0\,,$$

that is:

$$\varrho\dot{S} = -e\mathcal{M}_0 c^2 - \tfrac{1}{2} m_{\mu\nu}\dot{b}_\mu^{(\xi)} b_\nu^{(\xi)}\,. \tag{20}$$

Then the equations relative to the space-like EK variables $\mathcal{C}_{\mu\nu}^{(r)}$ give:

$$\partial_\lambda(\tfrac{1}{2} m_{\nu\mu} v_\lambda b_\mu^{(r)} = \tfrac{1}{2} m_{\mu\nu}\dot{b}_\mu^{(r)} + 2\lambda_{\mu\nu} b_\mu^{(r)}$$

that is:

$$2m_{\mu\nu}\dot{b}_\lambda^{(r)} + \dot{m}_{\mu\lambda} b_\lambda^{(r)} - 4\lambda_{\mu\lambda} b_\lambda^{(r)} = 0\,, \tag{21}$$

while the equation relative to $b_\mu^{(4)}$ gives in the same way:

$$\partial_\lambda(\tfrac{1}{2} m_{\nu\mu} v_\lambda b_\mu^{(4)}) = \tfrac{1}{2} m_{\mu\nu}\dot{b}_\mu^{(4)} + 2\lambda_{\mu\nu} b_\mu^{(4)} + \tfrac{1}{2}\varrho[\varepsilon_{\mu\nu\lambda\beta} s_\nu \dot{b}_\beta^{(\xi)} b_\lambda^{(\xi)} + it_\nu(\dot{b}_\mu^{(\xi)} b_\nu^{(\xi)} - \dot{b}_\nu^{(\xi)} b_\mu^{(\xi)})]$$

or else:

$$(22)\quad 2m_{\mu\lambda}\dot{b}_{\lambda}^{(4)} + \dot{m}_{\mu\lambda}b_{\lambda}^{(4)} - 4\lambda_{\mu\lambda}b_{\lambda}^{(4)} + + \varrho\varepsilon_{\mu\lambda\varkappa\beta}\dot{b}_{\lambda}^{(\xi)}s_{\alpha}b_{\beta}^{(\xi)} - \\ - \varrho i t_{\lambda}(\dot{b}_{\mu}^{(\xi)}b_{\lambda}^{(\xi)} - \dot{b}_{\lambda}^{(\xi)}b_{\mu}^{(\xi)}) + icm_{\alpha\beta}b_{\alpha}^{(\xi)}\partial_{\mu}b_{\beta}^{(\xi)} - 2ic\varrho\,\partial_{\mu}S = 0\,.$$

Multiplying (21) by $b_{\mu}^{(r)}$ (with contraction with respect to r) and (22) by $b_{\mu}^{(4)}$ and adding, we get, taking into account relation (13):

$$2m_{\mu\lambda}\dot{b}_{\lambda}^{(\xi)}b_{\nu}^{(\xi)} + \dot{m}_{\mu\nu} - 4\lambda_{\mu\nu} + \varrho\varepsilon_{\mu\lambda\varkappa\beta}\dot{b}_{\lambda}^{(\xi)}s_{\alpha}b_{\beta}^{(\xi)}b_{\nu}^{(4)} - \\ - \varrho i t_{\lambda}b_{\nu}^{(4)}(\dot{b}_{\mu}^{(\xi)}b_{\lambda}^{(\xi)} - \dot{b}_{\lambda}^{(\xi)}b_{\mu}^{(\xi)}) + icb_{\nu}^{(4)}m_{\alpha\beta}b_{\alpha}^{(\xi)}\partial_{\mu}b_{\beta}^{(\xi)} - 2icb_{\nu}^{(4)}\varrho\,\partial_{\mu}S = 0\,.$$

Taking the antisymmetrical part, we eliminate $\lambda_{\mu\nu}$ because of its simmetrical character. Multiplying the resulting equation by $b_{\nu}^{(4)}$, we get, after a short calculation in which we use equations (18), (13) and (20):

$$(23)\quad 2ic\varrho\,\partial_{\mu}S = -2\varrho\mathcal{M}_0c^2b_{\mu}^{(4)} - 2i\varrho(\dot{t}_{\mu} + t_{\lambda}\dot{b}_{\lambda}^{(4)}b_{\mu}^{(4)}) + \\ + icm_{\alpha\beta}b_{\alpha}^{(\xi)}\partial_{\mu}b_{\beta}^{(\xi)} + \varrho\varepsilon_{\nu\lambda\alpha\beta}b_{\lambda}^{(\xi)}s_{\alpha}\dot{b}_{\beta}^{(\xi)}(\delta_{\mu\nu} - b_{\mu}^{(4)}b_{\nu}^{(4)})\,.$$

An important consequence of this relation is that:

$$(24)\qquad \mathcal{L} = 0\,.$$

Now we can easily show that the Lagrangian (19) gives the correct results, for the tensors $t_{\mu\nu}$ and $f_{\mu\nu\lambda}$ take the forms (10) and (11).

$$t_{\mu\nu} = \frac{\partial\mathcal{L}}{\partial(\partial_{\nu}S)}\,\partial_{\mu}S + \frac{\partial\mathcal{L}}{\partial(\partial_{\nu}b_{\lambda}^{(\xi)})}\,\partial_{\mu}b_{\lambda}^{(\xi)}$$

because of (24). An immediate calculation furnishes:

$$t_{\mu\nu} = v_{\nu}(\varrho\,\partial_{\mu}S + \tfrac{1}{2}m_{\lambda\alpha}b_{\alpha}^{(\xi)}\partial_{\mu}b_{\lambda}^{(\xi)})$$

so that we have a linear momentum density:

$$(25)\qquad g_{\mu} = \varrho\,\partial_{\mu}S + \tfrac{1}{2}m_{\lambda\alpha}b_{\alpha}^{(\xi)}\partial_{\mu}b_{\lambda}^{(\xi)}\,.$$

One sees immediately that the form (25) is the generalization of the classical relativistic expression for the momentum. S is just the relativistic Jakobi function, while the second term represents the contribution of the internal rotation.

If we replace $\partial_\mu S$ by its expression (23) we get:

$$g_\mu = ic\varrho\mathcal{M}_0 b_\mu^{(4)} - \frac{\varrho}{c}\,(\dot{t}_\mu + t_\lambda \dot{b}_\lambda^{(4)} b_\mu^{(4)}) + \frac{\varrho}{2ic}\,\varepsilon_{\nu\lambda\alpha\beta} b_\lambda^{(\xi)} s_\alpha \dot{b}_\beta^{(\xi)} (\delta_{\mu\nu} - b_\mu^{(4)} b_\nu^{(4)})\,.$$

That is, for the so called « transversal momentum »:

$$(26) \qquad p_\mu = ic\varrho\mathcal{M}_0 b_\mu^{(4)} - g_\mu = \frac{\varrho}{c}\left[\dot{t}_\mu + t_\lambda \dot{b}_\lambda^{(4)} b_\mu^{(4)} + \frac{i}{2}\,\varepsilon_{\nu\lambda\alpha\beta} b_\lambda^{(\xi)} s_\alpha \dot{b}_\beta^{(\xi)} (\delta_{\mu\nu} - b_\mu^{(4)} b_\nu^{(4)})\right].$$

Of course the conservation equation $\partial_\nu t_{\mu\nu} = 0$ provides as usual the hydrodynamical equation: $\dot{g}_\mu = 0$.

Let us show in the same way that the Rosenfeld-Belinfante tensor $f_{\mu\nu\lambda}$ takes the correct form (11).

We have

$$\frac{\partial \mathcal{L}}{\partial(\partial_\lambda b_\alpha^{(\xi)})} = \frac{1}{2} m_{\alpha\gamma}\, icb_\lambda^{(4)} b_\gamma^{(\xi)}\,.$$

The operator of an infinitesimal relativistic rotation for a vector is, as is well known:

$$\mathcal{Z}_{\mu\nu}^{\alpha\beta} = \tfrac{1}{2}(\delta_{\alpha\mu}\delta_{\beta\nu} - \delta_{\alpha\nu}\delta_{\beta\mu})$$

so that we have immediately:

$$f_{\mu\nu\lambda} = \tfrac{1}{4} icm_{\alpha\gamma} b_\lambda^{(4)} b_\gamma^{(\xi)} (\delta_{\alpha\mu}\delta_{\beta\nu} - \delta_{\alpha\nu}\delta_{\beta\mu}) b_\beta^{(\xi)} = \tfrac{1}{4} v_\lambda (m_{\mu\gamma} b_\nu^{(\xi)} - m_{\nu\gamma} b_\mu^{(\xi)}) b_\gamma^{(\xi)}\,.$$

Or because of relation (13):

$$f_{\mu\nu\lambda} = \tfrac{1}{2} m_{\mu\nu} v_\lambda\,,$$

which is just the correct form.

As we noticed above, we can obtain from our Lagrangian 6 relations too, concerning the 6 kinematical quantities whose evolution is not determined by the 10 dynamical equations. Namely:

Derivation with respect to t_μ gives:

$$icb_\nu^{(4)} b_\lambda^{(4)} (\partial_\lambda b_\nu^{(\xi)} b_\mu^{(\xi)} - \partial_\lambda b_\mu^{(\xi)} b_\nu^{(\xi)}) = 0\,,$$

that is

$$b_\nu^{(4)} (\dot{b}_\nu^{(\xi)} b_\mu^{(\xi)} - \dot{b}_\mu^{(\xi)} b_\nu^{(\xi)}) = 0$$

or in other words:

$$\omega_{\mu\nu} v_\nu = 0\,.$$

Derivation with respect to s_μ gives on the other hand:

$$ic b_\lambda^{(4)} \partial_\lambda b_\alpha^{(\xi)} b_\beta^{(\xi)} \varepsilon_{\mu\nu\alpha\beta} b_\nu^{(4)} = 0 .$$

That is

$$\varepsilon_{\mu\nu\alpha\beta} b_\nu^{(4)} \dot{b}_\alpha^{(\xi)} b_\beta^{(\xi)} = 0 .$$

Or, in other words:

$$\varepsilon_{\mu\nu\alpha\beta} \omega_{\alpha\beta} v_\nu = 0 .$$

Therefore the tensor $\omega_{\mu\nu}$ is zero.

So we see that the above Lagrangian formulation is not at all equivalent to the bare set of the 10 dynamical equations expressing the general motion of the relativistic droplet. It represents a very particular case of that motion, namely the one where the matter of the droplet, considered in a purely kinematical sense, has no instantaneous rotation. In this point of view, such a motion generalizes in a natural way the classical motion of the newtonian point-particle.

It might seem strange at first sight that one should have an angular momentum density without kinematical global internal rotation. But a close examination shows that $m_{\mu\nu}$ and $\omega_{\mu\nu}$ are very different kinds of physical quantities. $m_{\mu\nu}$ depends on the internal stresses of the droplet, so that if these stresses vary with time in such a way they would not disturb the global distribution of matter, one could have angular momentum without angular velocity (*).

Taking account of the above supplementary relations in the expression (26) of the transversal momentum, we get simply: $p_\mu = (\varrho/c)\dot{t}_\mu$. In other words, in the case considered, the non classical transversal momentum does not result from any internal rotation, but only from the variations of the vector t_μ, which represents, as is well known (1) the distance between the center of matter density and the so-called « center of mass ».

3. – According to our program, we shall particularize the general motion defined by the dynamical equations (6) and (7) with the aid of some supplementary conditions. The most interesting way is to state some relations between the dynamical angular momentum $m_{\mu\nu}$ and the set of kinematical vectors $b_\mu^{(\xi)}$. The simplest binding relation is naturally Weyssenhoff's one, which assumes that $m_{\mu\nu}$ is orthogonal to the four-velocity.

As is well known, such a relation added to the 10 preceeding ones, furnishes a set of 13 equations for 13 variables, these equations can be completely integrated and it seems that the motion is determined in an unique way. But

---

(*) This case corresponds to a complete decoupling between $M_{\nu\beta}$ and $\omega_{\nu\beta}$, which is evidently not the case in general.

we note that no statement has been made about the 3 other EK variables, so they are entirely arbitrary.

Now to treat this problem by Lagrange's method, we must add to the Lagrangian (19) a term $l_\mu t_\mu$, which will immediately furnish by derivation with respect to the Lagrange multiplyer l_μ the condition needed.

But then we get a supplementary term in the Euler equation relative to t_μ, which becomes:

$$\omega_{\mu\nu} v_\nu + l_\mu = 0$$

and then does no longer represent a restriction on $\omega_{\mu\nu}$, but gives the expression for the new variable l_μ: So we are left with the restrictive condition

$$\varepsilon_{\mu\nu\alpha\beta}\omega_{\alpha\beta} v_\nu = 0 \,. \tag{27}$$

If we express $\omega_{\alpha\beta}$ with the aid of the EK variables we have:

$$\varepsilon_{\mu\nu\alpha\beta}\dot{b}_\alpha^{(\xi)} b_\beta^{(\xi)} b_\nu^{(4)} = 0$$

and we see, multiplying by $b_\lambda^{(4)}$ and taking the dual, that we have:

$$\dot{b}_\mu^{(l)} b_\nu^{(4)} - \dot{b}_\mu^{(4)} b_\nu^{(k)} = 0 \,. \tag{28}$$

In other words, the derivatives of the three space-like EK vectors are parallel to the four-velocity. Or else, noting that with regard to the proper frame Σ_I of the center of matter density, $\omega_{\mu\nu}$ has only time components, we see that the kinematical motion in the frame Σ_I is purely accelerative without any rotation.

Furthermore, multiplying (27) by $b_\lambda^{(4)}$ and taking the dual, we obtain:

$$\dot{b}_\mu^{(k)} b_\nu^{(k)} - \dot{b}_\nu^{(k)} b_\mu^{(k)} = 0$$

that is

$$\dot{b}_\mu^{(k)} b_\nu^{(k)} = 0 \tag{29}$$

the set (28), (29) beeing equivalent to (27).

If we take into account the latter relations, and remove the terms containing t_μ, which vanishes, the expression (26) becomes

$$p_\mu = -\frac{1}{2}\frac{\varrho}{ic}\varepsilon_{\mu\lambda\alpha\beta} b_\lambda^{(4)} \varepsilon_\alpha \dot{b}_\beta^{(4)} \,,$$

that is

$$p_\mu = -\frac{1}{c^2} m_{\mu\nu} \dot{v}_\nu \,,$$

which is a well known consequence of Weyssenhoff's laws of motion.

Finally, we can impose a further restriction by the assumption that the dynamical spin vector s_μ is parallel to the kinematical vector $b_\mu^{(3)}$. We must then add to our Lagrangian a further Lagrange term,

$$\eta_{\mu\nu}\varepsilon_{\mu\nu\alpha\beta}s_\alpha b_\beta^{(3)}$$

so that the derivation with respect to the Lagrange multiplyer $\eta_{\mu\nu}$ (which is evidently antisymmetrical) gives the condition of parallelism:

$$\varepsilon_{\mu\nu\alpha\beta}s_\alpha b_\beta^{(3)} = 0\,.$$

Then the condition (27) becomes

$$\varepsilon_{\mu\nu\alpha\beta}\dot{b}_\alpha^{(\xi)}b_\beta^{(\xi)}b_\nu^{(k)} + \eta_{\alpha\beta}\varepsilon_{\alpha\beta\mu\nu}b_\nu^{(3)} = 0\,.$$

This introduces no longer any restriction to the motion, but simply provides the expression of the new variable $\eta_{\mu\nu}$.

The total Lagrangian is then finally:

$$\mathcal{L} = \varrho\mathcal{M}_0c^2 + \frac{ic\varrho}{2}[\varepsilon_{\mu\nu\alpha\beta}s_\alpha b_\beta^{(4)} + i(b_\mu^{(4)}t_\nu - b_\nu^{(4)}t_\mu)]b_\lambda^{(4)}\partial_\lambda b_\mu^{(\xi)}b_\nu^{(\xi)} + \\ + ic\varrho b_\mu^{(4)}\partial_\mu S + \lambda_{\mu\nu}(b_\mu^{(\xi)}b_\nu^{(\xi)} - \delta_{\mu\nu}) + l_\mu t_\mu + \eta_{\mu\nu}\varepsilon_{\mu\nu\alpha\beta}s_\alpha b_\beta^{(3)}\,.$$

We note that, with the latter assumption, the angular momentum density takes the form:

$$m_{\mu\nu} = \varrho\hbar_0\varepsilon_{\mu\nu\alpha\beta}b_\alpha^{(3)}b_\beta^{(4)}\,,$$

where $\hbar_0$ designes the magnitude of the spin s_μ.

Then the rotation energy becomes:

$$T = \tfrac{1}{2}\varrho\hbar_0\varepsilon_{\mu\nu\alpha\beta}b_\alpha^{(3)}b_\beta^{(4)}\dot{b}_\mu^{(\xi)}b_\nu^{(\xi)}\,.$$

The terms corresponding to $\xi = 3$ and $\xi = 4$ vanish

$$T = \tfrac{1}{2}\varrho\hbar_0\varepsilon_{\mu\nu\alpha\beta}b_\alpha^{(3)}b_\beta^{(k)}(\dot{b}_\mu^{(1)}b_\nu^{(1)} + \dot{b}_\mu^{(2)}b_\nu^{(2)})\,,$$

which becomes, taking into account the relation (12)

$$T = \varrho\hbar_0 b_\mu^{(1)}\dot{b}_\mu^{(2)} \equiv ic\varrho\hbar_0 b_\lambda^{(4)}b_\mu^{(1)}\partial_\lambda b_\mu^{(2)}\,.$$

Then, removing the redundant variables s_μ and t_μ and the corresponding

Lagrange conditions, we get for the Lagrangian the most simplified form

$$\mathcal{L} = \varrho \mathcal{M}_0 c^2 + ic\varrho h_0 b_\lambda^{(4)} b_\mu^{(1)} \partial_\lambda b_\mu^{(2)} + ic\varrho\, b_\mu^{(4)} \partial_\mu S + \lambda_{\mu\nu}(b_\mu^{(\xi)} b_\nu^{(\xi)} - \delta_{\mu\nu}) ,$$

which was already proposed by two of us (F.H. and J.-P. V. ([6,11])) and which appears to correspond to the particular case where the angular momentum and angular velocity are related in a very strict way. It is easy to show that in this case the expression (30) is also valid.

4. – Conclusion.

In conclusion we wish to indicate a few possible extensions of the theory developped in the paper.

Evidently this Lagrange formulation opens the way to wide developments of the relativistic hydrodynamics. Introducing more variables into the Lagrange function, it is possible in principle to describe more and more properties of the isolated liquid droplet.

Another possible extension is to introduce coupling terms between these droplets in order to develop the theory of relativistic hydrodynamics for fluids presenting internal angular momentum density (spinning fluids). The Lagrange formalism is very convenient to treat such theories, since it is only necessary to introduce in the Lagrange function suitable coupling terms. Some steps in this direction have already been made by one of us (F.H.) ([6]).

Another possibility is to study the isolated droplet in special physical conditions. In a further paper, for instance, we propose to study the relativistic hydrodynamics of rotating fluid droplets with negligible rest mass, moving with velocities approaching the velocity of light.

The Lagrange formalism also offers the possibility to quantize the preceeding theory in the conventional way: one deduces the hamiltonian from the lagrangian and replaces the Poisson brackets by the usual commutators. In this way one discovers a new class of relativistic wave equations corresponding to all possible states of relativistic spinning droplets. Some of these equations could eventually correspond to new types of particles which have been shown to exist in nature.

Finally, and this seems to be the most promising line of research, the preceeding model paves the way to quantize internal states of motion of relativistic fluid droplet. This results from common work made in Bristol by Professor Bohm and one of us (J.-P. V.).

([11]) B. C. Unal et J.-P. Vigier: *Comptes-Rendus Acad. Sciences*, **245**, 1787, 1890 (1957).

If we define internal stable quantum states by the physical property that the angular velocity $\omega_{\mu\nu}$ and angular momentum $m_{\mu\nu}$ come back periodically in the same relative positions inside the droplet, one can show that such states determine a new set of internal quantum numbers which characterize different types of periodic motions of these two quantities. As we shall see ([12]) these quantum numbers are very similar to the numbers introduced by NISHIJIMA, GELL-MANN and TIOMNO to classify elementary particles.

* * *

We wish to express our gratitude to Professors DE BROGLIE, BOHM and TAKABAYASI. This paper is a natural development of common researches carried out in Bristol with Professor BOHM; and professor TABAKAYASI's work and advices have greatly contributed to the clarification of the basic conceptions used therein.

([12]) In a further paper.

RIASSUNTO (*)

Si studia la teoria generale delle masse fluide in moto relativistico in termini di un gruppo di variabili originariamente proposte da Einstein e Kramers. Le equazioni generali del moto impostate direttamente da Bohm e uno di noi (J.-P. V.) appaiono allora come equazioni conservative dedotte da un lagrangiano scalare di queste nuove variabili. Questo procedimento apre la via ad una quantizzazione del moto interno di un modello di particelle estese in uno spazio reale; modello fortemente suggerito dai risultati sperimentali di Hofstadter.

(*) *Traduzione a cura della Redazione.*

IL NUOVO CIMENTO Vol. X, N. 5 1° Dicembre 1958

Hyperfragment Decay Energy and Angular Distribution - I.

J. Szymański

Institute of Theoretical Physics - Warsaw University, Warsaw

(ricevuto il 19 Settembre 1958)

Summary. — Impulse approximation is applied to the hyperfragment decay. π-mesons energy distribution is obtained for the ${}^5\mathrm{He}_\Lambda$ case neglecting π-α interaction. Results are compared with experiment and the validity of impulse approximation is discussed.

1. – Introduction.

Decays of bound Λ, both mesonic and non-mesonic, can serve as a source of a large quantity of data on hyperfragments, and, indirectly, on the interactions of Λ with nucleons. From the analysis of the decay we can draw conclusions concerning the role of singlet or triplet potential as suggested by Dalitz [1] and Chow-Širokov [2]. On the other hand, it seems that much valuable information can be obtained by analysing the angular and energy distribution in the case of the three-body hfr decay, *e.g.* ${}^4\mathrm{H}_\Lambda \to \mathrm{t}+\mathrm{p}+\pi$. If the strong interactions of the decay products can be successfully taken into account, it may be expected that with somewhat better statistics than those at present available it will be possible to check the wave functions obtained by calculating the binding energy [3,4] and indirectly the Λ-N potential. In this paper we deal merely with the mesonic decays, particular consideration

---

(1) R. H. Dalitz: *The nuclear interaction of the* Λ*-hyperon* (preprint).
(2) K. C. Chow and M. J. Širokov: *Nucl. Phys.*, **6**, 10 (1958).
(3) P. Zieliński: *Nuovo Cimento*, **3**, 1479 (1956).
(4) J. Schneps, W. F. Fry and M. S. Swami: *Phys. Rev.*, **106**, 1062 (1957).

being given to the interaction of the final decay products; that this influence is important is indicated by the angular distributions as regards $\cos\theta = \hat{p}\hat{k}$ in the apparent rest system of the Λ in which $k = -q$; here k, q, p is the momentum of the π-meson, proton, and the recoil, respectively for the decay $\mathrm{hf} \to R + \mathrm{p} + \pi$. By $\hat{a}$ we denote the versor with the direction of vector $\boldsymbol{a}$. For this decay we have a distinct anisotropy and asymmetry independent of the hyperfragment. If the interaction is neglected and it is assumed that Λ has a spin $\frac{1}{2}$ (which now seems rather certain) and is bound with an orbital momentum $l = 0$ we obtain *e.g.* for ${}^5\mathrm{He}_\Lambda$ an isotropic distribution. If Λ were to be bound with a higher orbital momentum, which is not very probable, then we can obtain an anisotropy, but it must be symmetric with respect to the plane $\cos\theta = 0$, while experiment ([5]) shows a distinct asymmetry. Eighteen cases have been found in which $\cos\theta$ is negative and only one case in which it is positive.

In principle, our calculations, which involve the decay products, coincide with the impulse approximation. The modification introduced is that we give the method by means of which the virtual protons may be taken into account, these protons becoming real ones only after scattering. The ratios of the cross sections for the scattering of protons and pions on light nuclei allows one to assume that the main interaction will be that of p with the core, and therefore in the present calculations too we limit ourselves to consideration of only this interaction. In addition to neglecting the interaction we make use of the following other assumptions: *a*) in light hyperfragments $Z \leqslant 2$ the greater part of the time is spent outside the core ([6,7]); *b*) if the decay occurs outside the core then the operator for the $\Lambda \to \mathrm{p} + \pi$ which already takes into account the basic part of the strong interactions has the form

$$H_1 = g \int \psi_\mathrm{p}^* (1 + \beta \boldsymbol{\sigma k}) \psi_\Lambda \varphi_\pi \, \mathrm{d}\tau \,. \tag{1}$$

where g and β are constants that are independent of the energy. For a free Λ the only possible shape of the transition operator is

$$H_1' = g' \int \overline{\psi}_\mathrm{p} (1 + \delta\gamma_5) \psi_\Lambda \varphi_\pi \, \mathrm{d}\tau \,. \tag{2}$$

([5]) R. Levi-Setti, W. Slater and V. L. Telegdi: *Reported on the VII Rochester Conference*, 1957 pag. VIII-9. A world survey of experimental data on hypernuclei preliminary report preprint.

([6]) N. Dallaporta and F. Ferrari: *Nuovo Cimento*, **5**, 111 (1957).

([7]) H. Wilhelmson and P. Zieliński: *Nucl. Phys.*, **6**, 219 (1958).

3797

This follows from the requirement of relativistic invariance (see *e.g.* STAPP [8]), J. WERLE [9]). The non-relativistic approximation of (2) is (1).

The adoption of the form (1) for the operator of the vertex of a weak interaction corresponds to an artificial separation of the decay process into two stages. In the first stage we have only p interacting with π, in the second we have p interacting with the core and π with the core. This separation seems justified if we note that the range of the π-p potential is of the order of the Compton wavelength of the nucleon. We shall now discuss assumption (*a*) is somewhat more detail. For this purpose we expand the wave function of the hyperfragment in terms of the eigenfunction of the core

$$\Psi_0(r\xi) = \alpha_0\chi_0(\xi)\, f_0(\boldsymbol{r}) + \sum_{n=1}^{\infty} \alpha_n \chi_n(\xi)\, f_n(\boldsymbol{r}) = \Psi_1 + \Psi_2 , \tag{3}$$

here ξ denotes the internal variables of the core $\boldsymbol{r} = \boldsymbol{r}_c - \boldsymbol{r}_\Lambda$, $\boldsymbol{r}_\Lambda$ and $\boldsymbol{r}_c$ denotes the corresponding co-ordinates of the center of mass of the core and the Λ particle. The functions $f_n(\boldsymbol{r})$ are defined by the formula

$$f_n(\boldsymbol{r}) = N \int \Psi_0(\boldsymbol{r}\xi)\, \chi_n^*(\xi)\, \mathrm{d}\xi \, . \tag{4}$$

N is the normalizing coefficient and α_n the coefficient of fractional parentage. It is seen at once that the function $f_n(\boldsymbol{r})$, $n \neq 0$ can be essentially different from zero only in the region of the core because the range of the Λ-N forces is small, and therefore a deformation of the core may be expected only when Λ is outside it. For nuclei with $Z = 2$ the probability of mesonic decay inside the core is decreased by the Pauli principle. Besides, inside the core there is a competitive non-mesonic decay because of the direct proximity of the nucleons. These the facts which allow us to suppose that even if there is some core deformation the chief contribution to the mesonic decay is made only by the first part of the function (3) $\Psi_1 = \alpha_0\chi_0(\xi)\, f_0(\boldsymbol{r})$, since $f_0(\boldsymbol{r})$ is essentially different from zero outside the core.

Our work has been divided into two parts. In the first part we discuss the computational method and we give the results obtained for the energy distribution of the π-mesons from the decay ${}^5\mathrm{He}_\Lambda \to \alpha + \mathrm{p} + \pi$. In a forthcoming paper, which will be published after completion of the numerical calculations, we shall discuss the angular distributions for the decay of light hyperfragments.

([8]) H. P. STAPP: *Phys. Rev.*, **103**, 425 (1956).

([9]) J. WERLE: *Phenomenological theory of the S-matrix* (to be published).

2. – Method of calculation.

The Schrödinger equation for the decay of a hyperfragment to an accuracy of g/g is the coupling constant of weak interactions and has the form

$$(E - H)\Psi = H_1\Psi_0 ,$$

here

$$H = H_c + K_\pi + K_A + W_1 + W_2 \qquad W_1 = \sum_{i=1}^{A-1} V_{iA} ,$$

$$H_c = \sum_{n=1}^{A-1} K_n + \tfrac{1}{2}\sum_{n\neq m}^{A-1} V_{nm} = K + V \qquad W_2 = \sum_{i=1}^{A-1} V_{i\pi} ,$$

where A is the atomic number of the hyperfragment K_n, K_π are the kinetic energies of the n-th nucleon and the π meson respectively, V_{ij}, $V_{i\pi}$ are the potential energies of the i-th nucleon with respect to the j-th and the π meson with respect to the i-th nucleon.

In the general case (4) the solution has the form (see *e.g.* CHEW-GOLDBERGER)

$$\Psi = \Phi_0 + \frac{1}{E - H + i\eta} H_1\Psi_0 , \tag{5}$$

where Φ_0 satisfies the equation $(E - H)\Phi_0 = 0$.

In our case $\Phi_0 = 0$, which means that initially we have only hyperfragments. We make the transformation

$$\frac{1}{E - H + i\eta} H_1 = \frac{1}{a - w} H_1 .$$

where

$$a = E - H_c - K_n - K_\pi + i\eta , \qquad W = W_1 + W_2 , \tag{6}$$

$$\frac{1}{a - w} H_1 = \frac{1}{a}(a - w + w)\left[\frac{1}{a - w} - \frac{1}{a} + \frac{1}{a}\right] H_1 =$$

$$= \frac{1}{a}\left[w + w\,\frac{1}{a - w}\,w\right]\frac{1}{a} H_1 + \frac{1}{a} H_1 = \frac{1}{a}\left[1 + T\frac{1}{a}\right] H_1 .$$

We denote by T the scattering operator defined *e.g.* in the papers of LIPPMAN-SCHWINGER ([10]) or CHEW-GOLDBERGER ([11-12])

$$T = w + w\,\frac{1}{a - w}\,w .$$

([10]) B. LIPPMAN and J. SCHWINGER: *Phys. Rev.*, **79**, 481 (1950).
([11]) G. F. CHEW and M. L. GOLDBERGER: *Phys. Rev.*, **87**, 778 (1952).
([12]) G. F. CHEW and G. C. WICK: *Phys. Rev.*, **85**, 636 (1952).

The probability of a transition on the basis of (6) is given by the formula

$$W = 2\pi\delta(E - E_0)\,|M|^2 \qquad M = \langle f|\left(1 + T\frac{1}{a}\right)H_1|\psi_0\rangle\,. \tag{6}$$

For the sake of discussion, in our further calculations we shall limit ourselves to the decay $^5\mathrm{He}_\Lambda \to \alpha + \mathrm{p} + \pi$. We denote the moments of the α particle, proton and π meson in final state by $\boldsymbol{pqk}$ and $\boldsymbol{q'p'k'}$ in the intermediate state; we take Ψ_0 in the form

$$\Psi_0\rangle = \int \frac{\mathrm{d}^3 p_\Lambda}{(2\pi)^3} f(p_\Lambda)\,|p_\Lambda k_0 \nu\rangle\,. \tag{7}$$

We omit here the indices describing the state of the core, remembering that all the while we have to do with the basic state of $^4\mathrm{He}$. K_0 is the center of mass momentum of the hyperfragment, p_Λ is the Λ momentum with respect to the core, $f(p_\Lambda)$ is the Fourier transform of $f_0(r)$, ν is the projection of the hyperfragment coinciding for $^5\mathrm{He}_\Lambda$ with the Λ spin. By (7) and (6) we obtain

$$M = \int \langle \boldsymbol{pqk}^\mu|H_1|\boldsymbol{p}_\Lambda \boldsymbol{K}_0\nu\rangle \frac{d^3 p_\Lambda}{(2\pi)^3} + \sum_\mu \int \langle \boldsymbol{pqk}^\mu|T|\boldsymbol{p'q'k'}\rangle \frac{1}{E - E(p'q'k') + i\eta}\cdot \tag{8}$$

$$\cdot \langle \boldsymbol{p'q'k'}|H_1|\boldsymbol{p}_\Lambda \boldsymbol{k}\nu\rangle \cdot f(\boldsymbol{p}_\Lambda)\frac{1}{(2\pi)^{12}}\,\mathrm{d}^3\boldsymbol{p'}\,\mathrm{d}^3\boldsymbol{k'}\,\mathrm{d}^3\boldsymbol{q'}\,\mathrm{d}^3\boldsymbol{p}'_\Lambda\,.$$

Introducing the variables

$$\boldsymbol{l} = \frac{M_\mathrm{p}}{M_1}\boldsymbol{p} - \frac{M_\alpha}{M_1}\boldsymbol{q}\,, \qquad \boldsymbol{t} = \boldsymbol{p} + \boldsymbol{q}, \boldsymbol{K} = \boldsymbol{p} + \boldsymbol{q} + \boldsymbol{k}\,, \qquad M_1 = M_\alpha + M_\mathrm{p}\,,$$

neglecting the interaction between π and α, and taking H_1 in the form (1), we obtain

$$\langle \boldsymbol{pqk}^\mu|H_1|\boldsymbol{p}_\Lambda \boldsymbol{k}_0\nu\rangle = g(2\pi)^3\,\delta(\boldsymbol{q} + \boldsymbol{k} - \boldsymbol{p}_\Lambda)\,\delta(\boldsymbol{k} - \boldsymbol{k}_0)\,U_\mu(1 + \beta\boldsymbol{\sigma}\boldsymbol{k})u_\nu\,. \tag{9}$$

$$\langle \boldsymbol{pqk}\mu|T|\boldsymbol{p'q'k'}\mu'\rangle = 2\pi)^6\,\delta(\boldsymbol{k} - \boldsymbol{k'})\,\delta(\boldsymbol{t} - \boldsymbol{t'})\langle \boldsymbol{l}\mu|T|\boldsymbol{l'}\mu'\rangle\,, \tag{10}$$

$$M = g\left\{u_\mu(1 + \beta\,\boldsymbol{\sigma}\,\boldsymbol{k})\,u_\nu f(\boldsymbol{l} - \boldsymbol{v}) + \sum_\mu \int \frac{\mathrm{d}^3 l'}{(2\pi)^3}\langle \boldsymbol{l}\mu|T|\boldsymbol{l'}\mu'\rangle\cdot\right. \tag{11}$$

$$\left.\cdot\frac{1}{E(l) - E(l') + i\eta}\,u_\mu(1 + \beta\boldsymbol{\sigma}\boldsymbol{k})u_\nu f(\boldsymbol{l'} - \boldsymbol{v})\right\}\,,$$

where

$$\boldsymbol{v} = \frac{M_\alpha M_\pi}{M M_1} \boldsymbol{t} + \frac{M_\alpha}{M} \boldsymbol{k}\,, \qquad M = M_\alpha + M_p + M_\pi\,.$$

$$E(l) = \frac{1}{2\mu_1'} l^2\,, \quad E(l') = \frac{1}{2\mu_1} l'^2\,, \quad \mu_1 = \frac{M_\alpha M_p}{M_\alpha + M_p}\,.$$

In order to integrate over 1 we put $1/(E(l) - E(l') + i\eta)$ in the form

$$-i\pi\delta(E(l) - E(l'))_{\cdot} + \frac{P}{E(l) - E(l')}\,. \tag{12}$$

Making use of the relations between the phase shifts and the diagonal in the energy part of the operator T (see *e.g.* LIPPMANN-SCHWINGER) we obtain

$$-i\pi\int \langle \boldsymbol{l}\mu \,|\, T \,|\, \boldsymbol{l}'\mu'\rangle \delta(E(l) - E(l'))\, u_{\mu'}(1 + \beta\boldsymbol{\sigma}\boldsymbol{k}) u_\nu f(\boldsymbol{l}' - \boldsymbol{v}) \frac{\mathrm{d}^3 l'}{(2\pi)^3} = \tag{13}$$

$$= \frac{i}{\varrho} \sum_{Jn M} \sin\delta_{Jn} \exp[i\delta_{Jn}]\, C_{n\frac{1}{2}}(JMM - \mu\mu)\, C_{n\frac{1}{2}}(JMM - \mu'\mu')\, Y^*_{nM-\mu}(\hat{\boldsymbol{l}})\cdot$$

$$\cdot Y_{nM-\mu'}(\hat{\boldsymbol{l}}')\, \delta(E(l) - E(l'))\, u_{\mu'}(1 + \beta\boldsymbol{\sigma}\boldsymbol{k}) u_\nu f(\boldsymbol{l}' - \boldsymbol{v})\, \varrho\, \mathrm{d}E(l')\, \mathrm{d}\Omega_i\,.$$

We shall now show that if the decay takes place outside the core then the part of the matrix element containing the integration in the principal value can be expressed by means of (13) by a known function $D_n(lV)$. To show this we transform into the space configuration that part of expression (11) which contains the operator T. We make the transformation only with respect to l and l', that is, the center of mass of the α particle and the proton; we continue to describe the meson in the momentum representation. After transformation (11) has the form

$$\sum_{\mu'} \int \mathrm{d}^3 r\, \mathrm{d}^3 r' \langle \boldsymbol{l}\mu \,|\, r\mu\rangle \langle r\mu \,|\, T \,|\, r'\mu'\rangle [G_1(\boldsymbol{r}'\boldsymbol{r}'') + G_2(\boldsymbol{r}'\boldsymbol{r}'')]\cdot \tag{14}$$

$$\cdot \exp[i\boldsymbol{v}\boldsymbol{r}'']\, u_{\mu'}(1 + \beta\boldsymbol{\sigma}\boldsymbol{k}) u_\nu f_0(r'')\,,$$

$$\begin{cases} G_1(\boldsymbol{r}'\boldsymbol{r}'') = \langle \boldsymbol{r}'\mu' \,|\, -i\pi\delta(E(l) - E(\tilde{l}'))\,|\, \boldsymbol{r}''\mu'\rangle = iA \dfrac{\sin l\,|\boldsymbol{r}' - \boldsymbol{r}''|}{l\,|\boldsymbol{r}' - \boldsymbol{r}''|}\,. \\ G_2(\boldsymbol{r}'\boldsymbol{r}'') = \langle \boldsymbol{r}'\mu' \,|\, \dfrac{P}{E(l) - E(\tilde{l}')}\,|\, \boldsymbol{r}''\mu'\rangle = A \dfrac{\cos l\,|\boldsymbol{r}' - \boldsymbol{r}''|}{l\,|\boldsymbol{r}' - \boldsymbol{r}''|}\,. \end{cases} \tag{15}$$

$\tilde{\boldsymbol{l}}'$ denotes the operator whose eigenvalues were previously denoted $\boldsymbol{l}'$ ($\tilde{\boldsymbol{l}}' = i(\partial/\partial\boldsymbol{r})$). We note that if r or r' is greater than the range of the potential

W_1 then $T_{\mu\mu'}(\boldsymbol{r}\boldsymbol{r}') = \langle \boldsymbol{r}\mu \,|\, T \,|\, \boldsymbol{r}'\mu' \rangle$ vanishes; this is seen at once from the formal expression for T. Therefore if by R_0 we denote the radius of the α particle obtained from the scattering of nucleons on α, then we can assume that $T_{\mu\mu'} = 0$ if r or $r' > R_0$. If $r' < r''$ we can expand $(G_1(\boldsymbol{r}'\boldsymbol{r}''))$ and $G_2(\boldsymbol{r}'\boldsymbol{r}'')$ into a series of Legendre polynomials, respectively $\cos\gamma = \hat{\boldsymbol{r}}'\hat{\boldsymbol{r}}''$, in the form

$$(16)\qquad \begin{cases} G_1(\boldsymbol{r}'\boldsymbol{r}'') &= iA \sum\limits_n (2n+1) j_n(lr') j_n(lr'') P_n(\cos\gamma)\,, \\ G_2(\boldsymbol{r}', \boldsymbol{r}'') &= -A \sum\limits_n (2n+1) j_n(lr') n_n(lr'') P_n(\cos\gamma)\,. \end{cases}$$

Inserting (16) into (14), expanding $\exp[i\boldsymbol{v}\boldsymbol{r}'']$ into spherical harmonics and integrating over $\mathrm{d}\Omega_{r''}$, we obtain, if the decay occurs inside the core

$$(17)\quad B \sum_{\mu'} \int_0^{R_0} i^n \langle \boldsymbol{l}\mu \,|\, \boldsymbol{r}\mu \rangle \langle \boldsymbol{r}\mu \,|\, T \,|\, \boldsymbol{r}'\mu' \rangle j_n(lr') Y_{nm}(\hat{r}') Y_{n,}(\hat{k}) u_{\mu'} (1 + \beta\boldsymbol{\sigma}\boldsymbol{k}) u_\nu \,\mathrm{d}^3\boldsymbol{r}\,\mathrm{d}^3\boldsymbol{r}' \cdot$$
$$\cdot \left\{ i \int_{R_0}^{\infty} j_n(lr'') j_n(vr'') f_0(r'')\, r''^2\,\mathrm{d}r'' - \int_{R_0}^{\infty} j_n(vr'') n_n(lr'') f_0(r'') r''^2 \mathrm{d}r'' \right\}.$$

From (17) we find the ratio of matrix elements g_{1n} and g_{2n} containing the respective parts of the Green function G_1 and G_2 proportional to $P_n(\cos\gamma)$; we obtain

$$(18)\qquad \frac{g_{2n}}{g_{1n}} = i \frac{\int_{R_0}^{\infty} j_n(vr) n_n(lr) f_0(r) r^2\,\mathrm{d}r}{\int_{R_0}^{\infty} j_n(lr) j_n(vr) f_0(r) r^2\,\mathrm{d}r} = D_n(lv)\,.$$

By virtue of assumption (a) we neglect the decays taking place in the region $r'' < R_0$. By (18) and (13) we obtain

$$(19)\quad M_{\mu\nu} = g \Big\{ u_\mu (1 + \beta\boldsymbol{\sigma}\boldsymbol{k}) u_\nu f(\boldsymbol{l} - \boldsymbol{v}) + i \int \sum_{JnM} (1 + D_n(lv)) \sin\delta_{Jn} \exp[i\delta_{Jn}] \cdot$$
$$\cdot G_{n\frac{1}{2}}(JMM - \mu\mu) c_{n\frac{1}{2}}(JMM - \mu'\mu') Y^*_{nM-\mu}(\hat{l}) Y_{nM-\mu'}(\hat{l}') u_\mu (1 + \beta\boldsymbol{\sigma}\boldsymbol{k}) u_\nu \cdot$$
$$\cdot f(\boldsymbol{l}' - \boldsymbol{v}) \delta(E(l) - E(l'))\,\mathrm{d}E(l')\,\mathrm{d}\Omega_{l'} \Big\}.$$

Integrating over l' we have

$$(20)\quad M_{\mu\nu} = g \{ u_\mu (1 + \beta\boldsymbol{\sigma}\boldsymbol{k}) u_\nu f(\boldsymbol{l} - \boldsymbol{v}) + i \sum_{JnM} (1 + D_n(lv)) b_n(lv) \sin\delta_{Jn} \exp[i\delta_{Jn}] \cdot$$
$$\cdot C_{n\frac{1}{2}}(JMM - \mu\mu) C_{n\frac{1}{2}}(JMM - \mu'\mu') Y^*_{nM-\mu}(l) Y_{nM-\mu'}(l') \}.$$

and

$$b_n(lv) = 2\pi \sqrt{\frac{2\pi}{2n+1}} \int f(\boldsymbol{l} - \boldsymbol{v})\, Y_{n0}(\cos\vartheta)\, \mathrm{d}\cos\vartheta\,. \qquad \cos\vartheta = \hat{l}\,\hat{v}\,. \tag{21}$$

3. – Energetic distribution of the π-mesons.

Since we are not interested in the absolute value of the probability of transition and only in the relative energy distribution, we shall omit the energy-independent multiplicative constant. The probability of transition as a function of energy is given by the formula

$$W(\omega) \sim \sum_{\mu\nu} \int |\, M_{\mu\nu}\,|^2\, \delta(E - E_0)\, \varrho_l\, \varrho_k\, \mathrm{d}\Omega_k\, \mathrm{d}\Omega_l\, \mathrm{d}E_l\,. \tag{22}$$

In the center of mass system we have

$$\boldsymbol{v} = \frac{M_\alpha}{M_1}\,\boldsymbol{k}\,, \qquad l = \sqrt{2\mu_1 Q - \frac{\mu_1}{\mu_2}\,k^2}\,, \qquad \mu_2 = \frac{M_1 M_\pi}{M_1 + M_\pi}\,,$$

Q being the heat of the reaction. Integrating over $\mathrm{d}\Omega_k\, \Omega_l\, \mathrm{d}E$ we obtain

$$\begin{aligned} W(\omega) \sim 2F(vl)(1 + \beta^2 k^2) + \sum_{Jn} \Big[& (1 + \operatorname{Re} D_n(lv))\, b_n^2(lv) \sin^2\delta_{Jn} + \\ & + \frac{1}{2} \operatorname{Im} D(lv) b_n^2(lv) \sin 2\delta_{Jn} \Big] \Big[2(2J+1) + 2\,\frac{8\pi}{3}\,\beta^2 k^2 G(Jn) \Big] + \\ & + \sum_{Jn} |\, 1 + D_n(lv)\,|^2 b_n^2(lv) \sin^2\delta_{Jn} \Big[2J + 1 + \frac{8\pi}{3}\,\beta^2 k^2 R(Jn) \Big]\,. \end{aligned} \tag{23}$$

Here

$$F(v, l) = \int |\, f(\boldsymbol{l} - \boldsymbol{v}\,)\,|^2\, \mathrm{d}\Omega_l\, \mathrm{d}\Omega_v\,,$$

$$\begin{aligned} G(Jn) = \frac{1}{4\pi} \sum_{LMN\mu\mu'\nu} (-1)^{\mu+\mu'+1}\, \frac{9}{2L+1}\, C_{nn}^2(L000)\, C_{n\frac{1}{2}}(JMM - \mu\mu) \cdot \\ \cdot C_{n\frac{1}{2}}(JMM - \mu'\mu')\, C_{\frac{1}{2}\frac{1}{2}}(1\mu + \nu, \mu, \nu)\, C_{\frac{1}{2}\frac{1}{2}}(1\mu' + \nu, \mu', \nu) \cdot \\ \cdot C_{nn}(LN,\, M - \mu',\, \nu + \mu)\, C_{nn}(LMN - \mu\mu + \nu)\,, \end{aligned} \tag{24}$$

$$\begin{aligned} R(Jn) = \frac{1}{4\pi} \sum_{LMN\mu\mu'\mu''\nu} (-1)^{\mu+\mu'+1}\, \frac{9}{2L+1}\, C_{nn}(L, 0, 0, 0)\, C_{n\frac{1}{2}}(JM,\, M - \mu,\, \mu) \cdot \\ \cdot C_{n\frac{1}{2}}(JM,\, M - \mu,\, \mu)\, C_{n\frac{1}{2}}(JM,\, M - \mu',\, \mu')\, C_{n\frac{1}{2}}(JM,\, M - \mu'',\, \mu'')\, C_{\frac{1}{2}\frac{1}{2}}(1\mu' + \nu\,\mu', \nu) \cdot \\ \cdot C_{\frac{1}{2}\frac{1}{2}}(1\mu'' + \nu\,\mu''\nu)\, C_{nn}(LN,\, M - \mu'',\, \mu'' + \nu)\, C_{nn}(LNM - \mu'\,\mu' + \nu)\,. \end{aligned} \tag{25}$$

On the basis of data obtained from the scattering of protons on helium we see (JUVELAND JENTCHKE [13]) that only the phase shifts $\delta_{\frac{1}{2}0}$, $\delta_{\frac{1}{2}1}$, $\delta_{\frac{3}{2}1}$ are different from zero in the energy interval of interest to us.

Hence only the first three $G(Jn)$ and $R(Jn)$ will be of interest to us. After carrying out the summation we obtain the following values:

$$(30)\qquad \begin{cases} G(\tfrac{1}{2}\,0) = \dfrac{3}{4\pi}, & G(\tfrac{1}{2}\,1) = \dfrac{2.17}{4\pi}, & G(\tfrac{3}{2}\,1) = \dfrac{6.81}{4\pi}, \\ R(\tfrac{1}{2}\,0) = \dfrac{3}{4\pi}, & R(\tfrac{1}{2}\,1) = \dfrac{2.78}{4\pi}, & R(\tfrac{3}{2}\,1) = \dfrac{8.01}{4\pi}. \end{cases}$$

Furthermore, as $f_0(r)$ we take the function of Dallaporta and Ferrari

$$f_0(r) = N \exp[-\alpha r], \qquad \alpha = 3.67 \cdot 10^{12},$$

which gives a good binding energy. For such a form of it it turns out that $D_n(vl)$, $v \simeq l$ are of the order of $\frac{1}{3}$, and consequently, in the first approximation we neglect them. This considerably simplifies the calculations. For $b_n(vl)$ and $F(vl)$ we obtain

$$(31)\qquad \begin{cases} F(lv) = N^2 \dfrac{8\pi^2}{3B}\left[\dfrac{1}{(A-B)^2} - \dfrac{1}{(A+B)^2}\right], \\ b_0(lv) = \dfrac{4\pi}{A^2 - B^2}, \\ b_1(lv) = N \dfrac{2\pi}{B^2}\left[m \dfrac{A-B}{A+B} + \dfrac{2AB}{A^2-B^2}\right], \\ A = l^2 + v^2 + \alpha^2, \\ B = 2lv. \end{cases}$$

And for $W(\omega)$ we find, after making the above approximations,

$$(32)\qquad W(\omega) \sim F(lv) + 3b_0^2(lv)\sin^2\delta_{\frac{1}{2}0} + 3b_1^2(lv)[\sin^2\delta_{\frac{1}{2}1} + 2\sin^2\delta_{\frac{3}{2}1}] + \\ + \beta^2 k^2[F(lv) + 3b_0^2(lv)\sin^2\delta_{\frac{1}{2}0} + b_1^2(lv)[2.37\sin^2\delta_{\frac{1}{2}1} + 7.2\sin^2\delta_{\frac{3}{2}1}].$$

The results are given in Fig. 1 where the curves for the parts corresponding to scalar coupling and pseudoscalar coupling for weak interactions are given

---

[13] A. C. JUVELAND and W. Z. JENTHKE: *Zeits. f. Phys.*, **144**, 521 (1956).

separately. In both cases we also give the energy distribution that is obtained if the interactions of the decay products are neglected. All distributions are normalized to 1. In the experimental distribution the cross hatched area

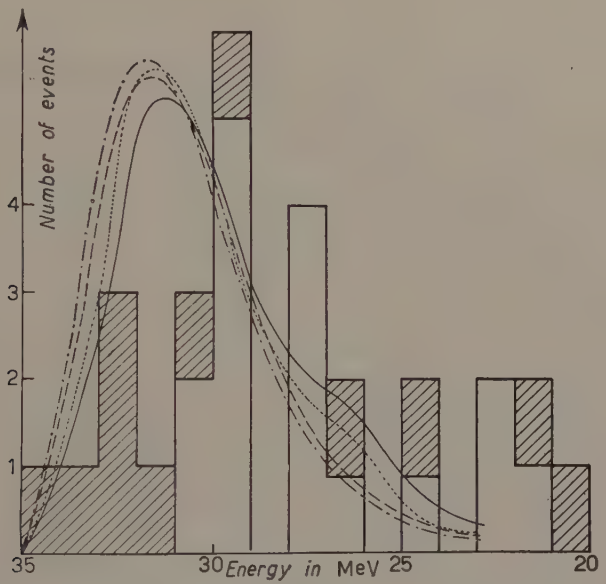

Fig. 1. -·-·- P.V. Coupling without interaction. ····· P.V. Coupling with interaction. - - - S Coupling without interaction. —— S Coupling with interaction. The theoretical distribution is given for the pion energy in the interval (23÷35) MeV. For ω smaller than 26 MeV, if the $D_n(vl)$ (proton virtual states) is taken into account the theoretical distribution can be considerably modulated.

represents cases that are not uniquely defined, while the remaining area represents the uniquely defined cases. The experimental data are taken from LEVI-SETTI. We shall discuss the results in the next part of this work along with the discussion of the angular distribution.

RIASSUNTO (*)

Si applica l'approssimazione impulsiva al caso del decadimento di un iperframmento. Si ottiene la distribuzione d'energia dei mesoni π nel caso del $^5He_\Lambda$ trascurando l'interazione π-α. Si confrontano i risultati con l'esperienza e si discute la validità dell'approssimazione impulsiva.

(*) *Traduzione a cura della Redazione.*

3805

IL NUOVO CIMENTO Vol. X, N. 5 1° Dicembre 1958

Penetration of a Magnetic Field into a One Dimensional Plasma.

A. Ron

Technion, Israel Institute of Technology - Haifa

(ricevuto il 22 Settembre 1958)

Summary. — In connection with the proposed compression and heating of a plasma through the application of an external magnetic field arises the problem of the penetration of such a field into a plasma. It is here investigated how an external magnetic field penetrates into a one dimensional bounded plasma which behaves as a compressible hydromagnetic fluid whose conductivity is proportional to density. The resulting mathematical problem is complicated, in particular as the movement of the boundary is not known beforehand. Transformation to a system of co-ordinates moving with the fluid simplifies the equations. In particular, in the case of a slowly varying magnetic field a single equation obtains with the magnetic field as only independent variable.

1. – Introduction.

Interest in the problem of the penetration of a magnetic field into a plasma arose recently in connection with astrophysics and high temperature plasma physics. The penetration of a magnetic field into a plasma must be studied in order to determine its pressure and movement and to gain some insight into the mechanism of its confinement. This investigation is of special interest in connection with recent proposals [1] to confine and heat plasma with the aid of an external magnetic field.

In previous works [2,3] the problem was introduced under the idealization of the plasma as an incompressible fluid of constant conductivity. Loughhead [4] was more realistic by considering the plasma as a compressible fluid

[1] G. Schmidt: to be published.
[2] E. N. Parker and M. Krook: *Astrophys. Journ.*, **124**, 216 (1956).
[3] S. Chandrasekhar: *Astrophys. Journ.*, **124**, 232 (1956).
[4] R. E. Loughhead: *Phys. Rev.*, **99**, 1678 (1955).

but introduces the simplification of infinite conductivity. We shall consider a compressible plasma of variable conductivity, but shall restrict ourselves to a simple geometry.

2. – Formulation of the problem.

We consider a one dimensional plasma confined by an external force to a given interval along the x-axis ($-a \leqslant x \leqslant a$) and unbounded in the other two dimensions. At a given moment ($t = 0$) an external, homogeneous and z directed magnetic field is applied to the plasma, and the external force is removed. The magnetic field, $B_0(t)$, outside the plasma is known, while its penetration into the plasma is to be studied. An ideal source of the magnetic field is assumed.

2·1. *Fundamental equations.* – The plasma is considered to be a magneto-hydrodynamic compressible fluid, to which the Maxwellian and Eulerian equations can be applied. Furthermore, we assume that the plasma is a homogeneous, isotropic, neutral and conducting medium. The fields we are going to deal with vary so slowly that the displacement current can be neglected and Maxwell's equations take the form

$$\nabla \times \boldsymbol{E} = -\frac{\partial \boldsymbol{B}}{\partial t} \tag{1}$$

$$\frac{1}{\mu} \nabla \times \boldsymbol{B} = \boldsymbol{j} , \tag{2}$$

$$\nabla \cdot \boldsymbol{B} = 0 , \tag{3}$$

$$\boldsymbol{j} = \sigma(\boldsymbol{E} + \boldsymbol{v} \times \boldsymbol{B}) , \tag{4}$$

$\boldsymbol{E}$ and $\boldsymbol{B}$ represent the electric and magnetic fields in the plasma, μ the permeability of vacuum (M.K.S. system), $\boldsymbol{j}$ the current density, σ the conductivity of the plasma and $\boldsymbol{v}$ the velocity of the fluid.

Neglecting any external forces except those caused by the magnetic field, we have for Euler's equations:

$$\varrho \left[\frac{\partial \boldsymbol{v}}{\partial t} + (\boldsymbol{v} \cdot \nabla) \boldsymbol{v} \right] = -\nabla p + \boldsymbol{j} \times \boldsymbol{B} , \tag{5}$$

$$\frac{\partial \varrho}{\partial t} + \nabla(\varrho \boldsymbol{v}) = 0 , \tag{6}$$

where ϱ and p are the density and pressure of the fluid.

Eliminating $\boldsymbol{E}$ and $\boldsymbol{j}$ we have from (1)–(4)

$$-\frac{\partial \boldsymbol{B}}{\partial t}+\nabla\times(\boldsymbol{v}\times\boldsymbol{B})=\nabla\times\left(\frac{1}{\mu\sigma}\nabla\times\boldsymbol{B}\right), \tag{7}$$

and from (5)

$$\varrho\left[\frac{\partial \boldsymbol{v}}{\partial t}+(\boldsymbol{v}\cdot\nabla)\boldsymbol{v}\right]=-\nabla p+\frac{1}{\mu}(\nabla\times\boldsymbol{B})\times\boldsymbol{B}\,. \tag{8}$$

The equation of state and the law giving the relation of the conductivity to the other quantities in question complete this set of equations. The pressure is assumed to be polytropic

$$p=C_1\varrho^{\gamma}\,, \tag{9}$$

with $\gamma=5/3$ and C_1 a constant. If we use for the conductivity Spitzer's relation [5]

$$\sigma=C_2T^{\frac{3}{2}}\,, \tag{10}$$

where C_2 is a constant, then, with the equation of state,

$$\frac{p}{\varrho}=C_3T\,, \tag{11}$$

where C_3 is another constant; with (9) we get

$$\sigma=c\varrho\,, \tag{12}$$

c is a constant which depends on C_1, C_2 and C_3.

2·2. *One-dimensional equations.* – In our one dimensional case, as the only space variable is x and the external magnetic field is z directed, we have

$$\boldsymbol{B}\equiv\{0,\,0,\,B(x,t)\}\,, \tag{13}$$

$$\boldsymbol{v}\equiv\{v(x,t),\,0,\,0)\}\,, \tag{14}$$

$$\varrho=\varrho(x,t)\,. \tag{15}$$

---

[5] L. Spitzer Jr.: *Physics of Fully Ionized Gases* (New York, 1956).

This reduces equations (7), (8) and (6) to

$$\frac{\partial B}{\partial t} + v\frac{\partial B}{\partial x} + B\frac{\partial v}{\partial x} = \frac{\partial}{\partial x}\left(\frac{1}{\mu\sigma}\frac{\partial B}{\partial x}\right), \tag{16}$$

$$\frac{\partial v}{\partial t} + v\frac{\partial v}{\partial x} = -\frac{1}{\varrho}\frac{\partial p}{\partial x} - \frac{1}{\mu\varrho}B\frac{\partial B}{\partial x}, \tag{17}$$

$$\frac{\partial \varrho}{\partial t} + v\frac{\partial \varrho}{\partial x} + \varrho\frac{\partial v}{\partial x} = 0\,. \tag{18}$$

The initial values of $\boldsymbol{B}$ and $\boldsymbol{v}$ are zero and those of ϱ and p are ϱ_i, p_i respectively, while on the moving boundary $B(x, t)$ is known to be $B_0(t)$.

Equations (9), (12), (16), (17) and (18) with the initial and boundary conditions given, form a complete set which governs the problem. Unfortunately, however, these equations are non-linear and one of them, (16), is not homogeneous in the first derivative. Moreover because of the compressibility of the plasma the boundary is moving in an unknown way, which can be found with the complete solution only. This gives the problem as formulated in x and t as independent variables a very formidable appearance indeed.

3. – Transformation to new coordinates.

3·1. *The equations of transformation.* – Let us introduce new independent variables ξ and τ for x and t

$$x = x(\xi, \tau)\,, \tag{19}$$

$$t = t(\xi, \tau)\,. \tag{20}$$

The functions $x(\xi, \tau)$ and $t(\xi, \tau)$ are to be chosen so as to give a stationary boundary in (ξ, τ) and, if possible, simplified equations.

Accordingly let ξ and τ be the space and time variables of a co-ordinate system of an observer moving with the fluid. Then

$$t = t(\xi, \tau) = \tau\,, \tag{21}$$

$$x = x(\xi, \tau) = \xi + \int_0^\tau v(\xi, \tau)\,\mathrm{d}\tau\,, \tag{22}$$

ξ is interpreted as the initial value of x

$$\xi = x(\xi, 0) \tag{23}$$

and we obtain a stationary boundary

$$\xi_b = \pm a \,.$$

The equations of transformation of the derivative are

$$\frac{\partial}{\partial t} = \frac{\partial}{\partial \tau} - \frac{x_\tau}{x_\xi}\frac{\partial}{\partial \xi}, \tag{24}$$

$$\frac{\partial}{\partial x} = \frac{1}{x_\xi}\frac{\partial}{\partial \xi}; \tag{25}$$

and the non-linear expression

$$\frac{\mathrm{d}}{\mathrm{d}t} = \frac{\partial}{\partial t} + v\frac{\partial}{\partial x}, \tag{26}$$

that appears in (16), (17) and (18) is simplified to $\partial/\partial\tau$.

In the Appendix (24)–(26) are derived in detail and it is formally shown that (21), (22) are indeed advantageous transformations.

3·2. *The transformed equations.* – Applying (24) and (25) to (16), (17) and (18) we have

$$\frac{\partial}{\partial \tau}\left(B\frac{\partial x}{\partial \xi}\right) = \frac{\partial}{\partial \xi}\left(\frac{1}{\mu\sigma(\partial x/\partial \xi)}\cdot\frac{\partial B}{\partial \xi}\right), \tag{27}$$

$$\frac{\partial v}{\partial \tau} = -\frac{1}{\varrho(\partial x/\partial \xi)}\left(\frac{\partial P}{\partial \xi} + \frac{B}{\mu}\frac{\partial B}{\partial \xi}\right), \tag{28}$$

$$\frac{\partial}{\partial \tau}\left(\varrho\frac{\partial x}{\partial \xi}\right) = 0 \,. \tag{29}$$

The equation of continuity (29) can be directly integrated, rendering

$$\varrho\frac{\partial x}{\partial \xi} = F(\xi) \,. \tag{30}$$

$F(\xi)$ is defined by initial conditions as

$$F(\xi) = \varrho(\xi, 0)\cdot\frac{\partial x}{\partial \xi}(\xi, 0) \,,$$

$$F(\xi) = \varrho_i \,,$$

since

$$\varrho(\xi, 0) = \varrho_i$$

and from (22)

$$\frac{\partial x}{\partial \xi}(\xi, 0) = 1 .$$

Thus

$$\varrho \frac{\partial x}{\partial \xi} = \varrho_i , \tag{31}$$

which simplifies (28):

$$\frac{\partial v}{\partial \tau} = -\frac{1}{\varrho_i}\left(\frac{\partial p}{\partial \xi} + \frac{B}{\mu}\frac{\partial B}{\partial \xi}\right), \tag{32}$$

or

$$\varrho_i \frac{\partial v}{\partial \tau} = -\frac{\partial}{\partial \xi}\left(p + \frac{B^2}{2\mu}\right). \tag{33}$$

Using (12) to eliminate σ from (27), we get

$$\frac{\partial}{\partial \tau}\left(B\frac{\partial x}{\partial \xi}\right) = \frac{\partial}{\partial \xi}\left(\frac{1}{\mu c \varrho (\partial x/\partial \xi)}\frac{\partial B}{\partial \xi}\right) \tag{34}$$

and with (31)

$$\frac{\partial}{\partial \tau}\left(B\frac{\partial x}{\partial \xi}\right) = k\frac{\partial^2 B}{\partial \xi^2} , \tag{35}$$

where k is

$$k = \frac{1}{\mu c \varrho_i} . \tag{36}$$

An important conclusion can immediately be drawn from (35) without solving the problem explicitly. Integrating (35) over ξ from $\xi = 0$ to the arbitrary plane $\xi = \xi'$

$$\frac{\partial}{\partial \tau}\int_0^{\xi'} B \cdot \frac{\partial x}{\partial \xi}\,\mathrm{d}\xi = k\int_0^{\xi'} \frac{\partial}{\partial \xi}\left(\frac{\partial B}{\partial \xi}\right)\mathrm{d}\xi , \tag{37}$$

or

$$\frac{\partial}{\partial \tau}\int_0^{x(\xi')} B \cdot \mathrm{d}x = k\left[\frac{\partial B}{\partial \xi}(\xi') - \frac{\partial B}{\partial \xi}(0)\right]. \tag{38}$$

The left-hand side integral is the magnetic flux, $\Phi(\xi')$ between the planes $x = 0$ and $x = x(\xi')$. Because of the symmetry of $B(\xi)$, $(\partial B/\partial \xi)(0) = 0$, thus

$$\frac{\partial}{\partial \tau}\Phi(\xi') = k\frac{\partial B}{\partial \xi}(\xi') , \tag{39}$$

or, with the help of (24) and (31),

$$\frac{\partial B}{\partial \xi}(\xi') = \frac{\partial x}{\partial \xi}(\xi')\frac{\partial B}{\partial x}(\xi') = \frac{\varrho_i}{\varrho(\xi')}\frac{\partial B}{\partial x}(\xi'),$$

and

$$\frac{\partial}{\partial \tau}\Phi(\xi') = k\frac{\varrho_i}{\varrho(\xi')}\frac{\partial B}{\partial x}(\xi'), \tag{40}$$

For incompressible media it can be shown on similar lines that

$$\frac{\partial}{\partial t}\Phi(x') = k'\frac{\partial B}{\partial x}(x'),$$

where k' is a constant.

Comparison of the last two equations shows that the flux through our particularly chosen surface changes more slowly in the compressible fluid the greater the density. This conclusion is important for the estimation of magnetization and demagnetization times of a compressible plasma.

4. – The magnetic field equation in the quasi-stationary case.

In the case of slowly varying magnetic fields we are led to considerations which resemble those appearing in connection with piston engines. The quasi-stationary case is of importance in plasma problems, just as the problem of the piston engine is solved under the assumption of a train of quasi-stationary states.

In the quasi-stationary case

$$\frac{\partial v}{\partial \tau} \approx 0,$$

giving for (33)

$$\frac{\partial}{\partial \xi}\left(p + \frac{B^2}{2\mu}\right) = 0; \tag{41}$$

integrating,

$$p + \frac{B^2}{2\mu} = G(\tau). \tag{42}$$

Outside the plasma $p = 0$ and $B = B_0(\tau)$; we thus have

$$p(\xi, \tau) + \frac{B^2(\xi, \tau)}{2\mu} = \frac{B_0^2(\tau)}{2\mu}. \tag{43}$$

If we write for (9)

$$p = \frac{p_i}{\varrho_i^\gamma}\varrho^\gamma ,$$

and substitute ϱ from (31), we have

$$p = \frac{p_i}{(\partial x/\partial \xi)^\gamma} . \tag{44}$$

We can now eliminate $\partial x/\partial \xi$ from (35), (43) and (44) give

$$\frac{\partial x}{\partial \xi} = \left[\frac{2\mu p_i}{B_0^2(\tau) - B^2(\xi, \tau)}\right]^{1/\gamma} , \tag{45}$$

and (35) changes to

$$\frac{\partial}{\partial \tau}\left[\frac{B}{(B_0^2 - B^2)^{1/\gamma}}\right] = K\frac{\partial^2 B}{\partial \xi^2} , \qquad K = \frac{k}{(2\mu p_i)^{1/\gamma}} . \tag{46}$$

The only dependent variable in (46) is the magnetic field $B(\xi, \tau)$. In principle this equation can be solved with the given initial and boundary conditions; in practice numerical methods would have to be applied.

* * *

This work was carried out in partial fulfilment of the requirements for the degree of Master of Science in Physics at Technion, Israel Institute of Technology, Haifa.

The help of Dr. George Schmidt who suggested the topic and served as thesis supervisor and of Dr. Gabor Kalman is gratefully acknowledged.

Thanks are also due to Dr. Amos Nathan and Reed Even for helping with the English formulation.

Appendix

Formal derivation of (22), (24) and (25).

In (19) we demand

$$\xi = x(\xi, 0) , \tag{47}$$

thus

$$x(\xi, \tau) = \xi + f(\xi, \tau) , \tag{48}$$

where

$$f(\xi, 0) = 0 . \tag{49}$$

Now, $f(\xi,\tau)$ can be chosen so as to linearize

$$\frac{\mathrm{d}}{\mathrm{d}t} = \frac{\partial}{\partial t} + v\,\frac{\partial}{\partial x}, \tag{50}$$

which appears in (16)-(18).

(50) is trasformed by

$$\frac{\partial}{\partial t} = \frac{\partial \tau}{\partial t}\,\frac{\partial}{\partial \tau} + \frac{\partial \xi}{\partial t}\,\frac{\partial}{\partial \xi}, \tag{51}$$

$$\frac{\partial}{\partial x} = \frac{\partial \tau}{\partial x}\,\frac{\partial}{\partial \tau} + \frac{\partial \xi}{\partial x}\,\frac{\partial}{\partial \xi}, \tag{52}$$

to the new independent variables, if we express the coefficients $\tau_t = \partial\tau/\partial t$, $\xi_t = \partial\xi/\partial t$ etc. as functions of ξ and τ.

Now

$$\frac{\partial(\xi,\tau)}{\partial(x,t)} = \left(\frac{\partial(x,t)}{\partial(\xi,\tau)}\right)^{-1}, \tag{53}$$

i.e.

$$\begin{Vmatrix} \xi_x & \xi_t \\ \tau_x & \tau_t \end{Vmatrix} = \begin{Vmatrix} x_\xi & x_\tau \\ t_\xi & t_\tau \end{Vmatrix}^{-1} = \frac{1}{x_\xi t_\tau - x_\tau t_\xi} \begin{Vmatrix} t_\tau & -x_\tau \\ -t_\xi & x_\xi \end{Vmatrix}. \tag{54}$$

Using (21) we get

$$t_\tau = 1, \tag{55}$$

$$t_\xi = 0, \tag{56}$$

yielding for (54)

$$\begin{Vmatrix} \xi_x & \xi_t \\ \tau_x & \tau_t \end{Vmatrix} = \begin{Vmatrix} \dfrac{1}{x_\xi} & -\dfrac{x_\tau}{x_\xi} \\ 0 & 1 \end{Vmatrix}, \tag{57}$$

(51) and (52) now reduce to

$$\frac{\partial}{\partial t} = \frac{\partial}{\partial \tau} - \frac{x_\tau}{x_\xi}\,\frac{\partial}{\partial \xi}, \tag{58}$$

$$\frac{\partial}{\partial x} = \frac{1}{x_\xi}\,\frac{\partial}{\partial \xi}. \tag{59}$$

Substitution into (50) gives

$$\frac{\mathrm{d}}{\mathrm{d}t} = \frac{\partial}{\partial \tau} - \left(\frac{x_\tau}{x_\xi} - \frac{v}{x_\xi}\right)\frac{\partial}{\partial \xi}, \tag{60}$$

it is therefore advantageous to fix x_τ as

$$x_\tau = v\,, \tag{61}$$

and thus

$$\frac{\mathrm{d}}{\mathrm{d}t} = \frac{\partial}{\partial \tau}\,, \tag{62}$$

which linearizes (50).

$f(\xi, \tau)$ can now be defined: from (48) and (61)

$$\frac{\partial}{\partial \tau} f(\xi, \tau) = v(\xi, \tau)\,, \tag{63}$$

thus

$$f(\xi, \tau) = \int_0^\tau v(\xi, \tau)\,\mathrm{d}\tau + g(\xi)\,,$$

which is reduced by (49) to

$$f(\xi, \tau) = \int_0^\tau v(\xi, \tau)\,\mathrm{d}\tau\,, \tag{64}$$

giving (48) in the form

$$x(\xi, \tau) = \xi + \int_0^\tau v(\xi, \tau)\,\mathrm{d}\tau\,.$$

RIASSUNTO (*)

In conseguenza della proposta di comprimere e riscaldare un plasma per mezzo dell'applicazione di un campo magnetico esterno sorge il problema della penetrazione di tale campo nel plasma. Si esamina nel presente lavoro come un campo magnetico esterno penetri in un plasma unidimensionale limitato che si comporti come un fluido idromagnetico compressibile la cui conduttività sia proporzionale alla densità. Il problema matematico che ne risulta appare complesso, particolarmente in quanto il moto del limite non è noto in precedenza. Il passaggio a un sistema di coordinate in moto col fluido semplifica le equazioni. In particolare, nel caso di un campo magnetico lentamente variabile si ottiene una equazione unica in cui figura il campo magnetico quale sola variabile indipendente.

(*) *Traduzione a cura della Redazione.*

IL NUOVO CIMENTO Vol. X, N. 5 1° Dicembre 1958

Covariant Description of Spin.

C. B. van Wyk (*)

Department of Physics, Columbia University - New York, N.Y.

(ricevuto il 22 Settembre 1958)

Summary. — The most general, finite, proper Lorentz transformation is generated in terms of an infinitesimal transformation. This generator is interpreted as a relativistic spin operator which is capable of describing in a relativistically covariant way the spin and electromagnetic properties of particles with spin $\frac{1}{2}$ and 1 and finite mass. Extensions of the method to particles with vanishing rest mass are indicated.

1. – Introduction.

According to a well established procedure finite Lorentz transformations, including space rotations, can be generated from suitable infinitesimal transformations. This procedure has the familiar advantage of linking these transformations of space and time directly with the spin angular momentum operator.

However, it has become customary to consider only those types of Lorentz transformations that leave invariant either two space vectors (four-vectors with vanishing time components) or one space vector and one time vector (four-vector with vanishing space components). The infinitesimal transformation generating such a finite transformation corresponds therefore only to a special type of relativistic spin operator that usually takes a non-covariant form.

In this paper the most general finite Lorentz transformation containing six independent parameters will be constructed in terms of a generator or spin angular momentum operator which is used as basis for the relativistically covariant description of the spin of particles with spin $\frac{1}{2}$ and 1. This spin operator contains a six-vector which, in the case of a particle with electromagnetic properties, is identified with its magnetic and electric moments.

(*) Now at the University, Bloemfontein, South Africa.

The covariant treatment of the spin of particles with vanishing rest mass presents a more complicated problem and two approaches to this problem are indicated.

2. – Discussion of an antisymmetric tensor.

The four-vectors m_μ and n_ν satisfying

$$m_\mu m_\mu = n_\nu n_\nu = 1, \qquad m_\mu n_\mu = 0\,, \tag{1}$$

where

$$m_4 = i m_0\,, \qquad n_4 = i n_0 \qquad (m_0 \text{ and } n_0 \text{ are real})$$

define the antisymmetric tensor

$$L_{\mu\nu} = -\,i(m_\mu n_\nu - m_\nu n_\mu) = m_\alpha (t_{\mu\nu})_{\alpha\beta}\, n_\beta \tag{2}$$

and the dual tensor

$$L^D_{\mu\nu} = \tfrac{1}{2}\varepsilon_{\mu\nu\varrho\sigma} L_{\varrho\sigma} = -\,i\varepsilon_{\mu\nu\varrho\sigma} m_\varrho n_\sigma\,,$$

where $\varepsilon_{\mu\nu\varrho\sigma}$ is the antisymmetric Levi-Civita tensor. These tensors have the invariants

$$L^D_{\mu\nu} L_{\mu\nu} = 0\,, \qquad L_{\mu\nu} L_{\mu\nu} = -\,2\,. \tag{3}$$

It follows that

$$L_{\mu\nu}(m_\nu \pm i n_\nu) = \pm\,(m_\mu \pm i n_\mu)\,, \tag{4}$$

and

$$L_{\mu\nu}\, k_\nu = 0\,, \qquad L_{\mu\nu}\, q_\nu = 0\,, \tag{5}$$

where

$$k_\nu m_\nu = k_\nu n_\nu = q_\nu m_\nu = q_\nu n_\nu = 0\,. \tag{6}$$

Without loss of generality q_μ and k_μ can be chosen to satisfy

$$k_\mu q_\mu = 0\,, \qquad q_\mu q_\mu = -\,1\,, \qquad k_\mu k_\mu = 1\,. \tag{7}$$

Then the dual tensor can be written

$$L^D_{\mu\nu} = q_\mu k_\nu - q_\nu k_\mu\,, \tag{8}$$

and corresponding to (4) and (5)

$$L^D_{\mu\nu}(k_\nu \pm q_\nu) = \pm\,(k_\mu \pm q_\mu)\,, \tag{9}$$

$$L^D_{\mu\nu}\, m_\nu = 0\,, \qquad L^D_{\mu\nu}\, n_\nu = 0\,. \tag{10}$$

The vectors

$$u_\mu^{\pm} = (m_\mu \pm i n_\mu)2^{-\frac{1}{2}}, \qquad v_\mu^{\pm} = (k_\mu \pm q_\mu)2^{-\frac{1}{2}}, \tag{11}$$

are null-vectors and satisfy

$$u_\mu^{+}u_\mu^{-} = 1 = v_\mu^{+}v_\mu^{-}, \qquad u_\mu^{\pm}v_\mu^{\pm} = 0. \tag{12}$$

Define the real three-vectors

$$\boldsymbol{a} = \boldsymbol{m} \wedge \boldsymbol{n}, \qquad \boldsymbol{b} = \boldsymbol{m}n_0 - \boldsymbol{n}m_0, \tag{13}$$

where where $\boldsymbol{x}$ denotes a three-vector as well as the space part of a four-vector x_μ. Then (3) becomes

$$\boldsymbol{a}\cdot\boldsymbol{b} = 0, \qquad a^2 - b^2 = 1 \quad \text{or} \quad (\boldsymbol{a} + i\boldsymbol{b})^2 = 1. \tag{14}$$

The antisymmetric tensor $L_{\mu\nu}$ defines a skew-symmetric 4×4 matrix $L = (L_{\mu\nu})$ such that [1]

$$L = \begin{pmatrix} 0 & -ia_3 & ia_2 & b_1 \\ ia_3 & 0 & -ia_1 & b_2 \\ -ia_2 & ia_1 & 0 & b_3 \\ -b_1 & -b_2 & -b_3 & 0 \end{pmatrix} =$$

$$= \boldsymbol{S}\cdot\boldsymbol{a} + \boldsymbol{K}\cdot\boldsymbol{b}, \tag{15}$$

where, in terms of the matrices defined in (2),

$$K_j = it_{j4}, \qquad S_j = t_{km},$$

(j, k, m is a cyclic permutation of 1, 2, 3) are the generators of Lorentz transformations and space rotations respectively and have the commutation properties

$$[t_{\mu\nu}, t_{\varrho\sigma}] = i(t_{\mu\varrho}\delta_{\nu\sigma} + t_{\nu\sigma}\delta_{\mu\varrho} - t_{\mu\sigma}\delta_{\nu\varrho} - t_{\nu\varrho}\delta_{\mu\sigma}).$$

The matrices $\boldsymbol{S}$ are the relativistic analogues of $\boldsymbol{s}$ of [1]. Similarly the dual tensor defines the matrix

$$L^D = i(\boldsymbol{S}\cdot\boldsymbol{b} - \boldsymbol{K}\cdot\boldsymbol{a}).$$

These two matrices satisfy

$$LL^D = 0 = L^D L, \qquad L^3 = L, \qquad (L^D)^3 = L^D. \tag{16}$$

---

[1] This part of the discussion follows the pattern of C. B. VAN WYK: *Nuovo Cimento*, **6**, 522 (1957).

Since they commute they have the common eigenfunctions (11) which can be written

$$(17) \qquad \begin{cases} u_\mu^{\pm} = 2^{-\frac{1}{2}}(\boldsymbol{N}_1 \pm ia\boldsymbol{N}_2,\ \mp b)\exp[\pm i\alpha) \\ v_\mu^{\pm} = 2^{-\frac{1}{2}}(\boldsymbol{N}_3 \pm b\boldsymbol{N}_2,\ \pm ia)\exp[\pm\beta]\,, \end{cases}$$

where $\boldsymbol{N}_j$ are the unit vectors

$$(18) \qquad \boldsymbol{N}_1 = \boldsymbol{b}/b\,; \qquad \boldsymbol{N}_2 = (\boldsymbol{a}\wedge\boldsymbol{b})/ab\,, \qquad \boldsymbol{N}_3 = \boldsymbol{a}/a$$

and α and β are undetermined parameters resulting from the lack of uniqueness with which m_μ, n_μ, k_μ, q_μ are determined by given L. In spite of this lack of uniqueness the structure and eigenvalue properties of L and L^D are most clearly exhibited by (2) and (8). The representation (15) of L has less structural simplicity but $\boldsymbol{a}$ and $\boldsymbol{b}$ have direct physical significance as will appear below.

From (16) follows that

$$\exp[iL\theta] = 1 + iL\sin\theta + L^2(\cos\theta - 1)$$

and similarly for $\exp[L^D\varphi]$. The most general, proper, single-valued Lorentz transformation containing six independent parameters can now be written

$$(19) \qquad x' = \exp[iL\theta + L^D\varphi]x\,, \qquad \text{with} \quad x_4 = ict\,,$$

where θ and φ are real « angular » variables.

The effect of the transformation (19) is easily understood in terms of (4), (5), (9) and (10). The parameter θ is the « angle of rotation » in the plane of m_μ and n_μ while φ is the hyperbolic angle measuring the « velocity » for the Lorentz transformation in the plane of k_μ and q_μ. If $b = 0$ then (19) describes a rotation about the space direction $\boldsymbol{a}$ as well as a Lorentz transformation relating to a velocity with direction $\boldsymbol{a}$.

3. – Application to particles with finite mass.

3·1. *Particles with spin unity.* – In interpreting L, the generator of the transformation (19), as a relativistic spin angular momentum operator, one is guided by the limit for which $b = 0$. The operator L then reduces for all practical purposes to the 3×3 operator $\boldsymbol{s}\cdot\boldsymbol{a}$ of [1] which describes the spin of a spin unity particle in its rest system.

This operator has the eigenvalue zero belonging to the eigenvector $\boldsymbol{a}$ which

can be called the non-relativistic spin vector. Generalizing from this observation it will now be assumed that a relativistic spin vector can be defined such that it is an eigenvector of L belonging to a zero eigenvalue.

Secondly, it is observed that the energy-momentum vector in the rest system has a vanishing space part and can in a formal way be regarded as a fourth eigenvector of $\boldsymbol{s}\cdot\boldsymbol{a}$ belonging to a zero eigenvalue. Therefore the second assumption is that the relativistic energy-momentum vector of a spin unity particle is another eigenvector of L belonging to a zero eigenvalue.

Since in the non-relativistic limit the spin and energy-momentum vectors can be regarded as orthogonal, it will be assumed that this is also the case in the relativistic description. Hence the spin pseudovector s_μ and the energy-momentum p_μ are vectors of the same type as k_μ and q_μ and satisfy

$$p_\mu p_\mu = -1\,, \qquad s_\mu s_\mu = 1\,, \qquad s_\mu p_\mu = 0\,. \tag{20}$$

From (8) follows that

$$L^D_{\mu\nu} = p_\mu s_\nu - p_\nu s_\mu \tag{21}$$

whence

$$s_\mu = L^D_{\mu\nu} p_\nu \tag{22}$$

and

$$\boldsymbol{a} = \boldsymbol{s}p_0 - \boldsymbol{p}s_0\,, \qquad \boldsymbol{b} = \boldsymbol{p}\wedge\boldsymbol{s} = (\boldsymbol{p}\wedge\boldsymbol{a})/p_0\,. \tag{23}$$

This vector $\boldsymbol{s}$ is the space part of the spin vector s_μ and must not be confused with the matrices $\boldsymbol{s}$ of [1]. Note that (22) expresses the spin vector in terms of the energy-momentum and the spin operator.

Within the above relativistic framework it is now possible to study the effect of Lorentz transformations. From (23) follows that in the rest system of the particle

$$\boldsymbol{a} = \boldsymbol{s} = \boldsymbol{a}^0\,, \qquad \boldsymbol{b} = 0\,, \tag{24}$$

where $\boldsymbol{a}^0$ is the spin vector of the particle in this system. Since $\boldsymbol{a}$ and $\boldsymbol{b}$ represent a six-vector it follows from (24) that when the particle has momentum $\boldsymbol{p}$, they become

$$\boldsymbol{a} = \boldsymbol{a}^0_1 + p_0\boldsymbol{a}^0_2\,, \qquad \boldsymbol{b} = \boldsymbol{p}\wedge\boldsymbol{a}^0 = \boldsymbol{p}\wedge\boldsymbol{a}^0_2\,, \tag{25}$$

where

$$\boldsymbol{a}^0 = \boldsymbol{a}^0_1 + \boldsymbol{a}^0_2\,, \qquad \boldsymbol{a}^0_1 \| \boldsymbol{p}\,, \qquad \boldsymbol{a}^0_2 \perp \boldsymbol{p}\,.$$

Similarly, the spin being a pseudovector is given by

$$\boldsymbol{s} = p_0 \boldsymbol{a}_1^0 + \boldsymbol{a}_2^0 , \qquad s_0 = p a_1^0 . \tag{26}$$

The consistency of (25) and (26) with (20) and (23) is evident. From (25) follows that b vanishes in the rest system while in any other system it depends on the spin direction in the rest system and the momentum.

In the case of a particle with a magnetic moment the six-vector $\boldsymbol{a}$, $\boldsymbol{b}$ is proportional to the magnetic and electric moment six-vector of the particle. This statement follows from (24) and (23).

The functions s_μ and $m_\mu \pm i n_\mu$ are eigenfunctions of L belonging to the eigenvalue 0, ± 1 and can therefore be regarded as the three relativistic spin states of the particle.

3·2. *Particles with spin* $\frac{1}{2}$. – The above procedure for spin unity particles can also be applied to spin $\frac{1}{2}$ particles ([2]). In this case the Lorentz group is represented by the Dirac matrices $-i(\gamma_\mu\gamma_\nu - \gamma_\nu\gamma_\mu)/4$ where $\gamma_j = -i\beta\alpha_j$, $\gamma_4 = \beta$. The most general double-valued Lorentz transformation is given by

$$\psi' = \exp\left[iT\theta/2 + T^D\varphi/2\right]\psi ,$$

where

$$\begin{cases} T = (1/2)\gamma_\mu\gamma_\nu L_{\mu\nu} = -i\gamma_\mu m_\mu \gamma_\nu n_\nu , \\ T^D = (1/2)\gamma_\mu\gamma_\nu L^D_{\mu\nu} = \gamma_\mu k_\mu \gamma_\nu q_\nu , \quad T T^D = T^D T = \gamma_5 , \end{cases} \tag{27}$$

and m_ν, n_ν, k_ν, q_ν are defined as in (1), (6) and (7).

If T is to be the covariant spin operator of the particle it must commute with the projection operators

$$\Lambda_\pm = (1/2)(1 \pm i\gamma_\mu p_\mu) ,$$

which distinguish between negative and positive energy states. Here p_μ is the energy-momentum vector of the particle normalized as above. Now T and Λ only commute if

$$L_{\mu\nu} p_\nu = 0 . \tag{28}$$

If $L_{\mu\nu}$ is written as a matrix L and L^D defined as above then (28) implies that

$$\boldsymbol{a}\cdot\boldsymbol{b} = 0 , \qquad L L^A = L^D L = 0 .$$

([2]) The relativistic description of electron spin has been approached from another angle by H. P. Stapp: *Phys. Rev.*, **103**, 425 (1956); Bouchiat and Michel, *Nuclear Physics*, **5**, 416 (1958).

Define s_μ as in (22) then s_μ and p_μ are again eigenvectors of L belonging to zero eigenvalues. From

$$T\psi_\pm = \pm\psi_\pm$$

and (27) follows that

$$\gamma_\mu(m_\mu \pm in_\mu)\psi_\pm = 0\,. \tag{29}$$

Hence (29) defines the four linearly independent eigenstates of T in terms of $m_\mu \pm in_\mu$, the eigenstates of L belonging to the eigenvalues ± 1.

If T commutes with $\Lambda_\pm$ so does

$$T\gamma_\mu p_\mu = i\gamma_5\gamma_\mu s_\mu = \beta(\boldsymbol{\sigma}\cdot\boldsymbol{s} - i\gamma_5 s_4)\,, \tag{30}$$

with s_μ defined by (22). If this pseudovector s_μ is interpreted as the spin vector of the spin $\frac{1}{2}$ particle, as the space part of (30) suggests, then the present situation is exactly the same as in (20)–(26) for spin unity particles. The spin operator can be expressed as

$$T = \boldsymbol{\sigma}\cdot\boldsymbol{a} + i\boldsymbol{\alpha}\cdot\boldsymbol{b}$$

and if the spin $\frac{1}{2}$ particle has a magnetic moment then $\boldsymbol{a}$ and $\boldsymbol{b}$ are again proportional to the magnetic and electric moments respectively.

4. – The case of zero mass particles.

In this case no rest system exists which can indicate a unique way of fitting relativistic spin into the above framework. The vanishing rest mass, however, requires that the energy-momentum vector must satisfy $p_\mu p_\mu = 0$ which suggests that p_μ and the spin vector s_μ be identified with the eigenstates $v_\mu^\pm$ of L and L^D. (17) can be normalized and rewritten as

$$p_\mu = (p_0/a)(\boldsymbol{N}_3 + b\boldsymbol{N}_2,\ ia)\,, \qquad s_\mu = (a/2p_0)(\boldsymbol{N}_3 - b\boldsymbol{N}_2,\ -ia)$$

whence

$$L^D_{\mu\nu}p_\nu = p_\mu\,, \qquad L^D_\mu s_\nu = -s_\mu$$

and

$$p_\mu p_\mu = 0 = s_\mu s_\mu\,, \qquad s_\mu p_\mu = 1\,. \tag{31}$$

With this physical interpretation the relations (21) and (23) between the spin and momentum four-vectors are still valid for zero mass particles. However, (22) is no longer valid.

The spin $\frac{1}{2}$ and 1 particles for which (31) would be valid would have some kind of inner structure described by the six-vector $\boldsymbol{a}$, $\boldsymbol{b}$ occurring in the spin operators L or T which are still 4×4 matrices. At present none of the known particles appear to be of this type.

5. – The photon and the neutrino.

Apart from the description of the spin of zero mass particles presented in Sect. **4**, there is another description which is suggested by the finite mass case when the mass $\to 0$. An equivalent procedure is to allow $p \to p_0 \to \infty$ in which case (26) becomes simply

$$s_\mu = \lambda p_\mu \,, \tag{32}$$

where λ is an undetermined constant and

$$s_\mu s_\mu = p_\mu p_\mu = s_\mu p_\mu = 0 \,. \tag{33}$$

Now the number of eigenstates of the spin operator has been reduced to three and L^p, as defined by (21), no longer serves a useful purpose. Consequently the spin operator for the spin unity particle becomes the 3×3 matrix $\boldsymbol{s}\cdot\boldsymbol{p}$ of [1] with the eigenstates $\boldsymbol{p}$ (the momentum) and $\boldsymbol{m} \pm i\boldsymbol{n}$ (the spin states), where, by (1) and (6),

$$\boldsymbol{m}\cdot\boldsymbol{p} = \boldsymbol{n}\cdot\boldsymbol{p} = \boldsymbol{m}\cdot\boldsymbol{n} = 0 \,, \qquad \boldsymbol{m}\cdot\boldsymbol{m} = \boldsymbol{n}\cdot\boldsymbol{n} = 1 \,.$$

For the spin $\frac{1}{2}$ particle the spin operator becomes the matrix $\boldsymbol{\sigma}\cdot\boldsymbol{p} = -i(\boldsymbol{\sigma}\cdot\boldsymbol{m})(\boldsymbol{\sigma}\cdot\boldsymbol{n})$ with the eigenstates $\psi_\pm$ given by

$$\boldsymbol{\sigma}\cdot(\boldsymbol{m} \pm i\boldsymbol{n})\psi_\pm = 0 \,.$$

In the absence of parity conservation for such a particle, $\boldsymbol{\sigma}$ can be regarded as a 2×2 matrix.

The most general 2×2 matrix with determinant unity can be written in the form $\exp[i\boldsymbol{\sigma}\cdot(\boldsymbol{a}+i\boldsymbol{b})(\theta+i\varphi)]$ with $\boldsymbol{a}$ and $\boldsymbol{b}$ satisfying (14). Since these matrices serve as representation for the Lorentz group, one might expect the Pauli matrix $\boldsymbol{\sigma}\cdot(\boldsymbol{a}+i\boldsymbol{b})$ rather than $\boldsymbol{\sigma}\cdot\boldsymbol{p}$ to be the spin operator for a spin $\frac{1}{2}$ particle that satisfies a two component theory. However this is not the case since the existence of a six vector implies the presence of an inner structure which, according to the above discussion, is only possible in the four component theory.

Since both the proton and the neutrino have zero mass and each has two spin states which appear to describe their inner structure completely, it must be concluded that their spins are described by (32) and (33) rather than by (31).

* * *

This work was completed with the assistance of the Carnegie Corporation of New York and the South African C.S.I.R. while the author was enjoying the hospitality of Columbia University.

Note added in proof.

The discussion in Sect. **4** does not take into account invariance under inversion of axes. Such invariance requires $s_\mu p_\mu = 0$ which, together with

$$s_\mu m_\mu = s_\mu n_\mu = p_\mu m_\mu = p_\mu n_\mu = p_\mu p_\mu = 0 ,$$

yields

$$s_\mu = \lambda p_\mu \qquad \text{and} \qquad s_\mu s_\mu = 0 .$$

Hence in this case the spin of a zero mass particle is described completely in terms of the energy-momentum vector and two linearly independent spin states as outlined in Sect. **5**.

RIASSUNTO (*)

Si genera la più generale trasformazione propria di Lorentz finita in termini di una trasformazione infinitesimale. Tale generatore si interpreta come operatore relativistico di spin capace di descrivere in modo relativisticamente covariante lo spin e le proprietà elettromagnetiche delle particelle di spin $\frac{1}{2}$ e 1 e massa finita. Si indica l'estensione del metodo a particelle di massa a riposo evanescente.

(*) *Traduzione a cura della Redazione.*

IL NUOVO CIMENTO Vol. X, N. 5 1° Dicembre 1958

On Sommerfeld's Approximation in High Energy Photoelectric Effect and one Quantum Annihilation of Positrons in the K-shell.

H. Banerjee

Department of Physics. Indian Institute of Technology. Kharagpur - India

(ricevuto il 26 Settembre 1958)

Summary. — The angular distribution and the total cross-section for high energy photoelectric effect and one quantum annihilation of positrons in the K-shell have been calculated with the use of the Sommerfeld-Maue approximation for the wave function of the scattering state of the fermion. The error in this procedure is of relative order (a/ε), where $a=Z/137$ and ε is the energy of the scattering state in units of mc^2, and is, therefore, negligible in the extreme relativistic case. Results have been obtained correctly up to terms of relative order a and methods for calculating the contributions from higher terms have also been indicated. The expression for the angular distribution of photoelectrons obtained in this paper does not show any marked qualitative difference from Sauter's formula. One may conclude from our results that the ratio of the forward to the maximum intensities of the photoelectrons diminishes as the primary energy is increased. The absorption coefficient for photoelectric effect has been presented in a form which is similar to Hall's results. Correction terms in the formulae of Bhabha and Hulme for the positron annihilation process have been found to be the same as those in Sauter's formula.

1. – Introduction and general discussion.

Although the photoelectric phenomenon is one of the basic physical processes of quantum electrodynamics, the only theoretical result for the angular distribution of photoelectrons that is available to experimental workers for ready reference is that of Sauter (1). Sommerfeld (2) has also obtained the

(1) F. Sauter: *Ann. Phys.*, **11**, 454 (1931).
(2) A. Sommerfeld: *Wellenmechanik* (New York, 1939), pp. 482-494.

same result following a different method of approximation. These results have been obtained only after neglecting terms of relative order a ($= Z/137$) which, however, is not too small for elements that are generally used as converters in experiments on photoelectric effect. The inadequacy of theoretical results which has prevailed since 1935, naturally makes one enquire whether with any one of the available methods of approximation an improved result in a closed form for the angular distribution can be obtained and thereby the discrepancies between Sauter's result and those recently reported by experimental workers ([3]) can be explained, at least partially.

The Born approximation method, which is commonly used in high energy scattering processes, is, however, not suitable for the photoelectric phenomenon. Although it gives the correct Z-dependence, the first Born approximation, which consists in representing the state of the scattered electron by a plane wave, introduces an error even in the approximation up to which Sauter's result is valid. This will be apparent from the calculations in this paper (Sect. 3). The reason for the failure of the first Born approximation is that important regions for the integrals occurring in the matrix element are at distances of the order of $\hbar/mc$, the Compton wavelength of the electron, from the nucleus. Consequently the wavefunction of the electron, which is appreciably distorted by the nuclear Coulomb field within this region, cannot be approximated by plane waves without vitiating the results. In fact, in order to obtain Sauter's results by this method, one has to take into account the contributions from the next higher approximation. So that, for any improvement on Sauter's results the third Born approximation in the nuclear Coulomb field has to be considered, which makes the calculation prohibitive.

If wave functions separated in polar co-ordinates are employed for the final state, as was done by SAUTER ([1]), one is confronted with the difficult task of summing an infinite series whose different terms correspond to the angular and magnetic quantum numbers l and m respectively of the final state, in addition to integration difficulties. In the derivation of the absorption coefficient in the extreme relativistic case, HALL ([4]) succeded in summing this series only after neglecting terms of $O(1/l)$. He has, however, expressed the absorption coefficient in the final steps of his calculation in terms of an integral which is not integrable in a closed form. For the angular distribution the situation further worsens and the only available result is that of SAUTER ([1]). A better approximation of the angular distribution by this method seems to be very difficult, even if some suitable simplification is found possible.

So far as the photoelectric effect is concerned, Sommerfeld's ([2]) method of

---

([3]) A. HEDGRAM and S. HULTBERG: *Phys. Rev.*, **94**, 498 (1954); S. HULTBERG: *Ark. f. Fys.*, **9**, 245 (1955).

([4]) H. HALL: *Revs. Mod. Phys.*, **8**, 358 (1936).

treatment has received the least attention. His method essentially consists in representing the state of the scattered electron by a wave function (5), known as the Sommerfeld-Maue wave function, of the form

$$\Psi_2 = N_2\left(1 - \frac{i\boldsymbol{\alpha}\cdot\boldsymbol{\nabla}_r}{2\varepsilon}\right) uF\,, \tag{1}$$

where N_2 is the normalization constant, $(\boldsymbol{p}, \varepsilon)$ the momentum and energy of the electron, F is a confluent hypergeometric function, u is the normalized Dirac spinor amplitude for an electron with momentum $\boldsymbol{p}$ and $\boldsymbol{\alpha} = (-\gamma^0\boldsymbol{\gamma})$ is the Dirac operator. With the above approximation for the final state and neglecting relativistic effects for the bound state, which amounted to Pauli approximation, SOMMERFELD was able to obtain Sauter's result. Sommerfeld's calculation in its original form could not be extended to obtain a better result; firstly, because the order of accuracy of the wave function (1) was not fully realized, and secondly, because of the Pauli approximation for the bound state one is forced to neglect terms of relative order a in the matrix element

It is only recently (6,7) that much attention has been focussed on the Sommerfeld-Maue wave function. Separating the wave function (1) in polar co-ordinates, BETHE and MAXIMON (6) have shown that the term of the resulting series corresponding to the angular momentum l coincides with the exact continuum Dirac wave function in spherical co-ordinates if in the latter terms of relative order (a^2/l) are neglected. As will be shown in Appendix C, in high energy photoeffect, the main contribution to the integrals in the matrix element comes from terms for which $l \sim \varepsilon$. Further, it will be apparent from the calculations in Sect. **3** that an error of $O(a^2)$ in the wave functions will lead to an error of $O(a)$ in the matrix element. Consequently the error committed in the matrix element by writing (1) for the wave function of the scattered electron will be of relative $O(a/\varepsilon)$. The Pauli approximation of the bound state, in which terms of relative $O(a^2)$ are neglected, is, however, not necessitated by the above approximation for the scattering state. In fact, in the high energy case one may represent the final state of the electron by a Sommerfeld-Maue wave function and still treat the bound state exactly without giving rise to any inconsistency. This is exactly the argument on which Hall's calculations for the photoelectric effect in the relativistic region have been based.

In the present work an attempt has been made towards treating the wave function of the K-electron exactly, while the state of the photoelectron has

---

(5) A. SOMMERFELD and A. W. MAUE: *Ann. Phys.*, **22**, 629 (1935).

(6) H. A. BETHE and L. C. MAXIMON: *Phys. Rev.*, **93**, 768 (1954).

(7) H. OLSEN, L. C. MAXIMON and H. WERGELAND: *Phys. Rev.*, **106**, 27 (1957); G. K. HORTON and E. PHIBBS: *Phys. Rev.*, **96**, 1066 (1954).

been approximated by a Sommerfeld-Maue type of wave function. The error committed, which is inherent in such a procedure, is of relative $O(a/\varepsilon)$. Integrals occurring in the matrix element do not appear to be integrable in a closed form. They have, however, been reduced to an elegant form from which successive approximations in powers of a may be possible. For our purpose, contributions to the matrix element only from terms of relative $O(a)$ have been obtained. It has been found that the correction term in the angular distribution leaves Sauter's result qualitatively unaltered. The expression for the absorption coefficient has been rendered in such a form which clearly brings out the similarity with Hall's result. The calculations for the photoelectric effect have been extended to the case of one quantum annihilation of a positron in the K-shell in Sect. **5**. For the latter process correction terms of relative $O(a)$ in the only available results of BHABHA and HULME [8] have been obtained. In the high energy limit the error in our results is of relative $O(a^2)$. Methods have, however, been indicated how our results could be further improved by finding higher order terms. In the light of this paper it will also be evident how easily the polarization effects of the photoelectrons, which will form the subject matter of a subsequent paper may be included in our consideration.

Although the present work has been carried out with Coulomb wave functions both for the initial and the final states of the electron, deviations due to the screening effects of internal and external charge distributions will not materially affect our results. Within distances from the nucleus of the order of the Compton wave length of the electron (see Appendix C), where the behaviour of our wave functions is important, the potential function $V(r)$ may be approximated with sufficient accuracy by

$$V(r) = -\frac{(Z-s)}{r} + V_0 ,$$

according to the Hartree self-consistent field. For heavy atoms the « inner screeing constant » is negligible, while the « outer screening constant », the only effect of which is to change the energy of the photoelectron by V_0, may be neglected in the high energy case.

2. – Matrix element.

Introducing m as the unit of mass, $\hbar/mc$ as the unit of length, and mc^2 that of energy, one can write the matrix element for the photoelectric effect

(8) H. J. BHABHA and H. R. HULME: *Proc. Roy. Soc.*, A **146**, 723 (1934).

as (9)

$$H_{12} = \frac{e}{\sqrt{4\pi k}} \int \overline{\Psi}_2 (\boldsymbol{e}\cdot\boldsymbol{\gamma}) \Psi_1 \exp[i\boldsymbol{k}\cdot\boldsymbol{r}]\, \mathrm{d}\tau\,, \tag{2}$$

where $\boldsymbol{e}$ is the polarization vector of the incident photon, and $(\boldsymbol{k}, k)$ are its momentum and energy. The energy of the photoelectron is given by Einstein's equation which may be written as

$$\varepsilon = k + \sqrt{1 - a^2} \approx k + 1\,, \tag{3}$$

if terms of $O(a^2/\varepsilon)$ are neglected. Ψ_1, the wave function of the K-electron, is given by

$$\Psi_1 = N_1 \left\{1 + \frac{a}{2-\delta}\cdot\frac{(\boldsymbol{\gamma}\cdot\boldsymbol{r})}{r}\right\} r^{-\delta} \exp[-ar]\, w\,, \tag{4}$$

where

$$\delta = 1 - \sqrt{1 - a^2}; \qquad N_1 = (2a)^{\frac{3}{2}-\delta} \left(\frac{2-\delta}{8\pi\Gamma(3-2\delta)}\right)^{\frac{1}{2}}. \tag{4a}$$

The normalized spinor w represents the polarization state of the K-electron. Ψ_2 is the Sommerfeld-Maue wave function as in (1). The normalization constant N_2 and the confluent hypergeometric function F are to be so chosen that asymptotically (6)

$$\Psi_2 \sim \frac{1}{(2\pi)^{\frac{3}{2}}}\cdot\frac{1}{\varepsilon^{\frac{1}{2}}}\cdot u \left\{\exp[i\boldsymbol{p}\cdot\boldsymbol{r}] + \frac{\exp[-ipr]}{r} f(\theta, \varphi)\right\}.$$

This condition may be satisfied if one chooses

$$F = F\{-ia_1;\, 1;\, -ipr - i\boldsymbol{p}\cdot\boldsymbol{r}\}\,, \tag{5a}$$

and

$$N_2 = \frac{1}{(2\pi)^{\frac{3}{2}}}\cdot\frac{1}{\varepsilon^{\frac{1}{2}}}\cdot \exp\left[\frac{\pi a_1}{2}\right] \Gamma(1 + ia_1)\,, \tag{5b}$$

where $a_1 = a\varepsilon/p$. Substituting (1) and (4) in the expression (2) for the matrix element we get

$$H_{12} = C\overline{u}\,[(\boldsymbol{e}\cdot\boldsymbol{\gamma})I_0 + (\boldsymbol{e}\cdot\boldsymbol{\gamma})(\boldsymbol{\gamma}\cdot\boldsymbol{I}_1) + (\boldsymbol{\alpha}\cdot\boldsymbol{I}_2)(\boldsymbol{e}\cdot\boldsymbol{\gamma}) + I_3]w\,, \tag{6}$$

(9) J. M. JAUCH and F. ROHRLICH: *The Theory of Photons and Electrons* (Cambridge Mass., 1955), pp. 318-326.

where

$$C = \frac{e}{\sqrt{4\pi k}} N_2^* N_1 . \tag{7}$$

In the above we have introduced the following abbreviations,

$$I_0 = \int \exp[i\boldsymbol{q}\boldsymbol{r}]\, F^* r^{-\delta} \exp[-ar]\, \mathrm{d}\tau = -\frac{\partial}{\partial a} J(-\delta) , \tag{8a}$$

$$\boldsymbol{I}_1 = \frac{a}{2-\delta} \int \exp[i\boldsymbol{q}\cdot\boldsymbol{r}]\, F^* \frac{\boldsymbol{r}}{r} r^{-\delta} \exp[-ar]\, \mathrm{d}\tau = -\frac{ia}{2-\delta} \nabla_q J(-\delta) , \tag{8b}$$

$$\boldsymbol{I}_2 = -\frac{i}{2\varepsilon} \int \exp[i\boldsymbol{q}\cdot\boldsymbol{r}] (\nabla_r F^*)\, r^{-\delta} \exp[-ar]\, \mathrm{d}\tau = \tag{8c}$$

$$= -\frac{ip}{2\varepsilon} \int \exp[i\boldsymbol{q}\cdot\boldsymbol{r}] \left(\frac{1}{r} \nabla_p F^*\right) r^{-\delta} \exp[-ar]\, \mathrm{d}\tau = -\frac{ip}{2\varepsilon} (\nabla_p J(-\delta)) ,$$

$$I_3 = -\frac{ia}{2\varepsilon(2-\delta)} \int \exp[i\boldsymbol{q}\cdot\boldsymbol{r}]\, (\boldsymbol{\alpha}\cdot\nabla_r F^*)(\boldsymbol{e}\cdot\boldsymbol{\gamma}) \left(\boldsymbol{\gamma}\cdot\frac{\boldsymbol{r}}{r}\right) r^{-\delta} \exp[-ar]\, \mathrm{d}\tau , \tag{8d}$$

where $\boldsymbol{q} = \boldsymbol{k} - \boldsymbol{p}$ is the momentum transferred to the nucleus and

$$J(-\delta) = \int \exp[i\boldsymbol{q}\cdot\boldsymbol{r}]\, F^* r^{-\delta} \exp[-ar]\, \frac{\mathrm{d}\tau}{r} . \tag{9}$$

Contributions to the matrix element from I_3 have been shown to be of relative $O(a/\varepsilon)$ in Appendix B and can, therefore, be neglected.

3. – Evaluation of integrals.

A convenient contour integral representation for the confluent hyper-geometric function F^* in the integral $J(-\delta)$ in (7) is

$$F^* = F(ia_1; 1; ipr + i\boldsymbol{p}\cdot\boldsymbol{r}) = \frac{1}{2\pi i} \oint^{(0+,1+)} \mathrm{d}t\, t^{ia_1 - 1} (t-1)^{-ia_1} \exp[i(pr + \boldsymbol{p}\cdot\boldsymbol{r})t] . \tag{10}$$

The contour encircles the point 0 and 1 in the t-plane once in the anticlockwise sense. At the point where the contour crosses the real axis to the right of 1 both $\arg t$ and $\arg(t-1)$ are zero. We substitute the above representation of F^* in the expression for $J(-\delta)$. Uniform convergence in t of the

space integral requires that the contour should not contain any singularity fo the space integral, which condition may be easily satisfied. With this understanding one can change the order of integration, perform the space integration first, and obtain in an elementary way

$$(11) \qquad J(-\delta) = -\Gamma(1-\delta)\oint^{(0+,1+)} \mathrm{d}t\, t^{ia_1-1}(t-1)^{-ia_1} \cdot \frac{\{(a-ipt+i\chi)^{1-\delta} - (a-ipt-i\chi)^{1-\delta}\}}{\chi\{(a-ipt)^2+\chi^2\}^{1-\delta}} .$$

where

$$(12) \qquad \chi = \sqrt{t^2p^2 + 2t\boldsymbol{p}\cdot\boldsymbol{q} + q^2} .$$

The possible singularities of the integrand in (11) are the branch points of χ and the zero of $\{(a-ipt)^2+\chi^2\}$. One can show easily that the integrand is regular at the branch points of χ. The only singularity is thus at $t=\sigma$, where

$$(13) \qquad \sigma = -(a^2+q^2)/2(\boldsymbol{q}\cdot\boldsymbol{p} - ipa) .$$

Let us now extend the contour to a large circle Γ of radius ϱ excluding the branch point at $t=\sigma$ by a small circle γ of radius η as shown in Fig. 1. We have then

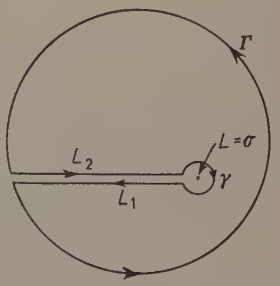

Fig. 1. – The contour in the t-plane.

$$(14) \qquad J(-\delta) = J_\Gamma + J_{L_2} + J_\gamma + J_{L_1} ,$$

where the respective contours are denoted by the subscripts and have been shown in Fig. 1. The lines L_1, L_2 have been chosen to extend from σ to the left so that they may not contain the branch points of χ. It can be shown in an elementary way that as $\varrho \to \infty$ and $\eta \to 0$ both J_Γ and J_γ vanish. We fix the branch of χ in such a way that $\chi = i(a-ipt)$ at $t=\sigma$. We further define

$$(15a) \qquad J' = \Gamma(1-\delta)\int \mathrm{d}t\, t^{ia_1-1}(t-1)^{-ia_1} \frac{(a-ipt-i\chi)^{1-\delta}}{\chi\{(a-ipt)^2+\chi^2\}^{1-\delta}} ,$$

and

$$(15b) \qquad J'' = -\Gamma(1-\delta)\,\mathrm{d}t\, t^{ia_1-1}(t-1)^{-ia_1} \frac{(a-ipt+i\chi)^{1-\delta}}{\chi\{(a-ipt)^2+\chi^2\}^{1-\delta}} .$$

The integrand of J'' is regular at $t=\sigma$. Therefore,

$$J''_{L_2} + J''_{L_1} = 0 .$$

We choose arg $(t-\sigma)$ to be π on L_2 and $-\pi$ on L_1. After considerable simplification we then have from (14) and (15)

$$J(-\delta) = C'\left(\frac{\boldsymbol{p}\cdot\boldsymbol{q}}{p} - ia\right)^{\delta} J_0 K\,, \tag{16}$$

where

$$C' = \Gamma(1-\delta)(2\exp[-\tfrac{1}{2}\pi i])^{\delta}, \tag{17}$$

$$K = \frac{(\exp[2\pi i\delta]-1)}{4\pi i}\int_0^{\infty} \mathrm{d}\xi (1-u\xi)^{ia_1-1}(1-v\xi)^{-ia_1}\frac{\{1-\xi+R\}^{1-\delta}}{R\xi^{1-\delta}}\,, \tag{18}$$

and

$$J_0 = \frac{4\pi(a^2+q^2)^{ia_1-1}}{\{(a-ip)^2+(\boldsymbol{p}+\boldsymbol{q})^2\}^{ia_1}}\,. \tag{19}$$

In the above

$$\left\{\begin{array}{l} u = 1+\dfrac{ia}{p\sigma}; \qquad v = \dfrac{p\sigma+ia}{p(\sigma-1)}\,, \\ \text{and} \\ R = \sqrt{\xi^2-2\xi x+1} \qquad \text{with} \qquad x = \dfrac{p^2\sigma+\boldsymbol{p}\cdot\boldsymbol{q}}{p^2\sigma+ipa}\,. \end{array}\right. \tag{20}$$

It may be observed that the integral in the expression for K in (18) behaves as $2/\delta$ for small δ. The presence of the factor $(\exp[2\pi i\delta]-1)$ however, ensures that the value of K is finite. The expression for K in (18) may be further simplified if one remembers that in our formulation we can always neglect terms of relative $O(a/\varepsilon)$. For this purpose, we observed that in high energy photoeffect the angle of emission $\theta(=\sphericalangle\, \boldsymbol{k},\boldsymbol{p})$ for most of the photoelectrons is of $O(1/\varepsilon)$. Therefore, q is of $O(1)$ and v, as defined in (20), is of order $1/\varepsilon$. The integral K exists if $v=0$, so that, if it be expanded in powers of v in the neighbourhood of $v=0$, only positive powers of v will appear in the expansion and, that too, in terms of $O(a^3)$. We may, therefore, put $v=0$ in the expression for K, the error committed thereby being of $O(a^3/\varepsilon)$. We thus have

$$K = \frac{(\exp[2\pi i\delta]-1)}{4\pi i}\int_0^{\infty} \mathrm{d}\xi (1-u\xi)^{ia_1-1}\frac{\{1-\xi+R\}^{1-\delta}}{R\xi^{1-\delta}}\,. \tag{21}$$

It can be easily shown that

$$K = 1+O(a^2)\,. \tag{22}$$

Neglecting terms of $O(a^2)$ we can therefore write from (16)

$$J(-\delta) \approx C'J_0 = C' \cdot \frac{4\pi(a^2+q^2)^{ia_1-1}}{\{(a-ip)^2+(\boldsymbol{p}+\boldsymbol{q})^2\}^{ia_1}}. \tag{23}$$

This is exactly the value obtained by SOMMERFELD (2). Substituting this approximate value of $J(-\delta)$ in eqs. (8) we obtain after some simplifications and neglecting terms of relative $O(a/\varepsilon)$ and $O(a^2)$

$$I_0 = \frac{C'J_0 a(1-ia)}{(\varepsilon-1)}\left\{\frac{1}{\varepsilon(1-\beta\cos\theta)}-\varepsilon\right\}, \tag{24a}$$

$$\boldsymbol{I}_1 = \frac{iC'J_0 a(1-ia)}{2(1-\frac{1}{2}\delta)(\varepsilon-1)}\left\{\frac{1}{\varepsilon(1-\beta\cos\theta)}\boldsymbol{q}-ia\boldsymbol{k}\right\}, \tag{24b}$$

$$\boldsymbol{I}_2 = \frac{C'J_0 a(1-ia)}{2(\varepsilon-1)}\boldsymbol{q}, \tag{24c}$$

where β is the electron velocity and $\theta = \sphericalangle(\boldsymbol{k}, \boldsymbol{p})$ is the angle of scattering. The correction terms for I_0 and $\boldsymbol{I}_1$ in (24a) and (24b) due to the approximation of $J(-\delta)$ by J_0 are of relative $O(a)$ and $O(a^2)$ respectively. The integral $\boldsymbol{I}_2$ is already of $O(1/\varepsilon)$ relative to I_0 and $\boldsymbol{I}_1$, so that its correction terms will contribute only terms of relative $O(a/\varepsilon)$ in the matrix element, which we shall neglect. It is thus evident, up to terms of relative $O(a)$, only the expression for I_0 in (24a) will be affected.

In eqs. (24) terms of relative $O(a^2)$ have been intentionally retained in order to preserve symmetry. It may be pointed out here that even in the approximation up to which eqs. (24) are valid, the Born approximation would not give the same results as ours. In fact, in the Born approximation the integral $\boldsymbol{I}_2$ and the second terms within the braces in (24a) and (24b) do not arise.

The problem of obtaining a suitable expression for the integral $J(-\delta)$ in (16) thus reduces to evaluating K in a closed form, which, however, does not appear to be possible. Derivation of a closed expression for K correctly up to terms even of $O(a^2)$ will prove to be a difficult task. But so far as our matrix element is concerned we need find only the derivatives of K with respect to the parameters u and x in terms of which it has been defined. It will be presently shown that these derivatives, though not exactly integrable, admit of suitable approximations.

From (20) and (21) we have,

$$\frac{\partial K}{\partial u} = \frac{(\exp[2\pi i\delta]-1)}{4\pi i}(1-ia_1)\int_0^\infty d\xi(1-u\xi)^{ia_1-2}\frac{\xi^\delta(1-\xi+R)^{1-\delta}}{R}, \tag{25a}$$

and

$$(25b)\quad \frac{\partial K}{\partial x} = \frac{(\exp[2\pi i\delta]-1)}{4\pi i}\int_0^\infty d\xi(1-u\xi)^{ia_1-1}\frac{\xi^\delta(1-\xi+R)^{1-\delta}}{R^2}\left[\frac{1}{R}-\frac{1-\delta}{1-\xi+R}\right].$$

The integrals in (25) are now convergent as $\delta \to 0$ and the factor $(\exp[2\pi i\delta]-1)$ ensures that $\partial K/\partial u$ and $\partial K/\partial x$ are both of $O(a^2)$. We may, therefore, put $\delta = 0$ in the integrands if terms of relative order a^3 are neglected in the matrix element and obtain

$$(26a)\quad \frac{\partial K}{\partial u} = \frac{\delta}{2}(1-ia_1)\int_0^\infty d\xi(1-u\xi)^{ia_1-2}\frac{(1-\xi+R)}{R} + O(a^4),$$

and

$$(26b)\quad \frac{\partial K}{\partial x} = \frac{\delta}{2}\int_0^\infty d\xi(1-u\xi)^{ia_1-1}\cdot\frac{(1-\xi)}{R^3} + O(a^4).$$

The values of $\partial K/\partial u$ and $\partial K/\partial x$ in the first approximation, as derived in Appendix B, are

$$(27a)\quad \frac{\partial K}{\partial u} = \frac{\delta}{2}\left(-1+\frac{\pi i}{\sqrt{2(1-x)}}\right) \approx \frac{a^2}{4}\left(-1-\frac{\pi i pq}{2\boldsymbol{p}\cdot\boldsymbol{q}}\right),$$

and

$$(27b)\quad \frac{\partial K}{\partial x} = \frac{\delta}{2}\cdot\frac{1}{1-x} \approx \frac{a^2}{8}\cdot\left(\frac{pq}{\boldsymbol{p}\cdot\boldsymbol{q}}\right)^2.$$

Therefore

$$(28)\quad \frac{\partial K}{\partial a} = \frac{a^2}{4}\left(\frac{2ip}{\boldsymbol{p}\cdot\boldsymbol{q}}-\frac{\pi}{q}\right).$$

The expression for I_0, correct up to terms of relative $O(a)$, may now be easily calculated from (8a), (16) and (28)

$$(29)\quad I_0 = C'J_0\frac{a(1-ia)}{(\varepsilon-1)}\left\{\frac{1}{\varepsilon(1-\beta\cos\theta)}-\varepsilon+\frac{\pi a}{4\sqrt{2}}\cdot\frac{1}{(1-\beta\cos\theta)^{\frac{1}{2}}}\right\}.$$

Substituting the values of $\boldsymbol{I}_1$, $\boldsymbol{I}_2$, and I_0 from (24b), (24c), and (29) in the matrix element H_{12} in (6) one now gets the result correctly up to terms of relative $O(a)$. For a better approximation the values of $\partial K/\partial u$ and $\partial K/\partial x$, and hence of I_0 correctly up to terms of relative $O(a^2)$ have to be calculated from eqs. (26). For the evaluation of the correction terms of $\boldsymbol{I}_1$, the values of $\partial K/\partial u$ and $\partial K/\partial x$ as given in eqs. (27) are sufficient.

4. – Angular distribution and absorption coefficient.

Summing over the final and averaging over the initial spin states of the electron one now gets from (6)

$$(30)\quad |H_{12}|^2 = \tfrac{1}{2}|C|^2[(\varepsilon-1)|I_0|^2 + (\varepsilon+1)|\boldsymbol{I}_1 - i\boldsymbol{I}_2|^2 + \\ + 4(\varepsilon+1)\,\mathrm{Im}\,(\boldsymbol{e}\cdot\boldsymbol{I}_1)(\boldsymbol{e}\cdot\boldsymbol{I}_2^*) + 4(\boldsymbol{p}\cdot\boldsymbol{e})\,\mathrm{Im}\,I_0(\boldsymbol{e}\cdot\boldsymbol{I}_1^*) + 2\,\mathrm{Im}\,I_0^*\{\boldsymbol{p}\cdot(\boldsymbol{I}_1 - i\boldsymbol{I}_2)\}]\,.$$

In the above the symbol Im signifies that we are to take the imaginary part of the expression following. Substituting the expressions for I_0, $\boldsymbol{I}_1$, and $\boldsymbol{I}_2$ derived in the preceding section and neglecting terms of relative $O(a/\varepsilon)$ and $O(a^2)$ we get after some simplifications

$$(31)\quad |H_{12}|^2 = |M|^2\left[\frac{\beta^2\sin^2\theta}{2(1-\beta\cos\theta)^3}\cdot\right. \\ \left.\cdot\left\{(\varepsilon-1)^2 + \frac{4\cos^2\varphi}{\varepsilon(1-\beta\cos\theta)} - 2(\varepsilon-1)\cos^2\varphi\right\} - \frac{\pi a\beta\varepsilon}{\sqrt{2}(1-\beta\cos\theta)^{\frac{1}{2}}}\sin^2\frac{\theta}{2}\right],$$

where

$$(32)\qquad |M|^2 = |C|^2|C'|^2\cdot\frac{2\pi^2a^2(1+a^2)}{(1-\frac{1}{2}\delta)^2\varepsilon(\varepsilon-1)^4}\exp\left\{-2\pi a + 2a\,\mathrm{tg}^{-1}\frac{a}{1-\delta}\right\},$$

and φ is defined by $\boldsymbol{p}\cdot\boldsymbol{e} = p\sin\theta\cos\varphi$.

We observe that the result given in (31) does not differ qualitatively from Sauter's formula for the angular distribution. It is apparent from eq. (31) that up to our order of approximation there will be no emission of photoelectrons in the forward direction ($\theta = 0$). The experimental value 0.29 of HULTBERG and HEDGRAM [3], the exact theoretical value 0.27 and the first approximation value 0.21 obtained by SAUTER and WUSTER [10] for the ratio of the forward and maximum intensities of the photoelectrons ejected from Pb-converters by 1.3 MeV γ-rays show that most of the contributions to the forward distribution of photoelectrons come from terms of relative order a/ε in the matrix element. We are, therefore, led to conclude that the ratio of forward and maximum intensities of photoelectrons should diminish as the primary energy increases.

The absorption coefficient of the K-shell is given by [9]

$$(33)\qquad \tau_K = 2N_0(2\pi)^2\beta\varepsilon^2\int|H_{12}|^2\,\mathrm{d}\Omega\,,$$

---

[10] F. SAUTER and H. O. WUSTER: *Zeits. f. Phys.*, **141**, 83 (1955).

where N_0 is the number of atoms per cm^3. Substitution of the expression for $|H_{12}|^2$ from (31) then leads to

$$\tau_K = N_0 \frac{\exp\left[-\pi a + 2a \operatorname{tg}^{-1}(a/1-\delta)\right]\left(1+\left((33-2\pi^2)/6\right)\delta\right)}{a^{2\delta}} \cdot \frac{4\pi\alpha^6 Z^5}{(\varepsilon-1)^4} \cdot \beta\varepsilon^3 \left\{1 - \frac{4\pi a}{15} - \frac{2(\varepsilon-2)}{3\varepsilon^2} + \frac{\varepsilon-2}{2\beta\varepsilon^3} \ln\left(\frac{1-\beta}{1+\beta}\right)\right\}, \tag{34}$$

approximately, where α is the fine structure constant. Although our result is correct only up to terms of relative $O(a)$, we have retained higher order terms which appear naturally in our calculation so as to illustrate the close similarity of our result with the expression derived by HALL [4] for the absorption coefficient in the extreme relativistic case. It may, however, be pointed out that the a-dependent term within the braces in (34) viz., $(-4\pi a/15)$ differs from the corresponding term $0.05 \operatorname{tg}^{-1}(.63/a)$ in the expression given at the end of Section **21** of reference [4]. The difference may be attributed to the probable inaccuracy of the approximation of a very complicated double integral, which Hall was forced to make in the final steps of his calculation. In fact, from the way this approximation has been made by HALL it appears that the error in Hall's result is of relative order a^2 if not greater.

In view of the close agreement of the results of the exact numerical calculation of HULME *et al.* [11] with the formula of Hall, the validity of our correction term may be questioned. One may, however, argue that in the particular formula which is given in eq. (17) of reference [4] and to which HULME *et al.* have referred, the term $0.05a \operatorname{tg}^{-1}(.63/a)$ does not occur. Secondly, although the formula of Hall was modified by HULME *et al.* so that it might coincide with Sauter's formula in the limit $a \to 0$, it is, however, clear that in any such modification contributions from terms of relative order a/ε (which is not small in the range of energy considered by HULME *et al.*) can not be included. It is quite likely that these contributions would partially cancel the deviation of Hall's formula from the correct one. For further justification of our result (34) it may be pointed out that the diminishing effect of the term $(-4\pi a/15)$ would be sufficiently neutralized by higher order correction terms. This is apparent from the factor $\left(1+\left((33-2\pi^2)/6\right)\delta\right)$ in (34) and also from the fact that in the case of large Z (*viz.*, $Z=84$), where these correction terms are significant, numerical results obtained from the formula (17) of reference [4] are less than the corresponding results of HULME *et al.* [11], whereas for low Z the contrary is true.

---

[11] H. R. HULME, J. MCDOUGALL, R. A. BUCKINGHAM and R. H. FOWLER: *Proc. Roy. Soc.*, A **149**, 131 (1935).

5. – One quantum annihilation of positrons.

The process of simultaneous annihilation of a positron and a K-electron with the emission of one quantum of radiation may be considered as the transition of the bound electron to a state of energy $-\varepsilon$ and momentum $-\boldsymbol{p}$, where $(\boldsymbol{p}, \varepsilon)$ are the momentum and energy of the incident positron. One can thus directly obtain the matrix element for this process if in the matrix element (2) for the photoelectric effect $(\boldsymbol{k}, k)$ and $(\boldsymbol{p}, \varepsilon)$ are replaced by $(-\boldsymbol{k}, -k)$ and $(-\boldsymbol{p}, -\varepsilon)$ respectively, according to the well known substitution law. Calculating exactly by the method followed in the preceding sections one gets

$$(35) \qquad |H'_{12}|^2 = |A|^2 \frac{\alpha^6 Z^5}{8\pi^2\varepsilon^2(\varepsilon+1)^5}\left[\frac{\beta^2\sin^2\theta}{2(1-\beta\cos\theta)^3}\cdot\right.$$
$$\left.\cdot\left\{(\varepsilon+1)^2 - \frac{4\cos^2\varphi}{\varepsilon(1-\beta\cos\theta)} + 2(\varepsilon+1)\cos^2\varphi\right\} - \frac{\pi a\beta\varepsilon}{\sqrt{2}(1-\beta\cos\theta)^{\frac{1}{2}}}\cdot\sin^2\frac{\theta}{2}\right],$$

of the angular distribution of the polarized photon and

$$(36) \qquad \sigma'_K = |A|^2 4\pi\alpha^6 Z^5 \cdot \frac{\varepsilon}{\beta(\varepsilon+1)^2}\left[1 - \frac{4\pi a}{15} + \frac{2(\varepsilon+2)}{3\varepsilon^2} + \frac{\varepsilon+2}{2\beta\varepsilon^3}\ln\left(\frac{1-\beta}{1+\beta}\right)\right],$$

with

$$(37) \qquad |A|^2 = \frac{\exp\left[-\pi a + 2a\,\mathrm{tg}^{-1}\,(a/1-\delta)\right]}{a^{2\delta}}\cdot\left(1 + \frac{33-2\pi^2}{6}\delta\right),$$

for the annihilation cross-section due to the two electrons in the K-shell. The undefined symbols used in the above exactly correspond to those employed in the case of the photoelectric effect.

From eqs. (35) and (36) it is apparent that the expressions for both the angular distribution and the total cross-section can be obtained directly from the corresponding formulae for the photoelectric effect by applying the substitution law except for a factor $(\varepsilon+1)^2/\beta^2\varepsilon^2$ in σ'_K. The origin of this factor may be traced to the fact that while obtaining the total cross-section for positron annihilation, one has to integrate the expression for the angular distribution over the momenta of the emitted radiation and divide by the velocity β of the incident positron, whereas in the photoelectric effect the integration is over the momenta of the photoelectron and the velocity of the incident quantum is unity. One may further observe that the correction terms in the formulae of Bhabha and Hulme (8) are the same as those in Sauter's

formulae. Our results thus resolve the doubt [12] about the applicability of the correction terms for the photoelectric effect to the positron annihilation process without any modification.

* * *

The author wishes to thank Prof. S. Gupta and Dr. G. Bandyopadhyay for many helpful discussions and encouragement throughout the present investigation. I am also grateful to Prof. J. M. Jauch of Iowa State University, U.S.A., for his kind interest in this work.

Appendix A

The eqs. (27) will now be derived from (26) employing a proper limiting procedure. The difficulty that arises in our approximation is due to the singularity of the integrands in (26) at $\xi = 1/u$ which, according to eq. (21), approaches $\xi = 1$ as $a \to 0$.

The derivation of (27*b*) presents no difficulty as the integrand behaves properly at $\xi = 1$. One readily obtains setting $a = 0$ in the integrand in (26*b*)

$$\frac{\partial K}{\partial x} = \frac{\delta}{2}\int_0^\infty \frac{\mathrm{d}\xi}{R^3} = \frac{\delta}{2}\cdot\frac{1}{1-x}. \tag{A.1}$$

From (26*a*) one gets

$$\frac{\partial K}{\partial u} = \frac{\delta}{2}(1-ia_1)\left[-\frac{1}{u(1-ia_1)} + \int_0^\infty \mathrm{d}\xi\cdot\frac{(1-u\xi)^{ia_1-1}}{R} - (1-u)\int_0^\infty \mathrm{d}\xi(1-u\xi)^{ia_1-2}\cdot\frac{\xi}{R}\right]. \tag{A.2}$$

It should be observed that the integrals in (A.2) vanish identically if one directly sets $u = 1$ and $a = 0$ in the integrands. But, as will be shown presently, the first integral in (A.2) has a non-vanishing value in the limit $a = 0$. We write it as the sum of three integrals

$$\int_0^\infty d\xi\,\frac{(1-u\xi)^{ia_1-1}}{R} = \left[\int_0^{1-\eta} + \int_{1-\eta}^{1+\eta} + \int_{1+\eta}^\infty\right]\mathrm{d}\xi\,\frac{(1-u\xi)^{ia_1-1}}{R}, \tag{A.3}$$

[12] J. C. Jaeger and H. R. Hulme: *Proc. Camb. Phil. Soc.*, **32**, 158 (1936).

where η is a small positive quantity, but otherwise quite arbitrary. We take $\eta \gg |1-u|$ and a. The singularity $\xi = 1/u$ of the integrand lies outside the range of integration for the first and the third integral. One can, therefore, set $u=1$ and $a=0$ in these integrands and ultimately find that they cancel each other. Such a procedure is not permissible for the second integral because the singularity shifts from $1/u$ to 1 in the ξ-plane as $a \to 0$ and thus lies within the range of integration. From (21a) it is apparent that the point $1/u$ lies below the real axis in the ξ-plane. We can, therefore, replace the path $(1-\eta)$ to $(1+\eta)$ by a semi circle of radius η about $\xi = 1$ above the real axis (Fig. 2). Further, as R is analytic in the neighbourhood of $\xi = 1$, one can replace R by $\sqrt{2(1-x)(1+\theta')}$, where $|\theta'|$, which is small, vanishes as $\eta \to 0$, and this factor may be brought outside the sign of integration. So that

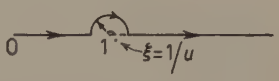

Fig. 2. – Contour in the ξ-plane.

$$\mathop{\mathcal{L}t}_{a\to 0} \int_{1-\eta}^{1+\eta} \mathrm{d}\xi \, \frac{(1-u\xi)^{ia_1-1}}{R} =$$

$$= \frac{1}{\sqrt{2(1-x)(1+\theta')}} \mathop{\mathcal{L}t}_{a\to 0} \int_{\pi}^{0} i\eta \, \exp[i\theta] \, \mathrm{d}\theta (1-u-u\eta \exp[i\theta])^{ia_1-1} =$$

$$= \frac{\pi i}{\sqrt{2(1-x)(1+\theta')}} .$$

We can now make $\eta \to 0$ and finally get

$$\mathop{\mathcal{L}t}_{a\to 0} \int_{1-\eta}^{\eta+1} \mathrm{d}\xi \, \frac{(1-u\xi)^{ia_1-1}}{R} = \frac{\pi i}{\sqrt{2(1-x)}} . \tag{A.4}$$

In a similar manner one can show that the second integral in (A.2) tends to zero with a. Neglecting terms of relative order a we, therefore, get

$$\frac{\partial K}{\partial u} = \frac{\delta}{2} \left(-1 + \frac{\pi i}{\sqrt{2(1-x)}} \right) . \tag{A.5}$$

Appendix B

The term I_3, neglected in the matrix element, can be written from eqn. (6d) in the form,

$$I_3 = -\frac{ap}{2\varepsilon(2-\delta)} (\boldsymbol{\alpha}\cdot\boldsymbol{\nabla}_p)(\boldsymbol{e}\cdot\boldsymbol{\gamma})(\boldsymbol{\gamma}\cdot\boldsymbol{\nabla}_q) J_1 , \tag{A.6}$$

where J_1 may be obtained from $J(-\delta)$ by replacing δ by $(1+\delta)$. One, therefore, gets from (16) and (21) neglecting terms of relative $O(a^2/\varepsilon)$

$$J_1 = \frac{\Gamma(-\delta)(\exp[2\pi i\delta]-1)}{4\pi i}(2\exp[-\tfrac{1}{2}\pi i])^{1+\delta}J_0K_1\,, \tag{A.7}$$

where

$$K_1 = \left(\frac{\boldsymbol{p}\cdot\boldsymbol{q}}{p}-ia\right)^{1+\delta}\int_0^\infty \mathrm{d}\xi(1-u\xi)^{ia_1-1}\frac{(1-\xi+R)^{-\delta}}{R\xi^{-\delta}}\,.$$

It follows from (20) that u and R and, therefore, K_1 are of zeroth order in p. So that $(\boldsymbol{\nabla}_p K_1)$ can at most have terms of $O(1/\varepsilon)$. Thus, if we neglect terms of $O(a/\varepsilon)$ in $(\boldsymbol{\nabla}_p K_1)$ and, therefore, of $O(a)$ in K_1 we get from Appendix A

$$K_1 = \frac{\boldsymbol{p}\cdot\boldsymbol{q}}{p}\cdot\frac{\pi i}{\sqrt{2(1-x)}} = -\frac{\pi i}{2q}$$

so that

$$(\boldsymbol{\nabla}_p K_1) = 0\,.$$

Therefore, $(\boldsymbol{\nabla}_p K_1)$ is of $O(a/\varepsilon)$. Further, from (24c) it is apparent that $(\boldsymbol{\nabla}_r J_0)$ is of $O(a/\varepsilon)$. Thus, from (A.6) and (A.7) it follows that the contribution of I_3 to the matrix element is of relative order a/ε and can, therefore, be neglected.

Appendix C

The following calculations are intended to show that the maximum contribution to the integral $J(-\delta)$ arises from: (a) regions within distances from the nucleus of the order of Compton wave-length (*i.e.*, $r \approx 1$) of the electron, and (b) final state wave functions which correspond to angular momenta $l \approx \varepsilon$.

a) Separating the confluent hypergeometric function in the integrand in (7) in polar coordinates [13] one obtains,

$$\exp[-i\boldsymbol{pr}]\,F(ia_1;1;ipr+i\boldsymbol{pr}) = \frac{1}{\Gamma(1-ia_1)}\sum_l (2l+1)(-i)^l L_l(r)P_l(\cos\vartheta)\,, \tag{A.8}$$

where

$$L_l(r) = [\Gamma(l+1-ia_1)/(2l+1)!]\,(2pr)^l\exp[ipr]\,F(l+1-ia_1;2l+2;-2ipr)\,,$$

[13] W. Gordon: *Zeits. f. Phys.*, **48**, 180 (1928).

and $\vartheta = \sphericalangle(\boldsymbol{p}, \boldsymbol{r})$. Substituting (A.8) in (7) one obtains after performing the angular integrations

$$(A.9) \qquad J(-\delta) = \frac{\pi^{\frac{1}{2}}}{\Gamma(1-ia_1)} \sum_l \frac{\Gamma(l+1-ia_1)}{(2l)!\Gamma(l+\frac{3}{2})} (pk)^l P_l(\cos\theta) \cdot$$

$$\cdot \int_0^\infty \mathrm{d}r\, r^{2l+2-\delta} \exp[-ar - i(k-p)r]\, F(l+1-ia_1;\, 2l+2;\, -2ipr)\, F(l+1;\, 2l+2;\, 2ikr) .$$

Maximum contributions to the integrals thus come from the region

$$(A.10) \qquad r = \frac{1}{|a + i(k-p)|} \approx 1 ,$$

in the high energy limit. For distance larger than this the exponential factor falls off rapidly.

b) In order to find the relative order of contributions to $J(-\delta)$ from final state wave-functions corresponding to different l, it is enough to obtain an approximate expansion of the from

$$(A.11) \qquad J(-\delta) = \sum_l M(l) P_l(\cos\theta) ,$$

and consider the behaviour of $M(l)$. Neglecting terms of relative order a we obtain [14] from (19)

$$(A.12) \qquad J(-\delta) \approx \frac{2\pi}{pk}\left(\frac{1}{\beta} - \cos\theta\right)^{-1} = \frac{2\pi}{pk} \sum_l (2l+1) Q_l\left(\frac{1}{\beta}\right) P_l(\cos\theta) ,$$

where Q_l is a Legendre function of the second kind of order l. For small values of l and as $\beta \to 1$, the behaviour of Q_l is approximately given by [14]

$$(A.13) \qquad Q_l\left(\frac{1}{\beta}\right) \approx -\frac{1}{2} \ln\left(\frac{1-\beta}{2\beta}\right) - \gamma - \Psi(l+1) ,$$

in terms of the well-nown Ψ-function and the Euler constant γ. From (A.11) and (A.13) we therefore conclude that for small values of l, $M(l)$ increases

---

[14] A. ERDELYI: *Higher Transcendental Functions*, Vol. 1 (New York, 1953), pp. 168, 163.

as $(2l+1)\ln 2\varepsilon$. If, however, l is of $O(\varepsilon)$, so that $(l/p) = x$ is finite, we get [15]

$$Q_l\left(\frac{1}{\beta}\right) \approx \left(\frac{\pi}{2x}\right)^{\frac{1}{2}} \exp[-x], \tag{A.14}$$

asymptotically. Hence in this region M_l increases as $(2lp)^{\frac{1}{2}} \exp[-l/p]$, which is maximum for $l = p$.

([15]) H. JEFFREYS and B. S. JEFFREYS: *Methods of Mathematical Physics* (Cambridge, 1956), p. 656.

RIASSUNTO (*)

Si sono calcolate la distribuzione angolare e la sezione d'urto totale per l'effetto fotoelettrico alle alte energie e l'annichilamento monoquantico dei positroni nello strato K ricorrendo all'approssimazione di Sommerfeld-Maue per la funzione d'onda dello stato di scattering del fermione. L'errore commesso in questo procedimento è dell'ordine a/ε, dove $a = Z/137$ ed ε è l'energia dello stato di scattering in unità mc^2 ed è pertanto trascurabile nei casi relativistici estremi. Si sono ottenuti risultati corretti fino a termini di ordine relativo a e si sono anche indicati metodi per calcolare i contributi di termini più elevati. L'espressione per la distribuzione angolare dei fotoelettroni ottenuta nel presente lavoro non mostra differenze qualitative marcate dalla formula di Sauter. Si può concludere dai nostri risultati che il rapporto dell'intensità equiversa a quelle massime dei fotoelettroni diminuisce col crescere dell'energia primaria. Si presenta il coefficiente d'assorbimento per l'effetto fotoelettrico in forma simile ai risultati di Hall. Si è trovato che i termini di correzione per le formule di Bhabha e Hulme per il processo di annichilamento del positrone sono uguali a quelli della formula di Sauter.

(*) *Traduzione a cura della Redazione.*

High Z Nuclei in Cosmic Radiation.

V. Bisi, R. Cester, C. M. Garelli and L. Tallone

Istituto di Fisica dell'Università - Torino
Istituto Nazionale di Fisica Nucleare - Sezione di Torino

(ricevuto il 3 Ottobre 1958)

Summary. — Adding the results obtained by measuring the charges of 117 heavy nuclei ($Z \geqslant 10$) to those obtained in a previous paper, we determined the values of the ratio $N(Z \geqslant 15)/N(Z \geqslant 10)$ at flight altitude and at the top of the atmosphere, and of the ratio $N(Z=26)/N(Z \geqslant 10)$ at flight altitude, at the top of the atmosphere and at the C.R. source. It results that the chemical composition of the C.R. source differs from the average composition of the universe, being much richer in heavy nuclei ($Z \geqslant 15$) and in particular in Iron. The absorption mean free path in air was also determined studying the zenith angle dependence of C.R. flux.

1. – Introduction.

The knowledge of the detailed features of the Cosmic Ray charge spectrum, is of great interest in the problem of the Cosmic Ray origin.

In particular from the relative abundance of nuclei of charge $Z \geqslant 10$ (H-nuclei) information can be derived on the chemical composition of the C.R. source, since this part of the spectrum is qualitatively the less affected in the diffusion through space and, therefore, may reflect its original composition.

Unfortunately this part of the spectrum is the less well known owing both to lack of statistics and to experimental difficulty in obtaining a good charge resolution. In a previous paper [1] which will be referred to as paper I, the Turin group used for charge analysis of the heavy primary spectrum a photo-

[1] R. Cester, A. Debenedetti, C. M. Garelli, B. Quassiati, L. Tallone and M. Vigone: *Nuovo Cimento*, **7**, 371 (1958).

metric device (²) that allowed a good charge discrimination up to the heaviest C.R. nuclei ($Z \simeq 26$).

The present research was carried out, under experimental conditions comparable with those of (I), in order to improve statistics for H-nuclei.

The interaction mean free path in air for these particles was also obtained studying the flux dependence from the zenith angle.

2. – Exposure details.

The emulsion plates used in this research were part of a large G-5 stack flown with vertical geometry over Texas ($\Lambda = 41^\circ$ N) in January 1955, at an atmospheric depth of 13.5 g/cm². The flight curve is given in Fig. 1. To the amount of residual atmosphere a total of 3 g/cm² must be added in order to take into account the packing material (1 g/cm²) and a layer 5 mm thick of emulsion over the scanned area.

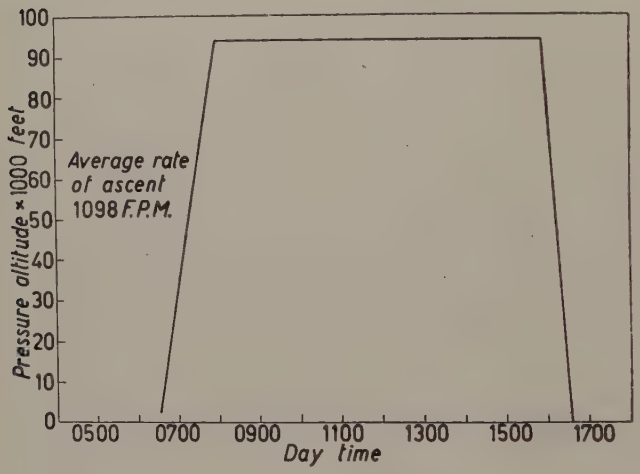

Fig. 1. – Time-altitude curve for Texas flight.

3. – Detection of particles.

A total area of 32.6 cm² of emulsion was scanned at 5 mm from the top edge of the stack. In order to improve statistics for large zenith angle tracks an additional area of 13.6 cm² (6.8 cm² from each side) was scanned at 5 mm from the lateral edges of the stack emulsions.

The selection criteria were the following:

1) range/plate $\geqslant 1.5$ mm.
2) number of δ-rays/100 μm $\geqslant 5.5$. This value had been found previously to correspond in our emulsion to a $Z = 8$ track (identified by its splitting products).
3) zenith angle $\theta \leqslant 70^\circ$.

(²) M. ARTOM, V. BISI and C. GENTILE: *Ricerca Scientifica* (1958), p. 287.

The problem of selecting the tracks to be followed through the stack, out of the observed ones, was made difficult by the fact that the range/plate of every track was changing near the upper edge of the stack due to emulsion distortions. We decided to trace through the stack only those tracks that had a range per plate $\geqslant 3$ mm in at least three plates. This criterium ensures the measurability of the photometric absorption of the track.

In order to avoid systematic errors, we added to these the tracks that came to an interaction before the end of the distorted region but that would have satisfied the measurability criterium if they did not interact. The charge of these tracks was estimated by δ-ray counting.

The main disadvantage due to this selection criterium consists in the indefiniteness of the solid angle cone of acceptance and, as a consequence, in the impossibility of estimating, in the present work, the H-nuclei absolute vertical flux.

4. – Charge identification.

Results of photometric absorption measurements on 68 H-nuclei tracks, entering the stack with zenith angle $\theta \leqslant 35°$ are reported on a histogram in Fig. 2*a*. The zenith angle limitation ensures us that the measured tracks are all due to H-nuclei of relativistic energy.

The measurement criteria were the same as described in paper (I). The photometric device was adjusted to give the maximum resolution in the region

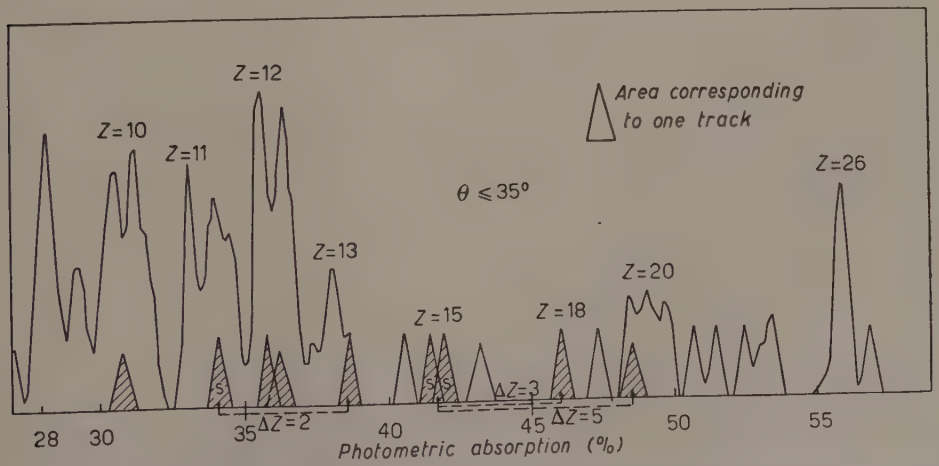

Fig. 2*a*. – Histogram showing the resolution in photometric measurements. Each track is represented by a triangle of constant area with a base equal to twice the standard deviation. The dashed areas correspond to the calibration tracks. Only tracks incident with a zenith angle $\theta \leqslant 3°5$ are reported.

of charge $Z \geqslant 10$. In this way we obtained well resolved peaks in the photometric absorption histogram (Fig. 2*a*, *b*).

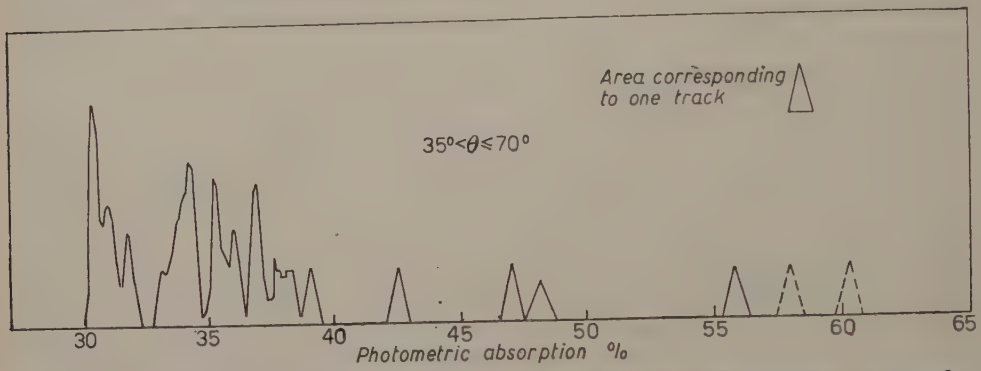

Fig. 2*b*. – Histogram showing the resolution in photometric measurements for tracks incident with a zenith angle $35° < \theta \leqslant 70°$. The broken line areas correspond to events which were determined to be not relativistic from the analysis of the interaction stars.

In order to establish a correct correspondence between photometric absorption and charge values, events in which charge could be unambiguously determined from the splitting products had to be carefully analyzed. Unfor-

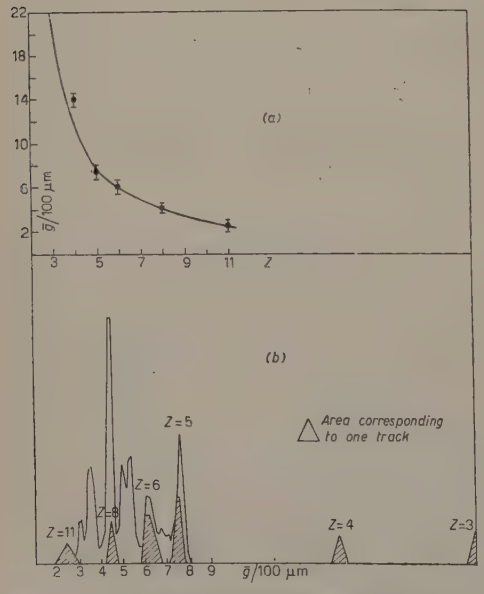

Fig. 3. – *a*) Total gap-length as a function of Z. *b*) Histogram showing the resolution in gap-length measurements. The dashed areas correspond to the calibration tracks.

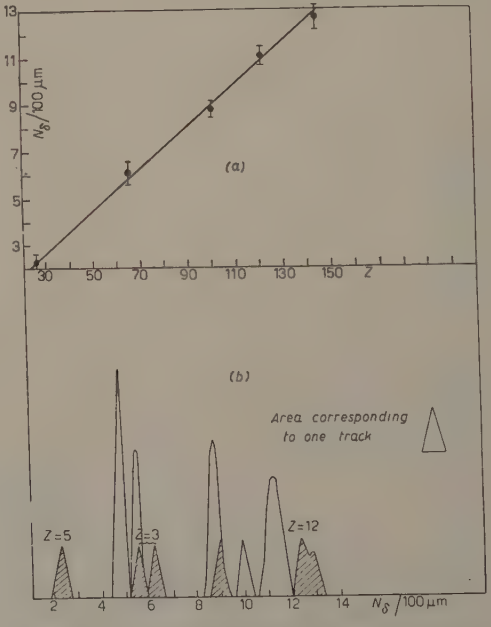

Fig. 4. – *a*) δ-ray density per 100 µm as a function of Z. *b*) Histogram showing the resolution in δ-ray counting. The dashed areas correspond to the calibration tracks.

TABLE I. – *Calibration events.*

Incoming nucleus	Target	Splitting	Charge measurements
Li	n	$\alpha+p$	Total gap length
Be	n	2α	Total gap length
B	n	$Li+\alpha$	Total gap length and δ-rays counting
	n	5p	Total gap length
C	n	$2\alpha+2p$	Total gap length
	n	6p	»
O	nucleus ($N_h=4$, $N_r=0$)	Be+2p	Total gap length
	nucleus ($N_h=3$, $N_r=0$)	B+3p	Total gap length and δ-ray counting
Ne	p (grey)	$B+\alpha+3p$	Ne: Phot. absorption; B: total gap length and δ-ray counting.
Mg	n	$0+2\alpha$	Mg: δ-ray counting and Phot. absorption; 0: total gap length and δ-ray counting.
	nucleus (*)	$N+\alpha+3p$	Mg: δ-ray counting and Phot. absorption; N: total gap length and δ-ray counting.
	nucleus (*)	$Li+3\alpha+3p$	Mg: Phot. absorption; Li: total gap length.
Al	nucleus ($N_h=18$, $N_r=0$)	Na+2p	Al: Phot. absorption; Na: Phot. absorption and total gap length.
A	n	$P+\alpha+p$	A and P: Phot. absorption.
Ca	p (grey)	$P+\alpha+3p$	Ca and P: Phot. absorption.

(*) In these events energy determination allowed us to definitely discriminate splitting protons from the other relativistic prongs of the star.

tunately such events become less frequent for higher charge values of primary nuclei.

All calibration events are reported in Table I. In most of them a heavy secondary particle is emitted and the accurate determination of its charge is essential in the interpretation of the event. Three methods have been used in the charge determination of heavy secondaries:

1) Total gap length for tracks of charge $3 \leqslant Z \leqslant 11$ (Fig. 3).

2) δ-ray counting for tracks of charge $5 \leqslant Z \leqslant 12$ (Fig. 4).

3) Photometric absorption measurements for tracks of charge $9 \leqslant Z$.

The photometric absorption values could then be plotted as a function of Z (Fig. 5) and were found to lie on a regular curve which can be represented by an analytic expression of the type:

$$A_m = a(1 - \exp[-b(Z - c)]) ,$$

where: $a = 66{,}67$; $b = 0{,}073$; $c = 1.45$.

The large peak at the upper limit of the spectrum belongs to this curve, corresponding to a charge value $Z = 26$.

In Fig. 2*b* are reported on a histogram 33 tracks entering the stack with a zenith angle $35° < \theta \leqslant 70°$.

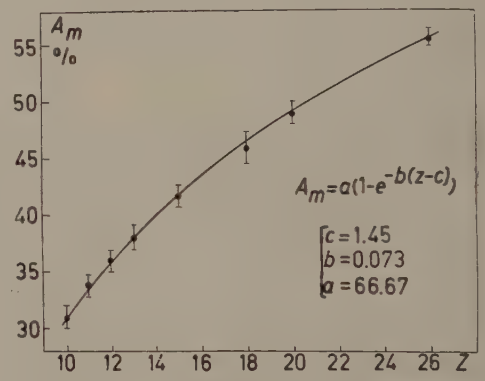

Fig. 5. – Variation of the photometric absorption with the charge.

Up to a charge value $Z = 14$ we calculated that at 41° geomagnetic latitude all measured tracks are relativistic. For charge values $Z > 14$ a percentage of the tracks incoming at the largest angles have a value of $\beta < 1$. Since most of the tracks in this charge region interact in the stack, an evaluation of the energy could be derived from the study of the interaction stars and as a consequence an indication for the charge could be obtained.

5. – Interaction mean free path in emulsion.

The interaction mean free paths in emulsion for all H-nuclei and for nuclei of charge $Z \geqslant 15$ were determined tracing through the stack the 117 tracks recorded. The values obtained are:

$$\lambda \text{ (emulsion)} = (42.9 \pm 4) \text{ g/cm}^2 \quad \text{for H-nuclei,}$$

$$\lambda \text{ (emulsion)} = (28.0 \pm 5) \text{ g/cm}^2 \quad \text{for nuclei of charge } Z \geqslant 15.$$

This set of values was used in the extrapolation of the charge spectrum to the top of the stack.

The result for H-nuclei is in very good agreement with the one reported in paper I.

6. – H-nuclei absorption in the atmosphere.

The analysis of the H-nuclei flux dependence from the zenith angle allows us to determine the absorption mean free path in air. Such method of determining the absorption mean free path is justified only if the cosmic ray flux incident on the top of the atmosphere, averaged over all azimuth angles, does not depend from the zenith angle. A recent experiment of DANIELSON and FREIER (3) seems to prove that this is the case at geomagnetic latitude 41° North, for zenith angles $\theta \leqslant 65°$.

In Fig. 6 are plotted in arbitrary units the flux values as a function of the thickness of air traversed, *a*) for H-nuclei, *b*) for nuclei of charge $Z \geqslant 15$.

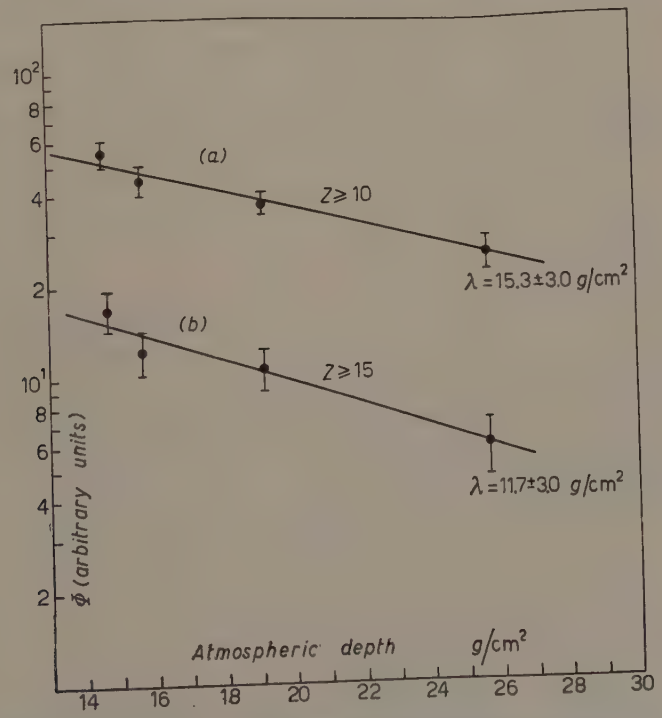

Fig. 6. – Dependence of the C.R. flux from the thickness of air traversed: curve *a*): for H-nuclei ($Z \geqslant 10$); curve *b*) for nuclei of $Z \geqslant 15$.

(3) R. E. DANIELSON and P. S. FREIER: *Phys. Rev.*, **109**, 151 (1958).

Every point was obtained as a result of a weighted mean of the T-stack (present work) and Y-stack (paper I) data. Statistical errors on each point are indicated.

The absorption curves are well represented by exponential laws. The absorption mean free path values, corresponding to the best fit exponential, are the following:

$$\lambda' \text{ (air)} = (15.3 \pm 3.0) \text{ g/cm}^2 \quad \text{for H-nuclei,}$$
$$\lambda' \text{ (air)} = (11.7 \pm 3.0) \text{ g/cm}^2 \quad \text{for nuclei of charge } Z \geqslant 15.$$

These results are in agreement, within the limits of statistical error, with the experimental values of FREIER *et al.* [4] and are not inconsistent with the values calculated following the method proposed by BRADT and PETERS [5], if the value for the fragmentation probability P_{III} is small ($\simeq 0.1$). It has been pointed out [6] that for atmospheric depths < 15 g/cm^2, the value of the H-nuclei absorption mean free path greatly increases, due to the fact that the main effect of H nuclei interactions at this stage results in a change of composition within the group itself, more than in an overall variation of the H-nuclei flux. In this case the H-flux dependence on atmospheric depth could not be represented by an exponential law.

The knowledge of a larger amount of data obtained at smaller atmospheric depths will clarify this point.

7. – Discussion of results.

The histogram in Fig. 7 gives the charge distribution of H-nuclei, entering the stack with a zenity angle $\theta \leqslant 35°$, at flight altitude, as obtained by adding to the results of the present work (T-stack) the previous results of paper I (Y-stack and B-stack). This could be done since latitude [7,8] and atmospheric depth of the three flights are comparable. The total number of tracks reported in the histogram of Fig. 7 is 153.

The good statistics and charge resolution guarantees the reliability of the results.

---

[4] P. S. FREIER, G. W. ANDERSON, J. E. NAUGLE and E. P. NEY: *Phys. Rev.*, **84**, 322 (1951).

[5] H. L. BRADT and B. PETERS: *Phys. Rev.*, **77**, 54 (1950).

[6] M. V. K. APPA RAO, S. BISWAS, R. R. DANIEL, K. A. NEELAKANTAN and B. PETERS: *Phys. Rev.*, **110**, 751 (1958).

[7] C. J. WADDINGTON: *Nuovo Cimento*, **6**, 748 (1957).

[8] J. A. SIMPSON, K. B. FENTON, J. KATZMAN and D. C. ROSE: *Phys. Rev.*, **102**, 1648 (1956).

In Table II are reported the ratios of nuclei of charge $Z \geqslant 15$ to H-nuclei and of Iron to H-nuclei as obtained *a*) at flight altitude, *b*) at the top of the

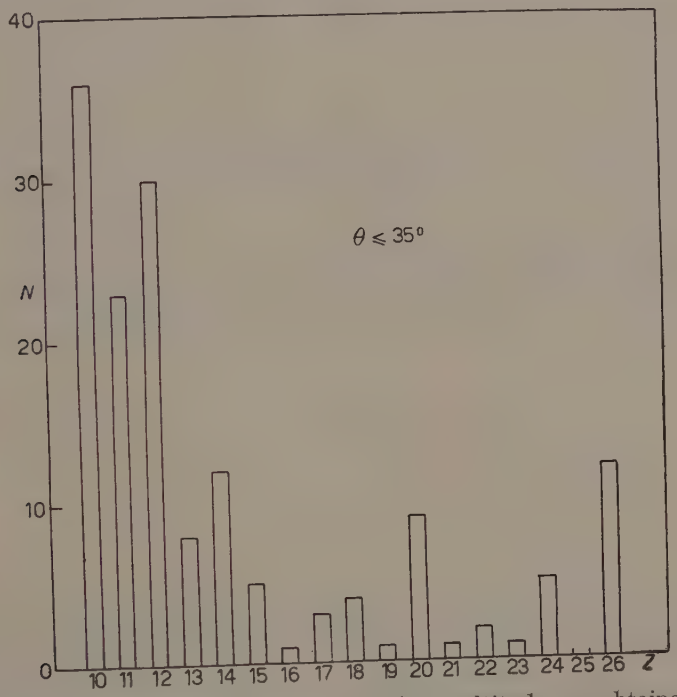

Fig. 7. – Relative abundance of H-nuclei at flight altitude, as obtained adding the results of experiment I (B and Y flights), and of the present experiment (T flight).

atmosphere. The extrapolation to the top of the atmosphere was made under the following assumptions:

1) H-nuclei, nuclei with charge $10 \leqslant Z < 15$ and Iron nuclei are absorbed according to exponential laws;
2) the absorption mean free path values are the ones obtained in Sect. 6 from a zenith angle dependence analysis. For Iron we used, as an approximated value, $\lambda'_{Fe}(\text{air}) = 11.7$.

TABLE II.

	$\frac{N(Z \geqslant 15)}{N(Z \geqslant 10)}$	$\frac{N(Z = 26)}{N(Z \geqslant 10)}$
Flight altitude	0.29 ± 0.03	0.08 ± 0.02
Top of atmosphere	0.65 ± 0.07	0.11 ± 0.02
C.R. source	—	0.16 ± 0.03
SUESS and UREY	0.10	0.05

As pointed out in Sect. 6, this method of extrapolation through the upper layers of the atmosphere may be inaccurate, if the assumption of an exponential depth dependence of H-nuclei will be proved to be incorrect.

An estimate of the ratio Iron to H-nuclei at the C.R. source was obtained by assuming an exponential attenuation for both the Iron and H-nuclei components.

The cross-sections used in extrapolation are the ones quoted by RAJOPADHYE and WADDINGTON ([9]). The composition of interstellar gas was assumed to be of 90% H and 10% He, with an average density of 0.1 atoms/cm^3 ([10]). The mean path traversed by cosmic rays was taken to be $R = 1.85 \cdot 10^{25}$ cm. This value was obtained using a set of one-dimensional diffusion equations with the following values of the parameters; for fragmentation probabilities in interstellar matter a weighted average of the Chicago ([11]) and Bristol ([9]) data:

$$P_{HH} = 0.29 \qquad P_{MM} = 0.09 \qquad P_{LL} = 0.07$$

$$P_{HM} = 0.36 \qquad P_{ML} = 0{,}34$$

$$P_{HL} = 0.27$$

$$P_{\text{Iron-Iron}} = 0 \ ;$$

for flux values at the top of the atmosphere, those obtained in paper I

$$\Phi_{L^0} = 1.67 \text{ particles/m}^2 \text{ sr s} \ ,$$

$$\Phi_{M^0} = 5.52 \text{ particles/m}^2 \text{ sr s} \ ,$$

$$\Phi_{H^0} = 2.82 \text{ particles/m}^2 \text{ sr s} \ .$$

The results of this calculation are reported in Table II.

A comparison with the SUESS and UREY data ([12]) (last row of Table II) definitely indicates that the composition of the C.R. source differs from the average chemical composition of the universe, being much richer in Iron and $15 \leqslant Z \leqslant 26$ elements.

From an analysis of the histogram of Fig. 7, giving the charge distribution at flight altitude, it appears that nuclei of even charge are more abundant than nuclei of odd charge. Interactions occuring during diffusion through the interstellar and atmospheric matter must have reduced the strength of this effect.

([9]) V. Y. RAJOPADHYE and C. J. WADDINGTON: *Phil. Mag.*, **3**,9 (1958).
([10]) V. L. GINZBURG: *Progress in elementary particles and C.R. Physics* (1958), p. 340.
([11]) H. KOSHIBA, G. SCHULTZ and M. SCHEIN: *Nuovo Cimento*, **9**, 1 (1958).
([12]) H. E. SUESS and M. C. UREY: *Rev. Mod. Phys.*, **28**, 53 (1956).

* * *

We wish to express our thanks to Professors R. DEAGLIO and G. WATAGHIN for their constant interest in our work.

We wish also to thank Drs. M. ARTOM and C. GENTILE of the Photometric Laboratory of the « Istituto Elettrotecnico Nazionale G. Ferraris » for the very useful technical assistance in the performance of photometric measurements, and to Drs. A. DEBENEDETTI, B. QUASSIATI and M. VIGONE for stimulating discussions.

Thanks are due to Mr. G. MORZO for carrying out some of the Phot. Ab. measurements and to Mr. G. ALGOSTINO and to Miss. C. NUNCIBELLO for their help in scanning and tracing the tracks.

RIASSUNTO

Riunendo i risultati ottenuti misurando le cariche di 117 nuclei pesanti di carica $Z \geqslant 10$ a quelli ottenuti in un precedente lavoro, si è determinato il valore del rapporto $N(Z \geqslant 15)/N(Z \geqslant 10)$ all'altezza di volo e alla sommità dell'atmosfera, e del rapporto $N(Z=26)/N(Z \geqslant 10)$ all'altezza del volo, alla sommità dell'atmosfera e alla sorgente della Radiazione Cosmica. I risultati indicano che la composizione chimica della sorgente della R.C. differisce dalla composizione media dell'universo, essendo più ricca di nuclei pesanti ($Z \geqslant 15$) ed in particolare di Fe. Si è anche determinato il cammino medio di assorbimento nell'aria analizzando la dipendenza del flusso dei primari pesanti dall'angolo zenitale.

IL NUOVO CIMENTO Vol. X, N. 5 1° Dicembre 1958

On the Connection between the S-Matrix and a Class of Non-Local Interactions - I (*).

Kh. Chadan

Ecole Normale Supérieure - Université de Paris - Paris.

(ricevuto il 7 Ottobre 1958)

Summary. — The problem of finding a phenomenological separable interaction from the S-matrix has been resolved by M. Gourdin and A. Martin who gave exact and explicit formulae relating the interaction to the phase-shift and bound state binding energy ([1,2]). We generalize their method to the case where the interaction is the superposition of a non-local separable interaction and a local one, both of them being central ([3]). The local part of the interaction is supposed to be known. We show how the separable part can be determined by the S-matrix. Except for a few modifications, the method and results are analogous to those of ([1,2]). The main result is that, given the local part of the interaction, the phase-shift and the bound states binding energies, it is then possible to determine exactly the separable part of the interaction if the phase-shift has a good behaviour ([4]).

1. – Introduction.

The mesonic theory of nuclear forces suggests that the interaction between two nucleons is local at great distances but becomes non-local and singular if the two nucleons come close together. For a phenomenological treatment of nuclear forces, it is then natural to superpose a non-local interaction on a

(*) Supported in part by the United States Air Force through the European Office Air Research and Development Command.

([1]) M. Gourdin and A. Martin: *Nuovo Cimento*, **6**, 757 (1957).

([2]) M. Gourdin and A. Martin: *Nuovo Cimento*, **8**, 699 (1958).

([3]) The case of tensor forces will be considered in a next paper. See also *C.R.A.S.*, **245**, 1597 (1957).

([4]) A preliminary report of this work has already been published in *C.R.A.S.*, **246**, 1513 (1958).

local one. We can suppose that the local part of the interaction is determined so as to agree with experimental data at low energies.

To determine a non-local phenomenological interaction from the S-matrix, it is always necessary to make some assumption about it. An arbitrary non-local interaction is too general to be uniquely determined by the S-matrix. There are a great variety of non-local interactions which are equivalent as far as their agreement with experimental data is concerned.

In absence of any detailed theoretical information about the nuclear forces at small distances ([2]), it is plausible to assume that, near the origin, the interaction is separable. This assumption has, as we shall see later, the advantage of simplicity. Then, there is some interest in connecting the separable part of the interaction to the S-matrix, the local part being known from low energy experimental data.

We take an interaction of the form ([1]):

$$(1.1)\qquad \begin{cases} U(\boldsymbol{r},\boldsymbol{r}') = V(r)\,\delta(\boldsymbol{r}-\boldsymbol{r}') + \sum_0^\infty \varepsilon_l u_l(r) u_l(r') P_l(\cos\theta)\,, \\ r = |\boldsymbol{r}|\,, \qquad r' = |\boldsymbol{r}'|\,, \qquad \theta = (\boldsymbol{r},\boldsymbol{r}')\,, \qquad \varepsilon_l = \pm 1\,. \end{cases}$$

We have then restricted ourselves to purely central forces.

The Schrödinger equation therefore reads:

$$(1.1)\qquad \frac{\hbar^2}{2M_r}\,\Delta\Psi(\boldsymbol{r}) + E\Psi(\boldsymbol{r}) = \int U(\boldsymbol{r},\boldsymbol{r}')\Psi(\boldsymbol{r}')\,\mathrm{d}\boldsymbol{r}' = V(r)\Psi(\boldsymbol{r}) + \sum_0^\infty \varepsilon_l \int u_l(r) u_l(r')\, P_l(\cos\theta)\Psi(\boldsymbol{r}')\,\mathrm{d}\boldsymbol{r}'\,.$$

M_r = reduced mass $= M/2$. In what follows, we put $\hbar = 2M_r = 1$.

It is well known that the l-th term of the expansion in the right-hand side of (1.2) acts only in the state of angular momentum l. ε_l is therefore the sign of the separable interaction acting in this state.

In the present paper, we consider only the case of zero angular-momentum (S-state). The extension of the method to higher angular momenta is straightforward.

The similar problem in which one tries to find a local potential from its S-matrix has extensively been treated by several authors: Levinson, Bargmann, Jost and Kohn, Gel'fand and Levitan, Newton and Fulton ([5,6]). Because of the presence of a local interaction in our problem, we make extensive use of the results of ([5]).

([5]) R. Jost and W. Kohn: *Dans. Mat. Fys. Med.*, **27**, 9 (1953).
([6]) R. Newton and T. Fulton: *Phys. Rev.*, **107**, 1103 (1957).

2. – S-state Schrödinger equation.

2·1. *Existence of the solution.* – The Schrödinger equation in the case of zero angular momentum is:

$$\psi'' + E\psi = \varepsilon U(r) \int_0^\infty U(r')\psi(r')\,\mathrm{d}r' + V(r)\psi(r)\,, \tag{2.1}$$

$$U(r) = \sqrt{4\pi}\, r u_0(r)\,, \qquad \varepsilon = \varepsilon_0\,,$$

where ψ is the reduced radial wave-function.

In order that this equation have a solution $V(r)$ and $U(r)$ must satisfy some conditions near the origin and near infinity. As we shall see later, it is essential that the «local» Schrödinger equation:

$$\varphi'' + E\varphi = V\varphi \tag{2.2}$$

offers good solutions. $V(r)$ is then assumed to satisfy ([5]):

$$\int_0^\infty r\,|\,V(r)\,|\,\mathrm{d}r < \infty\,, \tag{2.3}$$

$$\int_0^\infty r^2\,|\,V(r)\,|\,\mathrm{d}r < \infty\,. \tag{2.4}$$

On the other hand, we suppose that $U(r)$ satisfies the following conditions ([7]):

$$U(r) \underset{r\to 0}{\sim} r^{-\alpha} \qquad \alpha < \tfrac{3}{2}, \tag{2.5}$$

$$U(r) \underset{r\to\infty}{\sim} r^{-\beta} \qquad \beta > 2. \tag{2.6}$$

2·2. *The «local» Schrödinger equation.* – Here, we recall some properties ([5]) of solutions of (2.2). Consider first the case of $E > 0$ (scattering). (2.2) has many interesting solutions, each of them having either a given asymptotic form or a given behaviour near the origin. The most interesting are:

(a) $\qquad f(\pm k, r)\colon \quad \lim \exp[\pm ikr]\, f(\pm k, r) = 1\,, \qquad E = k^2,$

(b) $\qquad \varphi(E, r) \equiv \varphi(k^2, r)\colon \quad \varphi(E, 0) = 0\,, \qquad \varphi'(E, 0) = 1\,;$

$$\varphi(E, r) \underset{r\to\infty}{\sim} a \sin(kr + \delta_v)\,,$$

δ_v being the «local» phase-shift.

([7]) These conditions are obtained by considerations quite analogous to those of the begining of ([1]). Recall that $U(r) = ru(r)$.

In what follows, we write indistinctly $\varphi(E, r)$ or $\varphi(k^2, r)$ when $E = k^2 > 0$, The solution $\varphi(k^2, r)$ can be obviously written as:

$$\varphi(k^2, r) = \frac{1}{2ik}[f(k) f(-k, r) - f(-k) f(k, r)] , \tag{2.7}$$

$$f(k) \equiv f(k, 0) , \qquad f(-k) = f^*(k) .$$

It is easily seen from (2.7) that:

$$\varphi(k^2, r) \underset{r\to\infty}{\sim} \frac{\exp[-i\delta_v] f(k)}{k} \sin(kr + \delta_v) ; \tag{2 8}$$

$$\exp[2i\delta] = f(k)[f(-k)]^{-1} . \tag{2.9}$$

If there are bound states, their binding energies are given by the zero of $f(k)$ in the lower half of the complex k-plane. Under the conditions (2.3;4), $f(k)$ has a finite number of simple zeros along the negative imaginary axis. Call these zeros $-i\gamma_l$, $l = 1, 2, ..., n$. There are therefore n bound states with the binding energies $-\gamma_l^2 = -E_l$. The corresponding eigenfunctions are given by:

$$\varphi_l(r) = \varphi(-E_l, r) = \frac{-1}{2\gamma_l} f(i\gamma_l) f(-i\gamma_l, r) , \tag{2.10}$$

$\varphi_l(r)$ is not normalized to unity.

The function $f(k)$ enables us to define the spectral function $\varrho(E)$ by:

$$\varrho(0) = 0 ,$$

$$\begin{cases} \dfrac{d\varrho}{dE} = \sum c_l \delta(E + E_l) & E < 0 \\ \dfrac{d\varrho}{dE} = \dfrac{1}{\pi} \dfrac{k}{|f(k)|^2} & E = k^2 \geqslant 0 , \end{cases} \tag{2.11}$$

where

$$c_l = \left[\int_0^\infty [\varphi_l(r)]^2 \, dr\right]^{-1} .$$

The spectral function has the interesting property that for every square integrable function $F(r)$ we get the completeness relation:

$$\int_0^\infty [F(r)]^2 dr = \int_{-\infty}^{+\infty} d\varrho(E) \left[\int_0^\infty F(r) \varphi(E, r) \, dr\right]^2 . \tag{2.12}$$

This means that:

$$\int_{-\infty}^{+\infty} \varphi(E, r)\varphi(E, r')\,\mathrm{d}\varrho(E) = \delta(r - r')\,. \tag{2.13}$$

Moreover, the wave-functions $\varphi(k^2, r)$ and $\varphi_l(r)$ obey the usual orthogonality relations:

$$\begin{cases} \displaystyle\int_0^{\infty} \varphi(k^2, r)\varphi(k'^2, r)\,\mathrm{d}r = \frac{\delta(E' - E)}{\mathrm{d}\varrho/\mathrm{d}E} = \frac{\pi|f|^2\delta(k' - k)}{2k^2}\,, \\ \displaystyle\int_0^{\infty} \varphi_l(r)\varphi_{l'}(r)\,\mathrm{d}r = c_l^{-1}\,\delta_{ll'}\,, \\ \displaystyle\int_0^{\infty} \varphi_l(r)\varphi(E, r)\,\mathrm{d}r = 0 \qquad\qquad E = k^2 \geqslant 0\,. \end{cases} \tag{2.14}$$

These formulae permit us to define a kind of integral transform which is very similar to a Fourier sine transform. For any square integrable function $F(r)$ we define

$$\begin{cases} F(k^2) = \displaystyle\int_0^{\infty} F(r)\varphi(k^2, r)\,\mathrm{d}r\,, \\ F_l \quad\;\; = \displaystyle\int_0^{\infty} F(r)\varphi_l(r)\,\mathrm{d}r\,. \end{cases} \tag{2.15}$$

The inversion formulae read:

$$F(r) = \int_{-\infty}^{+\infty} \mathrm{d}\varrho(E)F(E)\varphi(E, r) = \sum c_l F_l \varphi_l(r) + \int_0^{\infty} \mathrm{d}\varrho(E')F(E')\varphi(E', r)\,. \tag{2.16}$$

2·3. *Solution of* (2.1) *with use of integral transforms.* – We write:

$$\psi(r) = \int_{-\infty}^{+\infty} \psi(E')\varphi(E', r)\,\mathrm{d}\varrho(E')\,, \tag{2.17}$$

$$U(r) = \int_{-\infty}^{+\infty} U(E')\varphi(E', r)\,\mathrm{d}\varrho(E')\,. \tag{2.18}$$

The equation (2.1) then reduces to:

$$\int_{-\infty}^{+\infty} \mathrm{d}\varrho(E')\psi(E', r) = \varepsilon N \int_{-\infty}^{+\infty} \mathrm{d}\varrho(E')\, U(E')\varphi(E', r)\,, \tag{2.19}$$

$$N = \int_0^{\infty} U(t)\psi(t)\,\mathrm{d}t = \int_{-\infty}^{+\infty} \mathrm{d}\varrho(E')\, U(E')\psi(E')\,. \tag{2.20}$$

Scattering, $E = k^2$. The wave-function is represented by $\psi(k, r)$ and its transforms by $\psi(k, p)$ and $\psi_l(k)$. (2.19) gives us:

$$\psi_l(k) = \varepsilon \frac{U_l}{k^2 + E_l} N(k)\,, \tag{2.21}$$

$$(k^2 - p^2)\psi(k, p) = \varepsilon N(k)\, U(p)\,. \tag{2.22}$$

The solution $\psi(k, r)$ which is of interest must have the following properties:

$$\psi(k, 0) = 0\,,$$

$$\psi(k, r) \underset{r\to\infty}{\sim} A \sin(kr + \delta)\,,$$

δ being the total phase-shift. Moreover, $\psi(k, r)$ must coincide with $\varphi(k^2, r)$ when $U(r) \equiv 0$. The solution of (2.22) satisfying all above conditions is:

$$\psi(k, p) = \frac{\delta(p^2 - k^2)}{\mathrm{d}\varrho/\mathrm{d}E} + \varepsilon N(k) P \frac{U(p)}{k^2 - p^2}\,. \tag{2.23}$$

Therefore:

$$\psi(k, r) = \sum \varepsilon c_l U_l N \frac{\varphi_l(r)}{k^2 + E_l} + \varepsilon N(k) \int_0^{\infty} \mathrm{d}\varrho(p^2)\, P \frac{U(p)\varphi(p^2, r)}{k^2 - p^2} + \varphi(k^2, r)\,. \tag{2.24}$$

By replacing (2.23) and (2.21) in (2.20) we find:

$$N(k) = \frac{U(k)}{1 + P\int_0^{\infty} \frac{\varepsilon U^2(p)}{p^2 - k^2}\, \mathrm{d}\varrho(p^2) - \sum \varepsilon \frac{c_l U_l^2}{k^2 + E_l}}\,. \tag{2.25}$$

When r goes to infinity, the first terms in (2.24) go to zero and therefore the behaviour of $\psi(k, r)$ is given by the remaining terms. It is easily seen that

one has [8]:

$$\psi(k,r) \underset{r\to\infty}{\sim} \frac{\exp[-i\delta_v]}{k} f(k)\left[\sin(kr+\delta_v) + \operatorname{tg}\delta_u^v \cos(kr+\delta_v)\right], \tag{2.26}$$

$$-\frac{2k}{\pi}\operatorname{tg}\delta_u^v = \frac{F(k)}{1 + P\int_0^\infty \frac{F(p)}{p^2-k^2}\,\mathrm{d}p - \sum \frac{\varepsilon c_l U_l^2}{k^2+E}} \tag{2.27}$$

$$F(k) = \frac{2\varepsilon k^2 U^2(k)}{\pi f(k) f(-k)}.$$

The right-hand side of (2.26) is of the form $A\sin(kr+\delta)$, as expected, with δ given by:

$$\delta = \delta_v + \delta_u^v, \tag{2.28}$$

$\delta_u^v(k)$ is the additional phase-shift due to $\varepsilon U(r)U(r')$. The superscript v indicates that a local potential $V(r)$ is present.

If $V(r)=0$, then $\varphi(k^2,r) = (\sin kr)/k$ and $f(k)=1$. (2.27) reduces to the classical form:

$$-\frac{2k}{\pi}\operatorname{tg}\delta_u = \frac{F(k)}{1 + P\int_0^\infty \frac{F(p)}{p^2-k^2}\,\mathrm{d}p}. \tag{2.29}$$

2·4. *Bound states.* – If there exists a bound state with binding energy $+X$ ($X<0$), (2.19) leads to:

$$\sum c_l \psi_l(E_l + X)\varphi_l(r) - \int_0^\infty \mathrm{d}\varrho(p^2)\psi(p)(p^2-X)\varphi(p^2,r) =$$

$$= \varepsilon N\left[\sum c_l U_l \varphi_l(r) + \int_0^\infty \mathrm{d}\varrho(p^2)\,U(p)\varphi(p^2,r)\right].$$

---

[8] To do this calculation, we substitute $\varphi(p^2,r)$ by (2.7),

$$\frac{1}{p^2-k^2} \quad \text{by} \quad \frac{1}{2}\left[\frac{1}{p^2-k^2-i\varepsilon} + \frac{1}{p^2-k^2+i\varepsilon}\right],$$

and then we get (2.25) by calculating the integral along an appropriate path in the complex p-plane.

Suppose first that all $U_l \neq 0$ and $U(p) \neq 0$. We deduce that:

$$\psi_l = \frac{\varepsilon N U_l}{E_l + X}, \tag{2.30'}$$

$$\psi(p) = \frac{-\varepsilon N U(p)}{p^2 - X}. \tag{2.30''}$$

By replacing these expressions into (2.20), we get the eigenvalue equation:

$$\Phi(X) = \sum \frac{c_l U_l^2}{E_l + X} - P\int_0^\infty \mathrm{d}\varrho(p^2)\, \frac{U^2(p)}{p^2 - X} - \varepsilon = 0. \tag{2.31}$$

More generally, we consider the equation (2.31) without any restriction on the sign of X. If $X = k^2 > 0$, $\Phi(X)$ is nothing but the denominator of (2.27) multiplied by $-\varepsilon$. In order to determine the number of negative roots of (2.31), we make use of a graphical method.

a) $\varepsilon = +1$. $\Phi(X)$ is represented in Fig. 1. One sees immediately that if

$$\Phi(0) = \sum \frac{c_l U_l^2}{E_l} - \int_0^\infty \mathrm{d}\varrho(p^2)\, \frac{U^2(p)}{p^2} - 1,$$

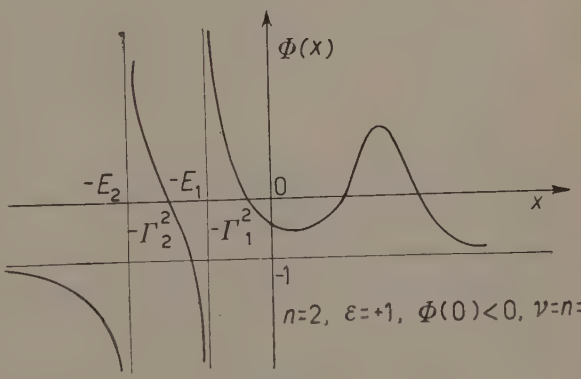

Fig. 1.

is positive, the eigenvalue equation has $n - 1$ negative roots. Otherwise, there are n eigenvalues. One sees also that the absolute value of all these eigenvalues are smaller than the corresponding E_l's. This is to be expected, the separable interaction being repulsive.

b) $\varepsilon = -1$. This case is very similar to the case *a*). The conclusions is:

if $$\Phi(0) = \sum \frac{c_l U_l^2}{E_l} - \int_0^\infty \mathrm{d}\varrho(p^2)\, \frac{U^2(p)}{p^2} + 1 > 0,$$

there are n eigenvalues; if $\Phi(0) < 0$, there are $n+1$ eigenvalues.

Hereafter, we designate the negative roots of (2.31) by $-\Gamma_\lambda^2$ ($\lambda = 1, 2, ..., \nu$) and the corresponding eigenfunctions by $\psi_\lambda(r)$. $\psi_{\lambda l}$ means $\int_0^\infty \psi_\lambda(r)\varphi_l(r)\,dr$.

Consider now the case in which one of the U_l's, say U_j, is zero. Then $\Phi(X)$ is continuous at $X = -E_j$ and one of the $\{-\Gamma_\mu^2\}$ desappears (see Fig. 2). As it can be directly seen from (2.1), the eigenvalue which desappears is replaced by $-E_j$, the eigenfunction being $\varphi_j(r)$. This means that if $U(r)$ is orthogonal to $\varphi_j(r)$, the superposition of $\varepsilon U(r)U(r')$ to $V(r)$ does not change the wave-function $\varphi_j(r)$ and its binding energy. The remaining eigenvalues are given as above, *i.e.* by (2.31). From these later, one, say $-\Gamma_\mu^2$, can be equal to $-E_j$. In this case, we have a degeneracy at $-E_j$. If it is so, the second wave-function, $\psi_\mu(r)$, can be chosen orthogonal to $\varphi_j(r)$. This is simply done by taking $\psi_{\mu j} = 0$.

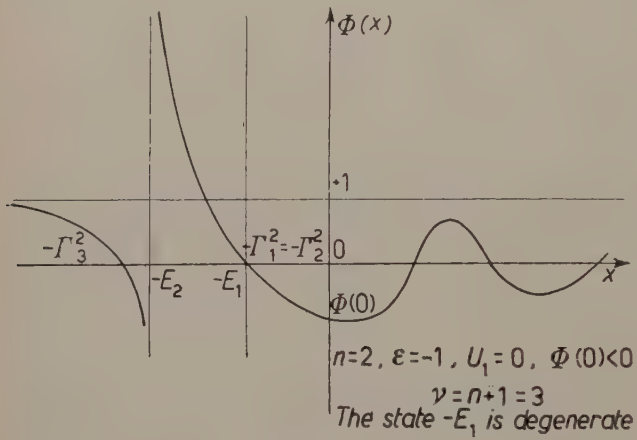

Fig. 2.

The case where many U_l are zero is very similar. The order of degeneracy at each $-E_j$ can never be greater than two.

If all $U_l = 0$, there are at least n bound states, namely all $\{E_l, \varphi_l(r)\}$. Therefore if $\nu = n - 1$, we are sure that at least one of U_l's is not zero.

Finally suppose that $U(k) \equiv 0$, *i.e.* $U(r) = \sum \alpha_l \varphi_l(r)$. (2.31) reduces to:

$$\sum \frac{c_l U_l^2}{E_l + X} - \varepsilon = 0 \,. \tag{2.32}$$

Here, however, one can never get more that n negative roots. This is because $\Phi(0) > -\varepsilon$. The bound states wave-functions are linear combinations of $\varphi_l(r)$. Besides, the scattering wave function $\psi(k, r)$ is identical to $\varphi(k^2, r)$. This is clear from (2.1). The only change concerns the bound states. Remark that (2.27) gives $\delta_u^v \equiv 0$.

The equation (2.32) can have sometimes one positive root. This occurs when $\varepsilon = +1$ and $\Phi(0) > 0$ This positive root corresponds, as we shall see later, to a positive energy degenerate state.

2·5. *Positive energy degeneracy.* – Consider again the equation (2.22). We have resolved it by imposing to $\psi(k, r)$ the asymptotic form $A \sin(kr + \delta)$ However, (2.22) can admit solutions with vanishing asymptotic form. Suppose that $\chi(k, r)$ is such a solution. $\chi(k, r)$ must vanish identically if $U(r) = 0$, because the local potentials considered here admit no such solutions. (2.22) gives immediately:

$$\chi_l(k) = \varepsilon \frac{U_l}{E_l + k^2} N , \tag{2.33}$$

$$\chi(k, p) = - \varepsilon N P \frac{U(k)}{p^2 - k^2} . \tag{2.34}$$

By replacing these values into (2.20), we are left with:

$$\Phi(k^2) = \left[\sum \frac{c_l U_l^2}{E + k_l^2} - P \int_0^\infty \mathrm{d}\varrho(p^2) \frac{U^2(p)}{p^2 - k^2} \right] - \varepsilon = 0 . \tag{2.35}$$

We see that positive energies at which degenerate solutions can exist are given by positive roots of the eigenvalue equation (2.31). However, this condition is not sufficient to insure the existence of $\chi(k, r)$. We must verify that $\chi(k, r)$ has really a vanishing asymptotic form. $\chi(k, r)$ is given by (dropping the normalization constant N):

$$\chi(k, r) = \varepsilon \sum \frac{c_l U_l}{k^2 + E_l} \varphi_l(r) - P \int_0^\infty \mathrm{d}\varrho(p^2) \frac{U(p)}{p^2 - k^2} \varphi(p^2, r) .$$

At infinity, only the integral contributes. This integral is evaluated as follows:

$$P \int_0^\infty \mathrm{d}\varrho(p^2) \frac{U(p)}{p^2 - k^2} \varphi(p^2, r) = P \int \mathrm{d}\varrho(p^2) \frac{U(p)}{p^2 - k^2} \frac{1}{2ip} [f(p) f(-p, r) - f(-p) f(p, r)] =$$

$$= \frac{1}{i\pi} \int_{-\infty}^{+\infty} \frac{p \, \mathrm{d}p}{f(-p)} \frac{U(p)}{p^2 - k^2} f(-p, r) \underset{r \to \infty}{\sim} \frac{1}{\pi i} \int_{-\infty}^{+\infty} \frac{p \, \mathrm{d}p}{f(-p)} \frac{U(p)}{p^2 - k^2} \exp[ipr] \simeq$$

$$\simeq \frac{i\pi}{2} \frac{U(k)}{f(-k)} [\exp[ikr] + \exp[-ikr] \exp[-2i\delta_v]] .$$

Therefore, $\chi(k, r)$ has a vanishing asymptotic form if and only if $U(k) = 0$. We conclude that:

Theorem: The necessary and sufficient conditions to have a degenerate state at the positive energy $E_0 = k_0^2$ are:

$$\Phi(k_0^2) = 0 , \tag{2.39}$$

$$U(k_0) = 0 . \tag{2.40}$$

The breakdown of the famous Levinson theorem is intimately related to the existence of such states ([9,10]).

In the special case considered in the end of Sect. 2·4, if (2.32) admits a positive root k_0^2, one obtains such a degenerate state. For the corresponding wave function is a linear combination of $\varphi_l(r)$ and therefore vanishes at infinity.

2·6. *Some properties of* δ_u^v. – δ_u^v is given by:

$$(2.41)\qquad -\frac{2k}{\pi}\operatorname{tg}\delta_u^v = F(k)\left[1 + P\int_0^\infty \frac{F(p)}{p^2-k^2}\,\mathrm{d}p - \sum \frac{\varepsilon c_l U_l^2}{E_l + k^2}\right]^{-1} = -\frac{\varepsilon F(k)}{\Phi(k^2)},$$

$$F(k) = \frac{2}{\pi}\varepsilon\, k^2 f(k)^2\, U^2(k)\,.$$

$F(k)$ has a constant sign, the same as ε. Equation (2.41) shows that $\operatorname{tg}\delta_u^v$ goes through zero at $k = k_0$ if and only if:

$$F(k_0) = 0\,,$$

$$\Phi(k_0^2) = 0\,.$$

These conditions, the same as (2.39), (2.40), are sufficient to insure that $\operatorname{tg}\delta_u^v$ goes effectively through zero at $k = k_0$. This is shown as follows:

Due to (2.3) and (2.4), $\varphi(k^2, r)$ is a well behaved function, *i.e.* it is a continuous function of r and has a continuous derivative $\partial\varphi/\partial k$. It is also an entire function of $E = k^2$. Then, (2.5) and (2.6) insure that $U(k)$ is also a well behaved function. Its derivative with respect to k, $\mathrm{d}U/\mathrm{d}k$, exists and is continuous everywhere except, may be, at the origin. Near each zero, k_0, of $U(k)$, we can therefore write:

$$(2,42)\qquad U(k) \underset{k\to k_0}{\simeq} (k-k_0)\,\bar{U}(k_0)\,, \qquad |\bar{U}(k_0)| < \infty.$$

Then, $F(k)$ has at least a double zero at $k = k_0$:

$$(2.43)\qquad F(k) \underset{k\to k_0}{\simeq} \varepsilon(k-k_0)^2\,\bar{F}(k_0)\,, \qquad 0 < \bar{F}(k_0) < \infty.$$

([9]) N. Levinson: *Dans. Mat. Fys. Med.*, **25**, 9 (1949).
([10]) A. Martin: *Nuovo Cimento*, **7**, 607 (1958).

This last equation shows that

$$\left(P\int_0^\infty \frac{F(p)}{p^2-k_0^2}\,\mathrm{d}p\right) \qquad \text{and} \qquad \left(P\int_0^\infty \frac{F(p)}{(p^2-k_0^2)^2}\,\mathrm{d}p\right)$$

exist and the latter expression is the derivative of the former with respect to k_0^2. It follows that:

$$\frac{\mathrm{d}\Phi}{\mathrm{d}k_0} = -2k_0\left[\sum \frac{c_l U_l^2}{(k_0^2+E_l)^2} + P\int_0^\infty \frac{\varepsilon F(p)}{(p^2-k_0^2)^2}\,\mathrm{d}p\right] < 0\,. \tag{2.44}$$

Therefore, in the neighbourhood of each k_0, one can write:

$$\frac{-2k}{\pi}\,\mathrm{tg}\,\delta_u^v \underset{k\to k_0}{\simeq} \frac{-(k-k_0)^2\overline{F}(k_0)}{(k-k_0)\Phi'(k_0)} = (k-k_0)\,A\,, \qquad A>0\,. \tag{2.45}$$

We infer that $\mathrm{tg}\,\delta_u^v$ goes effectively through zero at $k=k_0$. Incidentally, one sees also that:

$$\frac{\mathrm{d}\delta}{\mathrm{d}k_0} \leqslant 0\,. \tag{2.46}$$

One has therefore the two following theorems:

Theorem *a*): A necessary and sufficient condition for $\mathrm{tg}\,\delta_u^v$ to go through zero at $k=k_0$ is that there exists a degenerate state at $E_0=k_0^2$.

Theorem *b*): δ_u^v goes once and only once through each $n\pi$.

Most often, the zeros of the numerator and of the denominator of (2.41) do not coincide and the sign changes of $\mathrm{tg}\,\delta_u^v$ correspond to zeros of the denominator. In this case, δ_u^v remains between $n\pi$ and $(n+1)\pi$.

2·7. *The generalized Levinson theorem.* – As we shall see later, the value of $\delta_u^v(0)-\delta_u^v(\infty)$ is of great importance when one attempts to solve the integral equation connecting $U(k)$ to $\delta_u^v(k)$. It can be deduced from the Levinson theorem [9] generalized by A. Martin[10] for non-local interactions.

According to this theorem (*):

$$\delta(0) - \delta(\infty) = (\nu+\sigma)\pi\,,$$

$$\delta_v(0) - \delta_v(\infty) = n\pi\,.$$

(*) We disregard the possibility of a resonance at zero energy.

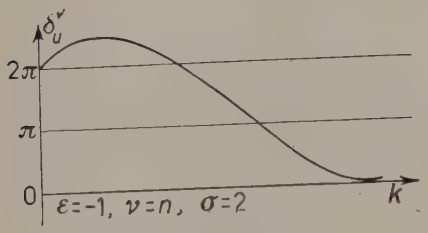

Fig. 3.

σ is the number of degenerate states at positive energies; ν and n respectively are the number of bound states of the total and local interactions. By subtracting these two equations, we find:

$$\delta_u^v(0) - \delta_u^v(\infty) = (\nu - n)\pi + \sigma\pi \,.$$

Generally, $\delta_u^v(0) - \delta_u^v(\infty)$ is non-negative. The only permissible negative value is $-\pi$, and occurs when $n \neq 0$, $\nu = n-1$ and $\sigma = 0$. This is in contrast to the purely separable case in which $\delta_u(0) - \delta_u(\infty)$ is always non-negative.

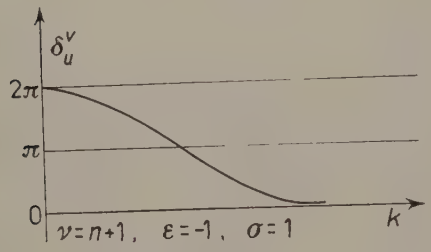

Fig. 4.

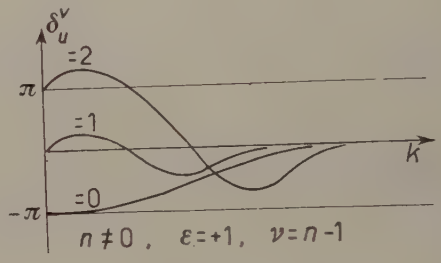

Fig. 5.

Fig. 3, 4 and 5 show some typical cases of variations of $\delta_u^v(k)$ against the momentum k.

3. – Derivation of the integral equation.

We have to determine $U(r)$, or its integral transform $\{U(k), U_i\}$, from, $V(r)$, $\delta(k)$ and the discrete spectrum. This is done as follows:

From $V(r)$, we calculate the phase-shift, $\delta_v(k)$. Then, we determine $\delta_u^v(k)$ by

$$\delta_u^v(k) = \delta(k) - \delta_v(k) \tag{3.1}$$

and therefore:

$$g(k) = -\frac{2k}{\pi} \operatorname{tg} \delta_u^v(k) \,. \tag{3.2}$$

$\delta_u^v(k)$ must have all properties previously established.

ε, the sign of the separable interaction, is given by the sign of $g(k)$ near infinity:

$$\varepsilon g(k) \to A \geqslant 0 \,, \qquad k \to \infty \,.$$

$g(k)$ and ε being determined, we have the following integral equation connecting $\{U(k), U_l\}$ to $g(k)$:

$$F(k) = g(k)\left[1 + P\int_0^\infty \frac{F(p)\,\mathrm{d}p}{p^2 - k^2} - \sum_l \frac{\varepsilon c_l U_l^2}{k^2 + E_l}\right], \tag{3.3}$$

$$F(k) = \frac{2\varepsilon}{\pi}\,\frac{k^2}{|f(k)|^2}\,U^2(k)\,.$$

This integral equation by itself is not sufficient to determine $F(k)$ and the constant U_l. Binding energies are also needed. This fact is in agreement with general theorems about the connection between the S-matrix and the interaction. There are therefore two steps to obtain $U(k)$ and U_l, $l = 1, 2, \ldots, n$.

We begin by supposing that the constants $\{U_l\}$ are known. In other words, we suppose that the inhomogeneous part of (3.3) is given. Some of the $\{U_l\}$ may be zero. This can be seen by simple examination of the discreet spectrum (see Sect. 2). Solving the equation (3.3) for $F(k)$, we find a solution depending on n constants U_l. Putting this solution $F(k; U_l)$ into the eigenvaule equation (2.31), we obtain a set of equations which determine $\{U_l\}$. As we shall see, our method cannot be applied in the particular case $\nu = n - 1$ and $\sigma = 0$.

Before solving equation (3.3), we establish some theorems connecting the sign of $g(k)$ near the origin and near infinity with the number of bound states in order that the integral equation can have admissible solutions, *i.e.* solutions with constant sign. These theorems are based on the discussion of (2.4) and the equation

$$g(k) = -\frac{\varepsilon F(k)}{\Phi(k^2)}\,.$$

Theorem 1: If $g(0)g(\infty) > 0$, the number of bound states must be equal to n.

Proof: There are two cases, according to the sign of $g(\infty)$.

If $g(\infty) > 0$, we have $\varepsilon = 1$ and $\Phi(0) < 0$. This shows that $\nu = n$.

If $g(\infty) < 0$, ε is equal to -1 and then $\Phi(0) > 0$. This requires also $\nu = n$.

Theorem 2. If $g(\infty) > 0$ and $g(0) < 0$, there is no admissible solution unless $\nu = n - 1$.

Proof: $g(\infty) > 0$ implies that $\varepsilon = 1$, and therefore ν cannot be greater than n. Besides, $g(0) < 0$ imposes to $\Phi(0)$ to be positive. This shows that $\nu = n - 1$.

Theorem 3: If $g(0) > 0$ and $g(\infty) < 0$, one must have $\nu = n + 1$.

Proof: ε is equal to -1 and $\Phi(0) < 0$. The number of bound states must therefore be equal to $n+1$, according to previous discussions.

Theorems 1, 2 and 3 give necessary conditions for the existence of solutions.

4. – Solution of the integral equation.

As in (2), we make the following changes of variable and of function:

$$x = k^2 + 1 ,$$

$$\varphi(x) = \frac{F(x)}{g(x)}\left[1 + i\pi \frac{g(x)}{2\sqrt{x-1}}\right].$$

Equation (3.3) then becomes:

$$\varphi(x) = 1 - \sum_l \frac{\varepsilon c_l U_l^2}{x + E_l - 1} + \frac{1}{\pi}\int_1^\infty \frac{h^*(y)\varphi(y)}{y - x - i\varepsilon}\,dy , \tag{4.1}$$

$$h(x) = \frac{\pi g(x)}{2\sqrt{x-1}}\left[1 - i\pi \frac{g(x)}{2\sqrt{x-1}}\right]^{-1} = -\sin\delta_u^v(x)\exp\left[-i\delta_u^v(x)\right]. \tag{4.2}$$

The new integral equation is of the same type as equation (2.1) of OMNÈS (11), with $\delta_n^v = -\eta$ and

$$\lambda(x) = 1 - \sum \frac{\varepsilon c_l U_l^2}{x + E_l - 1} . \quad (*)$$

We can therefore apply Muskhelishvili's method generalized by OMNÈS.

Inhomogeneous equation. – We define a function $H(Z)$ of the complex variable Z by (12):

$$H(Z) = \frac{1}{2\pi i}\int_1^\infty \frac{h^*(y)\varphi(y)}{y - Z}\,dy . \tag{4.3}$$

$$h(y) = \exp\left[i\eta(y)\right]\sin\eta(y) . \tag{4.4}$$

$H(Z)$ is holomorphic in the complex plane cut from 1 to ∞ along the real axis. Obviously, the solution of (4.1) is:

$$\varphi(x) = \lambda(x) + 2iH(x^+) . \tag{4.5}$$

Now, $H(Z)$ is put into the form:

$$H(Z) = \Omega(Z)\Phi(Z) , \tag{4.6}$$

---

(11) R. OMNÈS: *Nuovo Cimento*, **8**, 316 (1958), equation (2.1).

(*) To avoid confusion, we use the notations η and $\lambda(x)$ instead of δ and $f(x)$ used by Omnès.

(12) We suppose that δ_u^v is chosen so that $\delta_u^v(\infty) = 0$.

(13) Strictly speaking, there are some indications in favour of separable interactions. See, for example, LÉVY's repulsive core: M. M. LÉVY: *Phys. Rev.*, **88**, 725 (1952). Also the footnote (6) of Y. YAMAGUCHI's paper: *Phys. Rev.*, **95**, 1628 (1954).

where

$$\Omega(Z) = \exp[u(Z)], \tag{4.7}$$

$$u(Z) = \frac{1}{\pi}\int_1^\infty \frac{\eta(y)\,dy}{y - Z}. \tag{4.8}$$

$\Phi(Z)$ must be holomorphic in the complex cut plane. It must also go to zero in the limit $|Z| \to \infty$. From (4.1), one deduces that $\Phi(Z)$ must satisfy the following functional equation:

$$\Phi(x^+) - \Phi(x^-) = -\frac{1}{2i}\lambda(x)[\exp[-u(x^+)] - \exp[-u(x^-)]], \tag{4.9}$$

$$u(x^\pm) = \lim_{\varepsilon \to 0} u(x \pm i\varepsilon) = \alpha(x) \pm i\eta(x),$$

$$\alpha(x) = \frac{1}{\pi} P\int_1^\infty \frac{\eta(y)\,dy}{y - x}.$$

A particular solution of this equation is:

$$\Phi(Z) = -\frac{1}{2i}\left[\exp[-u(Z)]\,\lambda(Z) - 1 + \sum_{l=1}^{n} \frac{\varepsilon c_l U_l^2}{Z + E_l - 1}\exp[-u_l]\right], \tag{4.10}$$

$$u_l = u(1 - E_l) = \frac{1}{\pi}\int_1^\infty \frac{\eta(y)}{y + E_l - 1}\,dy.$$

We therefore deduce, from (4.5), (4.6) and (4.10) that:

$$\varphi(x) = \exp[u(x^+)]\left[1 - \sum_{l=1}^{n} \frac{\varepsilon c_l U_l^2}{x + E_l - 1}\exp[-u_l]\right]. \tag{4.12}$$

One must check that (4.12) is a solution of the integral equation (4.1). This is done in the same way as in [2] by assuming that $\eta(0) - \eta(\infty) \leqslant 0$ *This means that the solution* (4.12) *is not valid if* $\nu = n - 1$ and $\sigma = 0$. In fact $\varphi(x)$ is no longer finite at $x = 1$ in this last case.

Homogeneous equation. – The homogeneous equation corresponding to (4.1) is:

$$\varphi_0(x) = \frac{1}{\pi}\int_1^\infty \frac{h^*(y)\varphi_0(y)\,dy}{y - x - i\varepsilon}. \tag{4.13}$$

The same method as used for the inhomogeneous equation leads to:

$$\varphi_0(x) = \begin{cases} \exp[u(x^+)]\sum_1^N \dfrac{b_m}{(x-1)^m} & \text{if} \quad \eta(0 - \eta(\infty)) = -N\pi < 0, \\ 0 \qquad \text{otherwise}; \end{cases} \tag{4.14}$$

b_m are arbitrary constants. Therefore, the general solution of (4.1) is:

$$(4.15)\quad \varphi(x) = \exp[u(x^+)]\left[1 + \sum_1^N \frac{b_m}{(x-1)^m} - \sum_l \frac{\varepsilon c_l U_l^2}{x + E_l - 1} \exp[-u_l]\right].$$

Taking into account the changes of variable and of function, we deduce the general solution of (3.3):

$$(4.16)\quad F(k) = -\frac{2k}{\pi} \sin \delta_u^v(k) \exp[\alpha(k^2)]\left[1 + \sum_1^N \frac{b_m}{k^{2m}} - \sum_{l=1}^n \frac{\varepsilon c_l U_l^2}{k^2 + E_l} \exp[-u_l]\right].$$

This solution $F(k)$ depends on $N+n$ parameters, namely $\{U_l\}$ and $\{b_m\}$. It must keep a constant sign. Therefore, the changes of sign of $\sin \delta_u^v$ must coincide with the changes of sign of the expression between brackets in (4.16). This requirement gives us a set of relations between the parameters. These relations, added to those deduced from the eigenvalue equation, permit us to find the value of the parameters.

The particular case $v = n-1$ and $\sigma = 0$ must be excepted. We have not been able to find the solution of the integral equation in this case.

In all other cases ($v \geqslant n$ or $\sigma > 0$), it can be easily seen that there are at least as many equations as parameters.

The question of the uniqueness of $\{b_m\}$ and $\{U_l\}$ has not been clarified yet.

Note added in proof.

We shall give in a forthcoming paper the solution of the integral equation (4.1) in the particular case $v = n-1$, $\sigma = 0$, as well as the conditions of existence and uniqueness for the constants $\{U_l\}$.

RIASSUNTO (*)

Il problema di trovare dalla matrice S una interazione fenomenologica separabile è stato risolto da M. Gourdin e A. Martin che hanno dato formule esatte ed esplicite che mettono in relazione l'interazione con lo spostamento di fase e l'energia di legame dello stato legato ([1,2]). Generalizziamo il loro metodo al caso in cui l'interazione è la sovrapposizione di un'interazione non locale separabile e una locale, ambedue centrali ([3]). Mostriamo come si possa determinare la parte separabile per mezzo della matrice S. Eccettuate poche modificazioni, il metodo e i risultati sono analoghi a quelli di ([1,2]). Il risultato principale è che, data la parte locale dell'interazione, lo spostamento di fase e le energie di legame degli stati legati, è possibile determinare esattamente la parte separabile dell'interazione se lo spostamento di fase ha un andamento regolare.

(*) *Traduzione a cura della Redazione.*

LETTERE ALLA REDAZIONE

(La responsabilità scientifica degli scritti inseriti in questa rubrica è completamente lasciata dalla Direzione del periodico ai singoli autori)

Polarization of β^--Particles in ^{8}Li-Decay.

L. Keszthelyi and J. Zimányi

Central Research Institute for Physics, Department of Atomic Physics - Budapes

(ricevuto il 10 Ottobre 1958)

In their excellent experiment Goldhaber *et al.* have measured the helicity of the neutrino produced in K-capture (1). The helicity of the antineutrino produced in β^--decay, however, can be determined only if two joint experiments (β^--$\bar{\nu}$ angular correlation and β^--polarization) are carried out together. Therefore it seems worth while to perform these two experiments on the same β^--decay.

Mayer-Leibnitz *et al.* (2) have measured the angular correlation between β^- and $\bar{\nu}$-particles produced in ^{8}Li β^--decay. Since the polarization of β^--particles in ^{8}Li decay has not been measured yet, we have carried out this polarization experiment.

The half life of ^{8}Li is 0.85 s, the maximum β-energy $E_{max} = 12$ MeV (3). In order to determine the β^--polarization it has been found convenient, because of the high β^--energy, to measure the circular polarization of the external bremsstrahlung of β^--rays (4).

Radioactive ^{8}Li nuclei were produced by bombarding a natural Li target o about 1 mm thickness making use o the reaction ^{7}Li(d, p)^{8}Li. The $\sim$ 650 keV deuteron beam was produced by mean s of a Cockcroft-Walton generator. The β^--rays of ^{8}Li initiated bremsstrahlung in a Pb absorber. The circular polarization of bremsstrahlung was measured in the usual way (4).

In order to eliminate the direct γ radiation produced by the nuclear reactions, the d beam was periodically pulsed. An activation of 2 s was followed by a measurement of 1 s. The direction of the magnetic field was altered per 15 s.

In the Li+d reaction also fast neutrons are produced in a great number producing activities rather disturbing the measurement. We were particularly annoyed by the radioactivities of ^{20}F nuclei produced in NaI(Tl) crystal by (n, α) reaction and that of ^{16}N produced in the cooling water and in other material (*e.g.* the glass envelope of the multiplier) containing oxygen, by (n, p) reaction. Therefore, a CsI(Tl) crystal was used instead of NaI as γ-ray counter and the target was cooled by paraffine oil.

An integral discriminator connected to the detector was applied for meas-

(1) M. Goldhaber, L. Grodzins and A. W. Sunyar: *Phys. Rev.*, **109**, 1015 (1958).

(2) K. H. Lauterjung, B. Schimmer and H. Maier-Leibnitz: *Zeits. f. Phys.*, **150**, 657 (1958).

(3) F. Ajzenberg and T. Lauritsen: *Rev. Mod. Phys.*, **27**, 77 (1955).

(4) M. Goldhaber, L. Grodzins and A. W. Sunyar: *Phys. Rev.*, **106**, 826 (1957).

uring γ-rays of higher energy than ~ 5 MeV.

The effect of the magnetic field on detectors was studied by means of γ-rays of ^{60}Co, ^{24}Na and nuclear reactions ^{7}Li(p, γ)^{8}Be. It has been found that the number of pulses remained constant independently of the direction of the magnetic field within the error of measurement amounting to $\pm 0.15\%$.

Let us denote by n_+ the number of pulses in the case when the magnetic field in the measuring magnet is oriented towards the target (the spins of the electrons in the iron are oriented parallel to the momentum of the incident γ-radiation) and n_- will be the number of pulses in the case of an inverse magnetic field. In our experiment the value of

$$\varkappa = 2\,\frac{n_- - n_+}{n_- + n_+}\,,$$

was found to be

$$\varkappa_{exp} = +\,(3.4 \pm 0.8)\cdot 10^{-2}\,.$$

Since the disturbing activity of ^{16}N could not be completely eliminated, this value has to be corrected. By analysing the decay curve it has been found that of the total number of pulses a fraction of 72% was due to the bremsstrahlung of the β^--particles produced in ^{8}Li-decay. The correction being taken into account

$$\varkappa = +\,(4.85 \pm 1.1)\cdot 10^{-2}\,.$$

For completely left circularly polarized γ-rays we would obtain with the saturation magnetization of the analysing magnet of 7 cm effective length, applied in our experiment

$$\varkappa_{100\%} = +\,5.6\cdot 10^{-2}\,.$$

Thus it follows that the average polarization of the bremsstrahlung produced by β^--particles in ^{8}Li decay, is

$$P_\gamma = (86 \pm 20)\%\,,$$

for the energy range investigated in our experiment. The γ-rays are left handed circularly polarized (their spin is antiparallel to their momenta). It follows from this fact that the β^--particles of ^{8}Li are polarized in backward sense. It is rather complicated to determine accurately the degree of β^--polarisation from the value of P_γ. (The shape of the β^--spectrum and that of the bremsstrahlung, as well as the energy dependence of the polarization of bremsstrahlung γ-rays and the energy dependence of counter efficiency and so on, have to be taken into account).

In our measurement the sign of polarization is unambiguously obtained and the degree of polarization of electrons is found to be in agreement with the relation $P_e = v/c$.

By comparing our experiment with that of MAYER-LEIBNITZ *et al.* it follows that the spin of the antineutrino produced in β^--decay is parallel to its momentum in accordance with the result obtained by GOLDHABER *et al.* [1].

* * *

We have to thank our colleagues Dr. J. ERŐ and T. NAGY for their help in planning the experiment and L. SZABÓ for building the electronic equipment and G. SCHMIDT for his help in carrying out the measurements.

IL NUOVO CIMENTO Vol. X, N. 5 1° Dicembre 1958

The Selection Rules on Hyperon Decays.

K. Nakagawa and H. Umezawa

Department of Physics, University of Tokyo - Tokyo

(ricevuto il 21 Ottobre 1958)

Recently we have published a short note [1] with the same title. There, use has been made of the observed branching ratio

$$R_\Sigma \equiv \frac{w(\Sigma^+ \to \mathrm{p} + \pi^0)}{w(\Sigma^+ \to \mathrm{n} + \pi^+)} \simeq 1 \,, \tag{1}$$

the ratio of the life times

$$R'_\Sigma \equiv \frac{\tau(\Sigma^+)}{\tau(\Sigma^-)} \simeq \frac{1}{2} \,, \tag{2}$$

and the ratio of the anisotropy coefficients

$$\alpha_0/\alpha_+ \simeq 1 \,. \tag{3}$$

The symbol α denotes the anisotropy coefficients for the Σ-decay processes; α_0 for $\Sigma^+ \to \mathrm{p} + \pi^0$ and α^+ for $\Sigma^+ \to \mathrm{n} + \pi^+$. It was concluded in the previous note that the rule $|\Delta I| = \frac{1}{2}$ does not hold as far as the one-to-one law and the invariance under the time reversal (T-invariance) are assumed. The one-to-one law says that the coupling constants for the parity conserving and non-conserving terms are of a same magnitude.

We now come back to the same problem, because recent experiments have not always supported (3); the situation for the anisotropy coefficient now is quite obscure (*).

Assuming the rule $|\Delta I| = \frac{1}{2}$ and T-invariance, the Σ-decay interaction is of the form

$$H = \bar{\psi}_N \frac{1-\tau_3}{2} (A + B\gamma_5)\gamma_\mu \psi_{\Sigma i} \partial_\mu \varphi_{\pi i} + \left(\bar{\psi}_N \tau_i \frac{1-\tau_3}{2}\right)(A' + B'\gamma_5)\gamma_\mu \bar{\psi}_\Sigma t_i \partial_\mu \varphi_\pi + \mathrm{h.c.} \tag{4}$$

Notations here are as follows,

$$\psi_\Sigma = \begin{pmatrix} \psi_{\Sigma 1} \\ \psi_{\Sigma 2} \\ \psi_{\Sigma 3} \end{pmatrix}, \qquad \varphi_\pi \begin{pmatrix} \varphi_{\pi 1} \\ \varphi_{\pi 2} \\ \varphi_{\pi 3} \end{pmatrix}, \qquad \psi_N \begin{pmatrix} \psi_p \\ \psi_n \end{pmatrix}.$$

(1) K. Nakagawa and H. Umezawa: *Nuovo Cimento*, **8**, 945 (1958).

(*) The authors express their sincere thanks to Prof. F. S. Crawford for information on the experimental results under subject.

$$\begin{cases} \psi_{\Sigma^\pm} \equiv \dfrac{1}{\sqrt{2}}(\psi_{\Sigma 1} \pm i\psi_{\Sigma 2}), \\ \psi_{\Sigma^0} \equiv \psi_{\Sigma 3}, \end{cases} \qquad \begin{cases} \varphi_{\pi^\pm} \equiv \dfrac{1}{\sqrt{2}}(\varphi_{\pi 1} \pm i\varphi_{\pi 2}), \\ \varphi_{\pi^0} \equiv \varphi_{\pi 3}, \end{cases}$$

$$t_1 \equiv \begin{pmatrix} 0 & 0 & 0 \\ 0 & 0 & -i \\ 0 & i & 0 \end{pmatrix}, \quad t_2 \equiv \begin{pmatrix} 0 & 0 & i \\ 0 & 0 & 0 \\ -i & 0 & 0 \end{pmatrix}, \quad t_3 \equiv \begin{pmatrix} 0 & -i & 0 \\ i & 0 & 0 \\ 0 & 0 & 0 \end{pmatrix},$$

$$\tau_1 \equiv \begin{pmatrix} 0 & 1 \\ 1 & 0 \end{pmatrix}, \quad \tau_2 \equiv \begin{pmatrix} 0 & i \\ -i & 0 \end{pmatrix}, \quad \tau_3 \equiv \begin{pmatrix} 1 & 0 \\ 0 & -1 \end{pmatrix}.$$

Here, the constants A, B, A' and B' are real. The one-to-one law requires that

$$\begin{cases} A^2 = B^2, \\ A'^2 = B'^2, \end{cases} \tag{5}$$

This together with experimental results (1) and (2) leads us to the relations

$$\begin{cases} A/B \simeq -A'/B', \\ A^2 \simeq A'^2. \end{cases} \tag{6}$$

It should be noted that $A/B \simeq A'/B'$ was obtained in our previous letter where (3) was assumed. The relations (5) and (6) lead us to the interaction

$$H = g\bar{\psi}_N \frac{1-\tau_3}{2}(1+\varepsilon\gamma_5)\gamma_\mu \psi_{\Sigma i}\partial_\mu \varphi_{\pi i} \pm g\left(\bar{\psi}_N \tau_i \frac{1-\tau_3}{2}\right)(1-\varepsilon\gamma_5)\gamma_\mu \psi_\Sigma t_i \partial_\mu \varphi_\pi, \tag{7}$$

where g is a real coupling constant and $\varepsilon = \pm 1$. The anisotropy coefficients are calculated to be

$$\begin{cases} \alpha_0(\Sigma^+ \to \mathrm{p} + \pi^0) = -\varepsilon, \\ \alpha_+(\Sigma^+ \to \mathrm{n} + \pi^+) = 0, \\ \alpha_-(\Sigma^- \to \mathrm{n} + \pi^-) = 0. \end{cases} \tag{8}$$

The ratios R_Σ, and $R_{\Sigma'}$ are shown in the table. It should be noted that the one-to-one law depends on the expression for the interaction; it does on the definition of the coupling constants. Indeed, the one-to-one law would be lost if it would be formulated in terms of the coupling constants for the $\bar{\psi}_p \psi_{\Sigma^+} \varphi_{\pi^0}$ etc.

This is a situation different from that in our previous note where the relation (3) was assumed.

TABLE I. – *Branching ratios, the ratios of the life times and the anisotropy coefficients.*

A'/A	$B/A = \varepsilon$	$B'/A' = -\varepsilon$	R_Σ	$R_{\Sigma'}$	α_0	α_+	α_-
1	1	−1	0.88	0.44	−1	0	0
1	−1	1	0.88	0.44	1	0	0
−1	1	−1	1.28	0.75	−1	0	0
−1	−1	1	1.28	0.75	1	0	0

IL NUOVO CIMENTO Vol. X, N. 5 1° Dicembre 1958

Inelastic Scattering of Electrons from ^{6}Li and ^{14}N.

P. Cazzola

Istituto di Fisica dell'Università - Padova

C. Foglia

Istituto di Fisica dell'Università - Parma

(ricevuto il 15 Novembre 1958)

The inelastic scattering of electrons from ^{12}C has been calculated by Morpurgo [1] making use of the shell model in its most simple form, both in LS and JJ coupling. The agreement of these calculations with the experimental results is rather good: the very strong increase of the ratio inelastic to elastic scattering with the energy is given correctly and also the absolute value of the inelastic cross section differs at most by a factor of 3 from the experimental value.

It is then reasonable to ask whether an analogous situation is true also in other nuclei. We shall give here the results of calculations similar to the above mentioned ones for the case of ^{6}Li and ^{14}N; unfortunately no experimental data are as yet available on these nuclei; but we may reasonably hope that the experiments will be performed soon, and these calculations may be also useful in getting some idea of what one has to expect.

The reasons why we have chosen the above nuclei are: 1) the lower levels are sufficiently distant from each other so that the elastically and inelastically scattered electrons may be energetically resolved; 2) the shell model structure of the nuclei in question is rather simple; 3) the spin and parities of the levels involved are known.

Concerning the question of the resolution (point (1) above) we would like to mention that, in principle, also the cross section for excitation of rather close levels may be measured provided one takes the coincidences between the scattered electrons and the γ-rays from the de-excitation of the level in question. Such a technique is certainly much more complicated, but, once established, might give the possibility of getting by inelastic electron scattering very important information on a large variety of nuclei.

---

[1] G. Morpurgo: *Nuovo Cimento*, **3**, 430 (1956).

Coming back to the present case we have, for the ^{6}Li, considered the scattering from the ground state ($J=1^+$, $T=0$) to the first excited state ($J=3^+$, $T=0$) at 2.18 MeV. We have used in this case only the LS coupling — in which the two states in question are ^3S and ^3D respectively — because it is well known that the JJ coupling does not give correctly the order of the levels in ^{6}Li.

For the ^{14}N we have considered the scattering between the ground state and the state at 3.95 MeV which both have $J=1^+$ and $T=0$. In this case the calculations have been performed both in LS and JJ coupling. The calculations are very similar to the ones performed by MORPURGO for the ^{12}C; we have neglected recoil effects and the corrections arising from the form factor of the nucleons. Unless explicitly mentioned, the notation used in the following expressions will be the same as in ref. ([1]). The quantity to be calculated is, of course, the square of the inelastic form factor defined as:

$$F_{\text{in}}^2 = \frac{1}{2J+1} \sum_M \sum_{M'} |F_{\text{in}}^{MM'}|^2 ,$$

where J is the spin of the ground state and

$$F_{\text{in}}^{MM'} = \int \varrho_{0f}^{MM'} \exp[i\boldsymbol{q}\cdot\boldsymbol{r}] \, \mathrm{d}\tau .$$

The calculation of F_{in}^2 is most easily done choosing a system of coordinates with the z axis in the direction of $\boldsymbol{q}$, and using the expansion of $\exp[iqz]$ in series of spherical harmonics.

We list below the normalized wave functions which we have used, confining ourselves to the p nucleons and writing only the angular and spin part; 1 is proton and 2 is neutron; the isotopic spin is obviously 0 for all the wave functions written down.

^{6}Li (only LS coupling):

$$\psi_{\text{ground state}}^{M} = {}^3\sigma^M \sqrt{\tfrac{1}{3}} (p_1^+ p_2^- + p_1^- p_2^+ - p_1^0 p_2^0) ,$$

$$\psi_{\text{excited state}}^{M'} = \alpha_{M'} \, {}^3\sigma^{M'} \sqrt{\tfrac{1}{6}} (2p_1^0 p_2^0 + p_1^+ p_2^- + p_1^- p_2^+) + \text{other terms} .$$

Here $M = M' = -1, 0, 1$; are the triplet spin functions; $\alpha_{M'} = \sqrt{\frac{2}{5}}$ if $M' = \pm 1$ and $\alpha_{M'} = \sqrt{\frac{3}{5}}$ if $M' = 0$; the other terms in $\psi_{\text{excited}}^{M'}$ as well as the other values of M' do not intervene in the calculation, with our choice of the z axis.

^{14}N (LS coupling)

$$\psi_{\text{ground state}}^{M} = {}^3\sigma^M \sqrt{\tfrac{1}{3}} (\bar{p}_1^+ \bar{p}_2^- + \bar{p}_1^- \bar{p}_2^+ - \bar{p}_1^0 \bar{p}_2^0) ,$$

$$\psi_{\text{excited state}}^{M} = \alpha_{M'} \, {}^3\sigma^{M'} \sqrt{\tfrac{1}{6}} (2\bar{p}_1^0 \bar{p}_2^0 + \bar{p}_1^+ \bar{p}_2^- + \bar{p}_1^- \bar{p}_2^+) + \text{other terms} ,$$

with the same meaning of the symbols as above except that: 1) a bar indicates a hole; 2) $\alpha_{M'} = \sqrt{\frac{1}{10}}$ if $M' = \pm 1$ and $\alpha_{M'} = -\sqrt{\frac{2}{5}}$ if $M' = 0$.

^{14}N (JJ coupling):

$$\psi^M_{\text{ground state}} = \begin{cases} \bar{p}^{\,p}_{\frac{1}{2},\pm\frac{1}{2}}\,\bar{p}^{\,n}_{\frac{1}{2},\pm\frac{1}{2}}\,, & M = \mp 1\,, \\ \sqrt{\tfrac{1}{2}}\,(\bar{p}^{\,p}_{\frac{1}{2},-\frac{1}{2}}\,\bar{p}^{\,n}_{\frac{1}{2},\frac{1}{2}} + \bar{p}^{\,p}_{\frac{1}{2},\frac{1}{2}}\,\bar{p}^{\,n}_{\frac{1}{2},-\frac{1}{2}})\,, & M = 0\,, \end{cases}$$

$$\psi^M_{\text{excited state}} = \begin{cases} \sqrt{\tfrac{1}{2}}\,\{\pm\sqrt{\tfrac{1}{4}}\,\bar{p}^{\,p}_{\frac{3}{2},\pm\frac{1}{2}}\,\bar{p}^{\,n}_{\frac{1}{2},\pm\frac{1}{2}} \mp \sqrt{\tfrac{3}{4}}\,\bar{p}^{\,p}_{\frac{3}{2},\pm\frac{3}{2}}\,\bar{p}^{\,n}_{\frac{1}{2},\mp\frac{1}{2}} + \text{n} \rightleftarrows \text{p}\}\,, & M = \mp 1\,, \\ \sqrt{\tfrac{1}{2}}\,\{-\sqrt{\tfrac{1}{2}}\,\bar{p}^{\,p}_{\frac{3}{2},\frac{1}{2}}\,\bar{p}^{\,n}_{\frac{1}{2},-\frac{1}{2}} + \sqrt{\tfrac{1}{2}}\,\bar{p}^{\,p}_{\frac{1}{2},-\frac{1}{2}}\,\bar{p}^{\,n}_{\frac{1}{2},\frac{1}{2}} + \text{n} \rightleftarrows \text{p}\}\,, & M = 0\,, \end{cases}$$

where we have used n and p instead of 1 and 2 to indicate neutron and proton and we have symmetrized the wave function with respect to n, p interchange in order to have a total $T = 0$.

The expressions for F^2_{in} are summarized in the table below; we have also given the expressions for F^2_{el} (compare for this the formula (129) of the review paper by HOFSTADTER (2)).

TABLE I.

Nucleus	Coupling	Transition	F^2_{in}	F^2_{el}
^{6}Li	LS	(0÷4.18) MeV	$\frac{1}{Z^2}\,\frac{7}{270}\left(\frac{q^2}{\nu}\right)^2 \exp\left(-\frac{q^2}{2\nu}\right)$	$\left(1-\frac{q^2}{18\nu}\right)^2 \exp\left(-\frac{q^2}{2\nu}\right)$
^{14}N	LS	(0÷3.95) MeV	$\frac{1}{Z^2}\,\frac{1}{90}\left(\frac{q^2}{\nu}\right)^2 \exp\left(-\frac{q^2}{2\nu}\right)$	$\left(1-\frac{5}{42}\,\frac{q^2}{\nu}\right)\exp\left(-\frac{q^2}{2\nu}\right)$
^{14}N	JJ	(0÷3.95) MeV	$\frac{1}{Z^2}\,\frac{1}{72}\left(\frac{q^2}{\nu}\right)^2 \exp\left(-\frac{q^2}{2\nu}\right)$	

It appears that the inelastic to elastic ratio at 90° should be one in both cases around 230 MeV. The corresponding cross section is small but should nevertheless be measurable.

* * *

The authors wish to express their gratitude to Prof. G. MORPURGO for suggesting this problem and for helpful discussions.

(2) R. HOFSTADTER: *Ann. Rev. Nucl. Sci.*, **7**, 231 (1957).

LIBRI RICEVUTI E RECENSIONI

L. D. LANDAU and E. M. LIFSHITZ – *Statistical Physics*, Pergamon Press, London, 1958; pagg. 484, 80 scellini.

Si tratta del quinto volume del *Corso di Fisica Teorica*, il grande sforzo di questi autori di coprire in un trattato tanta parte di fisica. Una edizione in inglese era già stata pubblicata nel 1938, ma la presente edizione vuol essere una completa rielaborazione piuttosto che un rifacimento della precedente.

Indubbiamente si tratta di un libro notevole, che non dovrà mancare a nessuna biblioteca di fisica ed a cui gli specialisti dovranno continuamente riferirsi. Ma non si tratta di un libro facile e, tanto meno, da consigliare agli studenti. Il carattere un poco enciclopedico ne rende difficile lo studio sistematico, anche a causa delle forti discontinuità di livello degli argomenti trattati.

Dopo una parte generale di termodinamica statistica, che fa subito uso di concetti quantistici, seguono numerose le applicazioni che vanno dalle più tradizionali alle più moderne, e che in parte sono anche contributi originali degli autori. Così la teoria del liquido di Fermi e di Bose, le discontinuità nel calore specifico ed altri paragrafi ancora, sono molto preziosi perchè ci permettono una conoscenza diretta e concisa dei lavori originali dei due illustri autori e della scuola russa contemporanea.

G. CARERI

Direttore responsabile: G. POLVANI Tipografia Compositori - Bologna

Questo fascicolo è stato licenziato dai torchi il 31-XII-1958.